Università degli Studi di Salerno

Dipartimento di Chimica e Biologia "A. Zambelli"

Dottorato di ricerca in chimica -XXX ciclo

Ruthenium metathesis precatalysts with unsymmetrical N-heterocyclic carbene (NHC) ligands

Tutor:

Dr Fabia Grisi

Co-tutor: Candidata

Prof. Chiara Costabile   Veronica Paradiso

Coordinatore del dottorato:

Prof. Gaetano Guerra

Anno accademico 2016/2017

Preface

Olefin metathesis is one of the most important chemical transformations for the formation of carbon-carbon double bonds. The possibility to build up highly funtionalised alkenes starting from simple olefins makes this reaction indispensable in modern organic synthesis, giving access to a wide range of molecules that would be barely obtained through other synthetic routes.

The success of metathesis is due to the development of new and efficient catalysts which can be used in a wide variety of research fields, both in industry and in academia. In this context, the research of the 'perfect' metathesis complex still impassions scientists all over the word, and several research papers regarding the development of new catalytic systems are published every year.

The group I am part of focuses its attention on the development of new ruthenium metathesis catalysts. Our interest lies in the influence that nature and configuration of substituents on the N-heterocyclic carbene (NHC) ligand could have on the performances of the corresponding metal complexes.

In this doctoral thesis, the field of unsymmetrical N-heterocyclic carbene (u-NHC) ruthenium catalysts will be explored. Synthesis and characterisation of several novel complexes will be discussed. Catalytic performances will be evaluated in model metathesis reactions as well as in more attractive metathesis transformations. The relationship between NHC structure and complexes' behaviours will be investigated using NMR, X-Ray, IR, cyclic voltammetry and DFT calculations.

Chapters One and Two give an overview on olefin metathesis and on the most famous ruthenium-based systems.

In Chapter Three novel u-NHC ruthenium catalysts are investigated. Steric and electronic properties of the ligands are analysed in depth.

In Chapter Four, u-NHC ruthenium compounds are tested in homo- and copolymerisations.

In Chapter Five, the performances of a new series of u-NHC catalytic systems are studied. The application in various metathesis transformations, also involving renewable substrates, is investigated.

In Chapter Six, all the enantiomerically pure catalysts are tested in asymmetric metathesis transformations. A novel approach for the synthesis of enantiopure catalysts is also described.

Summary

Ruthenium metathesis precatalysts with unsymmetrical N-heterocyclic carbene (NHC) ligands

Chapter 1

Olefin Metathesis

The search of a synthetic route that combines efficiency and convenience has always excited chemists of all generations. Mild reaction conditions, high yields, considerable selectivities: nowadays these are the most important guidelines joined to a 'green' design that keeps also in consideration environmental issues.

However, there is something more. The appeal of a chemical synthesis lies also in the beauty of its stepwise construction and in the purity of the reaction sequence, a sort of complex feature that chemists call 'elegance'. In our society, in which numbers and quotes rule the scientific world, synthetic chemists persist in their pursuit of elegance, like creative architects that focus on the robustness of the structure without renouncing to an overall harmony.

Reactions of formation of carbon-carbon bonds build up organic molecules and are the beating heart of synthetic chemistry. In this context, olefin metathesis can be considered as a very elegant reaction of carbon bonds formation with a versatility and a simplicity that makes its application useful in several branches of chemistry. This metal catalysed reaction consists in an exchange of groups between double bonds that produces differently substituted alkenes (scheme 1.1).[1]
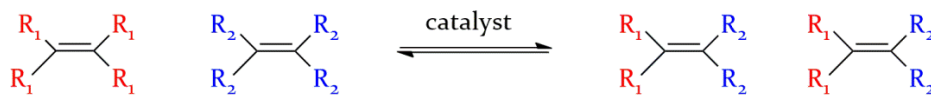
Scheme 1.1: Olefin Metathesis

In 2017, sixty years after the discovery, the interest toward this reaction is not decreasing. In fact many scientists all over the world are working on new applications of metathesis and on the development of new metal based catalytic systems, declaring it as one of the most important chemical transformation of the XX° century.

1.1 Discovery and early stages

The story of olefin metathesis started in the '50, when it was discovered that Ziegler-Natta heterogeneous catalytic systems (for example $WCl_6/EtAlCl_2$ or $MoCl_5/Al(C_2H_5)_3$) were able to convert simple olefins in a mixture of alkenes. After that, several industrial chemists independently observed the phenomena. In 1957 H. S. Euleterio at Du Pont Petrochemicals discovered the formation of an unsaturated polymer after the reaction of norbornene with molybdenum oxide on alumina with lithium aluminium hydride.[2] E. F. Peters and B. L. Evering of Standard Oil Company, in 1960, reported that when propylene reacted with

---

[1]a)*Olefin Metathesis: Theory and Practice,* Edited by K. Grela, John Wiley and Sons, Hoboken **2014;** b)*Handbook of Metathesis,* Edited by R. H. Grubbs, Wiley-VCH, **2015**.

[2]H.S. Eleuterio, *Ger. Pat. 1 072 811* **1960**, *Chem. Abstr.* **1961**, 55, 16005; H.S. Eleuterio *US. Pat. 3 074 918* **1963**.

molybdenum oxide on alumina and triisobutyl aluminium, a mixture of ethylene and butane was achieved. [3] The same reaction was described few years later by R. L. Banks and G. C. Bailey of Phillips Petroleum and was called 'disproportionation'.[4]

At this point, many scientists all over the world focused on this chemical transformation, intrigued by its novelty and great industrial potential. In 1967 Calderon and co-workers from Goodyear had the right intuition: in this reaction new olefins were formed by the breakage of reagents which then recombine to give new alkenes with a longer or a shorter carbon chain. It was an exchange of groups, a transposition or, in Greek, metathesis (μεταθεσις) (figure 1.1).[5]

OLEFIN METATHESIS – A NOVEL REACTION FOR
SKELETAL TRANSFORMATIONS OF UNSATURATED HYDROCARBONS

Nissim Calderon, Hung Yu Chen and Kenneth W. Scott
The Goodyear Tire and Rubber Company, Research Division, Akron, Ohio
(Received 29 May 1967)

It has been discovered that when an internal olefin is exposed to a catalyst comprised of tungsten hexachloride, ethanol and ethylaluminum dichloride, the following metathesis reaction occurs:

$$2\ R_1\text{-CH} = \text{CH-}R_2 \rightleftharpoons R_1\text{-CH} = \text{CH-}R_1 + R_2\text{-CH} = \text{CH-}R_2$$
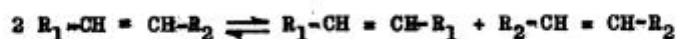
Thus, 2-pentene will undergo an interchange process resulting in the formation of a mixture containing at equilibrium 25, 50, and 25 mole percent of 2-butene, 2-pentene and 3-hexene, respectively.

Figure 1.1: The term 'olefin metathesis' appears for the first time (1967).

1.2 Reaction mechanism

Heterogeneous catalysis, which is often very easy and convenient, is still a black hole. Few catalytic mechanisms have been well clarified and most of the times what happens at the surface between catalyst and substrate is unknown. Of course, without an exhaustive elucidation of the reaction mechanism, olefin metathesis would have hardly become so widespread and the development of new homogeneous systems would not have been possible.

In 1971, Y. Chauvin and J. L. Hèrisson from the French Petroleum Institute proposed a mechanism in which the key role is played by a metal carbene (scheme 1.2).[6] In the catalytic cycle, the carbene (I) coordinates the olefin and forms, via a [2+2]cycloaddition, a metal cyclobutane intermediate (II) which then opens to give a new carbene (III). The new metal complex coordinates another olefin to form a new metalcyclobutane (IV) from which cycloreversion (I) is regenerated and a new olefin is formed. All stages are equilibrium steps.

---

[3] E. F. Peters, B. L. Evering *US Pat. 2 963 447* **1960**.
[4] R. L. Banks, G. C. Bailey *Ind. Eng. Chem. Prod. Res. Dev.* **1964**, 3 , 170.
[5] N. Calderon, H. Y. Chem, K. W. Scott *Tetrahedron Lett*. **1967**, 34, 3327.
[6] J. L. Hèrisson, Y. Chauvin *Makromol. Chem.* **1971**, 141, 161.
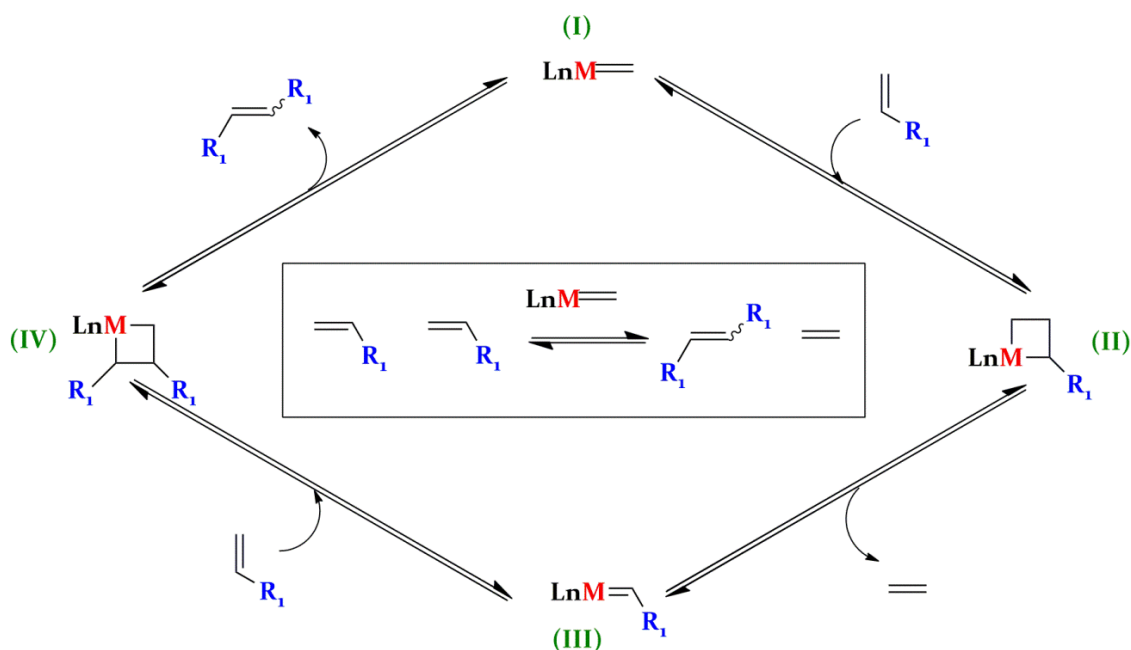
Scheme 1.2: Chauvin's mechanism.

1.3 Metathesis Reactions

The versatility of olefin metathesis has made it a method of choice to form carbon-carbon double bonds in organic chemistry, polymer chemistry, as well as in green chemistry and material science.

On the base of the type of alkenes involved in the transformation, it is possible to distinguish different metathesis reactions. The most important, with some relevant applications, are shown below:

- **Ring Closing Metathesis (RCM)** is an intramolecular reaction in which a polyolefin

Scheme 1.3: Ring Closing Metathesis

cyclises to form a cyclic alkene (scheme 1.3). During the catalytic cycle a gaseous molecule is formed and this makes the reaction ruled by an entropic driving force and essentially irreversible.

Between all metathesis transformations, RCM is one of the most successful, mainly thanks to all the pharmaceutical applications in which, frequently, the closure of a ring is one of the last steps. SIMEPREVIR, used for the cure of hepatitis C and PACRITINIB, currently under investigation for the treatment of lymphoma and myeloma are just few of the more recent examples (scheme 1.4).[7]

---

[7] D. S. Higman, J. A. M. Lummiss, D. E. Fogg *Angew. Chem.* **2016**, 55, 3552.

SIMEPREVIR
(synthesis in kilogram scale)

PACRITINIB
(synthesis in gram scale)
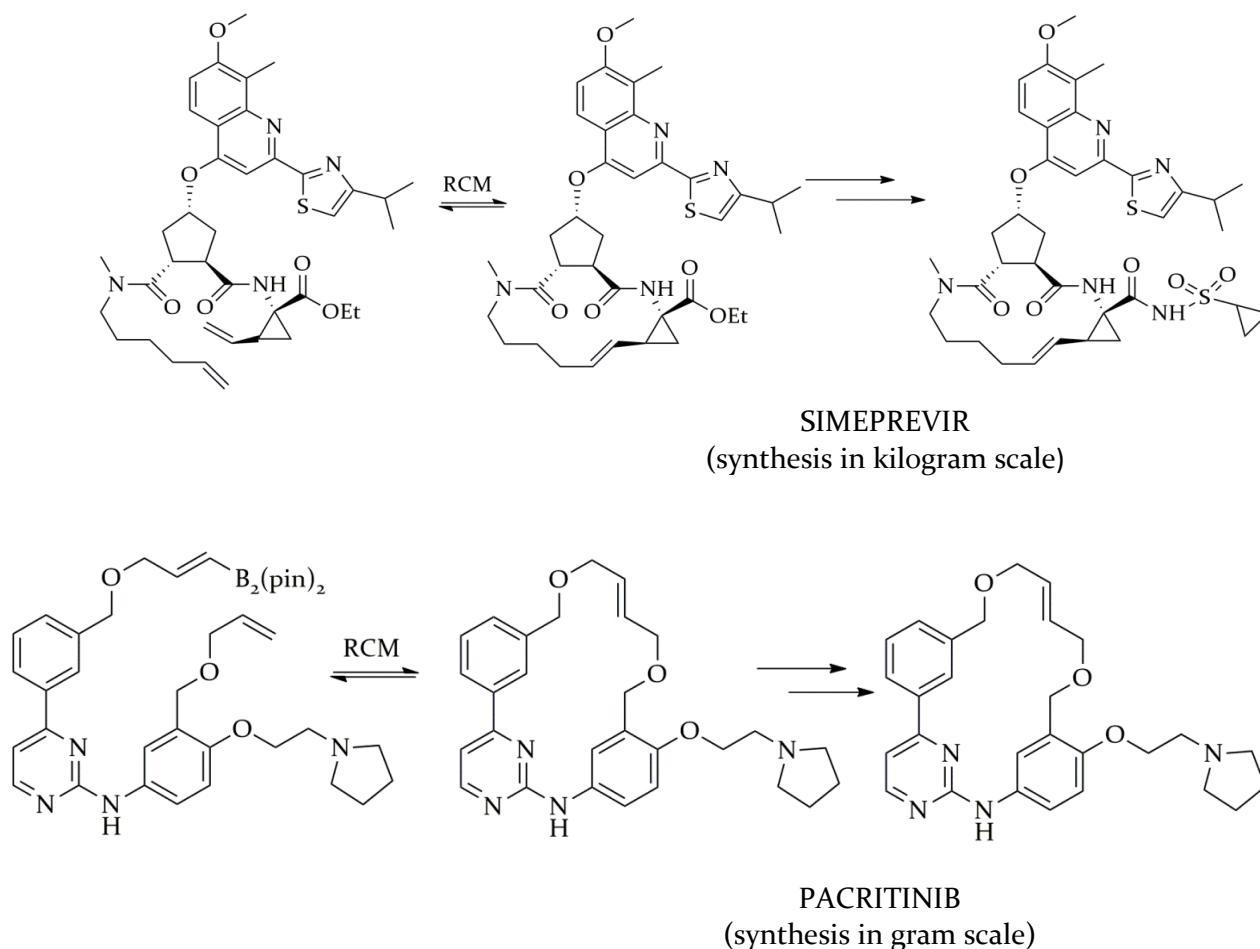
Scheme 1.4: Last steps of synthesis of SIMEPREVIR (top) and PACRITINIB (bottom)

- **Ring Opening Metathesis Polymerization (ROMP)** is a reaction in which cyclic unsaturated olefins polymerise through the opening of the ring to give unsaturated polymers which can be successively crosslinked or further functionalised (scheme 1.5).

Scheme 1.5: Ring Opening Metathesis Polymerisation

Olefins involved are usually ring strained, so this polymerisation is normally driven by an enthalpic driving force.

As discussed in paragraph 1.1, metathesis was discovered as a polymerisation reaction and is nowadays applied in many big scale polymerisation processes, with a range of ROMP products commercially available.

Poly(dicyclopentadiene) (pDCPD) (scheme 1.6) is probably the most relevant industrial product of ROMP, with a global production of 25000 metric tons per year (2014).[8]

It shows a good acids and alkali tolerance and, due to the rigidity of the bicyclic structure, a high impact resistance. These properties make it useful in various applications including wastewater treatment and body panels for cars.[9]

---

[8]C. Slugovic *Industrial Applications of Olefin Metathesis Polymerization,* chapter of *Olefin Metathesis: Theory and Practice*, Edited by K. Grela, John Wiley and Sons, Hoboken **2014**
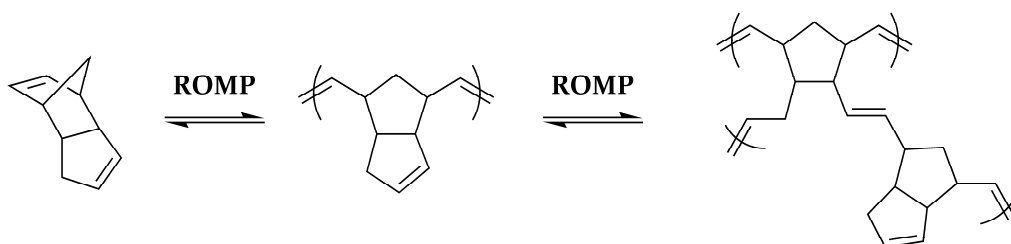
Scheme 1.6: pDCPD, sold as Telene®, Menton®, Pentam® and Proxima™

Scheme 1.7: Poly(norbornene) (Norsorex®)

Poly(norbornene) produced via ROMP is also known as Norsorex® (scheme 1.7) and was the first metathesis polymer commercialised (1976). It is characterised by a very high molecular weight (3000000 g/mol) and a considerable trans content (90%). This rubber can be blended with many other elastomers in order to adapt the properties on the market demands.[10]

NatureWax® represents a more recent application of ROMP.[11] The wax composition include a hydrogenated vegetable oil (typically triglyceride of soybean oil) (figure 1.2) and its metathesis oligomers. The main application lies in the production of candles.
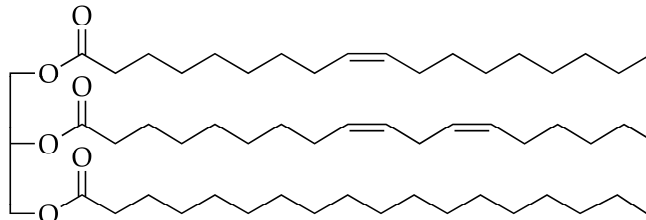
Figure 1.2: Triglyceride of soybean oil

- **Acyclic Diene Metathesis (ADMET)** is a condensation polymerisation used to convert acyclic dienes to linear polymers (scheme 1.8). Usually terminal α,ω-alkenes are used, with a release of a molecule of ethylene. Unfortunately, this is not sufficient to guarantee an efficient entropic driving force and for this reason ADMET is mainly ruled by equilibrium. Sometimes, in order to

Scheme 1.8: Acyclic Diene Metathesis

---

[9] www.telene.com, Last access October 22nd 2017.

[10]F.Lefebvre, J. M. Basset, *Industrial Applications of Olefin Metathesis Reaction*, chapter of *Metathesis Polymerization of Olefins and Polymerization of Alkynes*, Edited by Y. Imamogammalu, Springer Netherlands **1998**.

[11] A. Shofer, *US Pat. 8865118* **2014**

overcome the thermodynamic control, vacuum is used to remove gas and thus facilitate the transformation, leading to polymers with higher molecular weight and lower polydispersities.

ADMET has been used for many applications:[12] for example, the polymerisation of 1,4-bis(2-ethylhexyl)-2,5-divinylbenzene was used to obtain poly(p-phenylene vinylene) with all trans configurations (scheme 1.9).[13]

Scheme 1.9: ADMET of 1,4-bis(2-ethylhexyl)-2,5-divinylbenzene

- **Cross Metathesis (CM)** is the transalkylidenation of two olefins (scheme 1.10). When

Scheme 1.10: Cross Metathesis

at least one of the alkenes involved is terminal the reaction is entropically driven (a molecule of ethylene is released) while when both the alkenes are internal the reaction is particularly complicated.
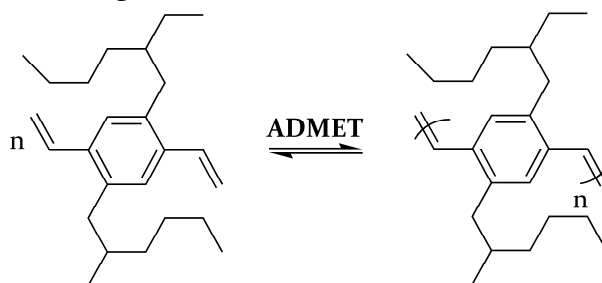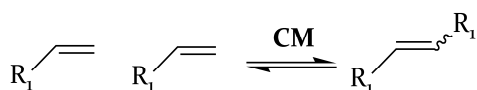
Selectivity is another important issue (scheme 1.11): in fact, beyond the desired cross-product **(I)**, also alkenes derived from self metathesis **(II)** and **(III)** are achieved. Particularly complex is the case of two alkenes having comparable reactivities. Indeed in this case, even if reagents were full converted, the cross metathesis product yield would not exceed 50%.
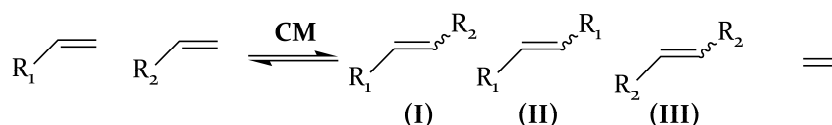
Scheme 1.11: Cross metathesis (I) and Self Metathesis (II, III) products

The cross metathesis involving ethylene as cross partner converts internal olefins into terminal alkenes and it is called ethenolysis. It represents the only cross metathesis industrially relevant application and it is mainly used for the conversion of fatty acid derivatives, tipically methyl esters with a long carbon chain, into shorter α-olefins (scheme 1.12) which are useful intermediates in the production of surfactants, cosmetics and antimicrobial.[14,15]

---

[12] H. Mutlu, L. M. deEspinosa, M. A. R. Meier *Chem. Soc. Rev.* **2011**, *40*, 1404.
[13] U. H. F. Bunz, D. Maeker, M. Porz Macromol. *Rapid Commun* **2012**, *33*, 886.
14J. Spekreijse, J. P. M. Sanders, J. H. Bitter, E. Scott *ChemSusChem* **2016**, *10*, 470.
[15] J. Bidange, C. Fischmeister, C. Bruneau *Chem. Eur. J* **2016**, *22*, 12226.
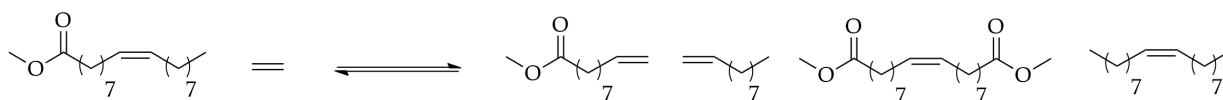
Scheme 1.12: Ethenolysis of methyl oleate

- **Enantioselective Metathesis Transformations**

  The development of an asymmetric version of a chemical reaction creates a wide list of new applications capable of adding value and broadening the scope of the whole transformation. Thanks to the advancement in the synthesis of new asymmetric catalysts, for all metathesis-related transformations an asymmetric version was developed. Some of the most important are Asymmetric Ring Closing Metathesis (ARCM) and Asymmetric Ring Opening Cross Metathesis (AROCM).

  ARCM has been the first asymmetric metathesis used and involves the formation of a cyclic alkene with a defined stereochemistry. It can be realized by desymmetrisation of prochiral polyenes or by resolution of racemic mixtures.

  In the synthesis of quebrachamine (an antispasmodic), ARCM is one of the last step and allows the enantioselective cyclisation of two sterically hindered double bonds (scheme 1.13).[16]
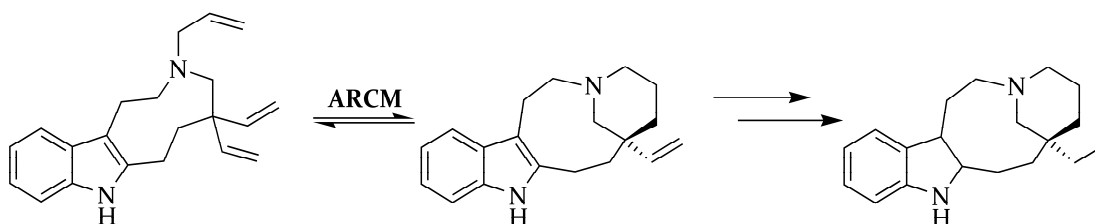
Scheme 1.13: Last steps of the synthesis of quebrachamine

  AROCM represents an example of different metathesis processes occurring in tandem: in fact, the asymmetric ring opening of a prochiral olefin is followed by the metathesis with a cross partner.

  This sequence of metathesis related process is used, for example, in the synthesis of (+)-baconipyrone C (a natural product derived from mollusks) (scheme 1.14).[17]
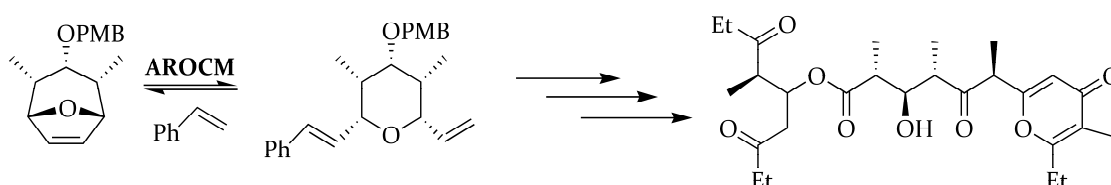
Scheme 1.14: Synthesis of (+)-baconipyrone C *via* AROCM.

1.4 'Standard' metathesis transformations

Since the advent of well defined ruthenium catalysts, the number of publications involving olefin metathesis has rapidly increased. In a few years, many metathesis catalysts were

---

[16] E. S. Sattely, S. J. Meek, S. J. Malcolmson, R.S. Schrock, A. H. Hoveyda *J. Am. Chem. Soc.* **2009**, *131*, 943.

[17] D. G. Gillingham, A. H. Hoveyda *Angew. Chem. Int. Ed.* **2007**, *46*, 3860.

published and the comparison between different systems (which is fundamental for the evaluation of the effective progresses in catalysis) soon became very difficult.

To solve this problem, in 2006 Grubbs proposed a set of 'standard' metathesis reactions with the respective reaction conditions: [18]

- **RCM of malonate derivatives**

    RCM is an excellent candidate to study complexes efficiency considering its facility and high reproducibility. Moreover reactions can be conveniently scaled down and monitored over time via NMR spectroscopy.

    Of course, the use of a closed reaction vessel (that is often a NMR screw tube) inhibits the removal of ethylene or other gaseous product but, since the scope of these reactions is comparison and not evaluation in absolute terms, this does not represent a limitation.

    Malonates derivatives were chosen as standard substrates (scheme 1.15). The increasing steric hindrance allows to investigate the efficiencies of catalysts in more challenging transformations. Reactions are carried out in deuterated methylene chloride at 30°C. Loadings are 1% mol for the formation of di- and trisubstituted olefins and 5% mol for the RCM forming the tetrasubstituted analogue.
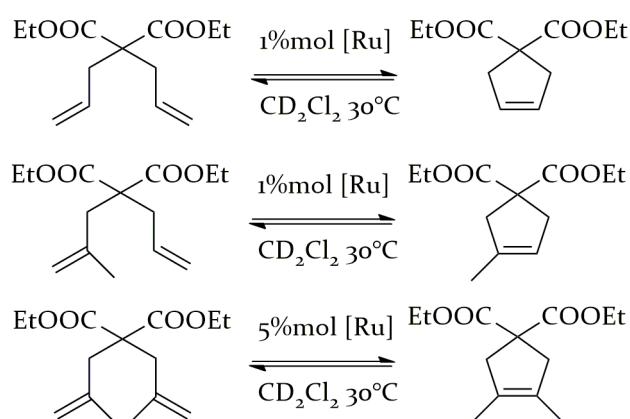
Scheme 1.15: RCM of malonate derivatives

Another class of common RCM substrates is constituted by the N-tosyl derivatives depicted in scheme 1.16. Tosyl is a very common protecting group in organic synthesis and thus these reactions represent an interesting test for catalysts.

[18] T. Ritter, A. Hejl, A. G. Wenzel, T. W. Funk, R. H. Grubbs, *Organometallics* **2006**, *25*, 5740.
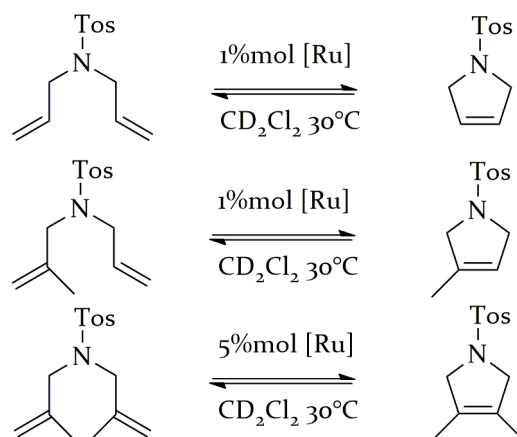
Scheme 1.16: RCM of tosyl derivatives

Alternatively to the approach proposed by Grubbs, in order to better appreciate catalytic activity of Hoveyda-type catalyst (which often need higher initiation temperature), standard RCM can be carried on also in deuterated benzene at 60°C.

- **ROMP of cyclooctadiene (COD)**
  ROMP is frequently used for evaluate catalytic activity and, in order to facilitate comparison, reaction monitoring via NMR spectroscopy is desirable. To prevent too fast reactions, which can be hardly controlled, highly strained monomers (like norbornene derivatives) should be avoided.
  Cyclooctadiene (COD) is a moderately active substrate for ROMP and gives polybutadiene without the formation of byproducts (scheme 1.17).
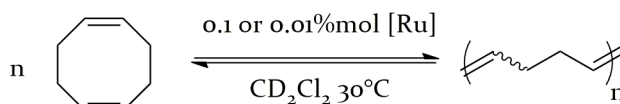
Scheme 1.17: ROMP of COD

Polymer NMR spectra are easily understandable and *E/Z* ratio can be also evaluated. Reactions are carried out in deuterated methylene chloride at 30°C. An increase of temperature (and the consequent change of solvent) for Hoveyda-type catalysts is often unnecessary. Loadings are 0.1% or 0.01% mol.

- **CM of allylbenzene and cis-2,4-diacetoxy-2-butene**
  Allylbenzene and cis-2,4-diacetoxy-2-butene are very convenient CM substrates for their structural semplicity and availability. Beyond the desired cross product, also stylbene is obtained, even if an excess of cis-2,4-diacetoxy-2-butene is used (scheme 1.18).
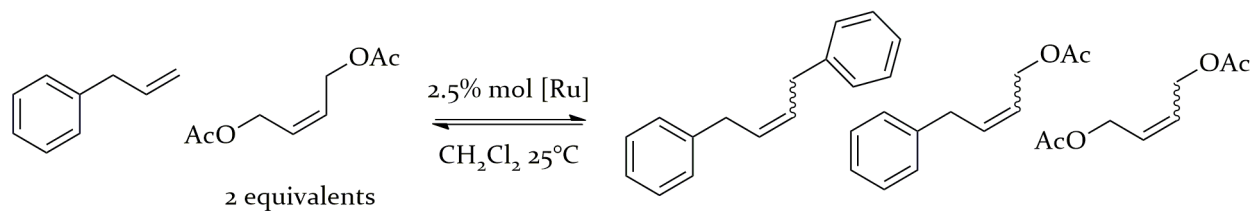
Scheme 1.18: CM of allylbenzene and cis-2,4-diacetoxy-2-butene

The *E/Z* ratio can be evaluated using NMR of purified reaction products. Conversions and geometry of the products can be also monitored using gas chromatography. Reactions are carried out in methylene chloride at 25°C.

1.5 Olefin Metathesis: rooted or outdated?

The fact that olefin metathesis is one of the few fundamentally novel organic reactions of the XX° century is undeniable. This reaction, like few others, is not restricted to organic handbooks and is not bordered into academic labs for applications in basic research. Indeed, it has gone overwhelmingly into people's every days life with widespread products (pharmaceuticals and polymer especially), which were made using processes involving metathesis in some steps.

The great contribution that metathesis has given to the advancement of chemistry has led three scientists to win the Nobel prize in 2005: Yves Chauvin, who proposed the reaction mechanism which is a milestone of all organometallic chemistry, and Richard Schrock and Robert Grubbs for the development of new catalytic systems.

But now, twelve years after the Nobel prize with hundreds of catalysts and applications developed, is there in olefin metathesis something interested or useful to be discovered yet? The answer is given in figure 1.3, in which are depicted the issued US patent and patent applications related to metathesis within the last years.[19]

The graphic shows an increase of metathesis-related topic in the US patent literature, with a significant improvement between 2012 and 2013. This is because, even if metathesis has been applied in industry since its discovery, just recently many technical obstacles (high dilution, impurities incompatibility) have been resolved.
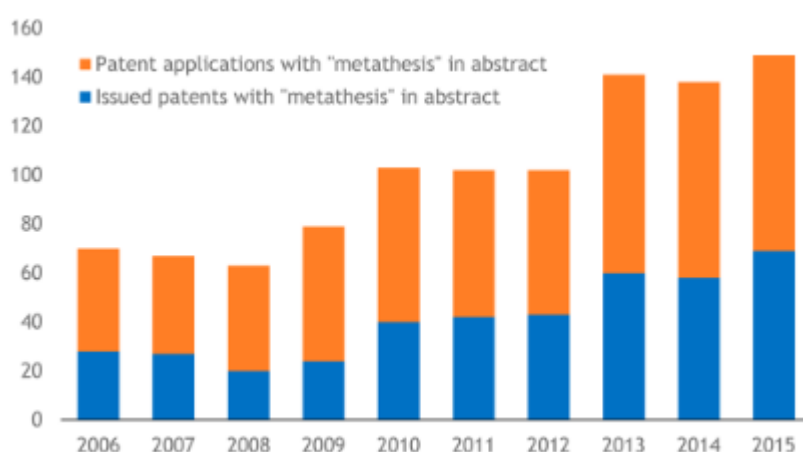
Figure 1.3: US patent and patent application related to olefin metathesis (taken from reference 19).

---

[19] D. L. Hughes *Org. Process. Res. Dev*. **2016**, *20*, 1008.

In fact, the most important commercial application of metathesis is dated just 2011 and is the Elevance-Wilmar biorefinery of Surabaya (Indonesia), that processes 180k MT of seed oil (400 million pounds). In this system natural alkenes (soy, palm, canola etc.) are converted to α-olefins, oleochemicals or specific chemicals using metathesis followed by other derivatisation reactions.[20]

These industrial progresses do not just implicate novel big scale productions but also represent a considerable incentive in the development of new catalysts, designed to answer to industrial needs considered impossible to satisfy so far.

In conclusion, even if the recognition with a Nobel prize represents the maximum goal for a chemical reaction and for its discover, for olefin metathesis it should not be considered as a finish line. It is, instead, a new starting point for new industrial applications, as well as academic studies.

---

[20] D. Stoianova, A. Johns, R. Pederson, *Commercial Application and Future Opportunities,* chapter of *Handbook of Metathesis, Vol. 2: Application in Organic Synthesis*, Edited by R. H. Grubbs and D. O'Leary, Wiley-VCH Verlag Gmbc & Co., **2015**.

Chapter 2

Evolution of Ruthenium-based catalytic systems

Since the elucidation of the reaction mechanism, many homogeneous systems based on different transition metals have been proven to initiate olefin metathesis.[21] The versatility of the reaction and the different kinds of olefins that could be potentially involved make the design of an "universal" metathesis catalyst impossible. Indeed, the initiation system's characteristics have to be modulated on the base of the specific reaction of interest.

Between all the catalysts applied in olefin metathesis, those based on ruthenium, molybdenum and tungsten are the most investigated.

Molybdenum and tungsten metal complexes have been successfully applied in all metathesis reactions and their efficiency is subject of many in-depth studies.[22] Advantages include the considerable activity and selectivity beyond the relatively low price of the two metals. Moreover problems related to their manipulation, due to their pronounced oxophilicity, have been recently solved by using easy to handle and air stable wax caps.[23]

Unfortunately, the low tolerance towards most of the functional groups (OH, OR, NH2 *etc.*) continues to be a hurdle which, *de facto*, strongly limits the field of applications.

Ruthenium is a low oxophilic late transition metal with a great tolerance towards many functional groups. These characteristics have made it the only metal suitable for big scale applications and renewables' metathesis reactions (renewable feedstocks often present oxygen containing functional groups and a considerable amount of impurities).

The only disadvantage consists in its high price (2643.4 €/kg)[24]. This aspect is of course very relevant, but the robustness of ruthenium complexes (which can be manipulated also by non-specialised employees) satisfies industrial needs to such an extent that economic evaluation on the ruthenium price has moved to the background.

During the years, the evolution of homogeneous ruthenium-based catalytic systems went hand in hand with the development of olefin metathesis and, in this path, the introduction of an N-heterocyclic carbene (NHC) as ancillary ligand represents a crucial point. In this chapter, a short overview on ruthenium homogeneous systems will be given. Special attention will be dedicated on latest NHC-Ru catalysts whose versatility and potentiality have inspired this doctoral thesis.

---

[21] a)J. Feldman, R. R. Schrock, *Prog Inorg Chem* **1991**, *39*, 1;b)R. R. Schrock, *Dalton Trans* **2001**, 2541; c) R. R. Schrock, *Chem. Rev.* **2002**, *102*, 145.

[22] a)R. R. Schrock, *Journal of Molecular Catalysis A: Chemical* **2004**, *1*, 21; b)R. R. Schrock, *Chimia* **2015**, *69*, 388.

[23] www.ximo-inc.com, last access October 22nd 2017.

[24] a) Live quotation of ruthenium: www.infomine.com, last access October 23th 2017; b) Similar quotations for pure molybdenum and tungsten, which are non-precious metals, are not easy to trace. The 2016 average price of molybdenum, which can be a comparison aid, is about 15.7€/kg. Source: www.quadl.com, last access October 23th 2017.

2.1 A historical background

In 1992, Grubbs and co-workers reported the first ruthenium alkylidene complex metathetically active (figure 2.1)[25]. This catalysts was tested in the ROMP of norbornene and,

Figure 2.1: The first Ru-alkylidene complex applied in metathesis

even if it exhibited a pronounced robustness, its activity was limited to strongly strained, electron rich olefins.

For this kind of complex, the basicity of phosphine is crucial, since it was demonstrated that the more basic is the phosphine ligand, the more active is the corresponding catalyst.[26]

This consideration, together with the substitution of a vinyl alkilydene with a benzylidene, led to the complex benzylidene-bis(tricyclohexylphosphine)dichlororutheniu m, which represents a cornerstone of metathesis development and is commercially known as Grubbs catalyst first generation (**GI**)(figure 2.2).[27]

Thanks to the enhanced tolerance toward oxygen and functional groups, this catalyst is diffusely used by chemists working in different fields and is perhaps present in most of the synthetic laboratories all over the world.
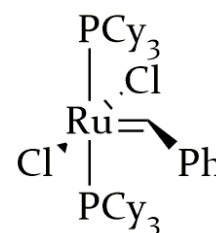
Figure 2.2: Grubbs catalyst first generation
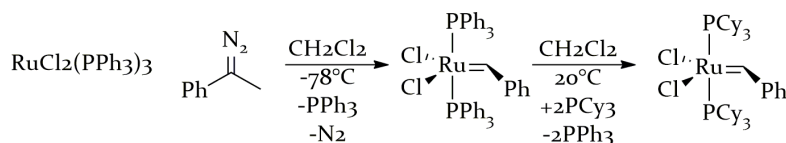
Scheme 2.1: Synthesis of **GI**

Of course, a crucial point in the commercial success of this catalyst lies in the scalable synthetic procedure which consists in the reaction of $RuCl_2(PPh_3)_3$ with a diazoalkane compound and subsequent treatment with tricyclohexylphosphine (scheme 2.1).

GI extended the scope of metathesis and was the first complex able to polymerise less strained alkenes and to perform RCM (scheme 2.2),[27b] thus creating a new synthetic strategy and giving access to a large number of ring systems.

N-heterocyclic carbenes are Lewis bases and act as a strong σ-donors and poor π-acceptors. They are widely used in transition metal catalysis,[28] thanks also to their low lability which implicates

Scheme 2.2: Examples of RCM with **GI**

[25] S. T. Nguyen, L. K. Johnson, R. H. Grubbs, J. W. Ziller, *J. Am. Chem. Soc.* **1992**, *114*, 3974.

[26] S. T. Nguyen, R. H. Grubbs, J. W. Ziller, *J. Am. Chem. Soc.* **1993**, *115*, 9858.

[27]a)P. Schwab, M. B. France, J. W. Ziller, R. H. Grubbs, *Angew. Chem. Int. Ed.* **1995**, *34*, 2039; b)P. Schwab, R. H. Grubbs, J. W. Ziller, *J. Am. Chem. Soc.* **1996**, *118*, 100.

[28] S. Diez Gonzàlez, N. Marion, S. P. Nolan, *Chem. Rev* **2009**, *109*, 3612.

a considerable stability of the corresponding metal complex. In metathesis, the substitution of a tricyclohexylphosphine with an NHC created a new family of complexes called second generation Grubbs catalysts (**GII**)(figure 2.3).[29]
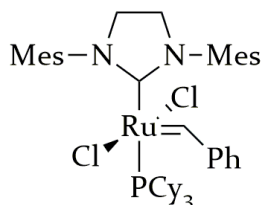
Figure 2.3: A Grubbs second generation catalyst. The depicted NHC ligand is H2IMes(1,3 dimesitylimidazolidine)

The synthesis of these complexes, published in 1999 but almost unchanged until nowadays,
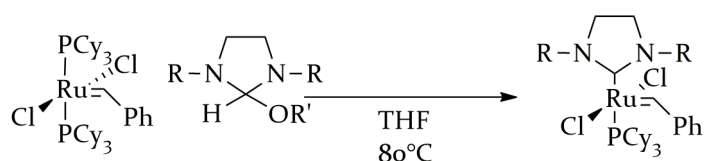
Scheme 2.3: Synthesis of **GII**

consists in a reaction between **GI** and an appropriate NHC ligand precursor (scheme 2.3)

GII showed an improved air and water tolerance and thermal stability and these characteristics allow use at higher temperatures, with lower loadings and unrefined olefins.

The possibility to fine tune catalysts' performances by modulating the steric and electronic properties of the NHC ligand has opened the window to unlimited catalytic opportunities and is the reason why this family of catalysts is one of the most important and investigated in olefin metathesis.

The substitution of a phosphine ligand with an ortho-isopropoxystyrene framework, proposed independently by Hoveyda and Blechert in 2000 [30] was "the most significant
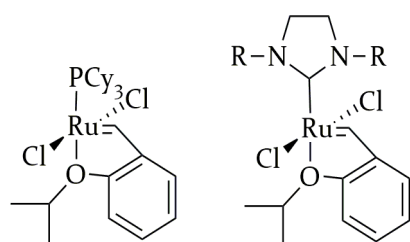
Figure 2.4: Hoveyda first (right) and second (left) generation catalysts

development in the improvement of the properties of the Grubbs catalysts since the introduction of the NHC ligand".[31] This new group of ruthenium complexes are called, analogously to the Grubbs', Hoveyda first and second generation catalysts (**HI** and **HII**)(figure 2.4).

HII has an exceptional air and moisture robustness, enough to be used in water or other polar solvents. This is because of the absence of any phosphinic ligand which can activate or accelerate decomposition pathways of the active species. Phosphines are damaging also because they could

[29] M. Scholl, S. Ding, C. W. Lee, R. H. Grubbs, *Org. Lett.* **1999**, *1*, 953.

[30] a) J. S. Kingsbury, B. L. Gray, A. H. Hoveyda, *J. Am. Chem. Soc.* **2000**, *122*, 8168; b) S. Gessler, S. Randl, S. Blechert, *Tetrahedron Lett.* **2000**, *41*, 9973.

[31] Y. Ginzburg, N. G. Lemcoff, *Hoveyda-type Olefin Metathesis Complexes*, chapter of *Olefin Metathesis: Theory and Practice*, Edited by K. Grela, John Wiley and Sons, Hoboken **2014**

determine a reduction of the activity of the complex, competing with the olefin in the coordination to the metal centre.[32]

Therefore, another peculiarity of **HII** is the improved reactivity towards electron-poor olefins, including fluorinated alkenes, sulfones, acrylonitriles, *etc.* [33]

The synthesis can be carried out using two strategies, both involving an exchange of one phosphine ligand: the first uses **HI** which reacts with an appropriate carbene precursor (scheme 2.4, top); the second starts from **GII** whose phosphine is substituted by isopropoxystyrene (scheme 2.4, bottom).[9a] Both synthetic pathways are efficient and can be used alternatively on the base of the available ruthenium precursor complex.
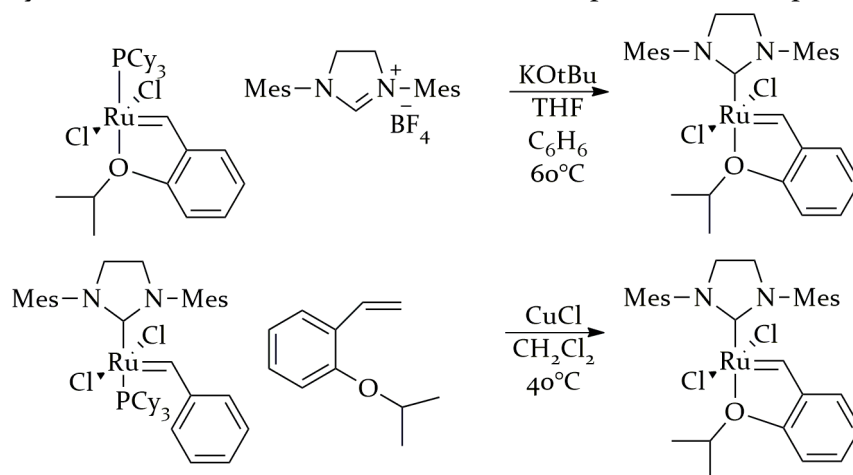
Scheme 2.4: Synthesis of **HII**

2.2 Catalytic mechanism
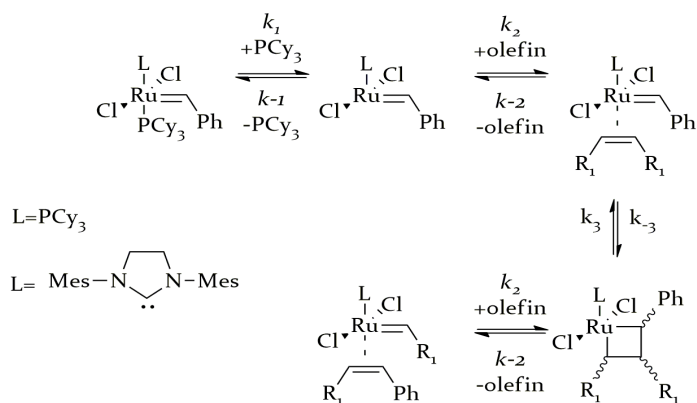
Scheme 2.5: Catalytic mechanism with Grubbs type catalysts

The general mechanism of olefin metathesis with Grubbs type catalysts involves a dissociative step (scheme 2.5) in which the loss of a phosphine generates a 14 electron intermediate.[34] The olefin coordinates to this species leading to the formation of a metallacyclobutane which can then evolve in a new olefin and a new metallocarbene. The pronounced reactivity of the second generation complexes, compared with the first generation analogues, is not due to the increased rate of phosphine dissociation as first

---

[32] N. B. Bespalova, A. V. Nizovtsev, V. V. Afanasiev, E. V. Shutko, *Metathesis Catalysts Stability and Decomposition Pathway,* chapter of *Metathesis Polymerization of Olefins and Polymerization of Alkynes,* Edited by Y. Imamogammalu, Springer Netherlands **1998**.

[33] a) S. Randl, S. Gessler, H. Wakamatsu, S. Blechert, *Synlett* **2001**, *3*, 430; b) S. Imhof,, S. Randl, S. Blechert, *Chem. Commun.* **2001**, *17*, 1692; c) A. H. Hoveyda, D. G. Gillingham, J. J. van Veldhuizen, O. Kataoka, S. B. Garber, J. S. Kingsbury, J. P. A Harrity, *Org. Biomol. Chem.* **2004**, *2*, 8.

[34] M. S. Sandford, J. A. Love, R. H. Grubbs, *J. Am. Chem. Soc.* **2001**, *123*, 6543.

supposed, but rather to the improved reactivity of the 14 electron intermediate bearing an NHC ligand.

The catalytic mechanism in the presence of **HII** type catalysts has not been completely clarified yet. The better performances of the Hoveyda catalysts, that were widespread with high olefin concentrations, were initially attributed to an associative initiation mechanism in which olefins led to rapid catalyst initiation.[35] Actually, the superior catalytic activity was preserved also in more diluted conditions,[36] thus suggesting a more complex situation. In fact, a detailed analysis of the initiation kinetics of Hoveyda catalysts with different alkenes showed that a dissociative and associative interchange mechanism can simultaneously occur. The prevalence of one path with respect to the other is determined by steric and electronic properties of both complex and olefin, thus explaining the largely different catalytic performances, even though the same active species is involved.[37]

Another key issue related to Hoveyda catalysts regards the so called "boomerang" or "release-return" mechanism, that is the re-bonding of the isopropoxystirene to the metal after the catalytic cycle.
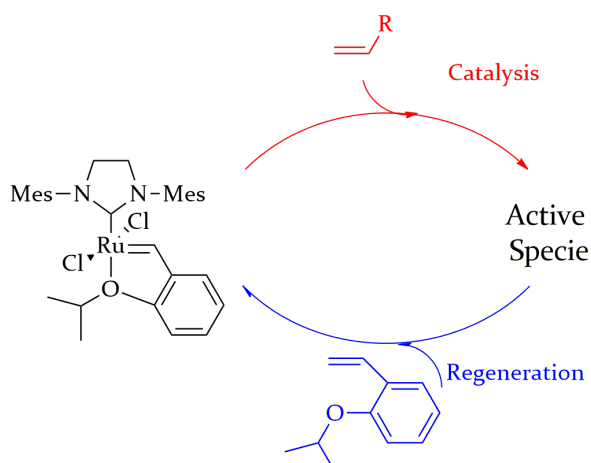
Figure 2.5: The boomerang (or release return) mechanism

This effect, initially proposed by Hoveyda, [38] have had for years no experimental evidence[39] until Fogg demonstrated it in different CM and RCM reactions.[40] The re-bonding of the styrenyl ether moiety has multiple consequences on the catalysis: definitely it implicates a competition between the ligand and the olefin but, more importantly, it protects catalyst and reduces decomposition pathways. This preservation represent another 'piece of the puzzle' in the explanation of the surprising reactivity of **HII** and of its improved performances with respect to **GII**.

2.3 Modifications on the NHC

The introduction of the NHC frameworks in ruthenium complexes has represented such a fundamental progress in ruthenium catalysed olefin metathesis that can perhaps be considered as a sort of point of no return. The possibility to fine modulate the catalytic performances of the resulting complex through the judicious variations of the hindrance and the electronic properties of the carbene ligand has given to synthetic chemists the access to a potentially infinite numbers of new catalysts.

[35] T. Vorfalt, K. J. Wannowius, H. Plenio, *Angew. Chem., Int. Ed.* **2010**, *49*, 5533.
[36] M. Bieniek, A. Michrowska, D. L. Usanov, K Grela, *Chem. Eur. J.* **2008**, *14*, 806–818.
[37] V. Tiel, M. Hendann, K. J. Wannowius, H. Plenio, *J. Am. Chem. Soc.* **2012**, *134*, 1104.
[38] J. S. Kingsbury, J. P A. .Harrity, P. J. Bonitatebus,, A. H. Hoveyda, *J. Am. Chem. Soc.* **1999**, *121*, 791.
[39] T. Vorfalt, K. J. Wannowius, V. Thiel, H. Plenio, *Chem. Eur. J.* **2010**, *16*, 12312.
[40] J. M. Bates, J. A. M. Lummiss, G A. Bailey, D. E. Fogg, *ACS Catal.* **2014**, *4*, 238.

NHCs are synthetically very versatile and inspire lots of chemical modifications. Among them, very relevant are the effects of substitution and configuration of the backbone and the influence of substituents on nitrogen atoms. These variations, for their historical importance and their increasing prominence, will be discussed in the following paragraphs.

2.3.1 Backbone substituents and absolute configuration
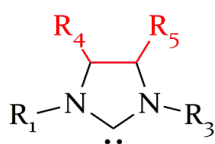
Figure 2.6: Positions 4 and 5 on the NHC

Positions 4 and 5 of the N-heterocyclic carbene rings are often called "backbone" positions (figure 2.6). Even though this portion of the NHC is far from the metal centre, it can strongly influence the stability and the activity of the complex.

Catalyst stability is a key factor in achieving effective ruthenium catalysts. Backbone substituents can enhance this important property by preventing C-H activation, which is a common decomposition pathway for second generation olefin metathesis catalysts (scheme 2.6).[41] This decomposition occurs in few steps: 1) the transfer of a hydrogen atom from one of the N-aryl groups of the NHC ligand to the benzylidene to form the ortho-metalled complex **(I)**; 2) the Ru-hydride species **(II)** is formed and the benzylidene moiety is regenerated; 3) the benzylidene is transferred to the N-aryl group by reaction with the Ru-C bond **(III).** In the presence of free phosphine, **(III)** can give the same C-H insertion on the other N-group to form **(IV)**. **(III)** and **(IV)**, in which ruthenium is η^6 coordinated, were experimentally observed.

Scheme 2.6: C-H activation decomposition pathway.

The just described decomposition mechanism is impeded or at least reduced thanks to the hindrance of backbone groups which simply reduce or prevent the rotation of the N-substituents.

Electronic factors play likewise an important role. An example is the first modification of the NHC ligand which consisted in a saturation of the backbone (figure 2.7).[28] The new 'backbone saturated' catalysts, thanks to an enhanced basic nature of the NHC, were more active with respect to the unsaturated analogues
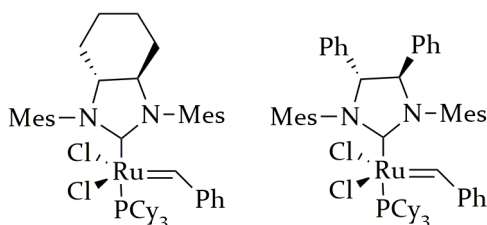
Figure 2.7: Ru-catalysts with saturated backbone

---

[41]S. H. Hong, A. Chlenov, M. W. Day, R. H. Grubbs, Angew. Chem. Int. Ed. **2007**, *48*, 5148.

known until then. This is not trivial, since backbone and active site are spatially distant. Beyond the steric and electronic properties of the backbone substituents, absolute configuration of the backbone stereogenic centers should be also taken in account.[42] The effect of backbone configuration on metathetical efficiency was observed by Grisi *et al.* in 2009.[43] It was observed that two complexes (figure 2.8), which differ just for the relative orientations of methyl groups in positions 4 and 5 (syn: groups on the same part of plane; anti: groups on the opposite part of plane) exhibited a pronouncedly different activity in the RCM of hindered olefins. In fact syn catalyst outperformed both **GII** and **GIItol** (GII with N-tolyl groups) in the RCM to form tetra substituted alkene, while its anti analogue showed a remarkably lower activity, reaching only half of the conversion in the same reaction.
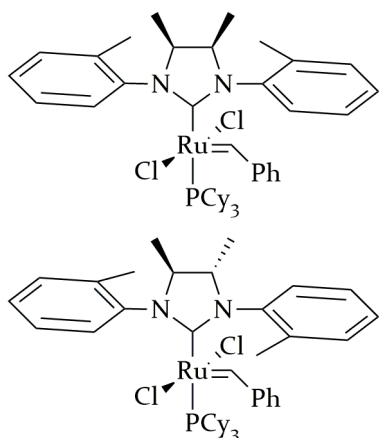
Figure 2.8: Ru-catalysts bearing syn or anti methyls on the NHC backbone
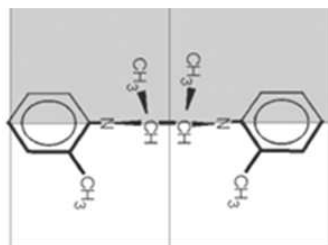
Figure 2.9: Up view of a catalyst with syn methyls on the NHC backbone (taken from ref. 23)

This big reactive gap was explained thanks to experimental and theoretical studies.[44] A syn substituted backbone forces the N-arylic groups to assume a cis conformation. (figure 2.9). The permanence of the two N-substituents on the same part of the NHC creates a larger reactive pocket which is of course more accessible for hindered olefins.

Another very important potential of catalysts with a defined backbone configuration, if enantiopure, is the possibility to be applied in asymmetrical metathesis transformations. This 'backbone ruled' induction of enantioselectivity is the most common in ruthenium NHC catalysis.

An emblematic example was reported by Grubbs in 2002.[45] In that study, several new enantiopure catalysts (an example is depicted in scheme 2.7) were tested for the first time in ARCM obtaining good yields and enantiomeric excesses.

The mechanism of induction of enantioselectivity was rationalised with computational chemistry.[46] The chiral information was transmitted from the anti phenyls through the N-aryl groups. These substituents impose a chiral orientation in the surroundings of the metal centre which can thus select between the two enantiofaces of the alkene. This effect is emphasized if the dimensions of the halide ligands increase. Indeed, by increasing the bulkiness of the halide ligands from chloride to iodide, higher enantioselectivity is experimentally observed.

[42] V. Paradiso, C. Costabile, F. Grisi, Molecules **2016**, *21*, 117.

[43]F. Grisi, A. Mariconda, C. Costabile, V. Bertolasi, P. Longo, *Organometallics* **2009**, *28*, 4988.

[44] a) K. Kuhn, J. B. Bourg, C. K. Chung, S. C. Virgil, R. H. Grubbs, *J. Am. Chem. Soc.* **2009**, *131*, 5313; b)C. Costabile, A. Mariconda, L. Cavallo, P. Longo, V. Bertolasi, F. Ragone, F. Grisi, *Chem. Eur. J.* **2011**, *17*, 8618.

[45]T. J. Seiders, D. W. Ward, D.W.; R. H. Grubbs, *Org. Lett.* **2001**, *3*, 3225.

[46] C. Costabile, L. Cavallo, *J. Am. Chem. Soc.* **2004**, *126*, 9592.
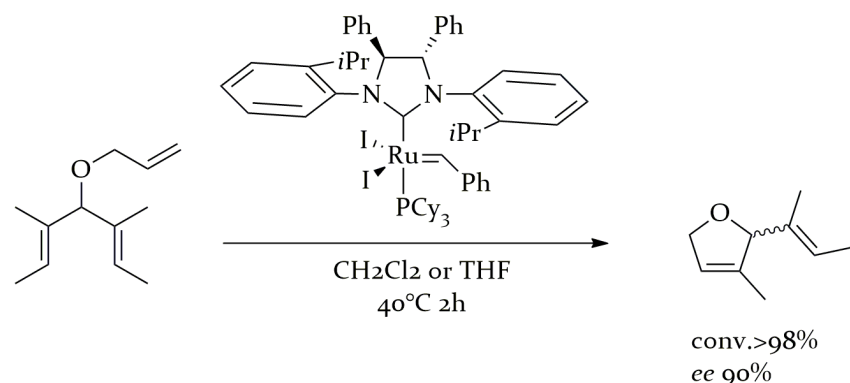
Scheme 2.7: ARCM of a prochiral triene

2.3.2 Groups on nitrogen atoms

The role of steric and electronic properties of the N-substituents on the NHC ligand (figure 2.10) was largely studied, thanks also to facile and consolidate synthetic strategies, which build up NHCs starting from a wide pool of commercially available amines.
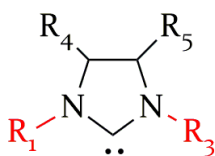
Figure 2.10: Positions 1 and 3 on the NHC

In the 2000's a very large number of Ru catalysts bearing N,N-diaryl substituents and their applications in all metathesis reactions were published. In fact their catalytic qualities, including stability, reactivity towards hindered olefins and enantioselectivity were sounded out in numerous papers and reviews.[47]

In contrast, much less investigated are catalysts bearing N-aryl, N-alkyl NHCs.

The introduction of an N-alkyl group on the NHC framework has always been attractive. As a matter of fact, the insertion of an electron donating group was expecting to enhance the σ-donor properties of the ligand, with positive effects on catalysis. Moreover, the design of catalysts which possessed a diversity of hindrance between the two sides of the NHC, was forecasted to create a moldable reactive pocket with interesting applications.

Actually, potential electronic effects were denied by Nolan, who demonstrated no increase of σ-properties of Pd-C(NHC) and of $Ni(CO)_3$(NHC) bearing N-alkyl groups.[48] At this point, steric features remained to be analysed in depth.

In 2003, Mol published the first Ru complex with an unsymmetrical NHC (u-NHC) bearing a N-adamantyl, N'-mesytil ligand, which unfortunately showed a very poor metathetical activity.[49]

Few years later, Blechert reported new u-NHC Ru catalysts with N-methyl, N'-mesytil groups. The decreased steric bulkiness conferred to this complexes comparable activities

[47] a) *Olefin Metathesis: Theory and Practice,* Edited by K. Grela, John Wiley and Sons, Hoboken **2014;** b)*Handbook of Metathesis, Volume 1: Catalyst development and mechanism,* Edited by R. H. Grubbs and A. G. Wenzel, Wiley-VCH, **2015.**

[48] a) M. S. Viciu, O. Navarro, R. F. Germananeau, R. A. Kelly III, W. Sommer, N. Marion, E. D. Stevens, L. Cavallo, S. P. Nolan, *Organometallics* **2004**, *23,* 1629; b) R. Dorta, E. D. Stevens, N. M. Scott, C. Costabile, L. Cavallo, C. D. Hoff, S. P. Nolan, *J. Am. Chem. Soc.* **2005**, *127,* 2485.

[49] M. B. Dinger., P. Nieczypor, J. Mol, *Organometallics* **2003**, *22,* 5291.

with respect to the symmetric akins. Moreover, the Z/E ratio of the olefins products, whose improvement is currently one of the aims of olefin metathesis, was remarkably raised.[50]

Verpoort reported several u-NHC complexes bearing N-mesityl and various alkyl groups. These compounds showed a pronounced reactivity only in polymerisation metathesis.[51]

A further advance was achieved by Buchmeiser, who used new u-NHC Ru catalysts for the synthesis via ROMP of alternating copolymers, impossible to obtain with symmetrical NHC complexes.[52]

More recently, an important progress was published by Grubbs, who reached a remarkable Z-selectivity in CM using u-NHC cyclometallated ruthenium complex.[53]

u-NHC ligands were also the subject of a 2014 study of Grela, who synthesized several new complexes with indenylidene ligands. These catalysts were very robust and metathetically active also in air and in the presence of unpurified solvents.[54]

Almost simultaneously, Mauduit published a small library of new catalysts with promising reactivity. These catalysts had an indenylidene moiety or other chelated benzylidene ligands.[55] All these complexes, which represent the breakthroughs of u-NHC Ru catalysts are reported in figure 2.11.

| Mol (2003) | Blechert (2006) | Verpoort (2006) | Buchmeiser (2009) |

| Grubbs (2011) | Grela (2014) | Mauduit (2014) |
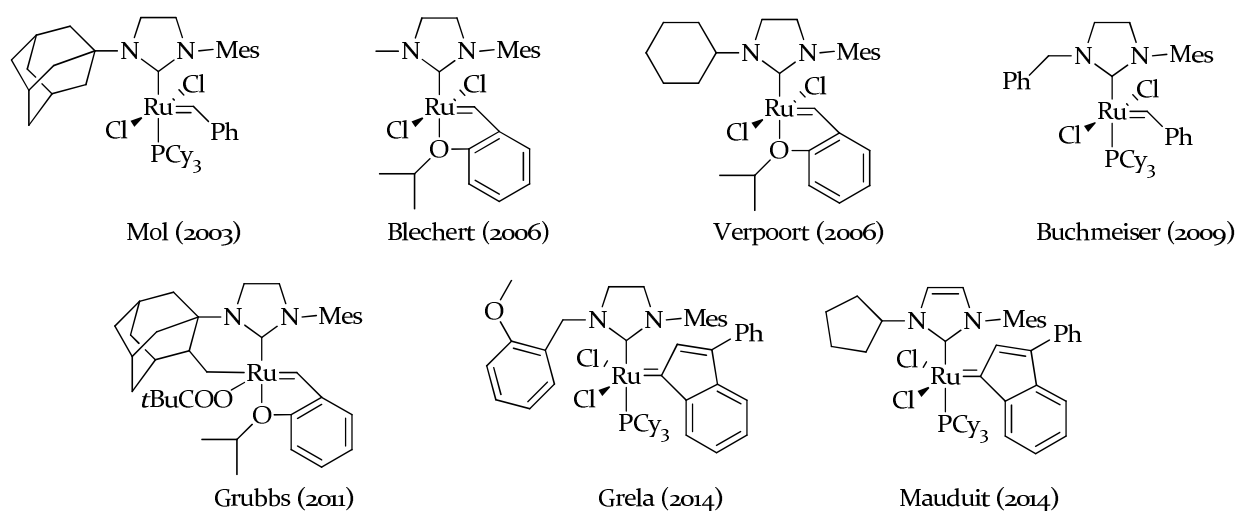
Figure. 2.11: u-NHC ruthenium complexes

2.3.3 Catalysts with N-alkyl, N'-aryl C₁-symmetric NHC ligands

[50] K. Vehlow, S. Maechling, S. Blechert, Organometallics **2006**, *25*, 25

[51] a) N. Ledoux, A. Linden,, B. Allaert, H. V. Mierde, F. Verpoort, *Adv. Synth. Catal.* **2007**, *349*, 1692; b) N. Ledoux, B. Allaert,, S. Pattyn, H. V. Mierde, C. Vercaemst, F. Verpoort, *Chem. Eur. J.* **2006**, *12*, 4654; c)N. Ledoux,B. Allaert, A. Linden, P. van der Voort, F. Verpoort, *Organometallics* **2007**, *26*, 1052.

[52] M. Lichtenheldt, D. Wang, K. Vehlow, I. Reinhardt, C. Kuhnel, U. Decker, S.Blechert, M.R. Buchmeiser, *Chem. Eur. J.***2009**, *15*, 9541.

[53] K. Endo, R. H. Grubbs, *J. Am. Chem. Soc.* **2011**, *133*, 8525.

[54] O. Ablialimov, M. Kędziorek, M. Malinska, K. Wozniak, K. Grela, *Organometallics* **2014**, *33*, 2160.

[55] M. Rouen, E. Borré, L. Falivene, L. Toupet, M. Berthod, L. Cavallo, H. Olivier-Bourbigoud, M. Mauduit, *Dalton Trans.* **2014**, *43*, 7044.
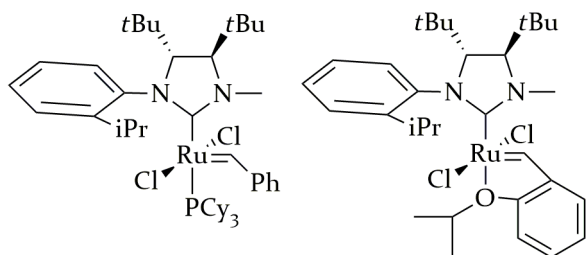
Figure 2.12: C*1*-symmetric NHC catalysts with N-methyl, N'-isopropylphenyl groups (Grubbs-type on left, Hoveyda-type on right)

The combination of chiral centres on the backbone and N-alkyl, N'-aryl substituents was totally unexplored until the innovative work of Collins.

In 2007 he published the synthesis of C*1*-symmetric NHC ruthenium catalysts with two anti tert-butyls on backbone and N-methyl, N'-isopropylphenyl groups (figure 2.12).[56]

This enantiopure catalyst was tested in several model ARCM reactions. Interestingly, enantioselectivity was eroded if the chloride ligands were replaced with more encumbered iodide. This was in contrast with the results obtained with symmetric analoguesand suggested a different mechanism of induction of the enantioselectivity.

It should be mentioned that the unsymmetrical substitution of the ligand makes two rotational isomers possible (figure 2.13): the syn isomer (N-alkyl on carbene) and the anti analogue (N'-aryl on carbene). For the Grubbs-type complex (figure 2.12, left), X-Ray analysis and NOE experiments revealed only the presence of the syn isomer. On the contrary, for the Hoveyda-type catalyst, both isomers were formed. Of course, the potential conversion between the two isomers during the catalytic cycle is a hurdle in the clarification of the mechanism of control of enantioselectivity.

syn isomer   anti isomer
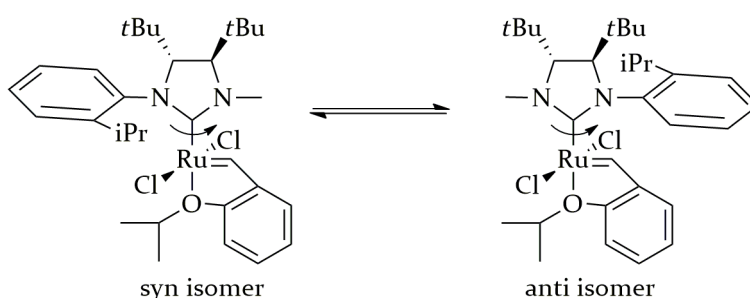
Figure 2.13: Rotation on the NHC-Ru bond

Generally talking, the replacement of an N-aryl group with an N-alkyl substituent determines a reduction in the stability of the corresponding complex. This is due to the inability of the alkyl group to make π-π interactions with the Ru-carbon double bond, which were demonstrated to play an important role in complex stability.[57] This is particularly true for the mentioned Collins' complexes, which unfortunately suffer of thermal sensitivity and instability in solution.

In order to improve robustness of this class of catalysts, new complexes with modified N-substituents were published
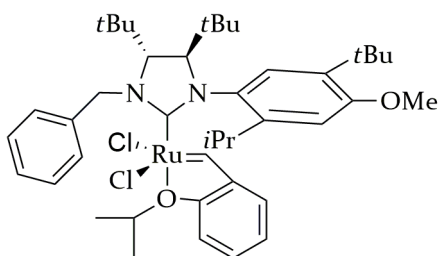
Figure 2.14: C*1*-symmetric NHC catalysts with modified nitrogens' groups

[56]a) P. Fournier, S. K. Collins, *Organometallics* **2007**, *26*, 2945; b) P. Fournier, J. Savoie, B. Stenne, M. Bédard, A. Grandbois, S. K. Collins, *Chem. Eur. J.* **2008**, *14*, 8690.

[57] M. Süßner , H. Plenio *Chem. Commun.*, **2005**, *43*, 5417.

by the same group (figure 2.14).[58] The enhanced stability led to the application in a more challenging reaction, such as the ARCM for the formation of tetrasubstituted olefins.

2.4 Aim of this work

Except for the just mentioned publications, there is no investigation about Ru-catalysts with C_1-symmetrical NHC ligands. As Collins demonstrated, the combination of a backbone definite configuration and appropriate nitrogens' group could led to the synthesis of innovative and promising catalysts.

Our interest lies in the study of new C_1-symmetrical NHC ruthenium catalysts, both Grubbs-type and Hoveyda-type, with syn or anti phenyls on the backbone and various aryl and alkyl groups on the nitrogens (figure 2.15).
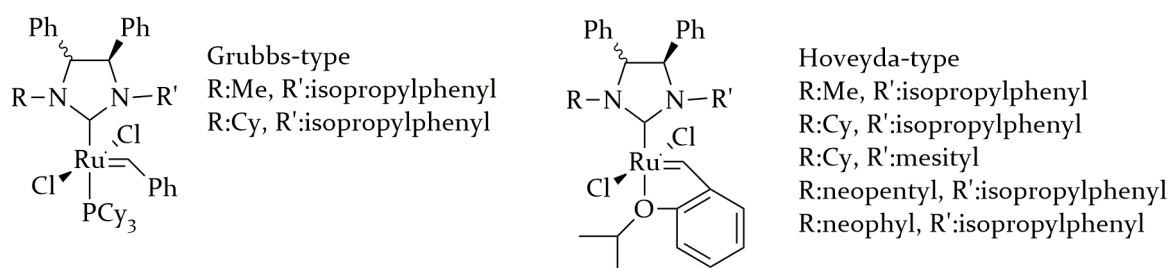
Figure 2.15: Catalysts subject matter of this doctoral study

The choice of phenyls on the backbone is due to the large commercial availability of the diphenylethylenediamine as starting material with the aim to simplify the synthesis of the ligand and lower its cost. Both syn and anti configurations are investigated.

The chosen alkyl groups have a different grade of hindrance and branching and involve methyl, cyclohexyl, neopentyl and neophyl. Aryl groups selected were isopropylphenyl and mesityl.

Our scopes include:

-the optimisation of the synthesis to few, easy,efficient, non-hazardous steps;

-the structural characterisation with NMR and X-Ray analysis;

-the evaluation of the electronic and steric properties, using both experimental (IR and Cyclic voltammetry) and theoretical studies;

-the test of the catalytic behaviours in several standard metathesis transformations as well as in more recent and attractive reactions.

Our work has the purpose to explore the correlation between chemical structure and catalytic performances, in order to lay the groundwork for the synthesis of even more efficient uNHC- catalysts.

The involvement of several experimental techniques has the aim to investigate the issue 'from different points of view' with a sort of multidisciplinary approach. This is typical of organometallics, which can thus be considered as one of the more versatile branches of chemistry.

---

[58]B. Stenne, J. Timperio, J. Savoie, T. Dudding, S. K. Collins, *Org. Lett.* **2010**, *12*, 2032.

Chapter 3

New *u*-NHC Ru catalysts: synthesis, characterisation and investigation of steric and electronic properties

The application of unsymmetrical, backbone substituted NHCs as ruthenium ancillary ligands in olefin metathesis is very promising. Starting from the pioneristic work of Collins, discussed in the previous chapter, several issues emerged:

- Which is the role of backbone substituents?
  Tertbutyl groups on the NHC backbone of Collins' complexes have undoubtedly a positive influence on the enantioselectivity observed in ARCM reactions but, on the other hand, they are maybe responsible of the scarce stability detected for this class of catalysts. Moreover, the choice of backbone groups that allows the use of a commercial and less expensive amine as a starting material is highly desirable.

- Which is the impact of configuration?
  An important question lies in the role of configuration. In fact the potential influence of syn configuration on reactivity was so far not taken in consideration for u-NHC complexes.

- What is the effect of N-alkyl groups?
  Methyl is the smallest alkyl group. A more encumbered or ramified substituent can potentially modulate the reactive pocket with a dramatic effect on catalysis.

Inspired by all these questions, we synthesized four new *u*-NHC ligands with syn or anti phenyls on backbone, methyl or cyclohexyl as the alkyl group and isopropyl phenyl as the aryl group. By the reaction of these ligands with commercial **GI** or **HI**, new ruthenium complexes **1-8** were prepared (figure 3.1).
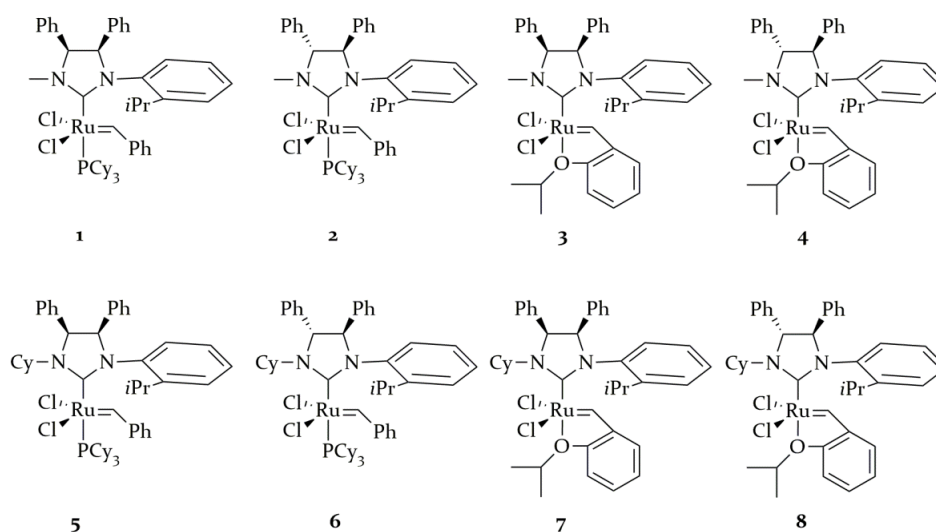
Figure 3.1: Catalysts **1-8**

Their catalytic activity was evaluated in several standard metathesis reactions and, surprisingly, **5** and **7** which are the catalysts bearing the syn version of the N-cyclohexyl and N'-isopropylphenyl ligand, showed an impressively different catalytic behaviour with respect to their anti analogues, **6** and **8**. This pronounced backbone effect was rationalised synthesizing new rhodium cyclooctadiene and rhodium dicarbonyl complexes and characterising them using NMR and IR spectroscopy, X-Ray analysis and computational chemistry.[59]

3.1 Synthesis of 1-8

Synthesis of complexes **1-8** are depicted in schemes 3.1 and 3.2.

Scheme 3.1: Synthesis of **1-4**

---
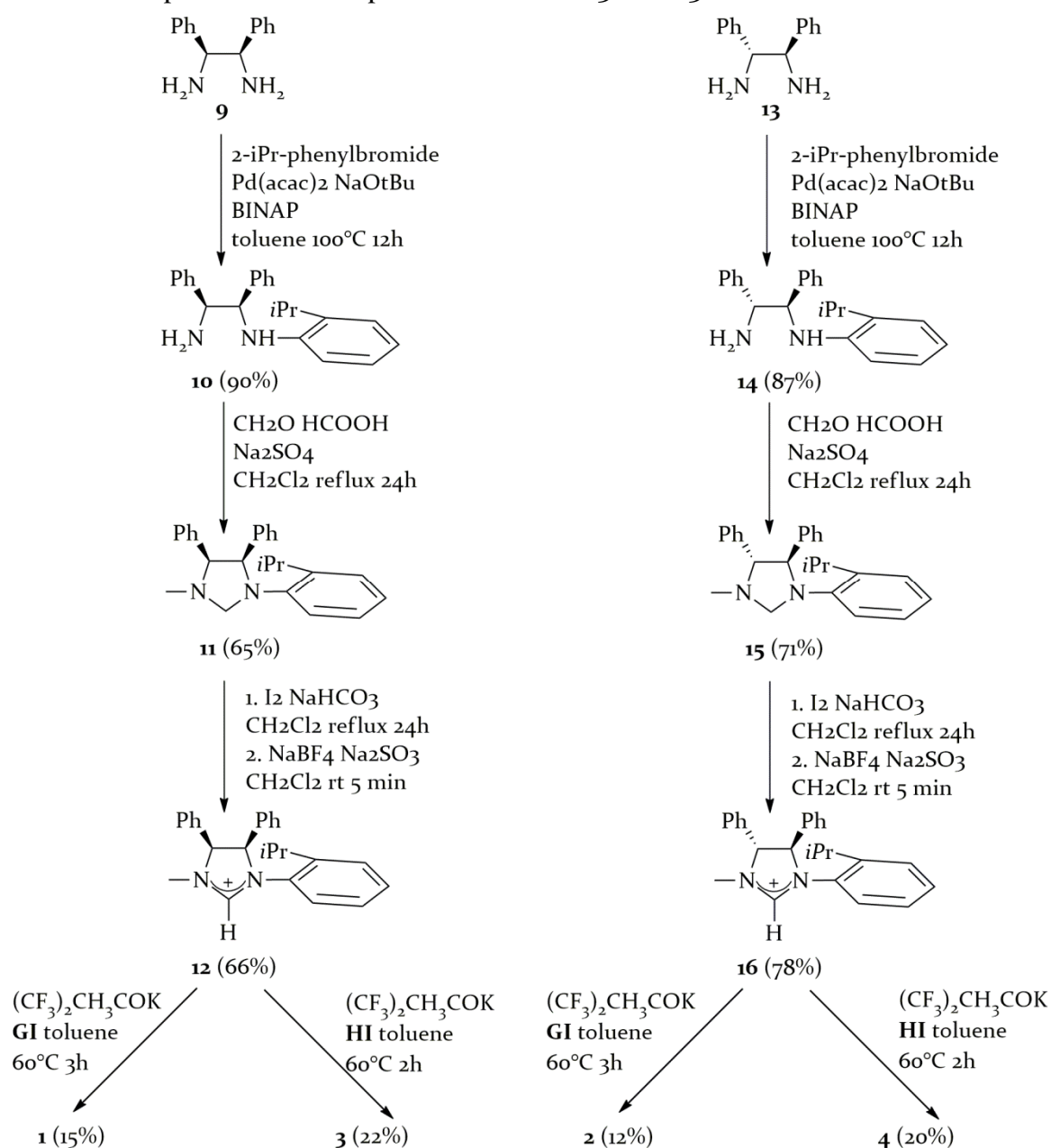
[59] Experimental data discussed in this chapter were published in: a)V. Paradiso, V. Bertolasi, F. Grisi, *Organometallics* **2014**, *33*, 5932; b)V. Paradiso, V. Bertolasi, C. Costabile, F. Grisi, *Dalton Trans.* **2016**, *45*, 561.

29
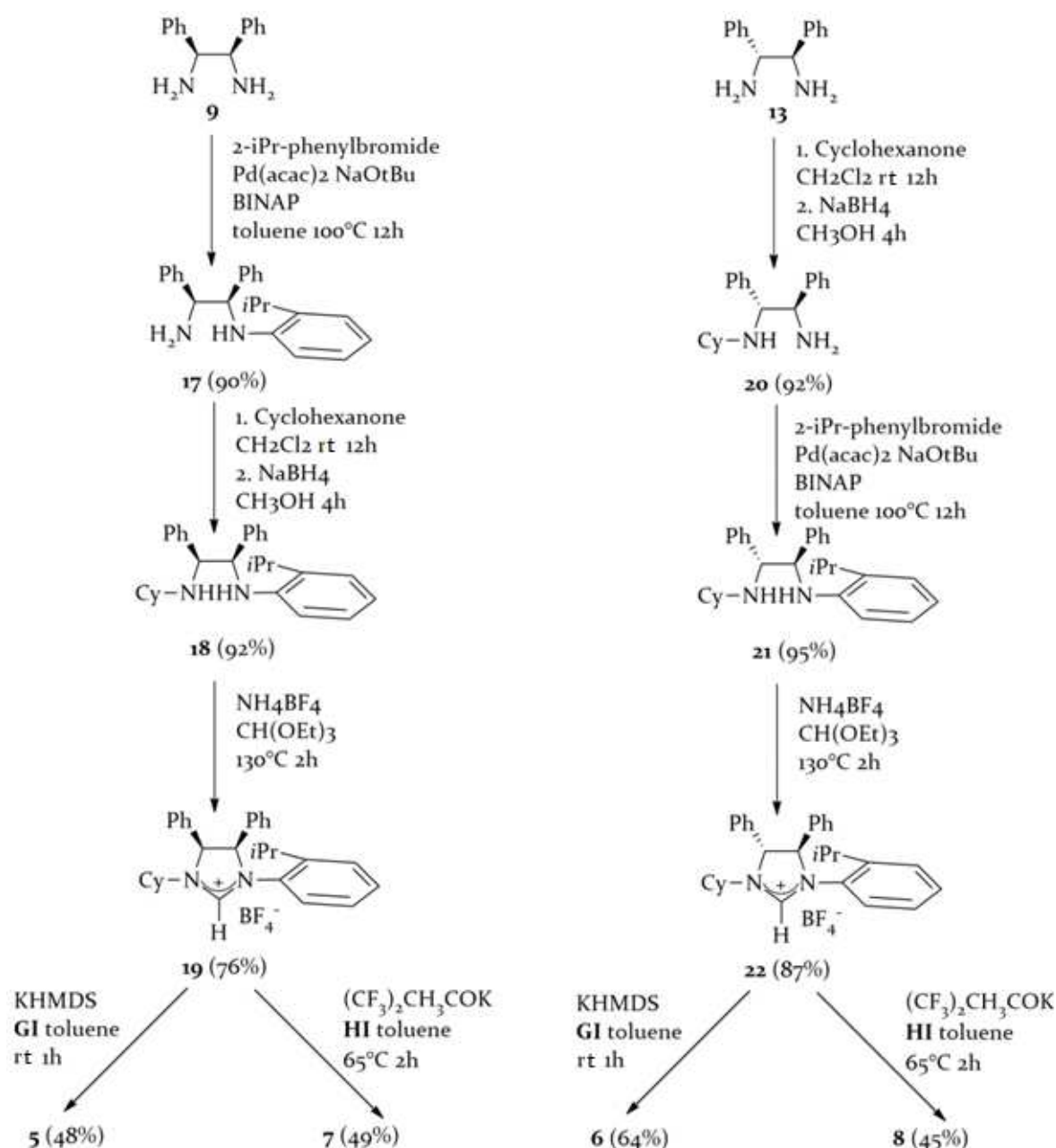
Scheme 3.2: Synthesis of **5-8**

Complexes **1-4** differ from the Collins' catalysts just for the configuration and the nature of groups of the NHC backbone. Synthesis of ligand precursors **12** and **16** were constituted by three easy synthetic steps with moderate-good yields (65-90%). The first step was a Pd-catalysed Buchwald-Hartwig arylation of diamines, followed by a reductive amination-condensation with formaldehyde and a deprotonation with sodium hydrogen carbonate. Carbenes were generated in situ by reaction with $(CF_3)_2CH_3COK$ and then reacted with with **GI** or **HI**. Unfortunately, **1-4** were synthesized with poor yields (12-22%). Any attempt to optimise reaction conditions was unsuccessful.

Complexes **5-8** differed from **1-4** for the presence of an N-cyclohexyl group in place of N-methyl. Cyclohexyl was chosen since its hindrance is comparable with isopropyl with the benefit of an easier reductive amination step.

Synthesis of **19** was similar to that of the analogues with the N-methyl group.

Synthesis of **22** was slightly different since it involved firstly a reductive amination and then the arylation step. This represented an advantage in the synthetic strategy because an excess of diamine, which is usually used to avoid diarylated product, was no more necessary. An analogue approach for **19** was not possible, since the syn monoalkylated product was not obtained selectively.

It should be underlined that **2**, **4**, **6** and **8**, obtained from (*1R, 2R*)-1,2-diphenylethylendiamine, were enantiopure while **1**, **3**, **5** and **7**, which were synthesized starting from (*meso*)-1,2-diphenylethylendiamine, were obtained under racemic form. The choice to develop the synthesis of enantiopure ligands was directed to investigate the potential enantioselectivity of the corresponding complexes. All data related to asymmetric metathesis catalysis will be separately discussed in chapter 6.

The first significant improvement of **1-8** with respect to Collins' complexes was the enhanced stability. In fact, the presence of phenyls instead of t-butyls on the backbone conferred to these new catalysts a very good solid state stability (at least 5-6 months) and a much higher solution stability (at least 1 week).

3.2 NMR and X-Ray characterisation

All complexes were analysed using 1D and 2D NMR spectroscopy. GII-type complexes **1** and **2** were obtained as a mixture of syn:anti rotational isomers (syn: N-alkyl on the same side of the carbene)(figure 3.2). 2D-EXSY experiments, at various mixing times, did not reveal any interconversion between isomers. Differently, phosphine-free complexes **3** and **4** were obtained as a single anti rotamer.

Spectroscopic NMR analysis of N-cyclohexyl complexes **5-8** revealed an analogue situation. In fact, phosphine-containing **5** and **6** were obtained as syn and anti isomers while for HII-type compounds **7** and **8** only the anti isomer was

Figure 3.2: syn and anti isomers of **1** and **2**

present. The enhanced stability of **5** and **6** with respect to the N-methyl analogues allowed variable temperature (VT) NMR investigation and no interconversion between isomers was observed up to 70°C. NMR data of rotational isomers of **1**, **2**, **5** and **6** at room temperature are summarised in table 3.1.

Table 3.1: NMR data of syn and anti isomers of **1**, **2**, **5** and **6**

complex	chemical shifts (δ) Ru=CH	syn:anti
1	20.64 (syn); 19.63 (anti)	0.4:1
2	20.73 (syn); 19.67 (anti)	0.5:1
5	21.07 (syn); 19.74 (anti)	0.3:1
6	21.04 (syn); 19.88 (anti)	0.8:1
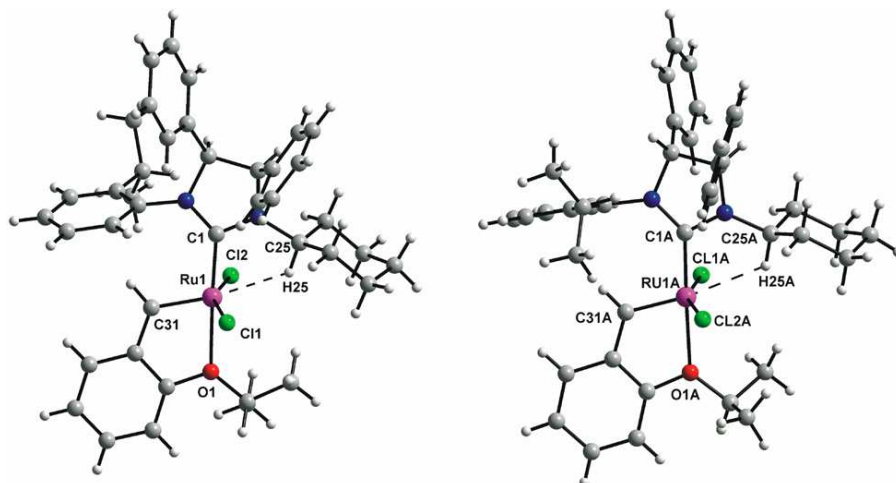
Figure 3.3: X-Ray structures of **7** (left) and **8** (right)

Good quality crystals of **7** and **8** were obtained (figure 3.3) from a hexane/diethyl ether saturated solution. X-Ray analysis revealed a short distance between the metal and the N-C(Cy)-H hydrogen (Ru1---H25 for **7** and Ru1A---H25A for **8**) that suggested the presence of anagostic interactions. Such interactions were confirmed by the NMR analysis of the complexes. In fact, it was observed the downfield shift of N-C(Cy)-H in comparison to those of their corresponding ligand precursors (figure 3.4) and a slightly lower value of $^1J(C25,H25)$ and $^1J(C25A,H25A)$ coupling constants (130 Hz), This proton has a characteristic broad triplet signal.
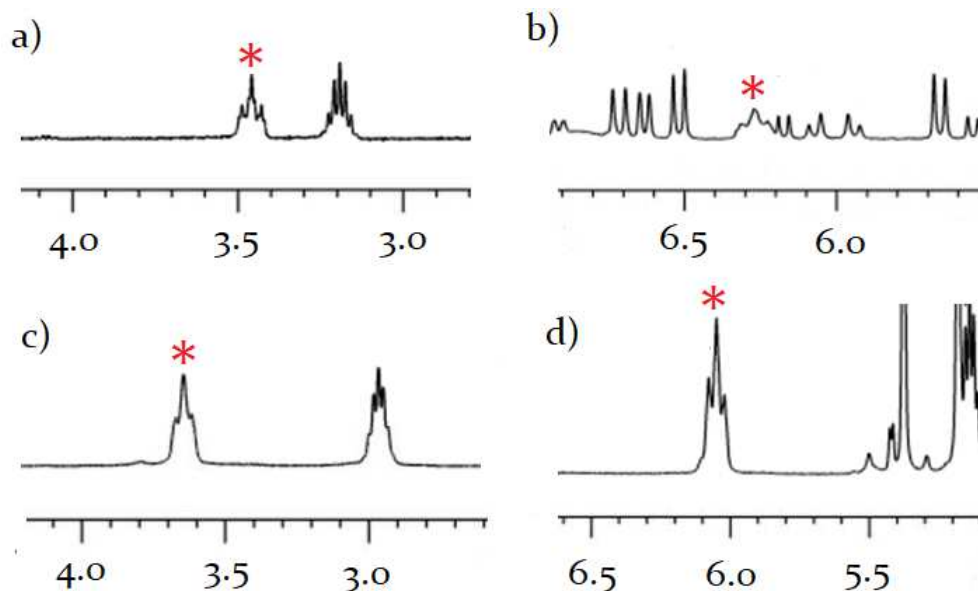
Figure 3.4: ^{1}H NMR signals of N-C(Cy)-H (indicated by the red star *) in: a) ligand precursor **19**, b) complex **7**, c) ligand precursor **22**, d) complex **8**

3.3 RCM of malonate and tosyl derivatives

The catalytic behaviours of **1-8** were investigated in the RCM of malonate and tosyl derivatives **23-28**. Each reaction was performed in an NMR tube under standard conditions (30°C in CD_2Cl_2 for phosphine catalysts, 60°C in C_6D_6 for phosphine free complexes) and conversions were monitored over time. For a better evaluation, the kinetic profiles of appropriate commercial catalysts (**GIItol** for Grubbs-type catalysts and **HIItol** for Hoveyda-type complexes) were also plotted.

Figure 3.5: RCM of **23** with: a)GII-type catalysts **1-2**, **5-6** and **GIItol**; b)HII-type catalysts **3-4**, **7-8** and **HIItol**

In the RCM of **23**, anti GII-type catalysts **2** and **6** surpassed their syn isomers **1** and **5**, as well as commercial **GIItol** (figure 3.5 a). This backbone configuration effect was more pronounced for N-cyclohexyl complexes. In the same reaction with phosphine-free analogues (figure 3.5 b) the same trend was observed, even if the gap between N-methyl catalysts was significantly reduced. Higher initiation temperatures perhaps contribute to render reactivity differences less assessable.

The RCM of **24** with phosphine-containing catalysts **1-2**, **5-6** (figure 3.6 a) was overall slower, if compared with the RCM of **23** catalysed by the same complexes. This finding is unusual, since the RCM of tosyl derivatives is generally easier to perform.[60] This surprisingly slower reaction highlighted more clearly the greater efficiency of anti catalysts, in fact the gap with the syn analogues appeared more pronounced. N-cyclohexyl complexes **5** and **6** showed the highest reactivity difference, confirming the noticeable backbone effect already observed also in the RCM of **23**.

In the ring closure of **24**, all GII-type catalysts were surpassed by **GIItol** that, albeit showing a slower initiation with respect to **2** and **6**, was the only able to reach full conversion.

---

[60]a) L. Vieille-Petit, H. Clavier, A. Linden,S. Blumentritt, S. P. Nolan, R. Dorta, *Organometallics* **2010**, *29*, 775; b) A. Perfetto, C. Costabile, P. Longo, F. Grisi, *Organometallics* **2014**, *33*, 2747.

The same reaction with Hoveyda-type complexes **3-4** and **7-8** (figure 3.6 b) was less informative, since **3-4**, and **8** had a very similar reactivity. The only behaviour appreciably different is showed by **HIItol**, that was incredibly efficient in this reaction, even at 0.1% mol, and by **7**, which confirmed itself as the less efficient phosphine-free catalysts.

Figure 3.6: RCM of **24** with: a)GII-type catalysts **1-2**, **5-6** and **GIItol**; b)HII-type catalysts **3-4**, **7-8** and **HIItol**
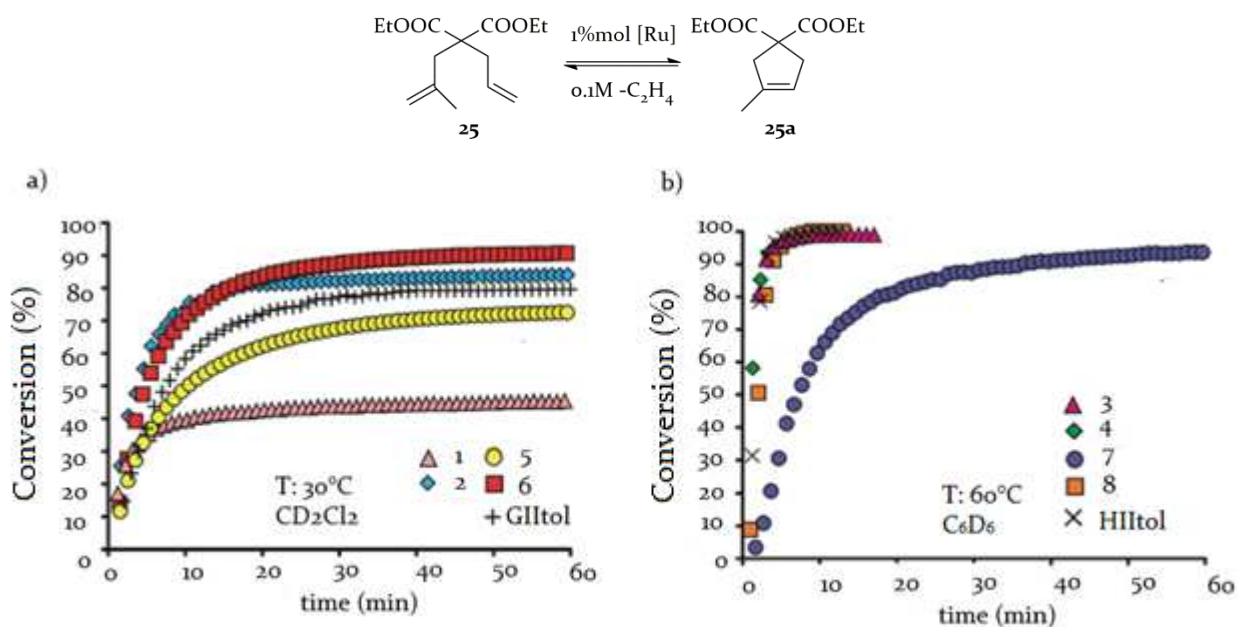
Figure 3.7: RCM of **25** with: a)GII-type catalysts **1-2**, **5-6** and **GIItol**; b)HII-type catalysts **3-4**, **7-8** and **HIItol**

The investigation of the ring-closing activity was extended to more hindered olefins **25** and **26**.

In the RCM of **25** (figure 3.7 a), Grubbs-type catalysts **2** and **6** corroborated their efficiency and outperformed **GIItol**. As in the RCM of less encumbered alkenes, **1** and **5** were the less efficient but, differently from the ring closing of **23** and **24**, N-cyclohexyl catalyst **5**

performed better than its N-methyl counterpart **1**. This was probably due to the lower stability of **1**, which had a very fast initiation, but a short solution lifetime.

In the ring closure of **25** catalysed by **3-4** and **7-8** (figure 3.7 b), all the complexes showed very similar kinetic plots, except to **7**, which was again the less performing.
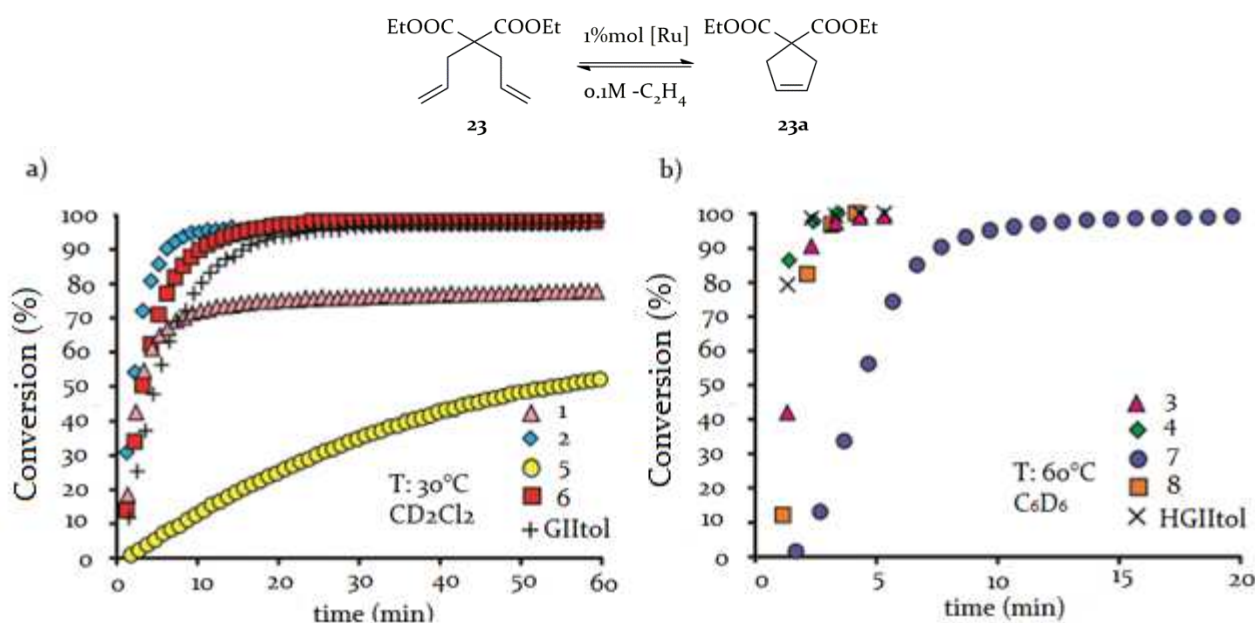

Figure 3.8: RCM of **26** with: a)GII-type catalysts **1-2**, **5-6** and **GIItol**; b)HII-type catalysts **3-4**, **7-8** and **HIItol**

The RCM of **26** was performed by **1-2** and **5-6** (figure 3.8 a) with less difficulty with respect to the malonate derivative with a comparable hindrance, coherently with the overall literature trend. Moreover, these two reactions shared the same catalysts' reactivity order. Indeed, anti **2** and **6** were the more active and, between the syn catalysts, N-cyclohexyl **5** performed better than its N-methyl analogue **1**, which had a lifetime of just ten minutes. **GIItol** reached full conversion albeit initiating slower than **2** and **6**.

In the ring closure of **26** carried out in the presence of Hoveyda catalysts **3-4** and **7-8** (figure 3.8 b), anti catalysts **4** and **8** slightly surpassed syn complex **3**. The fact that the backbone effect was relevant for N-methyl catalysts only if they were in the GII-type form, confirmed that for these complexes stability is a crucial factor. In fact, for the Hoveyda N-methyl **3** and **4**, which are more robust thanks to the presence of a chelating benzylidene ligand, this gap was absent or strongly reduced.

As for the RCM of **24**, in the ring closure of **26** HIItol was so efficient to show a kinetic plot comparable with the other catalysts at a catalyst loading ten times lower.

The ring closure of hindered olefins to obtain tetrasubstituted alkenes is one of the successes of olefin metathesis that often offers a solution to a thorny organic chemistry issue.

The RCM of hindered substrates **27** and **28** is a difficult metathesis transformation and is usually useful to more thoroughly examine and rationalise catalytic performances.

In the ring closing of **27** (figure 3.9 a), **GIItol** was the most performing catalyst. This was not surprising, since its competence in the RCM of hindered olefin is very well known.[61] Moreover, it should be noticed that **GIItol,** and more in general catalysts particularly competent in the RCM of **27**, are not exceptionally efficient in the ring closure of less encumbered alkenes.
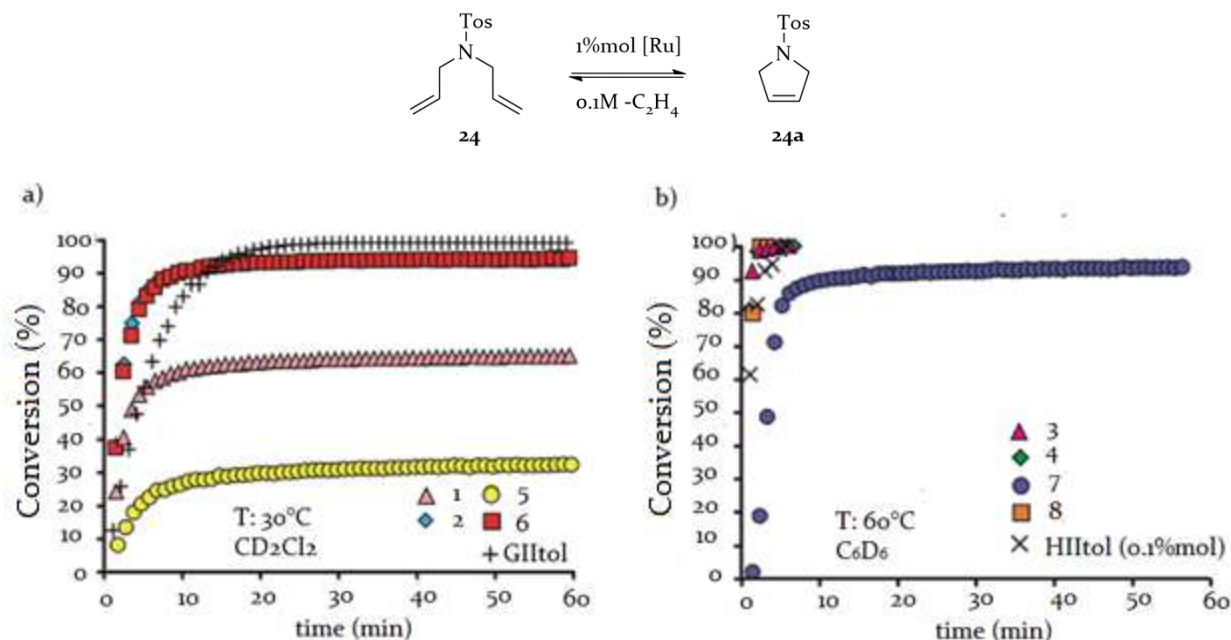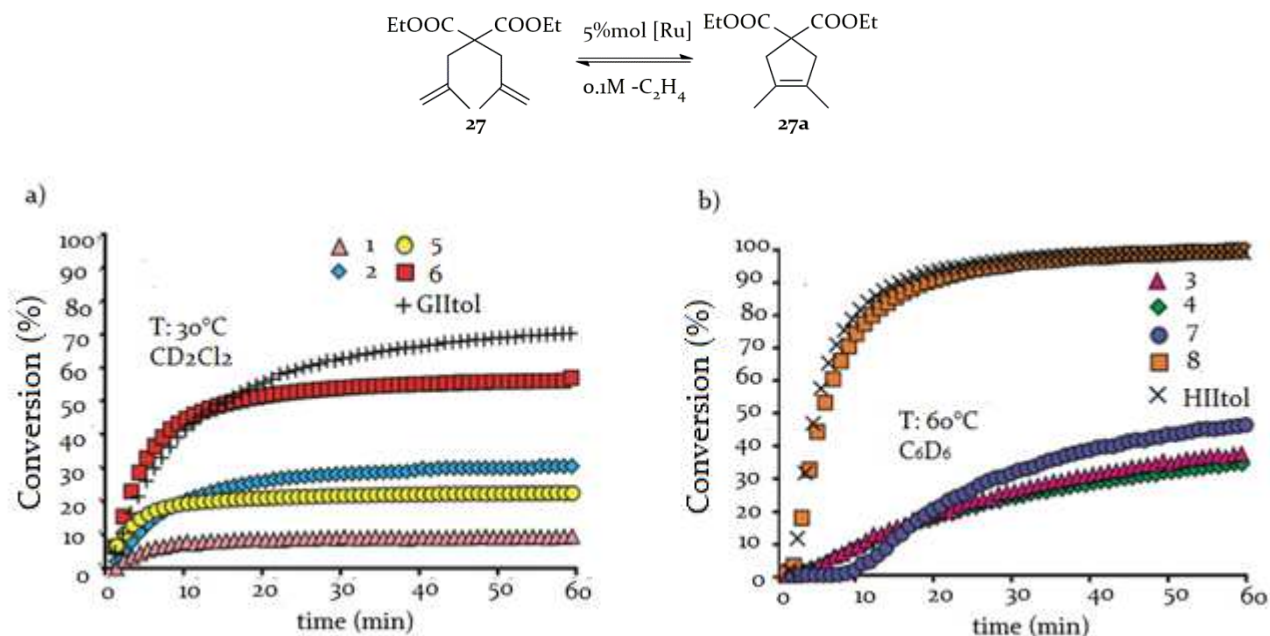

Figure 3.9: RCM of **27** with: a)GII-type catalysts **1-2**, **5-6** and **GIItol**; b)HII-type catalysts **3-4**, **7-8** and **HIItol**

Anti catalyst **6** significantly overcame its syn counterpart and all other u-NHC complexes. Also anti N-methyl **2** performed better than the syn analogue **1**, but the difference between their kinetic plots were less marked. Perhaps, the similar behaviours of **3** and **4** can be due to stability issues that, in such a difficult transformation, affect the reactivity of both catalysts, independently from the backbone configuration.

In the same reaction catalysed by phosphine-free complexes, the difference between reactivity of N-methyl and N-cyclohexyl complexes was accentuated (figure 3.9 b). Indeed anti N-cyclohexyl **8** had a reactivity comparable with HIItol and importantly surpassed its syn isomer and also N-methyl **3** and **4**. Syn N-cyclohexyl **7**, despite of a pronounced induction time, performed better than **3** and **4**, which showed a very similar kinetic plot. Conversions slightly increasing over time suggested for **7**, **3** and **4** a poor efficiency not due to complexes' stabilities but rather to the difficulty of the reaction.

The catalytic behaviours of phosphine containing catalysts **1-2** and **5-6** in the RCM of **28** were similar to those observed in the ring closure of malonate analogue **27** (figure 3.10 a). Comparing the two reactions, it was noticeable that all catalysts were more performing in the ring-closure of the tosyl derivative.

In the ring closing of **28** with phosphine-free catalysts (figure 3.10 b), a very great efficiency of **HIItol**, at just 0.1%mol of loading, could be observed. Anti N-cyclohexyl **8** was again the

---

[61] I. C. Stewart, T. Ung, A. A. Pletnev, J. M. Berlin, R. H. Grubbs, Y. Schrodi, *Org. Lett.* **2007**, *9*, 1589.

more efficient in the pool of u-NHC complexes. **3**, **4** and **7** reached comparable conversions, even if **7** displayed a slower initiation rate.

In conclusion, the RCM of malonate and tosyl derivatives was very informative in the investigation of the potentialities of these new catalysts. **1-8** had an overall appreciable efficiency, which led their application valuable also in difficult ring closures.

For GII-type complexes, an intriguing backbone effect was observed, in fact anti catalysts were more competent than their syn isomers. This was quite unexpected, since for ruthenium catalysts with symmetrical NHC an opposite trend was observed.[39]

Also the role of the N-alkyl group was well highlighted, indeed cyclohexyl substituent conferred to catalysts an overall increased efficiency. This was more evident for catalysts with syn backbone.
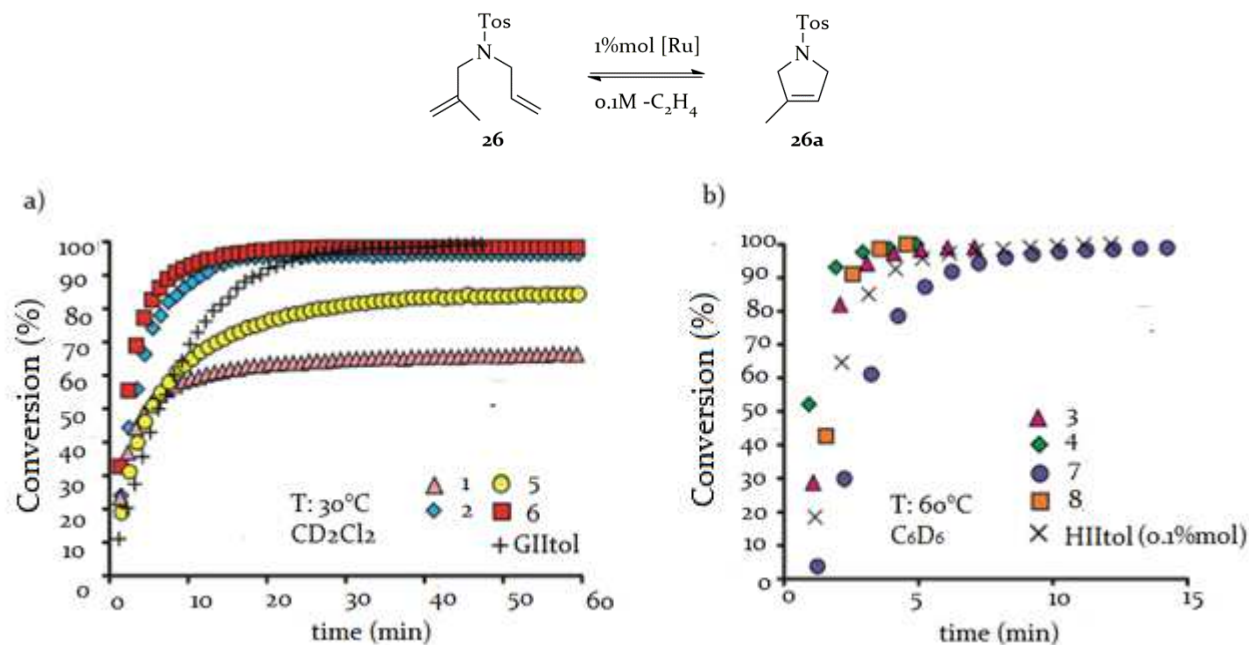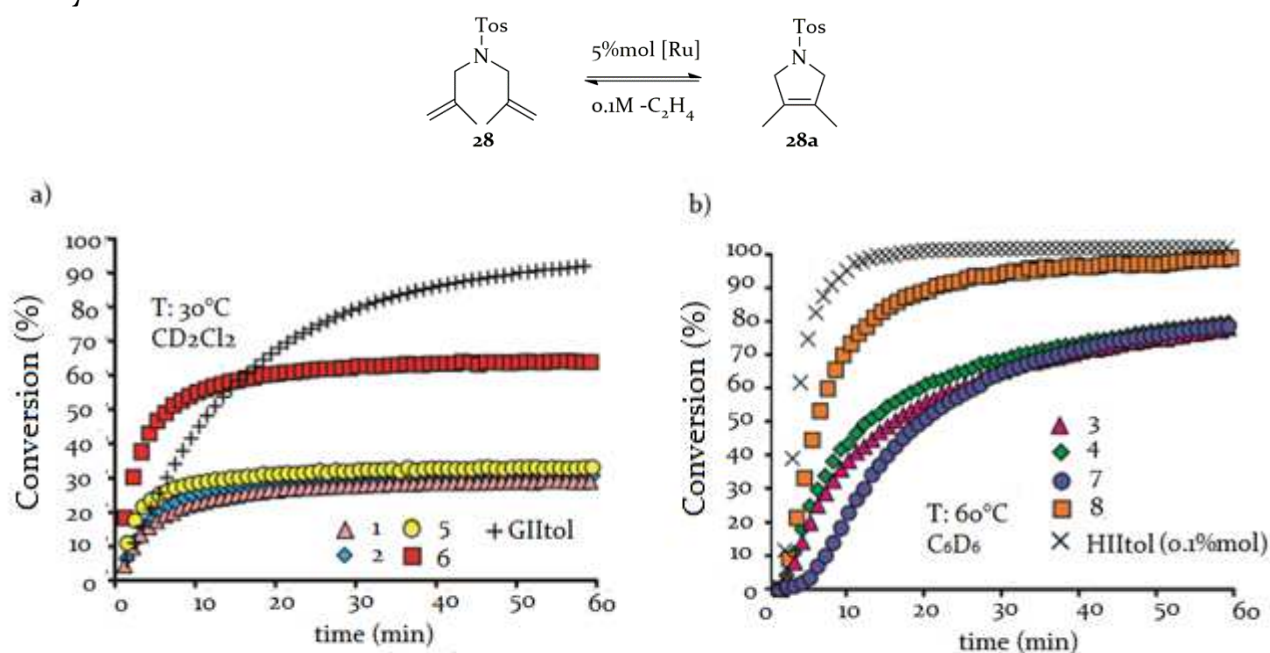

Figure 3.10: RCM of **28** with: a)GII-type catalysts **1-2**, **5-6** and **GIItol**; b)HII-type catalysts **3-4**, **7-8** and **HIItol**

For HII-type complexes, differences in catalytic performances were often less appreciable. Nevertheless, the backbone effect was visible for N-cyclohexyl catalyst while for N-methyl analogues differences in performances were generally scarce. This could suggest that for N-methyl complexes the backbone influence seen in phosphine containing catalysts has probably its origin in stability issues.

Among all catalysts, **5** showed the more intriguing behaviour. Indeed it differs from **6** just for the absolute configuration but gave dramatically lower performances.

Very emblematic was the ring closure of **23**, in which **5** was scarcely efficient. This unexpected behaviour encouraged the study of the energy profile of the reaction using molecular modelling.

In figure 3.11 are depicted free energy profiles of the RCM of a model of **23** (-COOEt groups were replaced by CH_3 groups) (blue line) and of nonproductive events for the same reaction (red line). The rate determining step was **P2** (figure 3.12, left) that was the first CM between substrate and alkylidene. The latter was orientated under the aryl group, coherently with

literature data.[62] Its $\Delta G^{\ddagger}$ was esteemed to be 15.2 kcal/mol, notably higher if compared with those of similar symmetrically substituted NHC systems already published.[44b]

NP2 (figure 3.12, right), the transition state in nonproductive events pathway, was calculated to be 14.1 kcal/mol. So, there was a gap of 1.1 kcal/mol with **P2**, that suggested that nonproductive events would be favourable. This is not unusual in u-NHC ruthenium metathesis,[63] and was perhaps the reason of the peculiar reactivity of **5**.
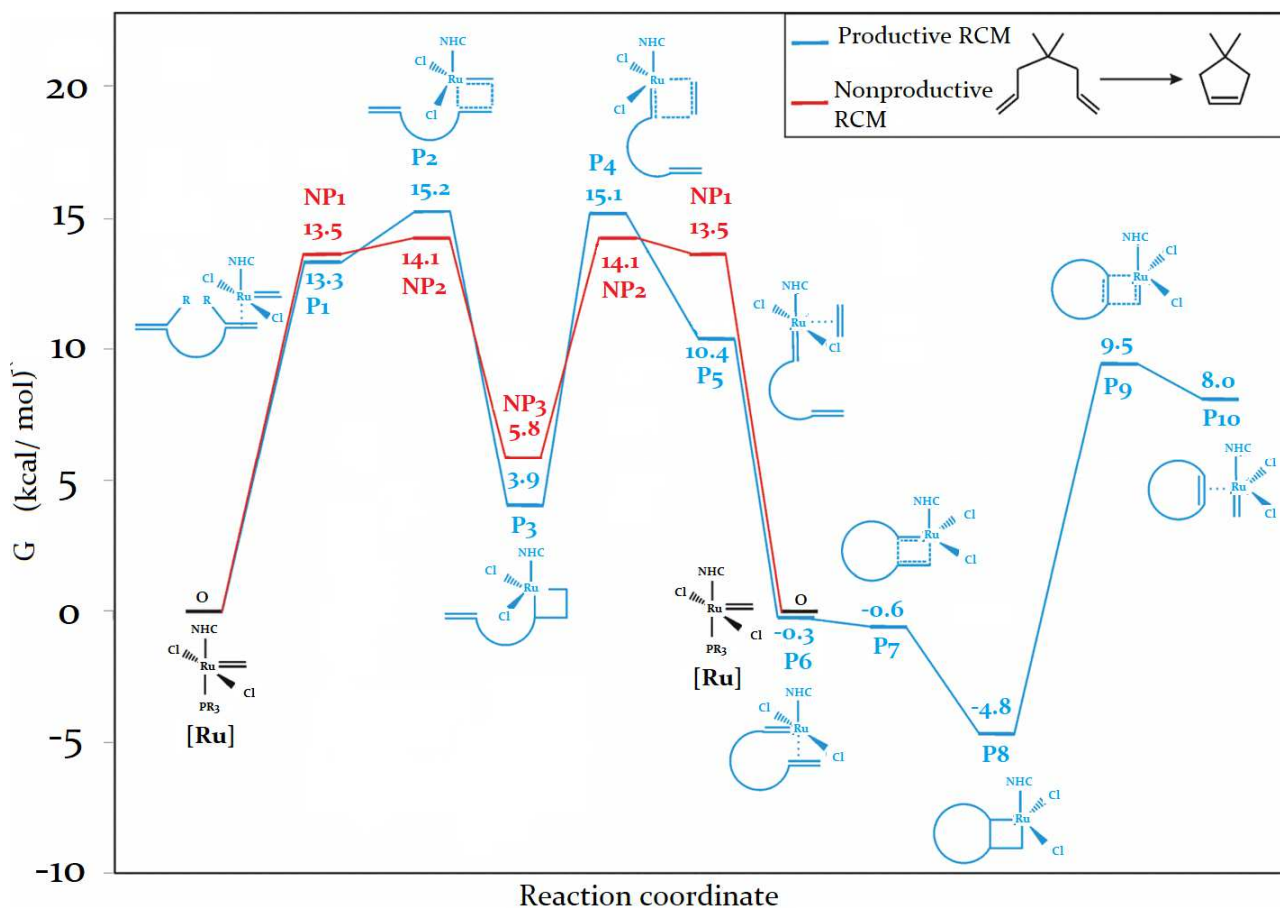
Figure 3.11: Comparison between free energy profile and nonproductive events energy profile in the RCM of **23** catalysed by **5** (calculated in methylene chloride)

[62] a)C. Costabile, A. Mariconda, L. Cavallo, P. Longo, V. Bertolasi, F. Ragone , F. Grisi, *Chem. Eur. J.* **2011**, *17*, 8618; b) A. Perfetto, C. Costabile, P. Longo, V. Bertolasi and F. Grisi, Chem. Eur. J. **2013**, *19*, 10492.

[63] I. C. Stewart, B. K. Keitz, K. M. Kuhn, R. M. Thomas, R. H. Grubbs, *J. Am. Chem. Soc.* **2010**, *132*, 8534.
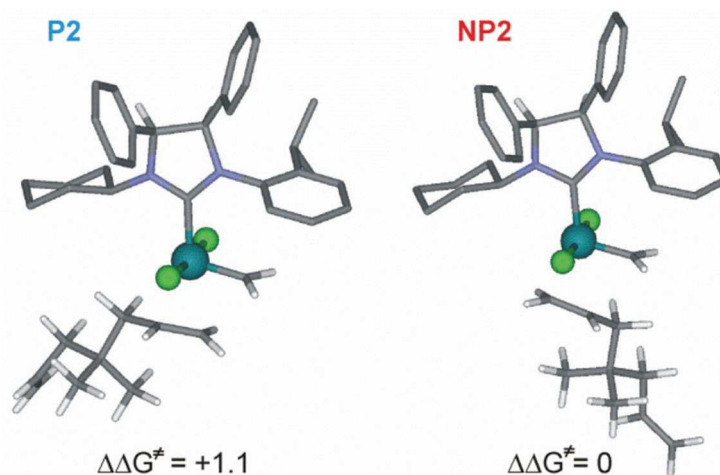
Figure 3.12: Structures of the transition states of the productive (**P2**) and non-productive (**NP2**) free energy profiles

3.4 ROMP of COD
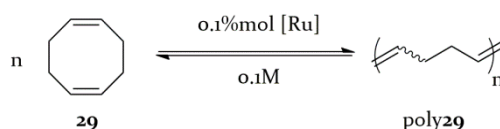
Scheme 3.3: ROMP of **29**

Complexes **1-8** were evaluated in the model ROMP of COD (**29**, scheme 3.3). Analogously to RCM, polymerisations were conducted in an NMR tube and monitored over time using NMR spectroscopy. Results are summarised in table 3.2.

Table 3.2: ROMP of **29** with **1-8**, **GIItol** and **HIItol**

catalyst	time (min) of complete conversion	*E:Z*
GIItol	4	1.3
1	14	0.8
2	9	0.5
5	30	1
6	20	1
HIItol	2	3.8
3	8	0.9
4	4	2
7	12	2
8	5	2.5

ROMP with GII-type complexes were carried on in CD_2Cl_2 at 30°C while polymerisations with phosfine free akins were conducted in C_6D_6 at 60°C

Commercial complexes **GIItol** and **HGIItol** were the most active among the Grubbs type and the Hoveyda type catalysts, respectively. Phosphine-containing complexes **1** and **2** with N-methyl ligands reached full conversion faster than N-cyclohexyl **5** and **6** moreover showing a certain degree of Z-selectivity.

Anti catalysts were more efficient than syn, independently from the N-alkyl group.

Hoveyda-type catalysts showed a similar reaction trend, in which catalysts bearing the smaller alkyl group displayed a higher activity and an overall lower *E:Z* ratio. Very likely, the smaller methyl substituent promoted both the coordination of **29** than the enhanced percentage of *Z*-double bonds in the polymer.

The pronounced efficiency of anti catalysts with respect to the syn was also confirmed.

3.5 CM activity
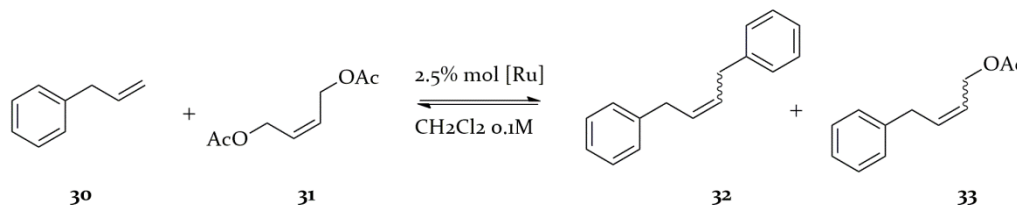
Scheme 3.4: CM of **30** and **31**

The intriguing backbone effect and the interesting N-alkyl group influence showed in both RCM and ROMP made the catalysts' investigation in CM very promising. The CM of **30** and **31** (scheme 3.4) was performed with **1-8**. Yields and *E:Z* ratio of **33** are reported in table 3.3.

Table 3.3: CM of **30** and **31** catalysed by **1-8**

catalyst	yield 33 (%)[a]	E/Z 33[b]
1	66	7.4
2	53	9.5
3	86	8.0
4	57	8.6
5	88	3.6
6	53	8.5
7	72	2.6
8	67	7.6

a)isolated yield; b)evaluated with NMR spectroscopy

All catalysts were able to full convert **30** (reactions were carried out with 2 equivalents of **31** in order to reduce homodimerisation) and to selectively reach the cross product **33**.

Syn N-methyl catalysts **1** and **3** reached **33** in higher yields, with respect to **2** and **4**. The backbone configuration did not affect the geometry of the double bond of **33**, in fact *E:Z* ratio differences between **1-4** catalysed reactions were not impressive.[64]

The catalytic results of the CM with N-Cyclohexyl catalysts **5-8** showed a more complex and interesting scenario. Indeed, with these complexes the backbone configuration impressively influences the *E/Z* ratio, with syn catalysts showing a more pronounced *Z*-preference. Very relevant is the case of **7** and **8**, which gained **33** with almost the same conversion albeit with a *E/Z* ratio of 2.6 and 7.6, respectively. This is the first published example of a so pronounced backbone influence in cross metathesis. Unfortunately, there is so far no study in the

---

[64] E:Z ratios of **33** with **1-4** were comparable with those obtained in commercial catalyst promoted reactions (~8).

literature clarifying the CM mechanism in u-NHC metal catalysed reaction. This make risky any rationalisation attempt.

3.6 More insight into the steric and electronic properties of u-NHC

Standard metathesis reactions highlighted an impressive backbone configuration influence in the reaction catalysed by N-cyclohexyl u-NHC catalysts **5-8**. The pronounced reactivity of anti complex respect to the syn in RCM, as well as their different E/Z ratios selectivity in cross metathesis inspired more in depth study.

Catalytic properties of a metal complex are often caused by a combination of steric and electronic reasons. Of course, an exhaustive clarification of aspects mainly influencing efficiency is crucial, albeit difficult and sometimes not possible.

In this context, NHCs confirm their pivotal role in metal catalysis. In fact, thanks to their availability (facile synthesis makes library of ligands usable) and to their reactivity towards many metals (different metal complexes allow to sound out various aspects in dependence on the same ligand architecture), investigation on steric and electronic properties is easy and gives diverse causes for reflection.

Scheme 3.5: Synthesis of **34** and **35**

NHC rhodium complexes are very informative and often used to study NHCs' properties'.[65] Rhodium cyclooctadiene complexes can be useful to estimate the steric hindrance of NHCs. Moreover they are the synthetic precursors of the rhodium cis-dicarbonyl complexes whose IR characterisation well appraises electron donating properties of these ancillary ligands.

To this end, **34** and **35**, bearing respectively the syn and the anti N-cyclohexyl u-NHC ligand, were synthesized (scheme 3.5). **34** and **35** were obtained through a deprotonation of the ligand precursors **19** and **22**, respectively. Carbenes thus generated reacted with chloro(1,5-cyclooctadiene) rhodium(I) dimer. Complexes were isolated as yellow microcrystalline solids.

^{1}H NMR analysis revealed for **34** the presence of two isomers in a 1:0.2 ratio, due to the rotation around the Rh-NHC bond or around the N-Aryl bond[66]. The signal of the carbenic carbon in the ^{13}C NMR spectrum was observed at 216.9 ppm (major isomer, d, J_{Rh-C}=48.1 Hz). Instead, just one isomer was detected by the proton NMR analysis of **35**. Carbon-13 NMR revealed the presence of the carbenic carbon at 214.9 ppm (d, J_{Rh-C}=47.2 Hz).

It was possible to characterise both **34** and **35** with X-Ray analysis (figure 3.13).

[65] K. M. Kuhn, J.-B. Bourg, C. K. Chung, S. C. Virgil and R. H. Grubbs, *J. Am. Chem. Soc.* **2009**, *131*, 5313.

[66] a) M. Iglesias, D. J. Beetstra, B. Kariuki, K. J. Cavell, A. Dervisi, I. A. Fallis, *Eur. J. Inorg. Chem.* **2009**, 1913; b) Y. Borguet, G. Zaragoza, A. Demonceau, L. Delaude, *Dalton Trans.* **2015**, *44*, 9744.
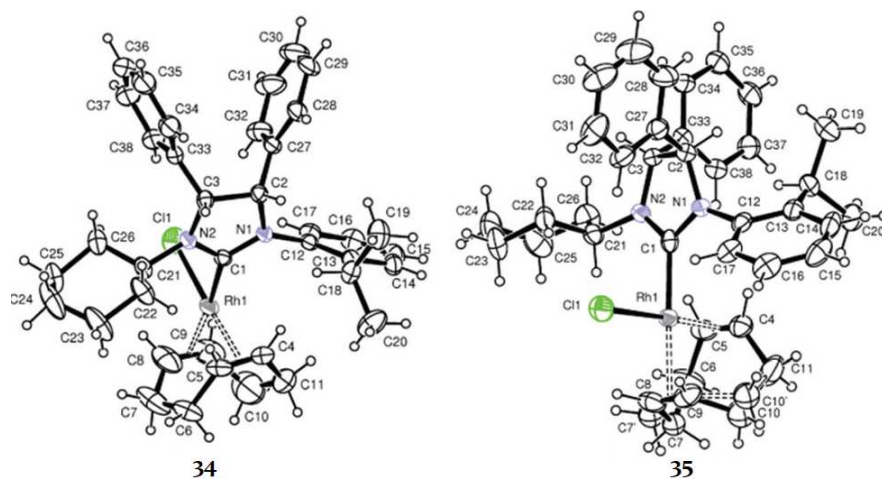
Figure 3.13: ORTEP view of complexes **34** and **35** with the thermal ellipsoids at 30% probability

In both complexes, the metals adopted a square planar coordination geometry. **34** crystallised in the centro-symmetric space group C2/c while **35** crystallised in the orthorhombic non-centrosymmetric space group P2$_1$2$_1$2$_1$. Absolute configurations (*R,S* and *S,R* for **34** and *R,R* for **35**) were determined from crystallographic data by means of the calculated Flack parameter of -0.02(5).[67] In both **34** and **35** distances between metal and the centroids of COD were longer for *trans*-NHC with respect to the *trans*-Cl. This was probably due to the greater *trans* influence of the N-heterocyclic carbene.

Some relevant crystallographic data are summarised in table 3.4.

As anticipated, **34** and **35** can be very useful for the investigation of the steric hindrances of their NHC frameworks. In fact, starting from selected crystallographic data it was possible to evaluate the percent of buried volume (%V*bur*) of the syn and anti N-cyclohexyl ligands.
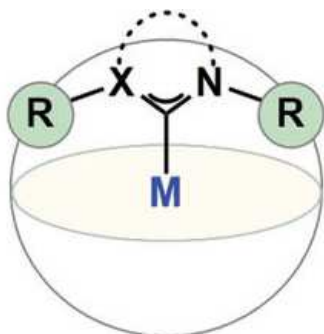
Figure 3.14: Representation of %V*bur* (taken from ref. 68)

The percent of buried volume (%V*bur*) of a certain ligand indicates the percentage of volume it occupies in a sphere (3.5 Å of radii) around the metal centre (figure 3.14).[68] In principle, it can be used to describe the hindrance of any ligand, independently from the denticity and the shape, and it is widely applied in the characterisation of the NHC's steric bulk.[69]

%V*bur* can be calculated using the SambVca program, developed by Cavallo,[68] using X-Ray CIF files or DFT coordinates of either the ligand nor the metal complex.

For **34** and **35**, values of %V*bur* were very similar (29.7 and 29.9, respectively), thus suggesting that the reactivity gap showed by syn and anti N-cyclohexyl ligands was not due to the difference in their steric hindrance. An analogue calculation on crystallographic data of **7** and **8** confirmed for the syn and anti frameworks a comparable encumbrance (%V*bur* were 29.1 and 29.4 for enantiomers of **7** and 29.9 for **8**)

At this point, to explain the observed backbone influence an in depth study of the electronic properties of these ligands seemed to be decisive At this scope, rhodium *cis*-dicarbonyl

[67] H. D. Flack, *Acta Crystallogr., Sect. A: Fundam. Crystallogr* **1983**, *39*, 876.

[68] A. Poater, B. Cosenza, A. Correa, S. Giudice, F. Ragone, V. Scarano, L. Cavallo, *Eur. J. Inorg. Chem.*, **2009**, 1759.

[69] A. Gomez Suarez, D. J. Nelson, S. P. Nolan, *Chem. Commun.* **2017**, 53, 2650.

complexes **36** and **37** were prepared by treating respectively **34** and **35** with carbon monoxide (scheme 3.6).

Table 3.4: X-Ray analysis of **34** and **35**

	34	**35**
centro-symmetric space group	C_2/c	$P_{2_1}2_12_1$
absolute configuration	R,S S,R	R,R
Distances (Å)		
Rh$_1$–C$_1$	2.016(2)	1.998(7)
Rh$_1$–C(C$_4$–C$_5$)	2.3825(8)	2.388(2)
Rh$_1$–C(C8–C9)	2.099(4)	2.102(8)
C$_1$–N$_1$	1.344(4)	1.3858(8)
C$_1$–N2	1.337(4)	1.348(7)
Angles (°)		
C$_1$–Rh$_1$–Cl$_1$	86.18(7)	90.0(2)
C$_1$–Rh$_1$–C(C$_4$–C$_5$)	95.0(1)	92.0(2)
C$_1$–Rh$_1$–C(C8–C9)	174.6(1)	177.8(2)
Cl$_1$–Rh$_1$–C(C$_4$–C$_5$)	176.8(1)	177.8(2)
Cl$_1$–Rh$_1$–C(C8–C9)	90.9(1)	91.0(2)
C(C$_4$–C$_5$)–Rh$_1$–C(C8–C9)	88.1(1)	87.0(2)
N$_1$–C$_1$–N2	109.0(2)	107.2(5)
C$_1$–N$_1$–C2	113.1(2)	112.9(5)
C$_1$–N2–C3	113.6(2)	113.4(5)

Proton NMR analysis of these dicarbonyl complexes revealed for both the presence of rotational isomers, due to the rotation around the Rh-NHC bond and/or around the N-Aryl bond, analogously with what observed for **34** (Isomers ratios were 1:0.5:0.3 for **36** and 1:0.3 for **37**).

Carbon-13 NMR spectra showed the carbenic signal at 206.3 ppm (major isomer, d, $J_{Rh–C}$ = 38.9 Hz) for **36**, and at 203.2 ppm (major isomer, d, $J_{Rh–C}$ = 40.4 Hz) for **37**. Chemical shifts of the two carbonyl ligands were

Scheme 3.6: Synthesis of **36** and **37**

observed for the major isomer of **36** at 186.8 (d, $J_{Rh–C}$ = 53.4 Hz) and 183.5 ppm (d, $J_{Rh–C}$ = 75.5 Hz), while for the major isomer of **37** at 186.7 (d, $J_{Rh–C}$ = 54.3 Hz) and 183.7 ppm (d, $J_{Rh–C}$ = 73.9 Hz).

IR CO stretching frequencies analysis of these compounds was very instructive.

Generally talking, stretching frequencies of carbon monoxide are influenced by the electron density at the metal centre which is, in turn, related to the electronic properties of the CO-trans ligand. An increased electron density determines a stronger M-C(CO) bond, because of

the improved π*-backbonding from the d orbitals of the metal into the π*CO anti-bonding orbital. It also causes a weaker C-O bond and thus lower C-O stretching frequencies. On the contrary, if the metal is less electron-rich, the degree of the π*-backbonding there will be lower, resulting in a weaker M-C(CO) bond, in a stronger C-O bond and higher C-O stretching frequencies (figure 3.15).
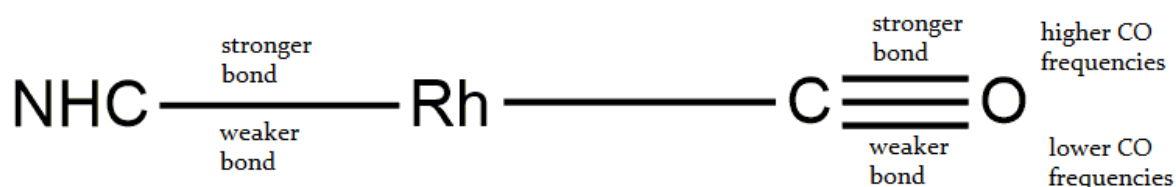
Figure 3.15: A schematic representation of NHC-Rh bond energy influence on trans CO stretching frequencies

The Tolman Electronic Parameter (TEP) describes ligand's electronic properties trough C-O stretching frequencies[70] and it can be calculated using the metal appropriate empirical formula, available in the literature.[71] For **36** and **37**, IR C-O average stretching frequencies[72] were respectively 2039.5 cm^{-1} and 2033.5 cm^{-1}. TEP was calculated [73] using the equation:

$$TEP = 0.8001\ CO_{av} + 420\ cm^{-1}$$

Calculated values were 2051.8 for **36** and 2047.0 for **37**, thus probing the more electro-donating nature of the anti ligand which can thus be the reason of the intriguing difference in reactivity between syn and anti N-cyclohexyl complexes **5-8**.
Coherently, Bond Dissociation Energy (BDE), calculated using DFT calculations to estimate the Rh-NHC bond energy, revealed that dissociation of anti ligand of **37** would be 0.6 kcal/mol more expensive with respect to dissociation of the syn in **36**, thus confirming the higher electro-donating nature experimentally observed for the anti NHC framework.

3.7 Conclusion
Ruthenium metathesis catalysts bearing backbone substituted u-NHC ligands are a family of complexes of increasing importance in the olefin metathesis scenario. In order to explore the potentialities of these complexes, compounds **1-8**, belonging to the Grubbs-type or the Hoveyda-type group, were synthesized and characterised using NMR and X-Ray techniques. They showed an improved stability both in solution and in solid state.

---

[70] C. A. Tolman, *Chem. Rev.* **1977**, 77, 313.
[71] D. J. Nelson, S. P. Nolan, *Chem. Soc. Rev.* **2013**, 42, 6723.
[72] Calculated considering the symmetric and asymmetric stretching frequencies, which were 2080 and 1999 cm^{-1} for **36** and 2075 and 1992 cm^{-1} for **37**. IR spectra were recorded at the solid state.
[73] a) T. Dröge F. Glorius, *Angew. Chem. Int. Ed.* **2010**, 49, 6940; b) A. R. Chianese, X. Li, M. C. Janzen, J. W. Faller R. H. Crabtree, *Organometallics* **2003**, 22, 1663; c) R. A. Kelly III, H. Clavier, S. Giudice, N. M. Scott, E. D. Stevens, J. Bordner, I. Samardjiev, C. D. Hoff, L. Cavallo, S. P. Nolan, *Organometallics* **2008**, 27, 202; d) S. Wolf, H. Plenio, *J. Organomet. Chem.* **2009**, 694, 1487.

Reactivity of **1-8** was studied in several model metathesis transformations. In RCM it was evident the higher efficiency of complexes with anti backbone absolute configuration with respect to their syn analogues. This was more visible for catalysts **5-8**, bearing cyclohexyl as the N-alkyl group.

The different catalytic behaviour of syn and anti isomers was very pronounced also in CM, in fact syn catalysts were found to be more Z-selective with respect to the anti isomers.

This intriguing backbone influence was analysed in depth synthesizing rhodium-COD (**34** and **35**) and rhodium dicarbonyl (**36** and **37**) complexes, bearing the syn and the anti N-cyclohexyl NHC ligands. %V_{bur}, calculated for **34** and **35**, revealed no significant difference in the steric hindrance generated by the two ligands in the surroundings of the metal centre. Instead, evaluation of CO stretching frequencies and bond dissociation energy of **36** and **37** demonstrated a prominent electro-donating nature of the anti ligand which is very likely responsible of the interesting reactivity gap observed in catalysis.

This study, which for the first time 'raises the curtain' on reactivity of backbone substituted u-NHC ruthenium complexes, clarified some aspects of their surprising reactivity with the aim to achieve an aware catalyst design.

3.8 Supporting Information

All reactions involving organometallic compounds were performed under nitrogen using standard Schlenk and glove-box techniques. Solvents were dried and distilled before use. Deuterated solvents were degassed under a N_2 flow and stored over activated 4 Å molecular sieves. Reagents were purchased from Sigma Aldrich Company and TCI chemicals and used without further purifications. Substrates for metathesis reactions were prepared according to the literature. Flash column chromatography of organic molecules were performed using silica gel 60 (230-400 mesh) from Sigma Aldrich Company and flash column chromatography of complexes were performed, under nitrogen flow, using silica gel 60 (230-400 mesh) from TSI Cambrige. Analytical thin-layer chromatography (TLC) was performed using silica gel 60 F254 precoated plates with a fluorescent indicator. The visualization was performed using UV-light and $KMnO_4$ or I_2 stains. NMR spectra were recorded on Bruker Avance 250 spectrometer (250 MHz for ^{1}H; 62.5 MHz for ^{13}C), Bruker AM 300 spectrometer (300 MHz for ^{1}H; 75 MHz for ^{13}C), Bruker AVANCE 400 spectrometer (400 MHz for ^{1}H; 100 MHz for ^{13}C; 161.97 MHz for ^{31}P) and Bruker ASCEND 600 spectrometer (600 MHz for ^{1}H; 150 MHz for ^{13}C). NMR samples were prepared dissolving about 10 mg of compounds in 0.5 mL of deuterated solvent. ^{1}H and ^{13}C chemical shifts are listed in parts per million (ppm) downfield from TMS and are referenced from the solvent peaks or TMS. ^{31}P chemical shifts are referenced using H_3PO_4 as external standard. Spectra are reported as follows: chemical shift (δ, ppm), multiplicity and integration. Multiplicity are abbreviated as follows: singlet (s), doublet (d), triplet (t), multiplet (m), broad (br), overlapped (o). Elemental analysis for C, H, N were recorded on a ThermoFinnigan Flash EA 1112 and were performed according to standard microanalytical procedures. ESI-MS were performed on a Waters Quattro Micro triple quadrupole mass spectrometer equipped with an electrospray ion source. Infrared

spectra were recorded with a Bruker Vertex70 spectrometer. Optical activity was determined using a JASCO P2000 polarimeter.

3.8.1 Synthesis of monoarilated diamines

Under nitrogen atmosphere, in a round bottom flask, 2,2'-bis(diphenylphosphino)-1,1'-binaphthyl (BINAP) (0.2 eq.), palladium acetate (0.1 eq.), sodium *t*butoxide (2 eq.) and toluene (C = 0.05 M) were introduced. The orange solution was stirred for a few minutes. Then the diamine (1.5 eq.) and *o-i*propylphenylbromide (1 eq.) were added and the reaction mixture was heated to 100 °C overnight. After this time the purple mixture was cooled at room temperature, diluted with hexane, then filtered through a plug of silica gel and eluting with methanol. The crude yellow oil was purified by flash column chromatography on silica gel (hexane:ethyl acetate 9:1 to 6:4) to give the desired products as yellow oils.

10 (MW=330.4 g/mol, Yield=90%).
^{1}H NMR (CD$_2$Cl$_2$, 250MHz): δ 7.32-7.20 (m, 10H), 7.04 (d, ^3J=7.5 Hz, 1H), 6.80 (t, ^3J= 7.5 Hz, 1H), 6.56 (t, ^3J=7.5 Hz, 1H), 6.26 (d, ^3J =7.5 Hz, 1H), 4.71 (br d, 1H), 4.51 (t, ^3J=5.6 Hz, 1H), 4.29 (d, ^3J=5.6 Hz, 1H), 2.84 (m, 1H), 1.25 (d, ^3J=6.8 Hz, 3H), 1.09 (d, ^3J=6.8 Hz, 3H).
^{13}C NMR (CD$_2$Cl$_2$, 62.5 MHz): 144.3, 143.1, 141.2, 133.1, 128.9, 128.7, 128.3, 128.1, 127.8, 127.7, 126.7, 125.2, 117.6, 112.1, 64.3; 62.0; 27.9, 22.6, 22.4.
ESI+MS: m/z= 331 (MH$^+$).

14 (MW=330.4 g/mol, Yield=87%).
^{1}H NMR (CD$_2$Cl$_2$, 400 MHz): δ 7.33-7.23 (m, 10H), 7.08 (d, ^3J=7.5 Hz, 1H), 6.80 (t, ^3J=7.9 Hz, 1H), 6.55 (t, ^3J=7.3 Hz, 1H), 6.14 (d, ^3J=8.2 Hz, 1H), 5.45 (br s, 1H), 4.52 (br s, 1H), 4.39 (d, ^3J=4.2 Hz, 1H), 3.06 (m, 1H), 1.36 (d, ^3J=6.8 Hz, 3H), 1.23 (d, ^3J=6.8 Hz, 3H).
^{13}C NMR (CD$_2$Cl$_2$, 75 MHz): δ 144.2, 143.8, 142.4, 132.6, 128.9, 128.7, 127.7, 127.5, 127.3, 127.1, 126.6, 125.1, 116.9, 111.5, 63.5, 61.6, 27.8, 22.8, 22.4.
ESI+MS: m/z =331 (MH$^+$).
[α]$_{20}$=+36.2° (*c*=0.5, CH$_2$Cl$_2$).

21 (MW= 412.6 g/mol, Yield=95%). The product was obtained by using the diamine and *o-i*propylphenylbromide 1:1.
^{1}H NMR (CDCl$_3$, 300 MHz): δ 7.32-7.18 (m, 11H), 6.92 (t, ^3J =7.5 Hz, 1H), 6.72 (t, ^3J =7.5 Hz, 1H), 6.29 (d, ^3J =7.5 Hz, 1H), 5.85 (br s, 1H), 4.37 (br d, 1H), 4.06 (br d, ^3J =7.4 Hz, 1H), 3.24 (m, 1H), 2.37 (br m, 1H), 1.97 (br d, 1H), 1,69 (br s, 2H), 1.46 (d, ^3J =6.8 Hz, 3H), 1.40 (d,^3J =6.8 Hz, 3H), 1.29-1.05 (om, 7H).
^{13}C NMR (CDCl$_3$, 75 MHz): δ 144.9, 142.0, 141.7, 133.1, 128.3, 127.8, 127.3, 127.1, 126.6, 124.8, 117.1, 112.1, 65.9, 64.4, 53.1, 35.0, 32.6, 27.7, 26.3, 24.9, 24.4, 23.1, 22.3.
ESI+MS: m/z = 414 (MH$^+$).

3.8.2 General procedures for the alkylation of diamines

For the synthesis of **11** and **15**, in a flask containing the amine (1 eq.), formaldehyde (5eq.), Na_2SO_4 (14.5 eq.), two drops of formic acid and CH_2Cl_2 (C= 0.1 M) were added. The reaction mixture was heated to reflux for 24 hours and then was filtered, concentrated and purified by flash column chromatography on silica gel (hexane:ethyl acetate 9:1).

For the synthesis of **18** and **20** a round bottom flask was charged with the diamine (1 eq.), cyclohexanone (7 eq. for **18** and 3 eq. for **20**) and CH_2Cl_2 (C=0.1 M). The reaction mixture was stirred overnight (**18**) or for 48 hours (**20**) at room temperature over activated molecular sieves 4Å. After filtration the solvent was removed under reduced pressure, anhydrous MeOH was added (C=0.1 M) and the solution was stirred at room temperature for 30 minutes. After that an equal volume of dry methanol (final concentration C=0.05 M) followed by a portionwise addition of $NaBH_4$ (4 eq.) was added under nitrogen atmosphere. The reaction mixture was stirred for 4h, diluted with methylene chloride and extracted with water. The organic layer was dried over anhydrous Na_2SO_4 and then the solvent was removed under vacuum to afford the product as a colourless oil.

11 (MW=356.5 g/mol, Yield=65%).
^{1}H NMR (CD_2Cl_2, 400 MHz): δ 7.22-6.93 (m, 14H), 5.02 (d, ^3J =8.5 Hz, 1H), 4.65 (d, ^3J =4.1 Hz, 1H), 4.06 (d, ^3J =8.5 Hz, 1H), 3.82 (m, 1H), 3.55 (d, ^3J =4.1 Hz, 1H), 2.32 (s, 3H), 1.29 (d, ^3J =7.0 Hz, 3H), 1.04 (d, ^3J =7.0 Hz, 3H).
^{13}C NMR ($CDCl_3$, 75 MHz): δ 146.8, 145.2, 140.7, 139.3, 129.3, 129.1, 127.8, 127.5, 127.0, 126.9,126.7, 125.1, 122.8, 80.3, 75.4, 70.9 , 38.7, 27.3, 24.9, 24.3.
ESI+MS: m/z =357 (MH$^+$).

15 (MW=356.5 g/mol, Yield=71%).
^{1}H NMR (CD_2Cl_2, 400 MHz): δ 7.19-6.95 (m, 14H), 4.61 (d, ^3J =8.5Hz, 1H), 4.35 (d, ^3J =4.5Hz, 1H), 4.29 (d, ^3J =4.5Hz, 1H), 3.59 (m, 1H), 3.41 (d, ^3J =8.5Hz, 1H), 2.24 (s, 3H), 1.29 (d, ^3J =6.8Hz, 3H), 1.06 (d, ^3J =6.8Hz, 3H).
^{13}C NMR (CD_2Cl_2, 100 MHz): δ 147.3, 144.2, 140.4, 139.0, 128.7, 128.6, 128.4, 128.1, 128.0, 127.7, 126.8, 126.5, 123.7, 120.4, 80.5, 79.8, 75.1, 38.6, 27.9, 24.6, 24.1.
ESI+MS: m/z =357 (MH$^+$).
$[\alpha]_{20}$ = +76.0° (c=0.5, CH_2Cl_2,).

18 (MW= 412.6 g/mol, Yield=92%).
^{1}H NMR (CD_2Cl_2, 250 MHz): δ 7.36-7.10 (om, 11H), 6.96 (t, ^3J = 7.5 Hz, 1H), 6.72 (t, ^3J =7.5 Hz , 1H), 6.37 (d, ^3J =7.5 Hz, 1H), 5.39 (br d, 1H), 4.68 (br t, 1H), 4.43 (d, ^3J =4.8 Hz, 1H), 3.09 (m, 1H), 2.44 (br m, 1H), 2.01 (br d, 1H), 1.76-1.64 (br m, 5H), 1.45 (d, ^3J =6.8 Hz, 3H), 1.40 (d, ^3J =6.8 Hz, 3H), 1.29-1.14 (br m, 4H).
^{13}C NMR ($CDCl_3$, 62.5 MHz): δ 143.9, 140.5, 140.1, 139.9, 132.2, 128.5, 128.2, 128.1, 127.9, 127.5, 127.2, 126.6, 124.8, 116.9, 111.8, 64.3, 62.4, 52.9, 34.7, 33.1, 27.9, 26.3, 25.0, 24.5, 22.4.
ESI+MS: m/z = 414 (MH$^+$).

20 (MW=294.4 g/mol, Yield= 92%).

^{1}H NMR and ^{13}C NMR signals were congruent with those reported in the literature.[74]

3.8.3 General procedures for the synthesis of tetrafluoroborate salts

For the synthesis of **12** and **16**, in a flask containing the cyclic amine (1eq.) were added NaHCO$_3$ (1.3 eq.), I$_2$ (1 eq.) and CH$_2$Cl$_2$ (C=0.1M). The purple reaction mixture was heated to reflux for 24 hours and then a saturated aqueous solution of Na$_2$SO$_3$ and NaBF$_4$ were added. When the organic phase became yellow it was extracted, concentrated, dried with MgSO$_4$ and purified by column chromatography (methylene chloride:methanol 40:1) to afford the product as a white solid.

For the synthesis of **19** and **22**, the diamine (1 eq.) and triethyl orthoformate (8 eq.) were introduced in a flask equipped with a magnetic stir and a condenser. The reaction mixture was stirred at room temperature for few minutes. Then NH$_4$BF$_4$ (1.2 eq.) was added and the solution was heated at 130°C for 2 hours. After that, the condenser was removed in order to facilitate the evaporation of the ethanol produced during the reaction. The crude orange oil was washed with diethyl ether and purified by flash column chromatography on silica gel (hexane:ethyl acetate 9:1 to 1:1) to obtain the product as a white solid.

12 (MW=442.3 g/mol, Yield=66%).
^{1}H NMR (CDCl$_3$, 400 MHz): δ 8.69 (s, 1H), 7.45-6.86 (m, 14H), 6.27 (d, 1H, ^3J =12.4 Hz), 5.83 (d, 1H, ^3J =12.4 Hz), 3.34 (s, 3H), 3.26 (m, 1H), 1.27 (d, 3H, ^3J =7.0 Hz), 1.21 (d, 3H, ^3J =7.0 Hz).
^{13}C NMR (CDCl$_3$, 100 MHz): δ 160.1, 144.9, 131.8, 130.7, 130.5, 129.9, 129.1, 129.1, 129.0, 128.9, 128.3, 128.1, 127.5, 127.3, 127.1, 73.1, 70.8, 34.6, 28.3, 24.6, 24.2.
ESI+MS: m/z =356[(M$^+$)-BF$_4$$^-$].

16 (MW=442.3 g/mol, Yield=78%).
^{1}H NMR (CDCl$_3$, 400 MHz): δ 8.53 (s, 1H), 7.51-6.68 (m, 14H), 5.25 (d, 1H, ^3J =9.6 Hz), 5.08 (d,1H, ^3J =9.6 Hz), 3.24 (s, 3H), 2.92 (m, 1H), 1.10 (d, 3H, ^3J =6.9 Hz), 0.98 (d, 3H, ^3J =6.9 Hz).
^{13}C NMR (CD$_2$Cl$_2$, 100 MHz): δ 158.5, 146.3, 134.6, 134.2, 131.6, 130.9, 130.7, 130.4, 129.9, 128.9, 128.3, 127.8, 127.6, 127.4, 78.2, 75.1, 34.3, 28.6, 24.4, 24.1.
ESI+MS: m/z =356 [(M$^+$)-BF$_4$$^-$].
$[\alpha]_{20}$ = +233.8° (c=0.5, CH$_2$Cl$_2$).

19 (MW=511.4 g/mol, Yield=76%).
^{1}H NMR (CDCl$_3$, 400 MHz): δ 8.36 (s, 1H), 7.42-6.86 (m, 14H), 6.38 (d, ^3J = 12.0 Hz, 1H), 6.00 (d, ^3J = 12.0 Hz, 1H), 3.45 (br t, 1H), 3.19 (m, 1H), 2.26-1.45 (m, 8H), 1.34-1.30 (o m, 6H), 1.24-1.13 (o m, 2H).
^{13}C NMR (CD$_2$Cl$_2$, 62.5 MHz): δ 157.2, 145.2, 132.4, 131.7, 130.9, 130.5, 129.6, 129.3, 128.6, 128.5, 128.1, 127.6, 127.3, 73.0, 68.7, 58.3, 32.5, 31.7, 28.9, 25.6, 25.3, 24.7, 24.4.
ESI+MS: m/z = 434 [M$^+$(-BF$_4$$^-$)].

---

22 (MW=511.4 g/mol, Yield=87%).

^{1}H NMR (CDCl$_3$, 400 MHz): δ 8.56 (s, 1H), 7.54-7.10 (o m, 14H), 5.42 (d, ^3J =7.4 Hz, 1H), 5.15 (d, ^3J =7.4 Hz, 1H), 3.62 (br t, 1H), 2.93 (br t, 1H), 2.16-2.05 (br d, 2H), 1.85-1.41 (o m, 9H), 1.46 (d, ^3J = 6.8 Hz, 3H) 1.08 (d, ^3J =6.5 Hz, 3H).

^{13}C NMR (CDCl$_3$, 100 MHz): δ 156.4, 145.4, 136.1, 134.7, 131.4, 130.7, 130.4, 130.3, 129.9, 128.7, 127.9, 127.5, 127.1, 126.9, 77.9, 72.1, 58.3, 31.9, 31.0, 28.4, 25.2, 25.1, 24.7, 24.3, 24.2.

ESI+MS: m/z = 434 [M$^+$(-BF$_4^-$)].

$[\alpha]_{20}$ = +230.6° (c= 0.5, CH$_2$Cl$_2$).

3.8.4 General procedure for the synthesis of catalysts 1-4

In glove box potassium hexafluoro*t*butoxide (1 eq.) and dry toluene (C = 0.1 M) were introduced in a vial followed by the tetrafluoroborate salt (1 eq.). After five minutes **GI** (synthesis of **1** and **2**) or **HI** (synthesis of **3** and **4**) (0.5 eq.) was added. The reaction mixture was stirred for three (Grubbs-type) or two hours (Hoveyda-type) and purified by flash column chromatography on silica gel (hexane:diethyl ether 9:1 for **1** and **2** and 5:1 for **3** and **4**)

1 (MW=897.0 g/mol, Yield= 15%). The product is a mixture of two isomers (major:minor 1:0.4) and was obtained as a brown solid

^{1}H NMR (C$_6$D$_6$, 400 MHz): δ 20.64 (minor isomer, d, $^3J_{\text{H-P}}$=9.4Hz, 0.4H), 19.63 (major isomer, s, 1H, Ru=CHPh), 8.63-6.17 (overlapped signals of both isomers, 28H), (only signals of major isomer are shown below), 5.31 (d, ^3J=10.6 Hz, 1H), 5.18 (d, ^3J=10.6 Hz, 1H), 3.97 (s, 3H), 3.81-3.66 (o m, 3H), 2.68 (br m, 3H), 2.45 (br m, 1H), 2.34 (s, 1H), 2.08-0.88 (overlapped signals of both isomers, 50H).

^{13}C NMR (C$_6$D$_6$, 100 MHz): δ 294.8 (Ru=CHPh), 223.8 (iNCN, $^2J_{\text{C-P}}$=75.1Hz), 151.7, 146.5, 137.5, 134.6, 134.5, 134.1, 133.9, 132.9, 131.4, 126.0, 75.1, 72.9, 36.4, 33.2, 33.1, 32.0, 31.9, 30.5, 30.1, 29.7, 29.6, 28.2, 28.1, 27.2, 27.0, 26.8, 25.6.

^{31}P NMR (C$_6$D$_6$, 161.97 MHz): δ 34.8, 19.8.

Anal. Calcd for C$_{50}$H$_{65}$Cl$_2$N$_2$PRu (897.0): C, 66.95, H, 7.30, N, 3.12. Found: C, 67.08, H, 7.49, H, 3.08.

2 (MW=897.0 g/mol, Yield= 12%). The product is a mixture of two isomers (major:minor 1:0.5) and was obtained as a brown solid

^{1}H NMR (C$_6$D$_6$, 400 MHz): δ 20.73 (minor isomer, d, $^3J_{\text{H-P}}$= 8.8 Hz, 0.5H), 19.67 (major isomer, s, 1H, Ru=CHPh), 8.44-6.21 (overlapped signals of both isomers, 28H), (only signals of major isomer are shown below) 4.85 (d, ^3J=3.7 Hz, 1H), 4.80 (d, ^3J=3.7 Hz, 1H), 3.90 (s, 3H), 3.51 (m, 1H), 2.72 (m, 3H), 2.08-0.92 (overlapped signals of both isomers, 53H).

^{13}C NMR (C$_6$D$_6$, 100 MHz): δ 303.6 (Ru=CHPh), 295.4, 219.9 (iNCN, $^2J_{\text{C-P}}$=72.3 Hz) 152.7, 151.5, 147.3, 146.7, 140.5, 140.2, 139.5, 138.3, 137.1, 79.1, 78.0, 77.7, 76.7, 36.8, 36.3, 33.3, 33.1, 32.0, 31.8, 30.5, 30.0, 29.8, 29.5, 29.7, 28.2, 28.1.

^{31}P NMR (C$_6$D$_6$, 161.97 MHz): δ 35.0, 20.8.

Anal. Calc. for C$_{50}$H$_{65}$Cl$_2$N$_2$PRu (897.0): C, 66.95, H, 7.30, N, 3.12. Found: C, 66.98, H, 7.42, N, 3.18.

3 (MW=674.7 g/mol, Yield= 22%). The product was obtained as a green solid.

^{1}H NMR (C$_6$D$_6$, 400 MHz): δ 16.22 (s, 1H, Ru=CH-o-OiPrC$_6$H$_4$), 7.51 (d, ^3J=7.9 Hz, 1H), 7.13-6.97 (o m, 5H), 6.89-6.86 (m, 3H), 6.74-6.64 (o m, 7H), 6.50-6.47 (o m, 2H), 5.49 (d, 3 ^3J=10.33 Hz, 1H), 4.80 (d, ^3J= 10.3 Hz, 1H), 4.72 (m, 2H), 4.06 (s, 3H), 3.52 (m, 1H), 1.77 (m, 6H), 1.24 (m, 6H).

^{13}C NMR (C$_6$D$_6$, 100 MHz): δ 289.4 (Ru=CH-o-OiPrC$_6$H$_4$), 214.9, 153.6, 149.0, 144.5, 139.8, 134.5, 134.2, 133.6, 122.8, 113.5, 75.6, 72.7, 37.5, 30.6, 28.6, 24.8, 24.7, 22.6, 22.5.

Anal. Calc. For C$_{35}$H$_{38}$Cl$_2$N$_2$ORu (675.7): C, 62.31, H, 5.68, N, 4.15. Found: C, 62.49, H, 5.96, N, 4.07.

4 (MW=674.7 g/mol, Yield= 20%).The product was obtained as a green solid.

^{1}H NMR (C$_6$D$_6$, 400 MHz): δ 16.16 (s, 1H, Ru=CH-o-OiPrC$_6$H$_4$), 7.52-6.92 (om, 15H), 6.68 (m, 1H), 6.58 (br s, 1H), 6.47 (d, ^3J=8.0 Hz, 1H), 4.79-4.70 (om, 4H), 3.99 (s, 3H), 3.48 (br m, 1H), 1.75 (m, 6H), 1.25 (br d, 3H) 1.01 (d, ^3J=6.8 Hz, 3H).

^{13}C NMR (C$_6$D$_6$, 100 MHz): δ 288.5 (Ru=CH-o-OiPrC$_6$H$_4$), 212.2, 153.8, 149.0, 144.6, 144.4, 140.8, 140.4, 139.8, 133.4, 130.1, 129.9, 129.6, 129.5, 127.7, 127.6, 127.5, 127.0, 123.0, 122.7, 113.7, 82.7, 80.5, 76.8, 76.2, 75.8, 37.8, 37.6, 32.9, 31.4, 30.8, 30.4, 28.4, 28.1, 26.8, 25.2.

Anal. Calc. for C$_{35}$H$_{38}$Cl$_2$N$_2$ORu (674.7): C, 62.31, H, 5.68, N, 4.15. Found: C, 62,45, H, 5,86, N, 4,10.

3.8.5 General procedure for the synthesis of catalysts 5-8

For the synthesis of **5** and **6**, in a glove box potassium hexamethyldisilazide (KHMDS) (1.5 eq.) and dry toluene (C = 0.1 M) were introduced in a vial. Then the tetrafluoroborate salt (1.5 eq.) was added followed, after few minutes, by **GI** (1 eq.). The reaction mixture was stirred for 1 hour and purified by flash column chromatography on silica gel (hexane:diethyl ether 5:1 to 1:1).

For the synthesis of **7** and **8**, in a glove box, to a suspension of tetrafluoroborate salt (1 eq.) in toluene (C = 0.1 M) was added potassium hexafluoro$t$butoxide (1.1 eq.). The reaction mixture was stirred for few minutes at room temperature and then **HI** (0.5 eq.) was added. The flask was removed from the glove box and stirred at 65°C for 2 hours. The reaction mixture was cooled at room temperature and purified by flash column chromatography on silica gel (hexane:diethyl ether 5:1 to 1:1).

5 (MW=965.1 g/mol, Yield= 48%). The product is a mixture of two isomers (major:minor 1:0.3) and was obtained as brown solid

^{1}H NMR (C$_6$D$_6$, 400 MHz): δ 21.07 (minor isomer, d, $^3J_{HP}$ = 4.0 Hz, 0.3H), 19.74 (major isomer, s, 1H, Ru=CHPh), 9.02-6.58 (overlapped signals of both isomers), 6.41 (t, ^3J = 7.5 Hz, 1H), 6.15 (br s, 2H), 5.91 (od, 1.3H), 5.30 (br t, 1H), 5.20 (od, 0.3H), 5.16 (d, ^3J = 9.4 Hz, 1H), 5.02 (br d, 0.3H), 3.89 (br m, 0.3H), 3.47 (om, 2.3H), 3.24 (br s, 1H), 2.54 (br d, 1.3H), 2.39 (br s, 5H), 2.04-0.91 (overlapped signals of both isomers). ^{13}C NMR (C$_6$D$_6$, 100 MHz): δ 299.4 (Ru=CHPh), 221.0 (iNCN, $^2J_{C-P}$ = 79.2 Hz), 152.3, 137.6, 134.4, 134.0, 133.8, 132.2, 130.6, 130.4,

129.8, 129.1, 127.5, 126.3, 125.9, 75.8, 67.5, 61.1, 33.9, 33.7, 33.5, 33.4, 33.0, 30.4, 30.2, 29.9, 29.8, 28.7, 28.6, 27.3, 26.0, 25.9, 25.4, 23.6.

^{31}P NMR (C_6D_6, 161.97 MHz): δ 24.9, 24.6.

Anal. Calcd for $C_{55}H_{73}Cl_2N_2PRu$ (965.13): C, 68.45, H, 7.62, N, 2.90. Found C, 68.48, H, 7.59, N, 2.92.

6 (MW=966.14 g/mol, Yield=64%). The product is a mixture of two isomers (major:minor 1:0.8) and was obtained as a light brown solid

^{1}H NMR (C_6D_6, 400 MHz): δ 21.04 (minor isomer, br s, 0.8H), 19.88 (maior isomer, s, 1H, Ru=CHPh), 8.87 (d, ^3J = 7.5 Hz, 2H), 8.37 (br s, 2H), 7.64 (d, ^3J = 7.5 Hz, 2H), 7.51 (d, ^3J = 7.5 Hz, 2H), 7.41-7.01 (overlapped signals of both isomers), 6.97 (t, ^3J = 7.5 Hz, 1H), 6.74 (d, ^3J = 7.5 Hz, 1H), 6.58 (t, ^3J = 7.5 Hz, 0.8H), 6.28 (t, ^3J = =7.5 Hz, 0.8H), 5.32 (br t, 1H), 5.10 (br s, 0.8H), 4.99 (br s, 1H), 4.80 (br s, 0.8H), 4.68 (br s, 1H), 3.86 (om, 1.8H), 3.46 (m, 1H), 3.14 (br d, 1H), 2.73 (br d, 1H), 2.6-0.98 (overlapped signals of both isomers), 0.86 (d, ^3J = 6.8 Hz, 3H).

13C NMR (C6D6, 100 MHz): δ 299.9 (Ru=CHPh), 217.5 ((iNCN, $^2J_{C-P}$ = 76.3 Hz), 152.9, 151.7, 147.9, 147.1, 143.9, 143.6, 140.2, 139.4, 137.8, 137.5, 133.3, 132.0, 130.0, 129.5, 127.2, 126.7, 126.0, 80.1, 79.3, 70.5, 69.4, 60.3, 58.7, 33.9, 33.7, 33.4, 33.3, 31.5, 30.4, 30.0, 29.4, 28.3, 27.2, 27.1, 26.9, 26.0, 25.6, 25.2, 25.0, 24.2.

^{31}P NMR (C_6D_6, 161.97 MHz): δ 25.8, 22.0.

Anal. Calcd for $C_{55}H_{73}Cl_2N_2PRu$ (965.13): C, 68.45, H, 7.62, N, 2.90. Found C, 68.34, H, 7.66, N, 2.91.

7 (MW=742.8 g/mol, Yield= 49%). The product was obtained as a green solid.

^{1}H NMR (C_6D_6, 400 MHz): δ 16.29 (s, 1H, Ru=CH-o-OiPrC$_6$H$_4$), 8.65 (br d, 1H), 8.06-6.66-6.50 (o m, 1.H), 6.15 (d, ^3J = 10.3 Hz, 1H), 6.06 (d, ^3J = 7.6 Hz, 1H), 5.95 (d, ^3J = 9.3 Hz, 1H), 5.70 (br t, 1 H), 5.09 (d, ^3J = 9.3 Hz, 1H), 4.69 (o m, 2H), 4.29 (d, ^3J = 10.2 Hz, 1H), 3.77 3.36 (br m, 1H), 3.11 (o m, 1.H), 2.82 (o m, 1H), 2.41 (m, 2H), 2.11-0.52 (o m, 46H).

^{13}C NMR (C_6D_6, 100 MHz): δ 290.4 (Ru=CH-o-OiPrC$_6$H$_4$), 213.7 (iNCN), 163.8, 153.5, 149.4, 148.9,148.6, 147.5, 144.8, 144.5, 144.2, 143.1, 141.6, 141.5, 139.9, 139.7, 139.1, 138.9, 137.2, 137.1,133.8, 133.1, 132.9, 130.9, 130.8, 130.6, 129.5, 129.2, 128.9, 128.8, 128.7, 127.7, 127.4, 127.3,127.2, 127.0, 122.7, 113.5, 79.1, 77.9, 76.3, 75.2, 69.5, 66.6, 65.5, 64.3, 63.6, 62.8, 61.1, 53.9, 54.2,53.4, 35.4, 35.3, 34.0, 33.6, 33.2, 33.1, 33.0, 28.0, 27.9, 27.5, 27.1, 27.0, 26.8, 26.7, 26.5, 26.0, 25.7, 25.5, 25.5, 25.4, 25.1, 23.9, 23.7, 23.1, 22.6, 22.5.

8 (MW=742.8 g/mol, Yield= 45%). The product was obtained as a green solid.

^{1}H NMR (C_6D_6, 400 MHz): δ 16.2 (s, 1H, Ru=CH-o-OiPrC$_6$H$_4$), 7.54 (d, ^3J =7.3 Hz, 2H), 7.42 (d, ^3J =8.0 Hz, 1H), 7.30-6.99 (om, 10H), 6.68 (t, ^3J =7.3 Hz, 1H), 6.57 (t, ^3J =7.3Hz, 1H), 6.49 (t, ^3J =8.0 Hz, 1H), 5.61 (br t, 1H), 4.93 (br s, 1H),4.70 (overlapped multiplets, 2H), 3.45 (m, 1H), 3.07 (br d, 1H), 2.70(br d, 1H), 1.88 (br t, 1H), 1.80 (d, ^3J =6.1 Hz, 3H), 1.76 (d, ^3J =6.1 Hz, 3H), 1.56 (om, 4H),1.33 (d, ^3J =6.7 Hz, 3H), 1.02 (d, ^3J =6.7 Hz, 3H), 0.90 (br m, 3H).

13C NMR (C$_6$D$_6$, 100 MHz): δ 289.2 (Ru=CH-o-OiPrC$_6$H$_4$), 211.1, 153.6, 148.6, 144.6, 143.6, 140.3, 139.6, 133.4, 129.6, 129.4, 129.3, 127.2, 126.9, 126.6, 122.8, 122.5, 113.5, 81.2, 75.2, 69.9, 63.2, 34.1, 32.2, 28.0, 27.0, 25.9, 24.9, 23.5, 22.6, 22.4.

Anal. Calcd for C$_{40}$H$_{46}$Cl$_2$N$_2$ORu (742.78): C, 64.68, H, 6.24, N, 3.77. Found C, 64.80, H, 6.10, N, 3.82.

3.8.6 General procedure for the synthesis of 34 and 35

In glove box the tetrafluoroborate salt (1 eq.), potassium bis(trimethylsilyl)amide (KHMDS, 1 eq.) and dry toluene (0.02M) were introduced in a vial. After few minutes, a solution of [RhCl(COD)]2 (2 eq.) in dry toluene was added. After two hours at room temperature the mixture was concentrated and purified by column chromatography on silica gel (methylene chloride:ethanol 95:5).

34 (MW=669.1 g/mol, Yield= 84%) The product is a mixture of two isomers (major:minor 1:0.2) and was obtained as a yellow solid.

1H NMR (CD$_2$Cl$_2$, 600 MHz): δ 8.71 (major isomer, d, 1H, ^3J=7.6 Hz), 8.31 (minor isomer, d, 0.2H, ^3J= 7.6 Hz), (only major isomer signals are shown below) 7.33-7.29 (o m, 3H), 7.23 (d, ^3J= 7.4 Hz, 2H), 7.07 (o m, 5H), 6.98 (br s, 4H), 5.66 (m, 1H), 5.65 (d, ^3J= 11.0 Hz, 1H), 5.35 (d, ^3J= 11.0 Hz, 1H), 4.93 (br s, 2H), 3.50 (br s, 1H), 3.08 (m, 1H), 2.82 (br s, 1H), 2.40-2.38 (o m, 2H), 2.25 (br s, 1H), 2.08 (br d, 1H), 1.93-1.82 (o m, 4H), 1.70-1.64 (o m, 4H), 1.56-1.54 (o m, 2H), 1.45-1.32 (om, 2H), 1.29 (d, ^3J= 6.6 Hz, 3H), 1.09 (d, ^3J= 6.6 Hz, 3H), 0.94 (o m, 1H), 0.84 (o m, 1H).

13C NMR (CD$_2$Cl$_2$, 150 MHz): δ 216.9 (J_{Rh-C}=48.1 Hz), 144.2, 138.3, 135.9, 134.4, 133.2, 128.1,128.0, 127.9, 127.7, 126.3, 126.0, 98.0 (J_{Rh-C}=6.6 Hz), 97.8 (J_{Ru-C}=6.3 Hz), 74.3, 68.8 (J_{Rh-C}=14.2 Hz), 68.1, 66.5 (J_{Ru-C}=13.3 Hz), 62.9, 33.6, 33.4, 33.3, 33.2, 31.9, 28.9, 28.8, 28.6, 27.0, 26.9, 25.9,24.7, 24.6.

Anal. Calc. for C$_{38}$H$_{46}$ClN$_2$Rh (669.1): C, 68.21, H, 6.93, N, 4.19. Found: 67.87, H, 7.05, N, 4.16.

35 (MW=669.1 g/mol, Yield= 79%). The product was obtained as a yellow solid.

1H NMR (CD$_2$Cl$_2$, 600 MHz): δ 8.48 (d, 1H, ^3J=7.8 Hz), 7.48-7.18 (o m, 14H), 5.61 (br t, 1H), 4.96 (br s, 1H), 4.86 (br m, 1H), 4.76 (d d, ^3J=15.4 Hz, 2H), 4.29 (br s, 1H), 3.82 (br m, 1H), 2.99 (m, 1H), 2.96 (br s, 1H), 2.54 (o m, 1H), 2.45 (m, 1H), 2.28 (m, 1H), 2.01 (m, 1H), 1.88-1.56 (o m, 7H), 1.48-1.36 (o m, 3H), 1.27 (d, ^3J=7.0 Hz, 3H), 1.03 (d, ^3J=6.7 Hz, 3H), 0.98 (o m, 1H), 0.80 (o m, 1H).

13C NMR (CD$_2$Cl$_2$, 150 MHz): δ 214.9 (J_{Rh-C}=47.2 Hz), 145.1, 142.5, 139.6, 137.5, 133.7, 129.5, 129.4, 129.3, 129.0, 128.9, 128.6, 128.3, 127.3, 126.3, 126.0, 125.9, 125.6, 98.9 (J_{Rh-C}=6.0 Hz), 97.9 (J_{Rh-C}=6.0Hz), 79.0, 78.9, 78.7, 70.4, 68.2 (J_{Rh-C}=14.7 Hz), 67.3 (J_{Rh-C}=14.1 Hz), 61.0, 34.7, 34.3, 31.6, 29.2, 28.3, 27.7, 26.9.

Anal. Calc. for C$_{38}$H$_{46}$ClN$_2$Rh (669.1): C, 68.21, H, 6.93, N, 4.19. Found: 68.32, H, 7.11, N, 4.10.

3.8.7 General procedure for the synthesis of 36 and 37

Carbon monoxide was bubbled into a solution of **34** or **35** in dry methylene chloride (C=0.013M) for 1 hour at room temperature. The light yellow solution was concentrated and the solid was washed three times with the minimum amount of cold pentane.

36 (MW=617.0 g/mol, Yield= 73%) The product is a mixture of three isomers and was obtained as a yellow solid (major:minor1:minor2 1:0.5:0.3).

^{1}H NMR (CD2Cl2, 600 MHz):), (only major isomer signals are shown below) δ 7.87 (d, 1H, ^3J=7.9Hz), 7.23-6.71 (o m, 14H), 5.78 (d, ^3J=10.8, 1H), 5.40 (d, ^3J=10.8, 1H), 4.56 (brt, 1H), 3.07 (m, 1H), 2.11-1.02 (o m, 17H).

^{13}C NMR (CD2Cl2, 150 MHz): δ 206.3 (J_{Rh-C}= 38.9 Hz), 186.8 (J_{Rh-C}= 53.4 Hz), 183.5 (J_{Rh-C}= 75.5Hz), 148.2, 145.5, 137.2, 135.7, 134.1, 133.1, 129.9, 129.4, 128.9, 128.4, 128.2, 128.1, 127.9, 126.8, 126.2, 74.7, 68.3, 61.9, 34.3, 33.0, 28.9, 27.7, 26.4, 26.2, 25.7, 25.6, 24.9.

IR (KBr): vCO 2080 (trans) and 1999 cm^{-1} (cis).

Anal. Calc. for C32H34ClN2O2Rh (617.0): C, 62.29, H, 5.55, N, 4.54. Found: C, 62.35, H, 5.87, N, 4.36.

37 (MW=617.0 g/mol, Yield= 64%) The product is a mixture of two isomers (major:minor 1:0.3) and was obtained as a yellow solid.

^{1}H NMR (CD2Cl2, 600 MHz): (only major isomer signals are shown below) δ 7.45-7.03 (o m, 14H), 5.01 (br d, 1H), 4.93 (br t, 1H), 4.76 (br d, 1H), 3.15 (m, 1H), 2.97 (m, 1H), 2.36 (o m, 1H), (2.32 br s, 2H), 1.85-1.03 (o m, 11H).

^{13}C NMR (CD2Cl2, 150 MHz): δ 203.2 (J_{Rh-C}= 40.4 Hz), 186.7 (J_{Rh-C}= 54.3 Hz), 183.7 (J_{Rh-C}= 73.9 Hz), 146.1, 141.4, 138.9, 136.5, 133.9, 129.7, 129.6, 129.4, 129.3, 129.2, 129.0, 127.5, 126.7, 126.4, 126.1, 79.0, 71.8, 61.1, 32.0, 31.7, 30.1, 27.8, 26.3.

IR (KBr): vCO 2075 (trans) and 1992 cm^{-1} (cis).

Anal. Calc. for C32H34ClN2O2Rh (617.0): C, 62.29, H, 5.55, N, 4.54. Found: C, 62.44, H, 5.39, N, 4.46.

3.8.8 NMR spectra
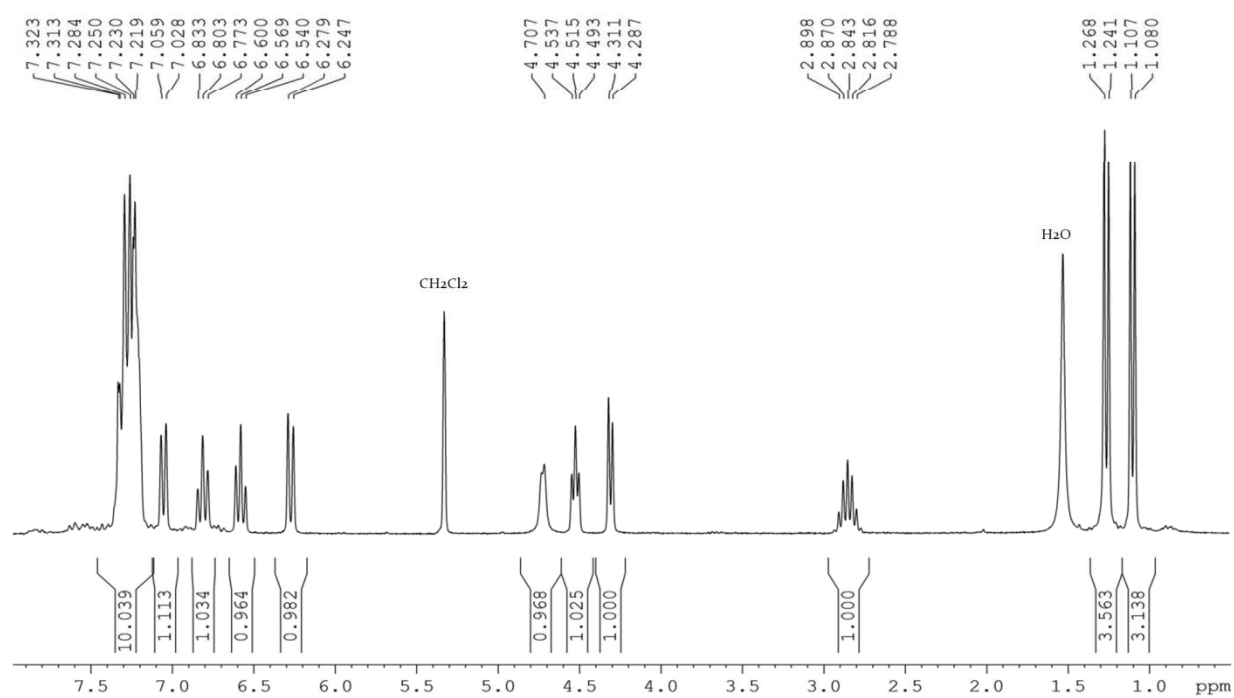
Figure S3.1: ¹H NMR of **10** (CD₂Cl₂, 250 MHz)
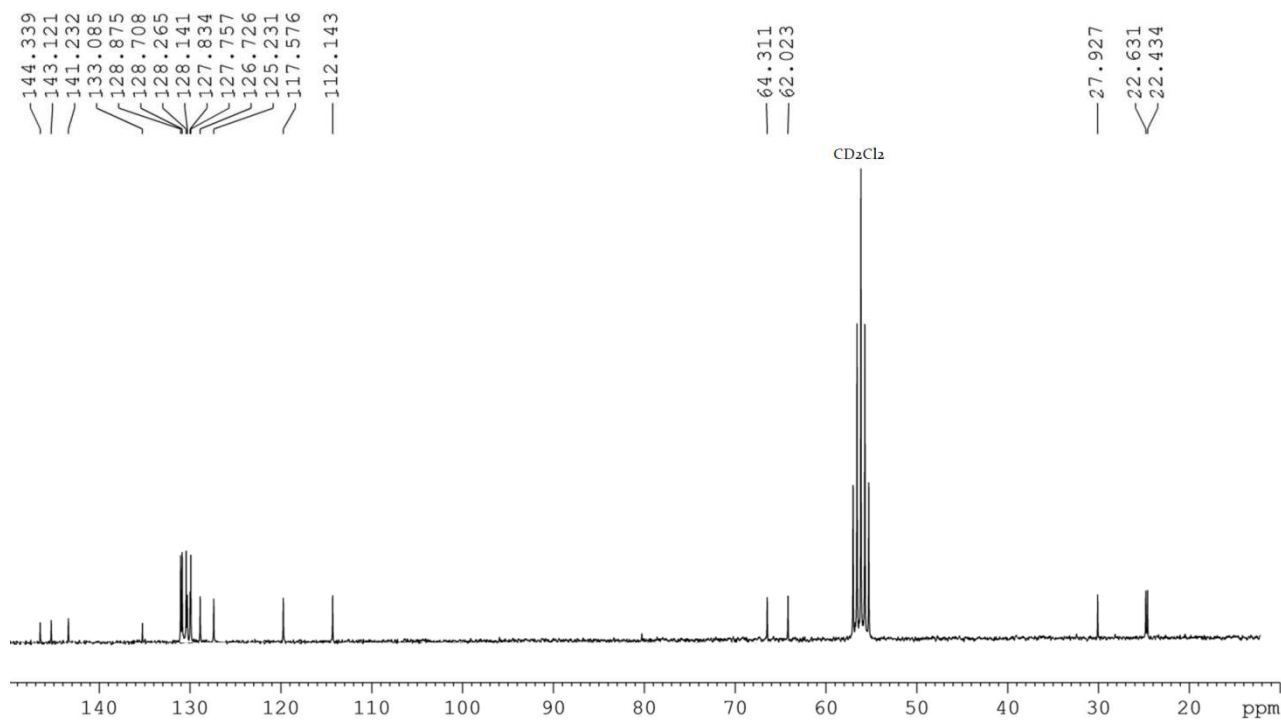
Figure S3.2: ¹³C NMR of **10** (CD₂Cl₂, 62.5 MHz)
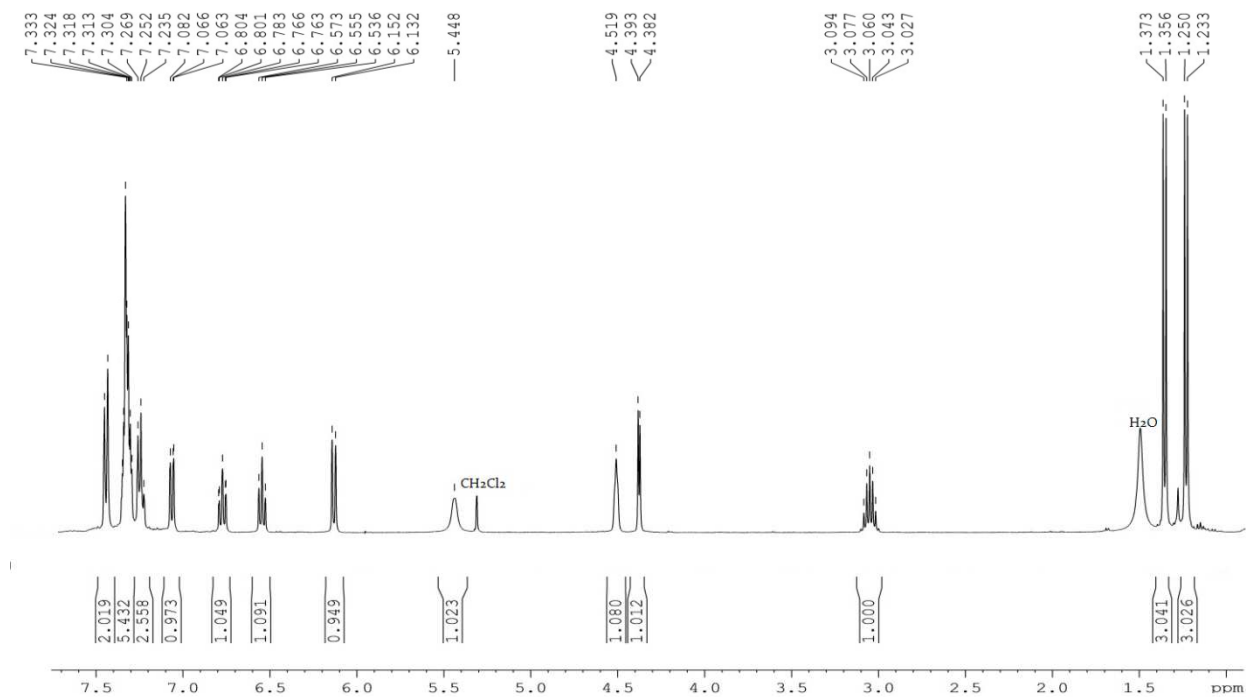
Figure S3.3: ¹H NMR of **14** (CD₂Cl₂, 400 MHz)
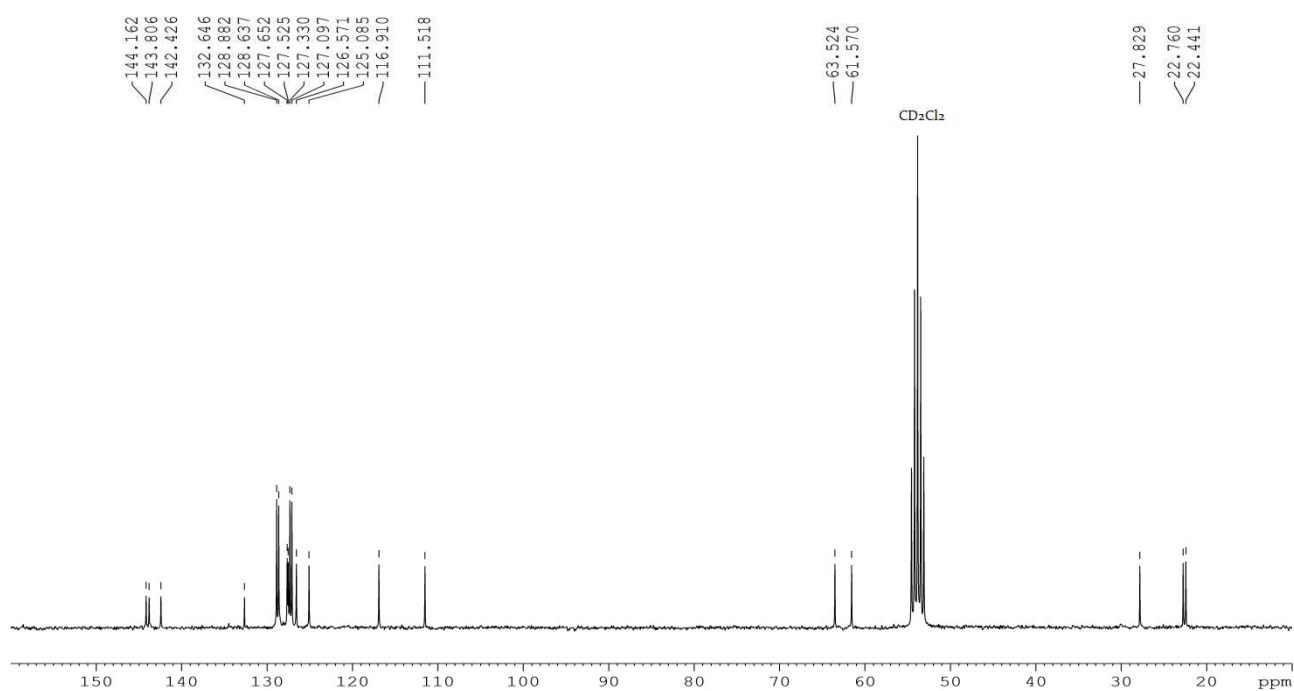
Figure S3.4: ¹³C NMR of **14** (CD₂Cl₂, 75 MHz)
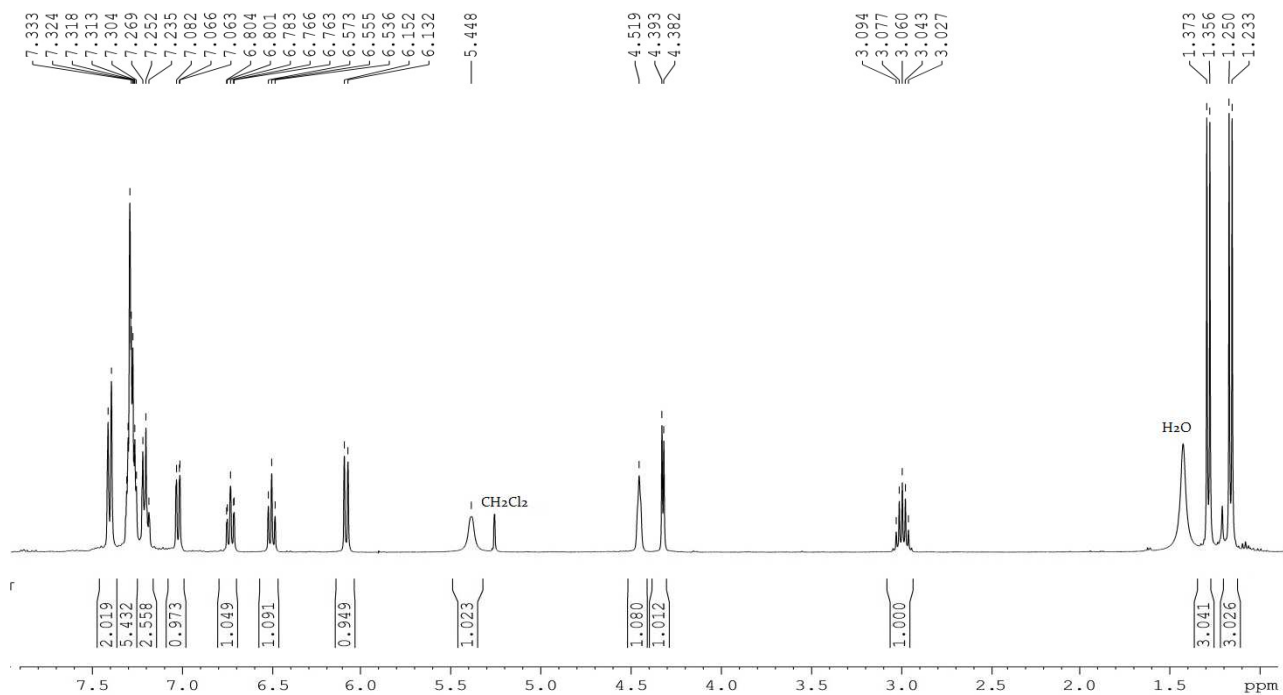
Figure S3.5: ^{1}H NMR of **21** (CD$_2$Cl$_2$, 400 MHz)
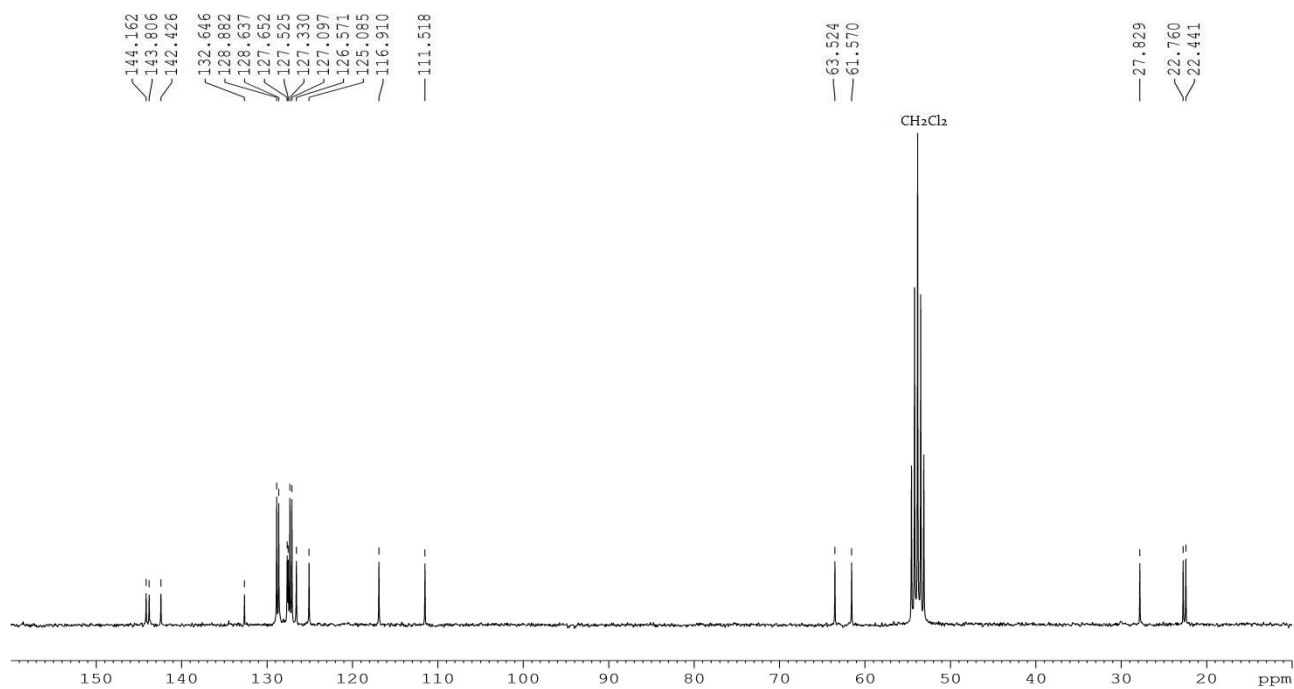
Figure S3.6: ^{13}C NMR of **21** (CD$_2$Cl$_2$, 75 MHz)
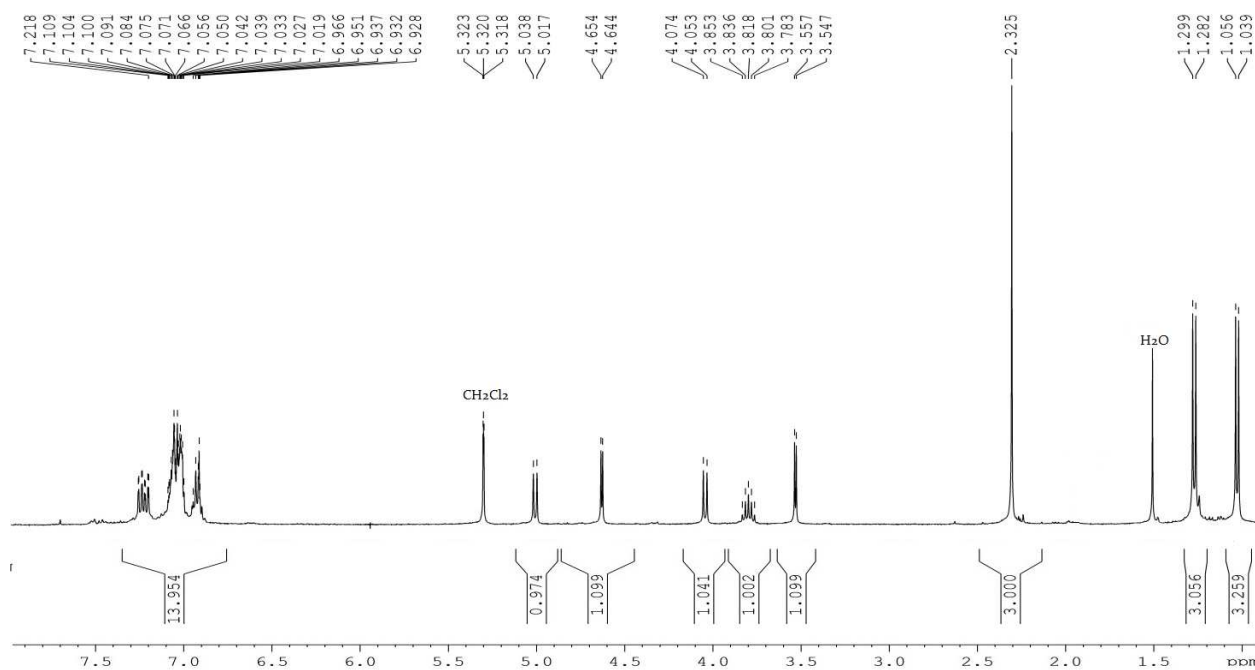
Figure S3.7: ^1H NMR of **11** (CD2Cl2, 400 MHz)
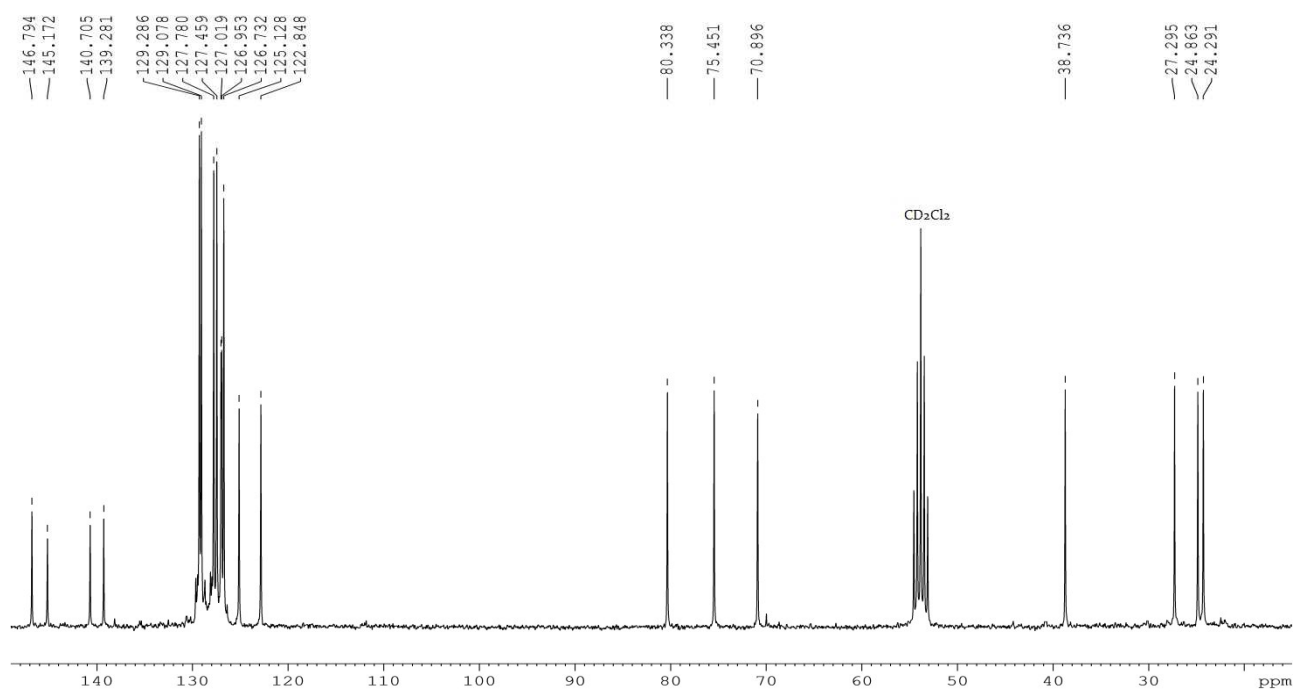
Figure S3.8: ^{13}C NMR of **11** (CD2Cl2, 75 MHz)
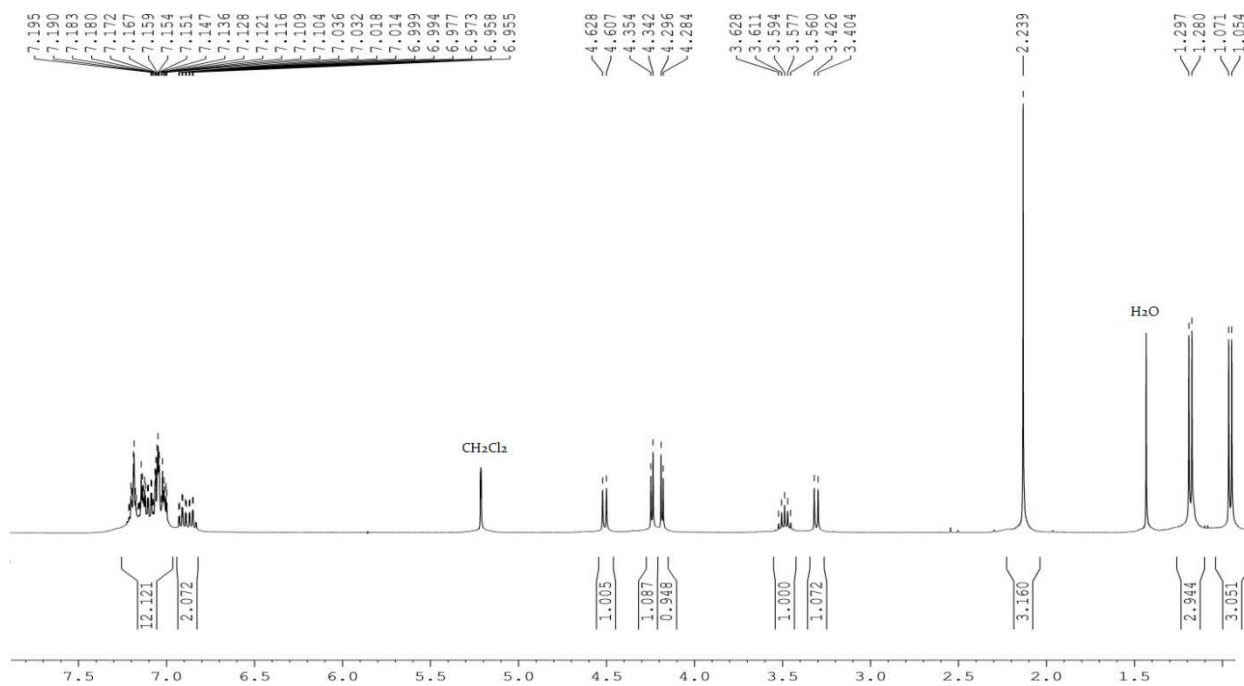
Figure S3.9: ^{1}H NMR of **15** (CD2Cl2, 400 MHz)
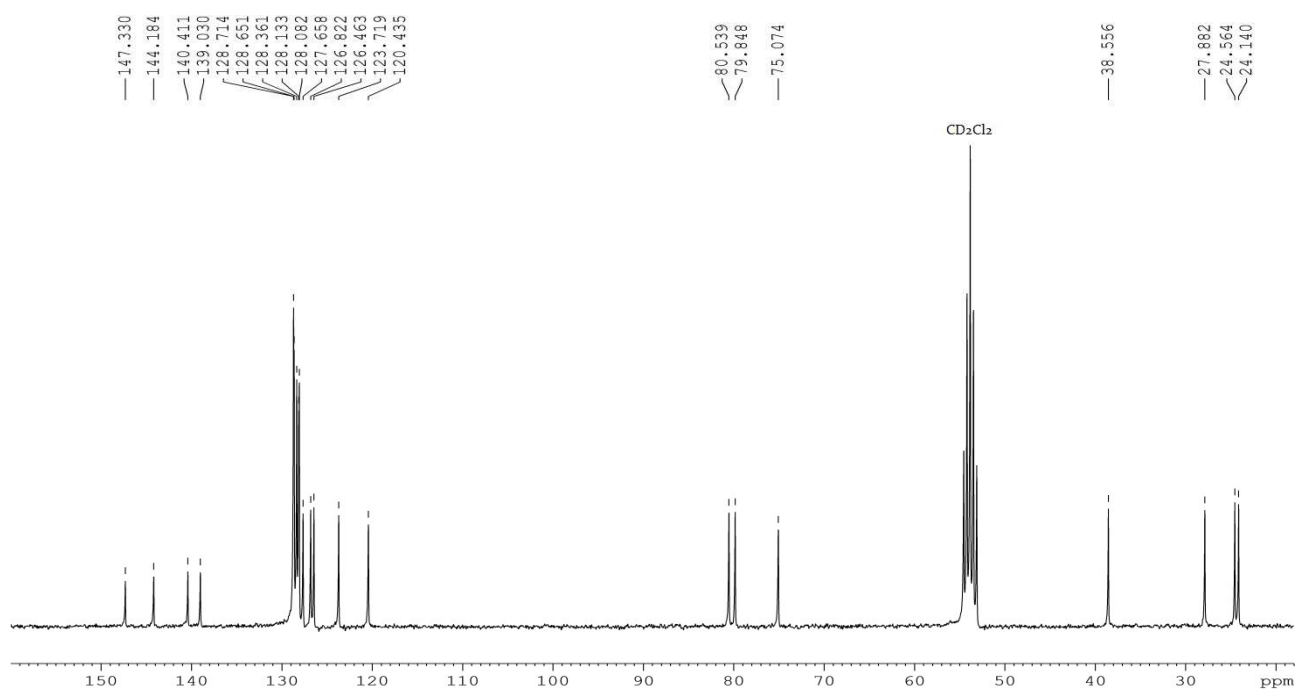
Figure S3.10: ^{13}C NMR of **15** (CD2Cl2, 100 MHz)
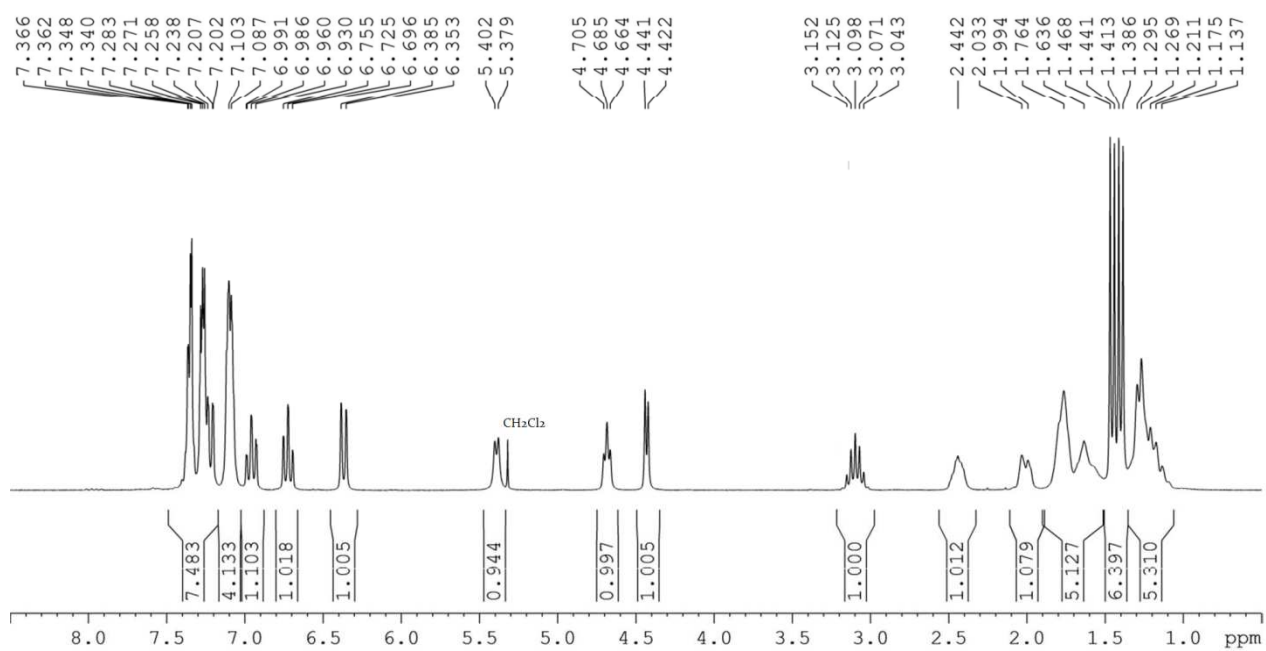
Figure S3.11: ¹H NMR of **18** (CD2Cl2, 250 MHz)
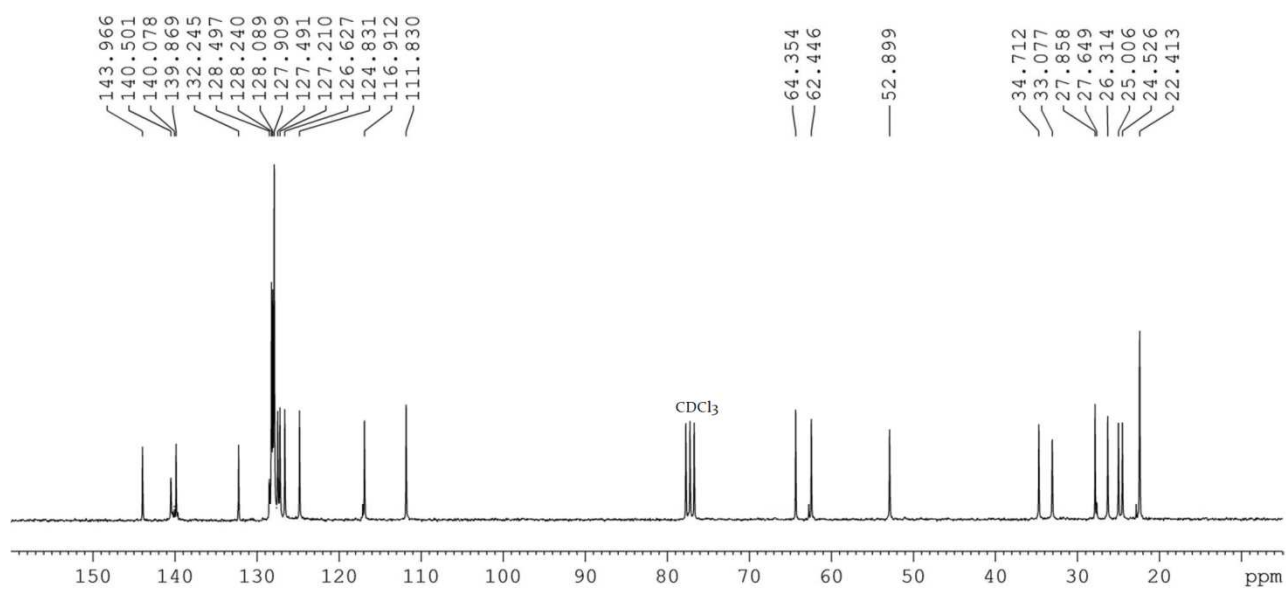
Figure S3.12: ¹³C NMR of **18** (CDCl3, 62.5 MHz)
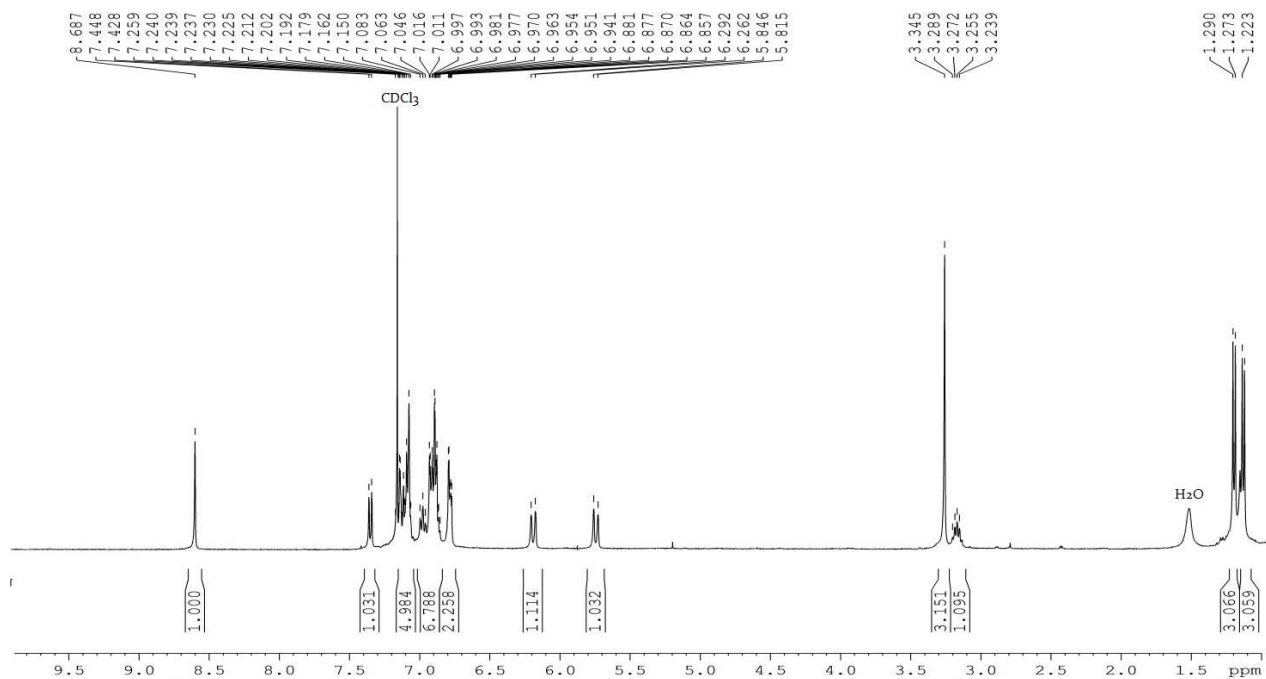
Figure S3.13: ¹H NMR of **12** (CDCl₃, 400 MHz)
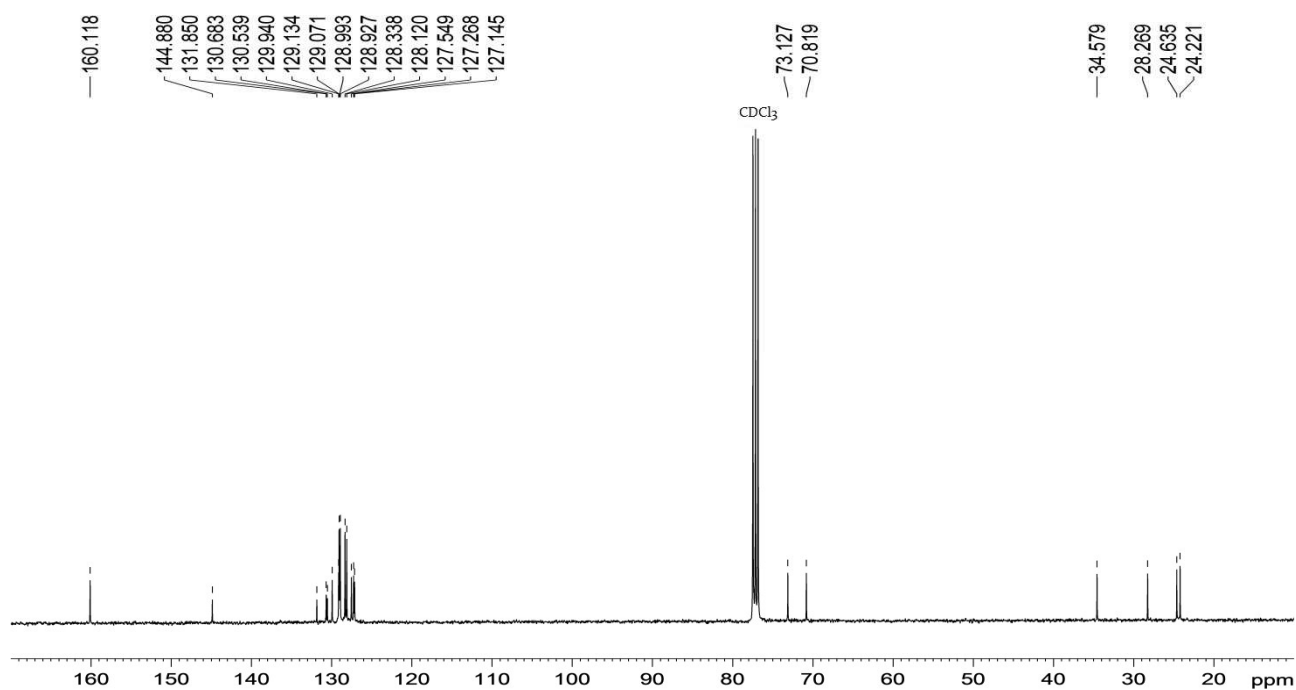
Figure S3.14: ¹³C NMR of **12** (CDCl₃, 100 MHz)
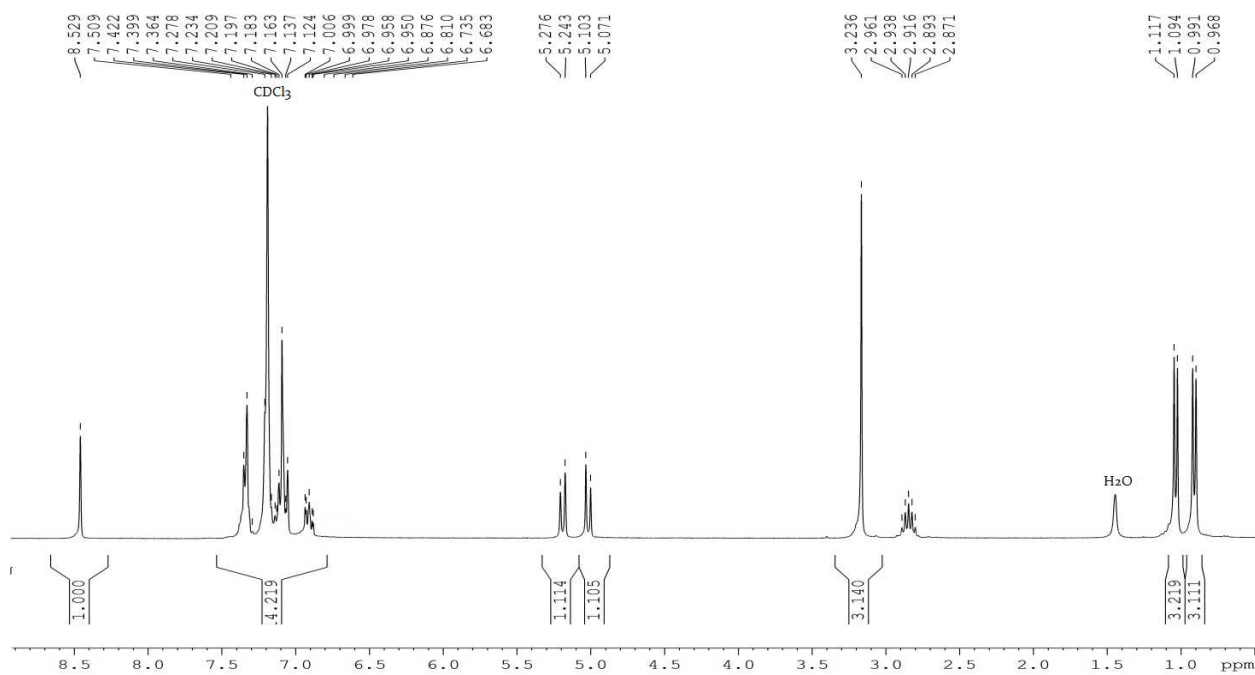
Figure S3.15: ^{1}H NMR of **16** (CDCl$_3$, 400 MHz)
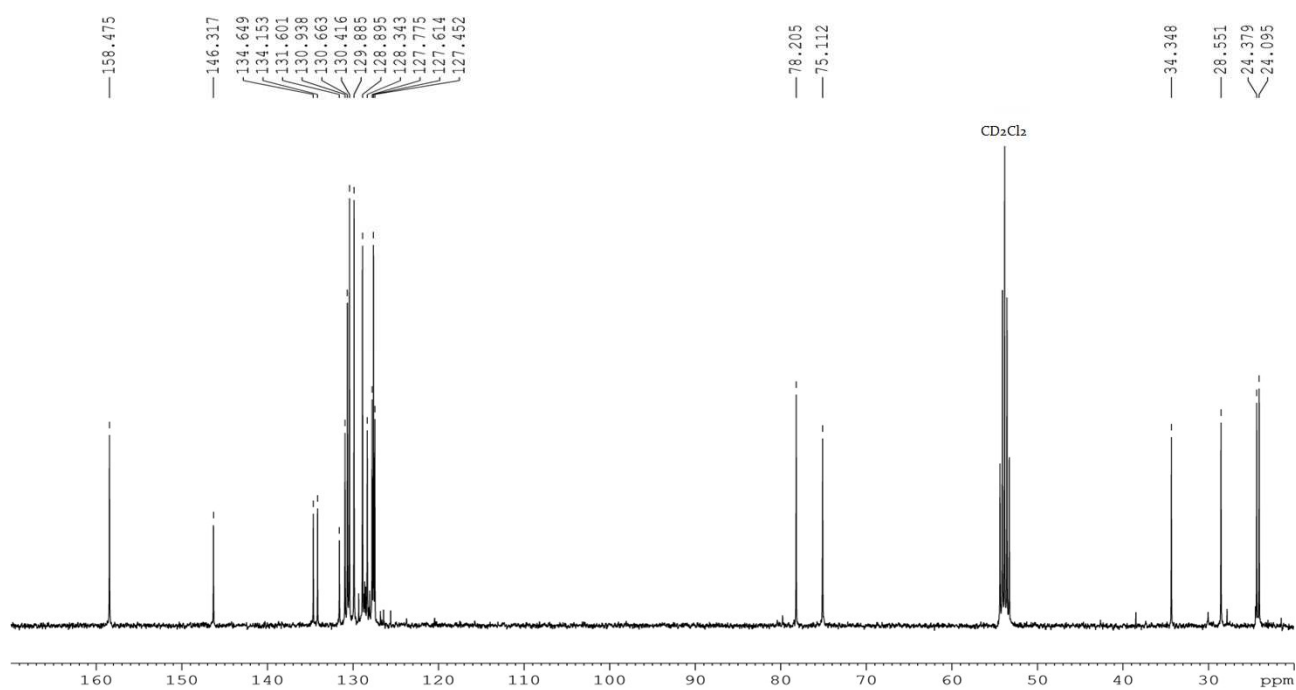
Figure S3.16: ^{13}C NMR of **16** (CD$_2$Cl$_2$, 100 MHz)
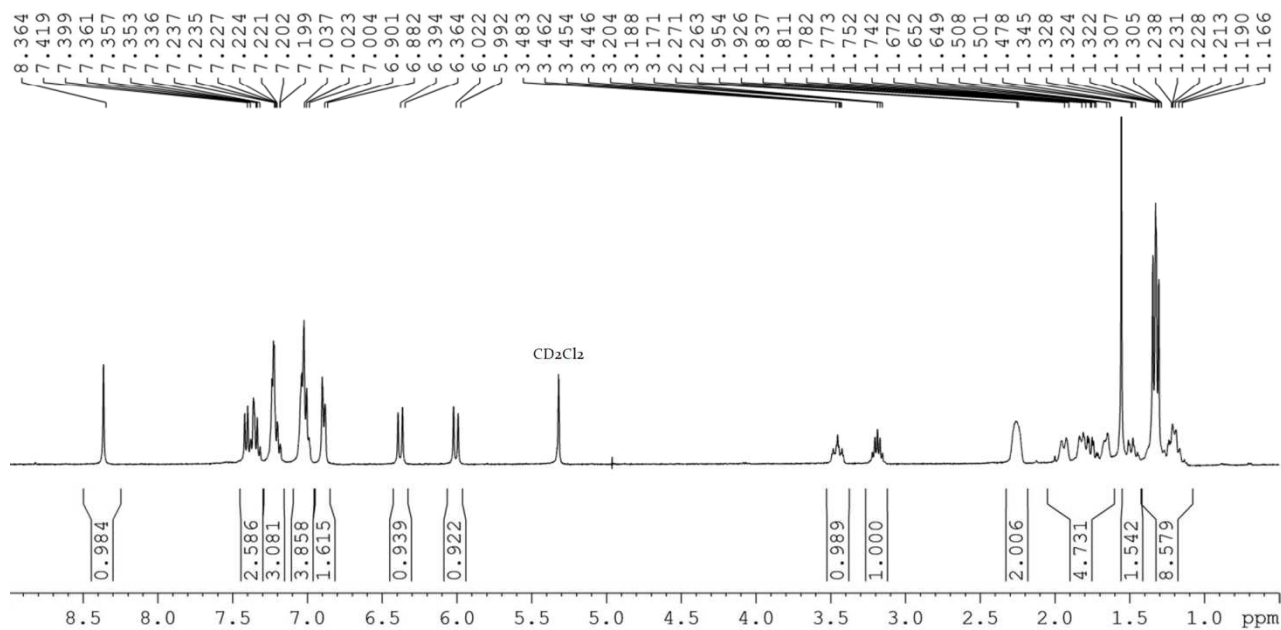
Figure S3.17: ¹H NMR of **19** (CD₂Cl₂, 400 MHz)
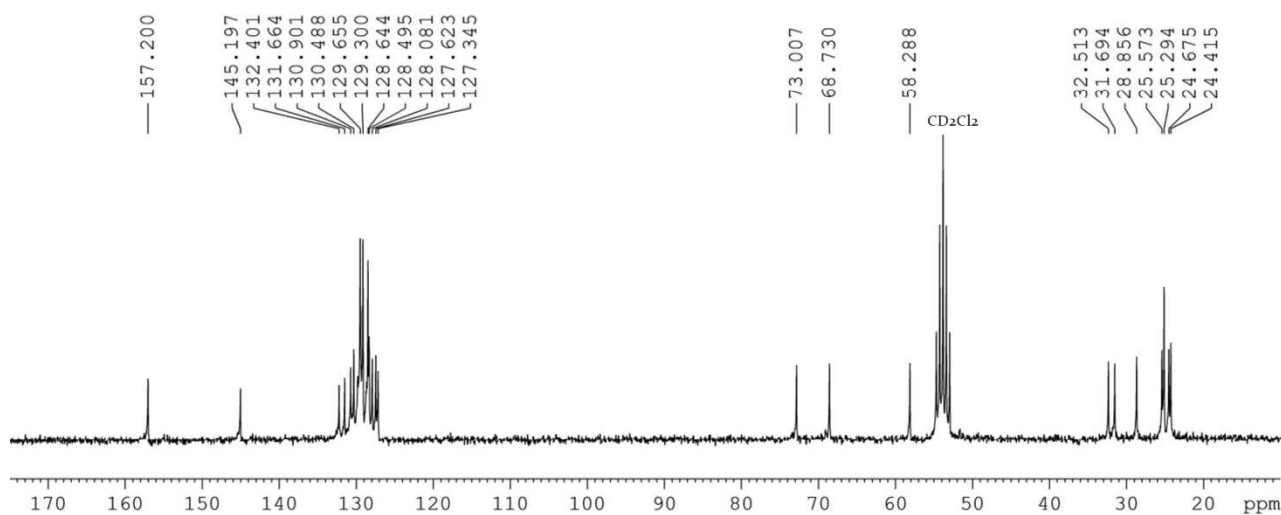
Figure S3.18: ¹³C NMR of **19** (CD₂Cl₂, 62.5 MHz)
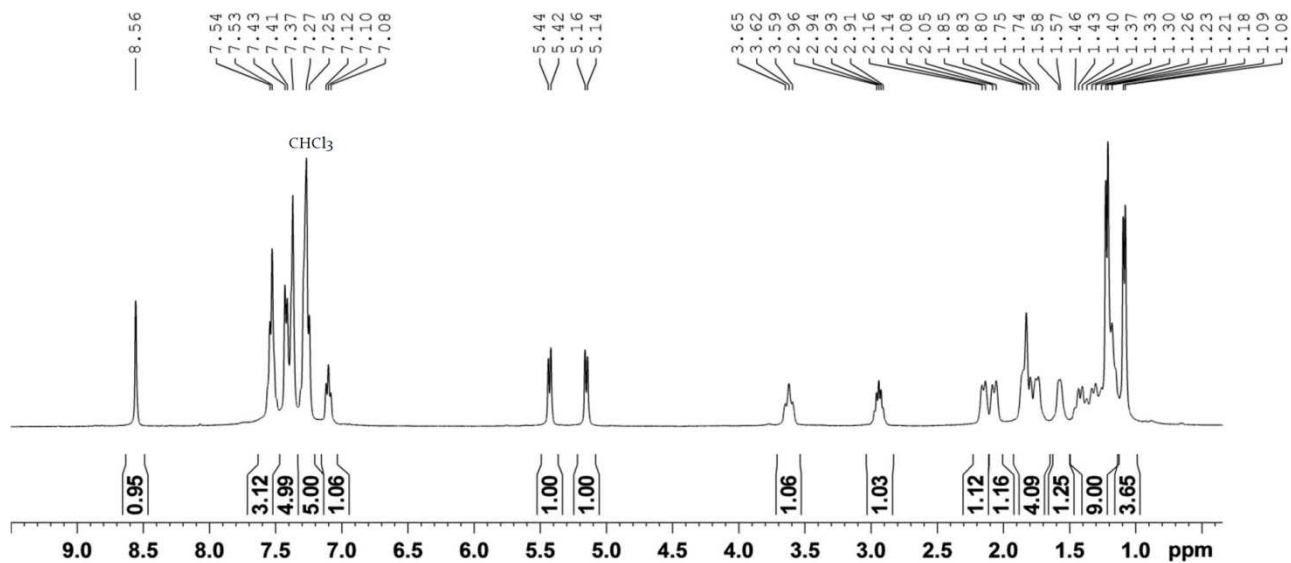
Figure S3.19: ¹H NMR of **22** (CDCl3, 400 MHz)
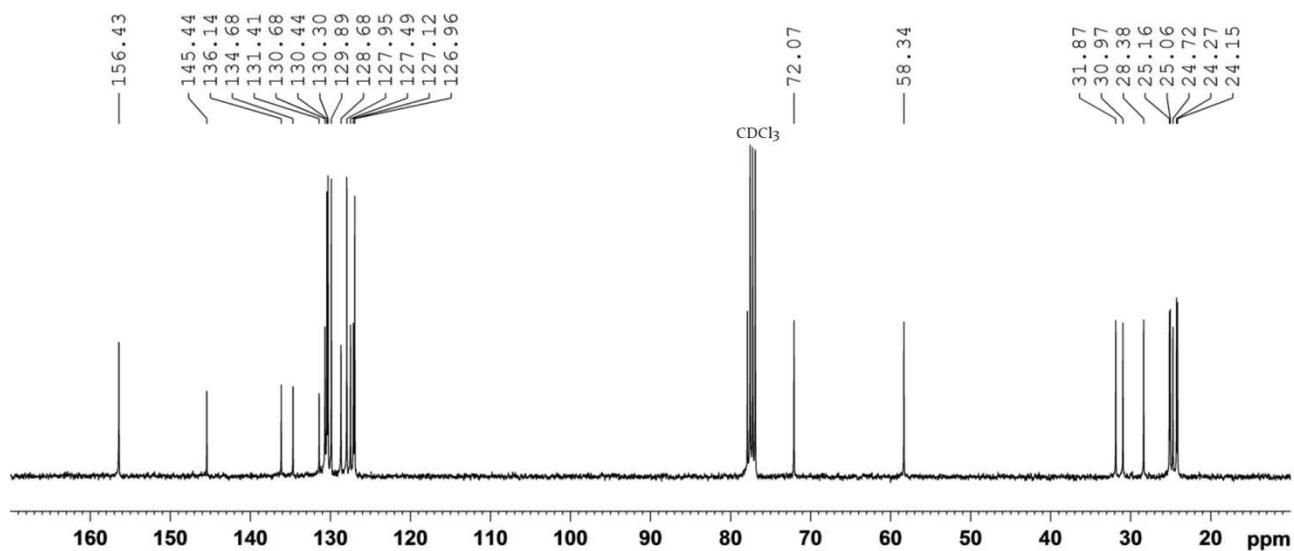
Figure S3.20: ¹³C NMR of **22** (CDCl3, 100 MHz)
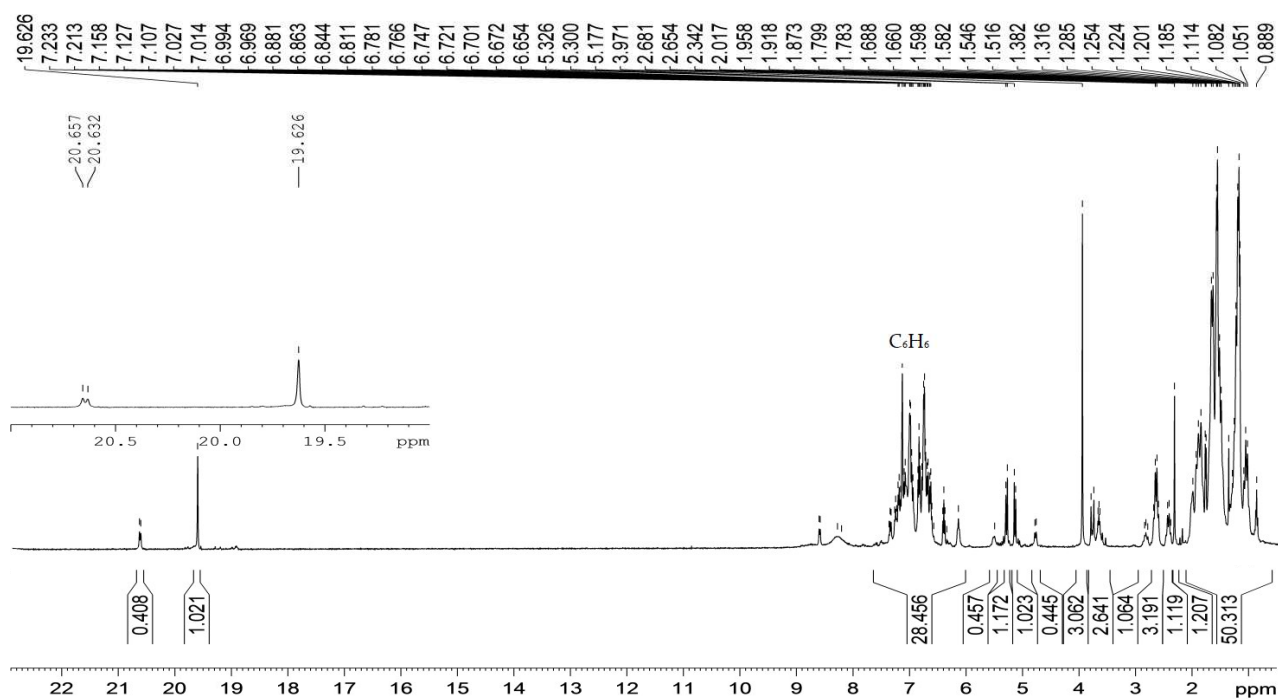
Figure S3.21: ¹H NMR of **1** (C₆D₆, 400 MHz)
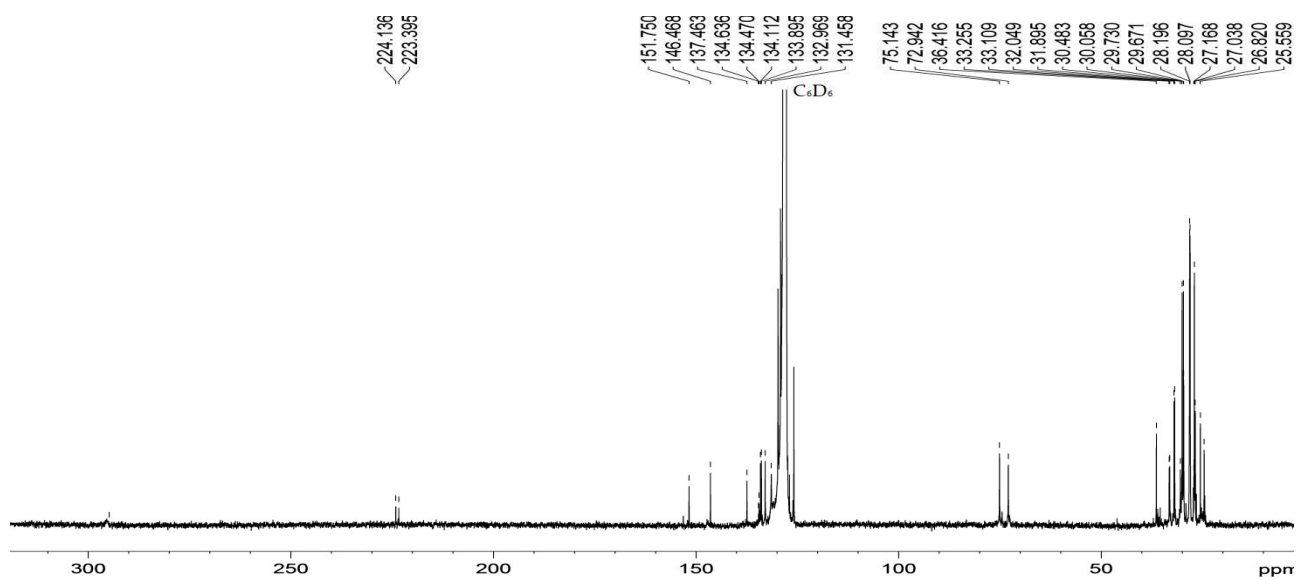
Figure S3.22: ¹³C NMR of **1** (C₆D₆, 100 MHz)
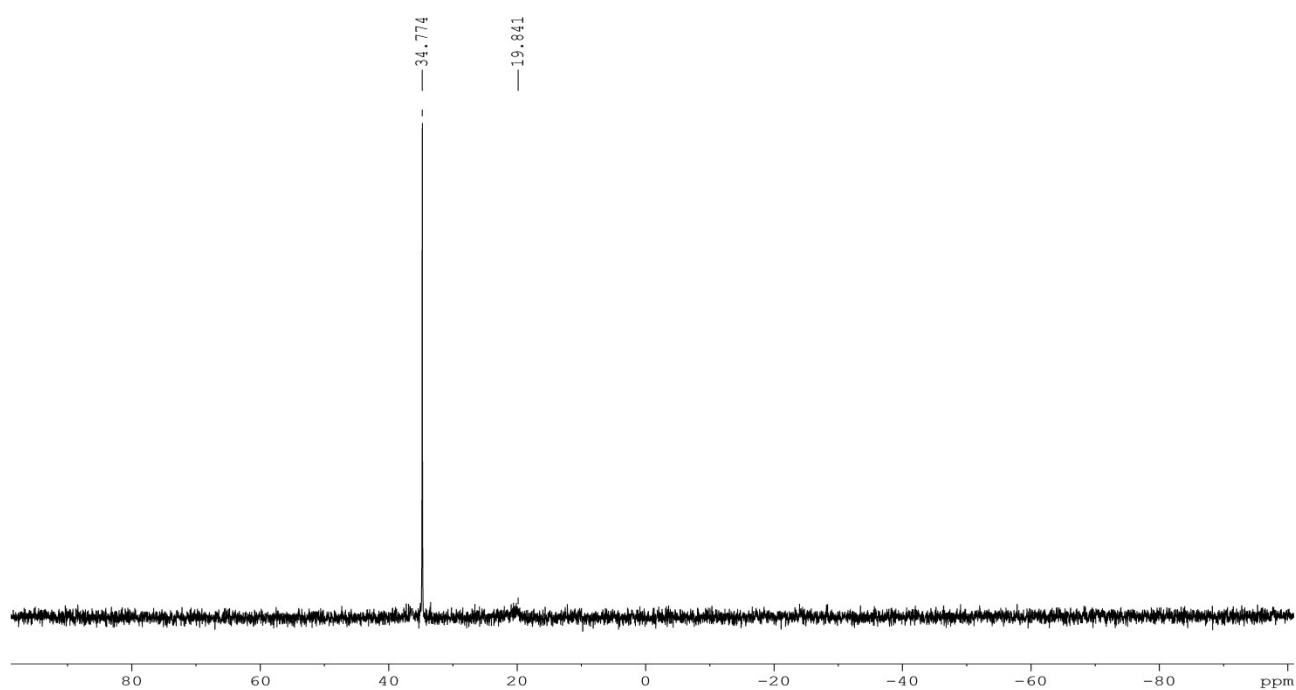
Figure S3.23: ^{31}P NMR of **1** (C$_6$D$_6$, 161.97 MHz)
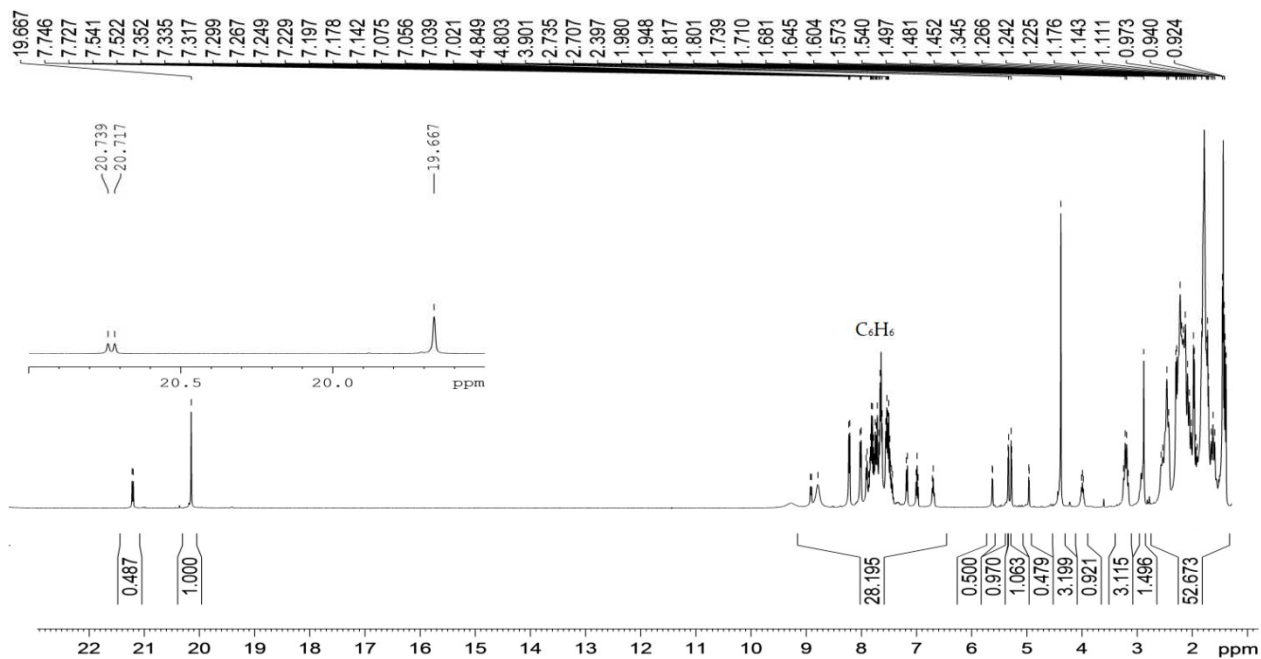
Figure S3.24: ¹H NMR of **2** (C₆D₆, 400 MHz)
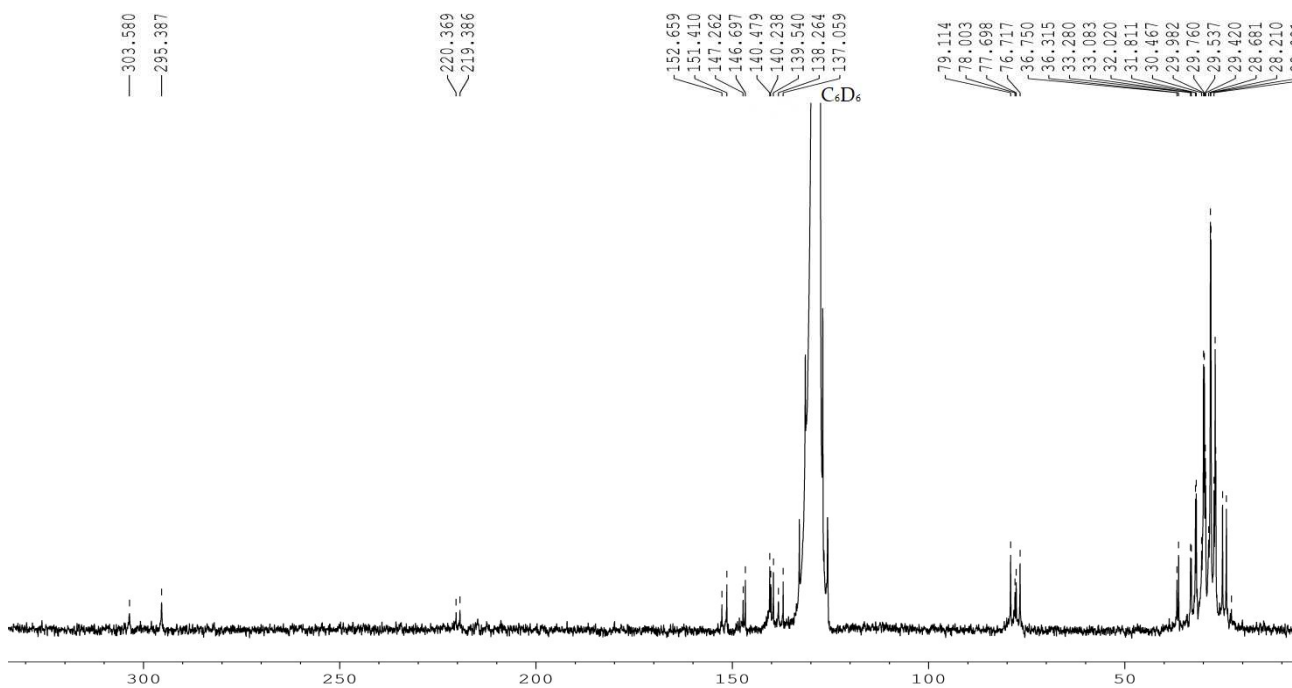
Figure S3.25: ¹³C NMR of **2** (C₆D₆, 100 MHz)

35.037

20.797

80   60   40   20   0   −20   −40   −60   −80   ppm
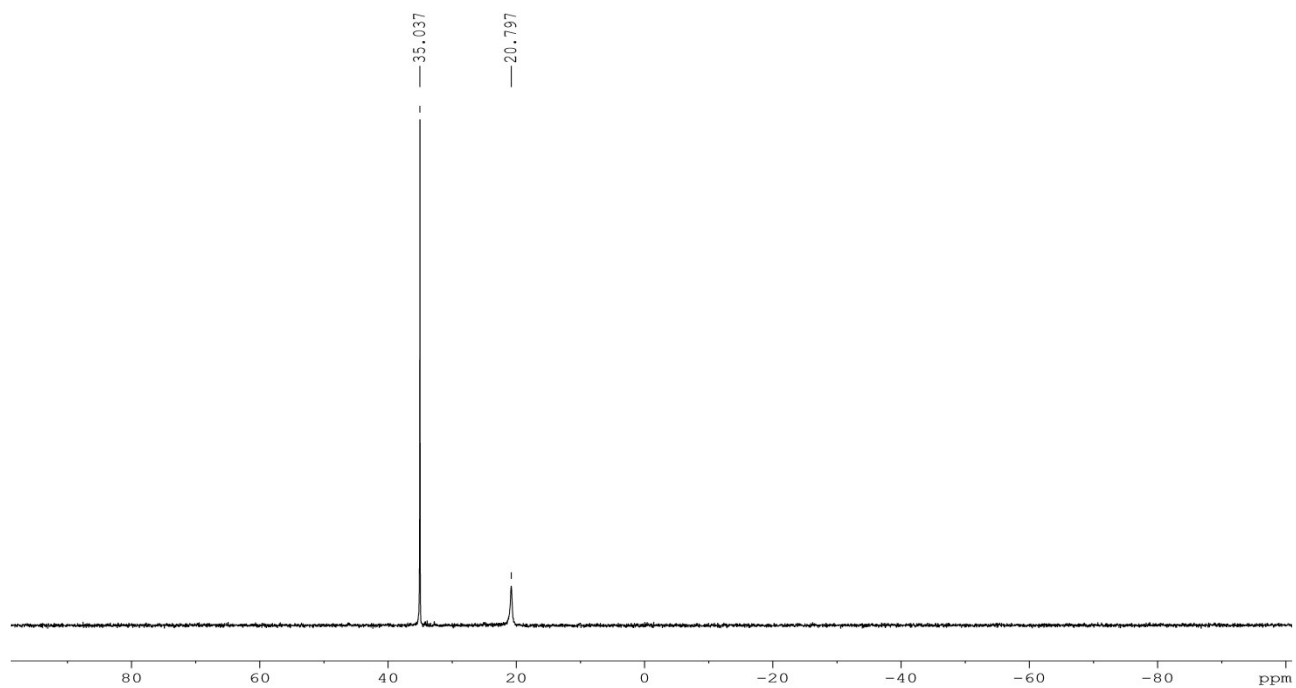
Figure S3.26: ^{31}P NMR of **2** (C$_6$D$_6$, 161.97 MHz)
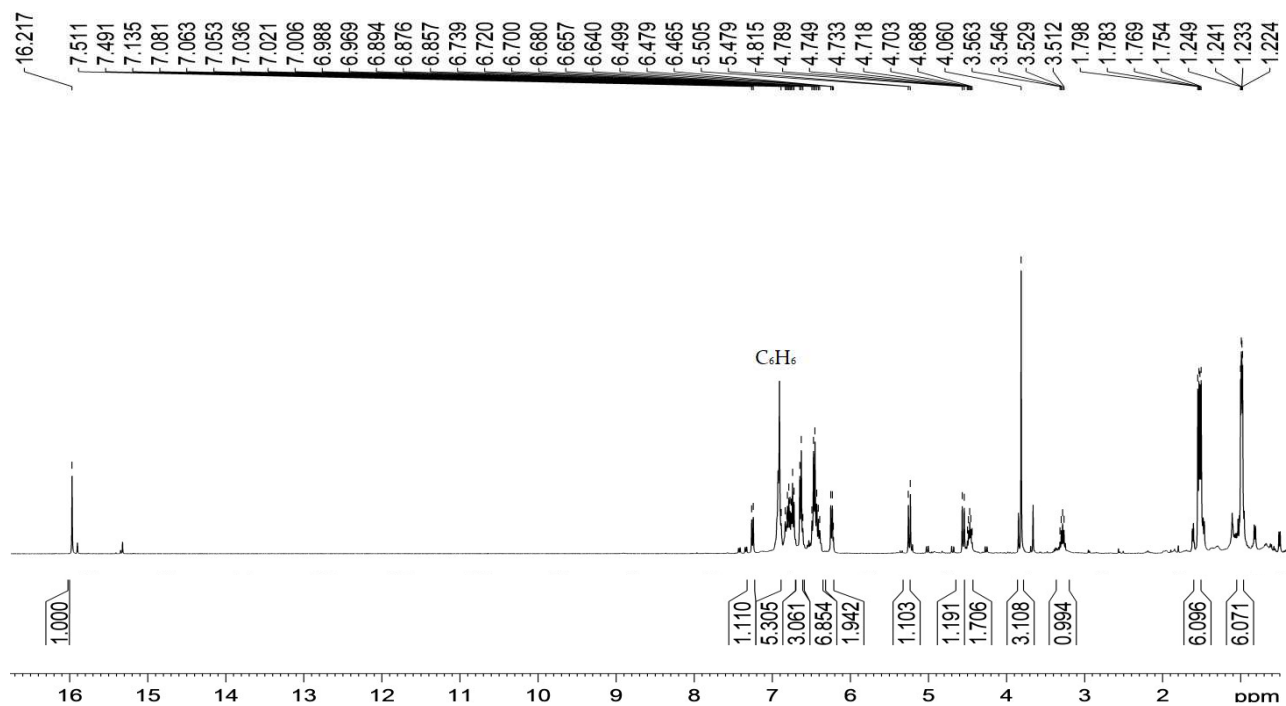
Figure S3.27: ^{1}H NMR of **3** (C$_6$D$_6$, 400 MHz)
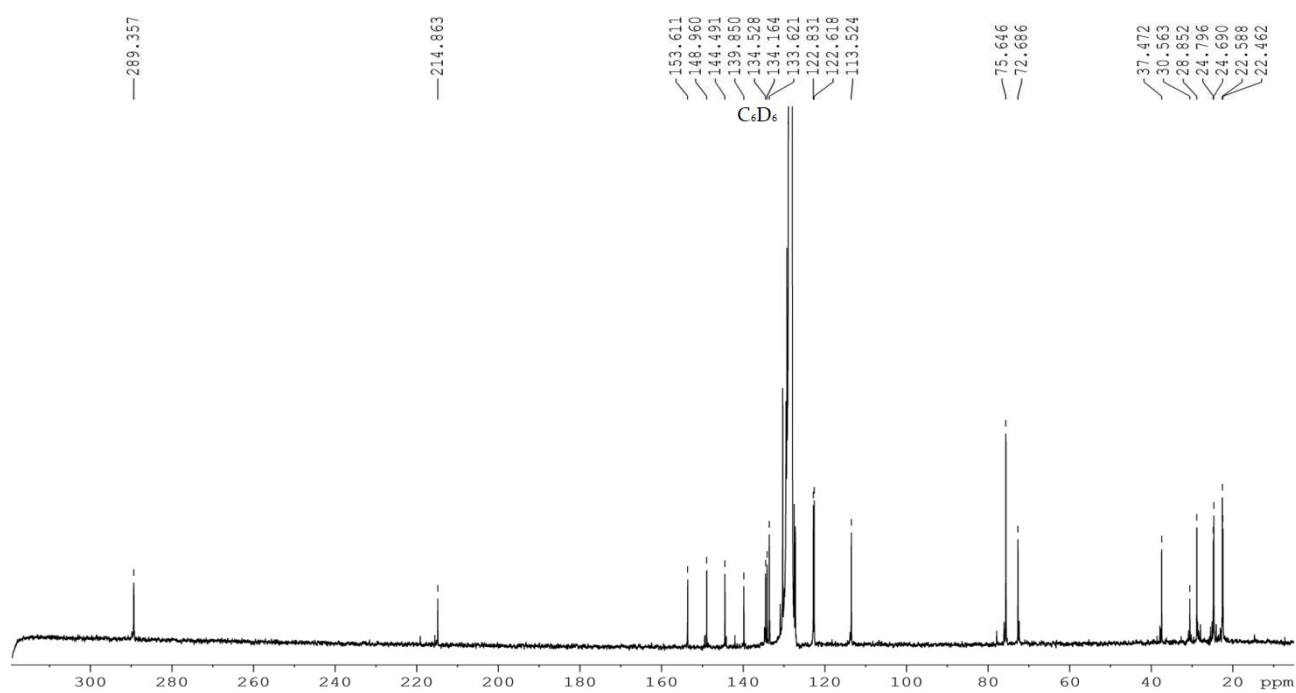
Figure S3.28: ^{13}C NMR of **3** (C$_6$D$_6$, 100 MHz)
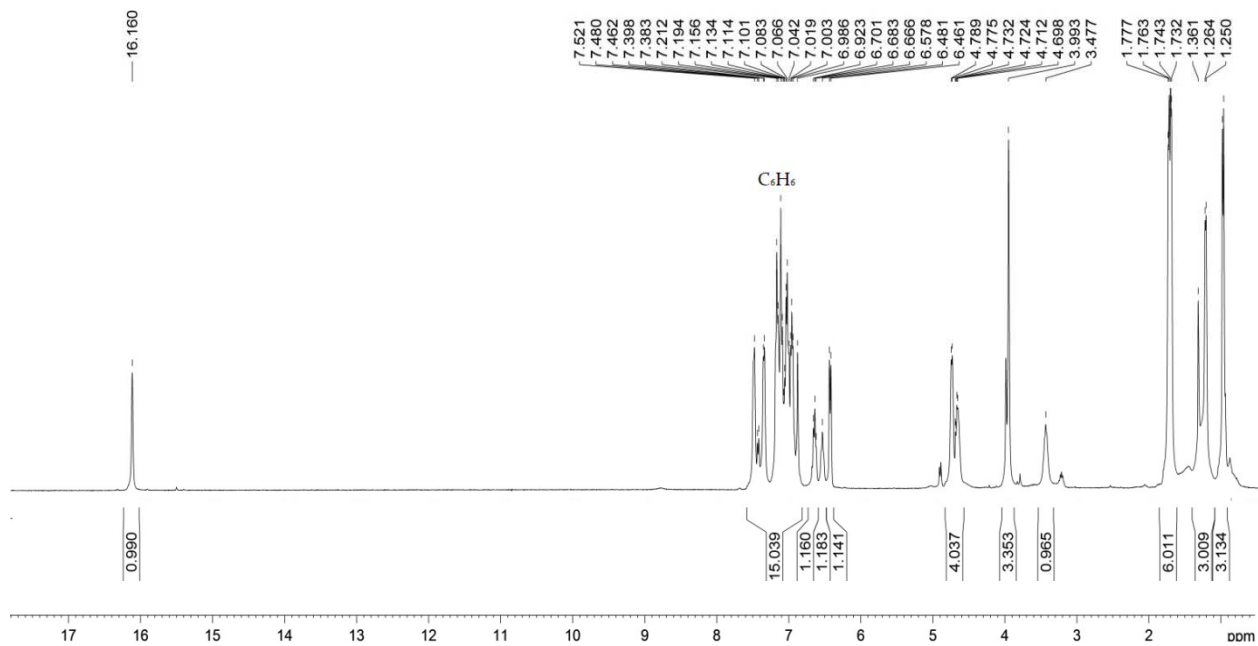
Figure S3.29: ^{1}H NMR of **4** (C$_6$D$_6$, 400 MHz)
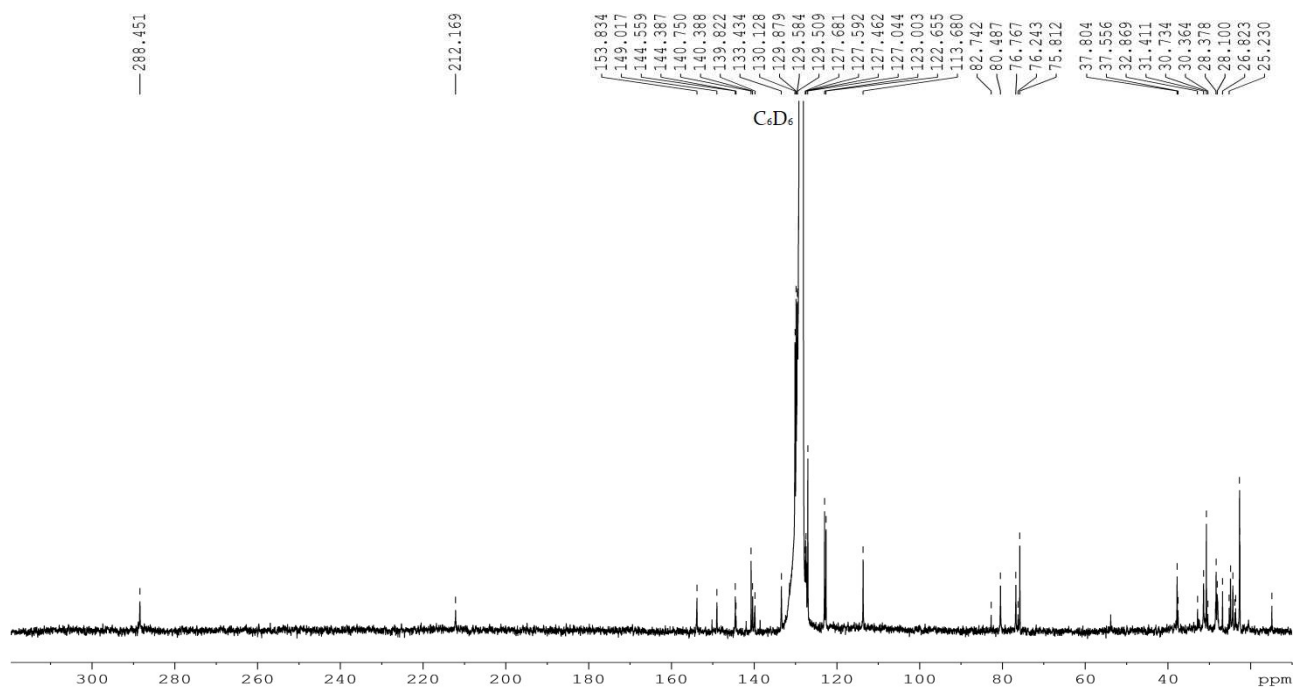
Figure S3.30: ^{13}C NMR of **4** (C$_6$D$_6$, 100 MHz)
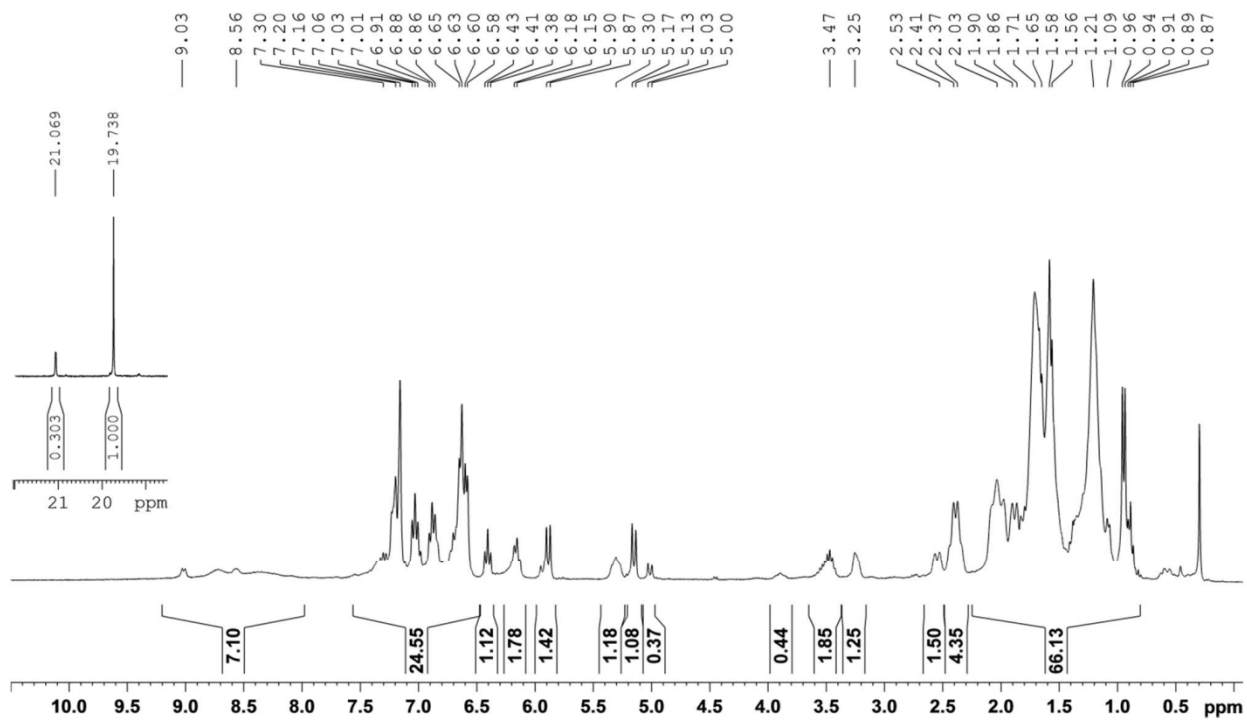
Figure S3.31: ^{1}H NMR of **5** (C$_6$D$_6$, 400 MHz)
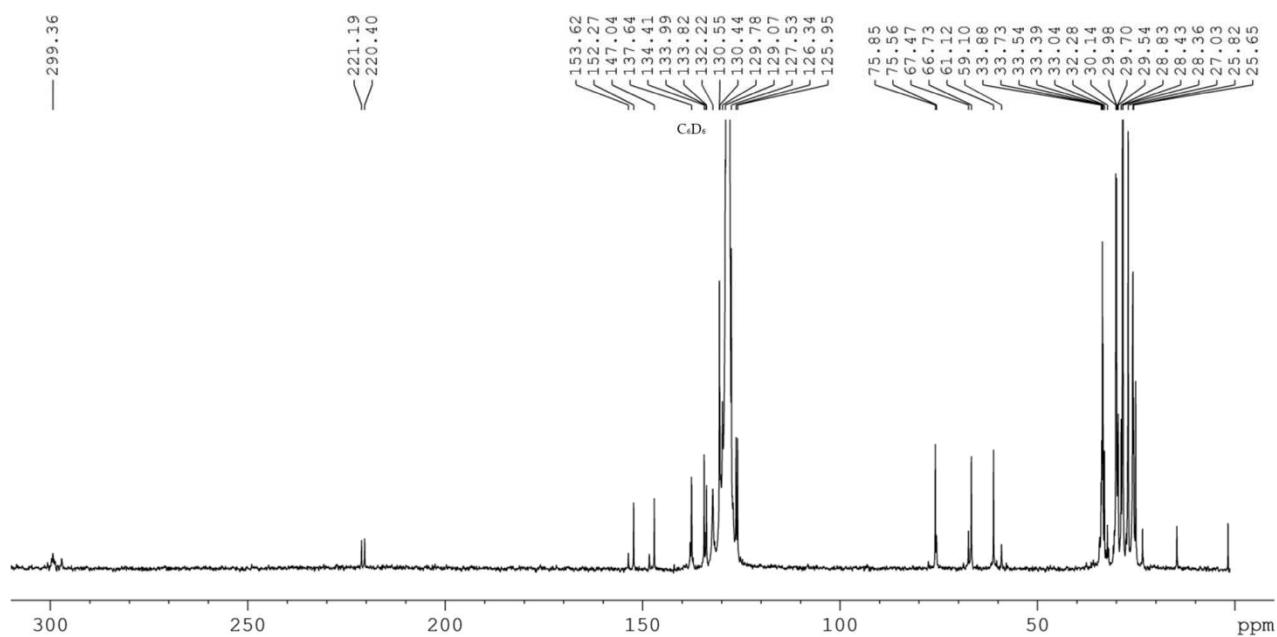
Figure S3.32: ^{13}C NMR of **5** (C$_6$D$_6$, 100 MHz)
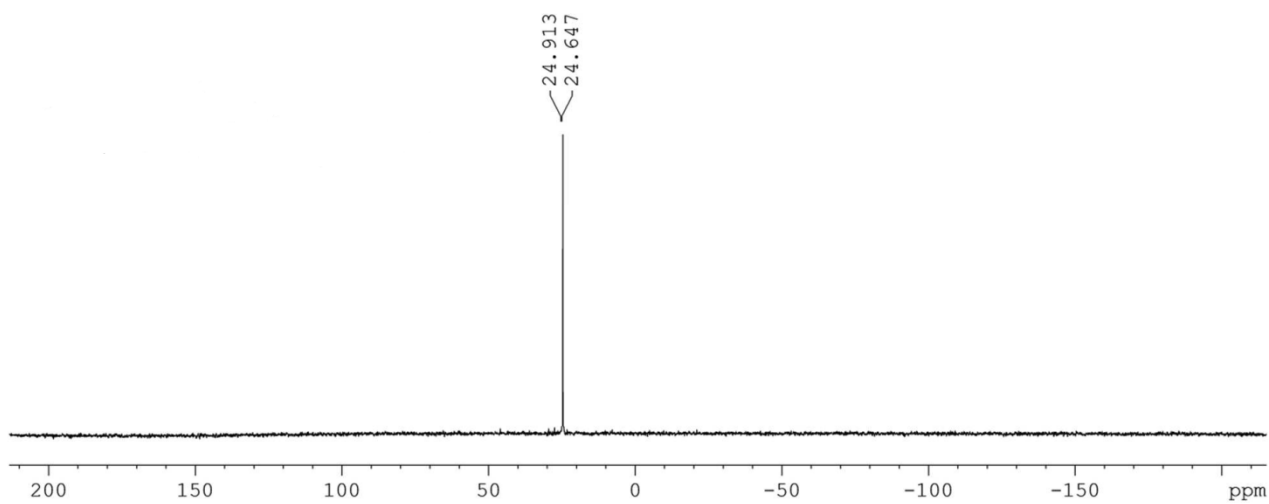
Figure S3.33: ^{31}P NMR of **5** (C$_6$D$_6$, 161.97 MHz)
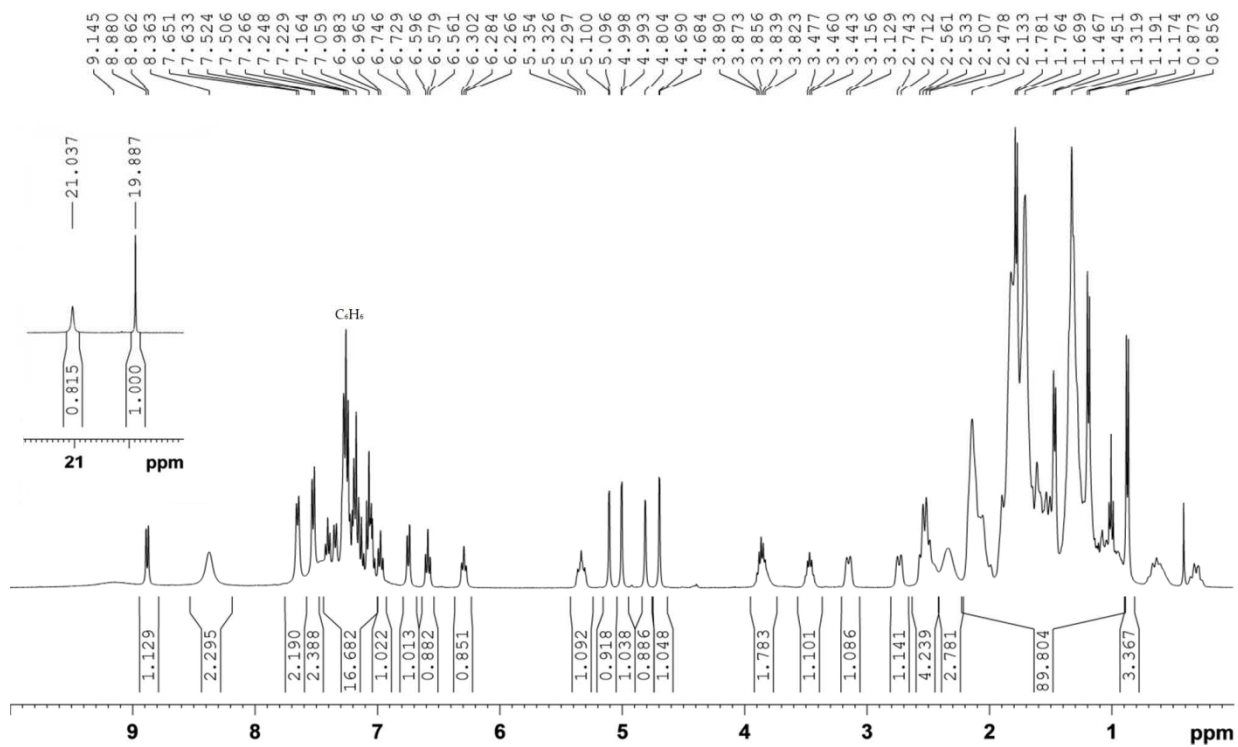
Figure S3.34: ^{1}H NMR of **6** (C$_6$D$_6$, 400 MHz)
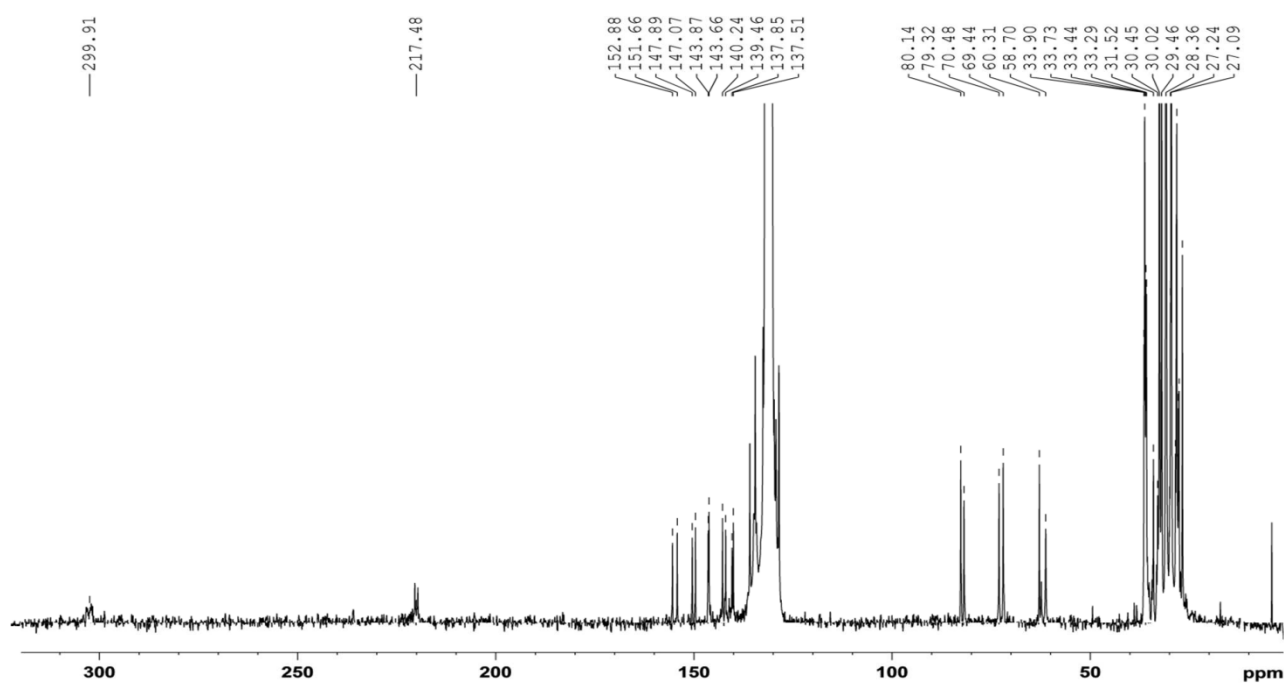
Figure S3.35: ^{13}C NMR of **6** (C$_6$D$_6$, 100 MHz)
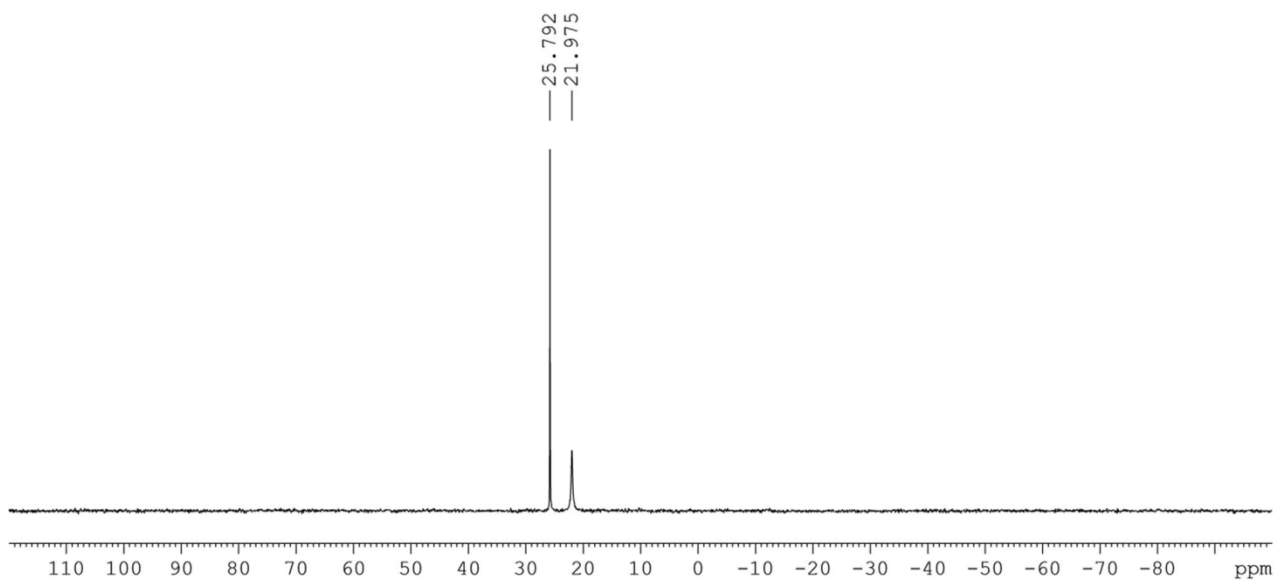
Figure S3.36: ^{31}P NMR of **6** (C$_6$D$_6$, 161.97 MHz)
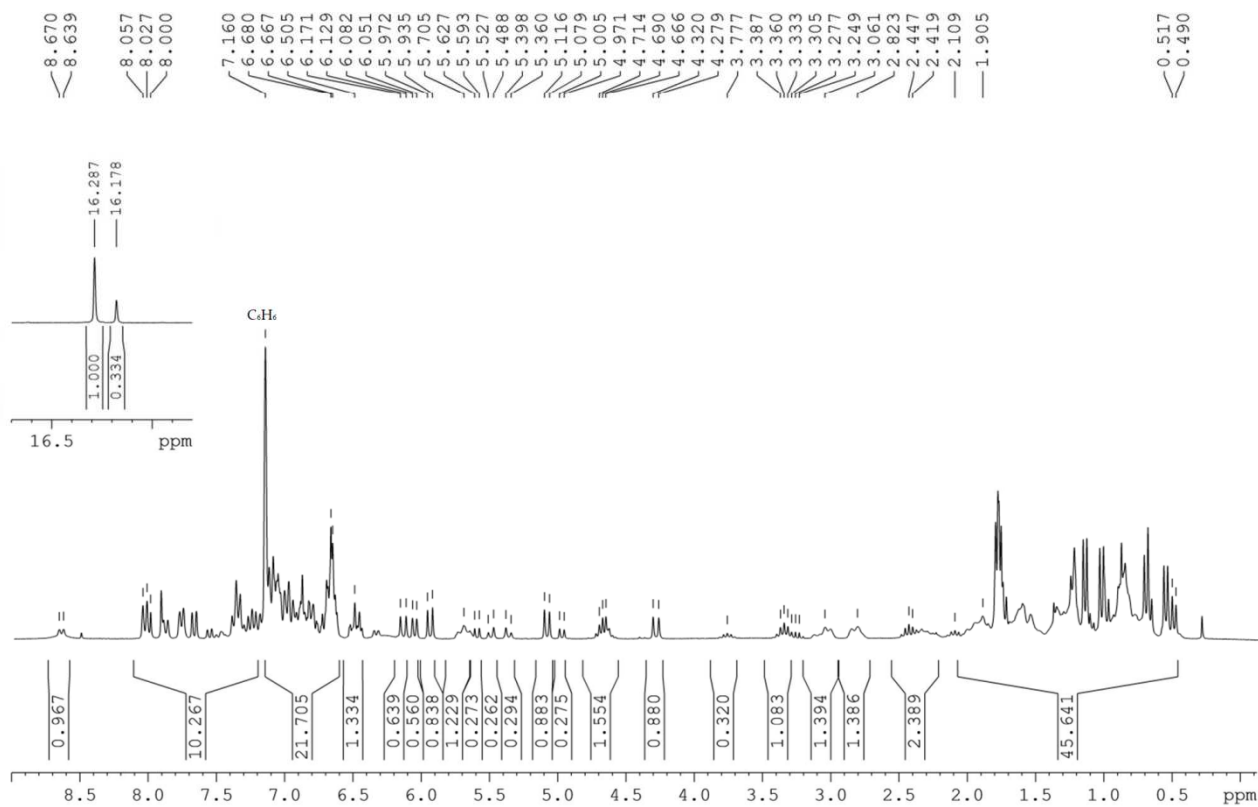
Figure S3.37: ¹H NMR of **7** (C₆D₆, 400 MHz)
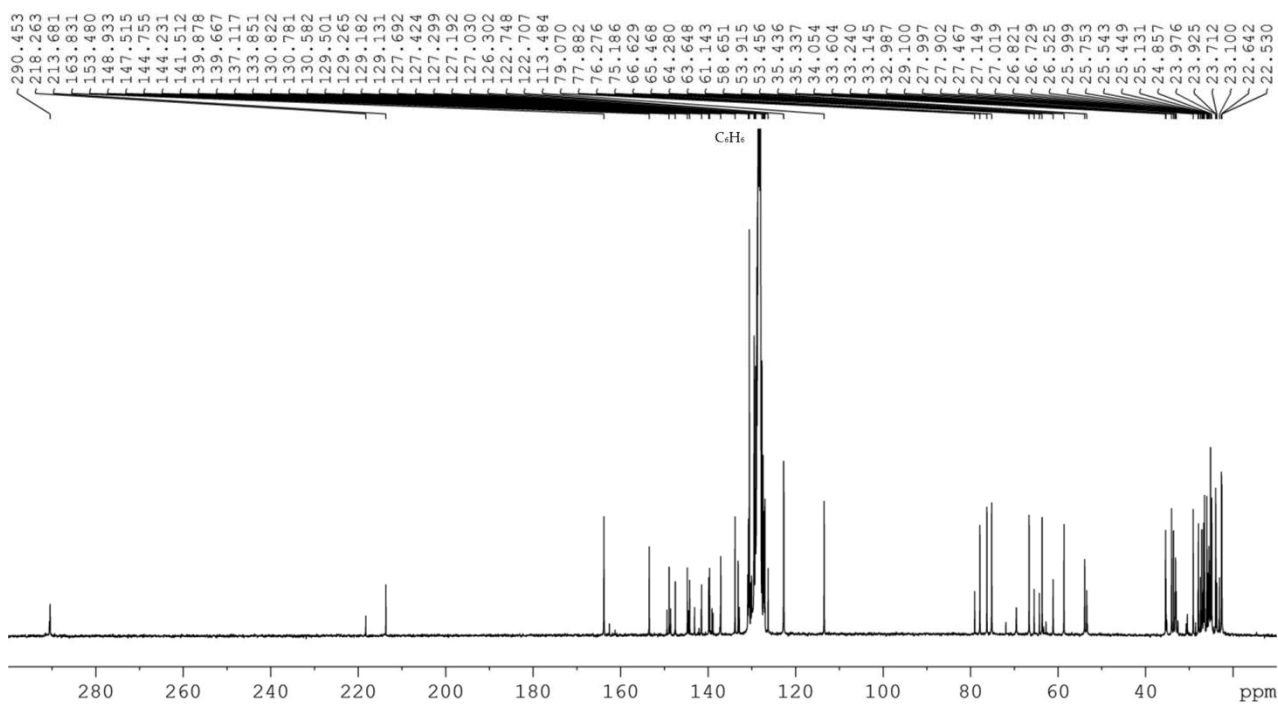
Figure S3.38: ¹H NMR of **7** (C₆D₆, 400 MHz)
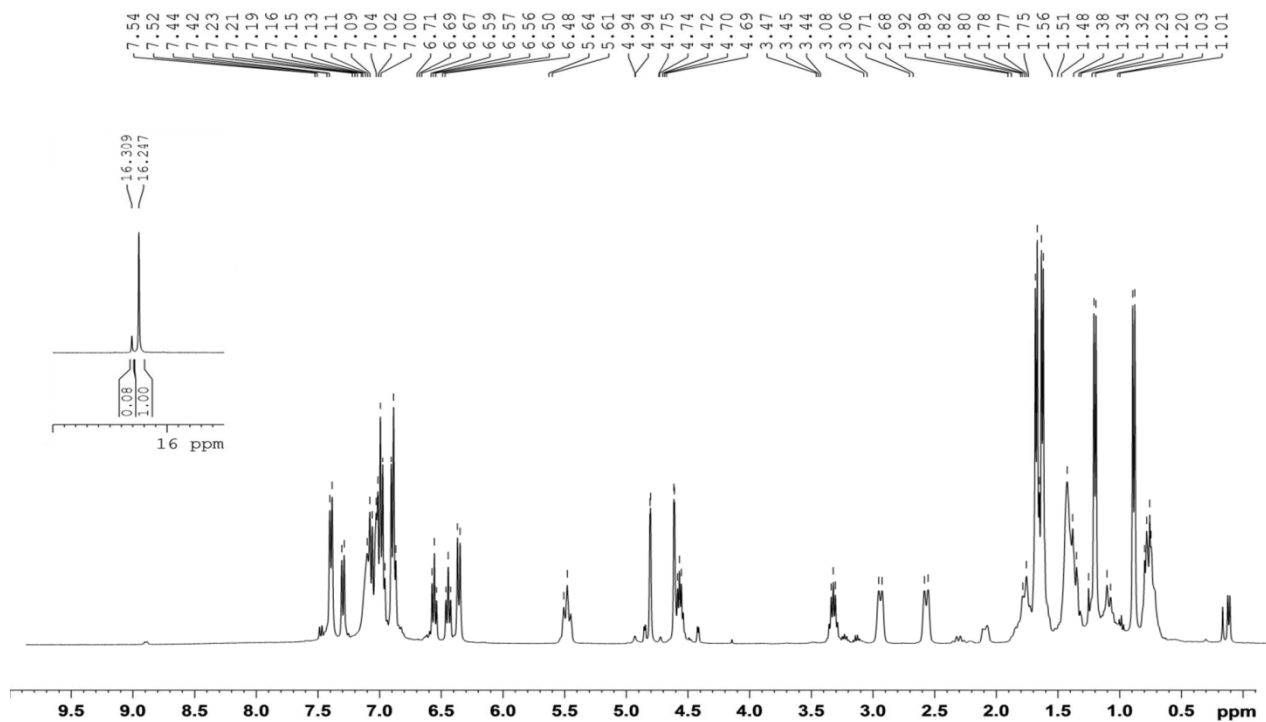
Figure S3.39: ¹H NMR of **8** (C₆D₆, 400 MHz)
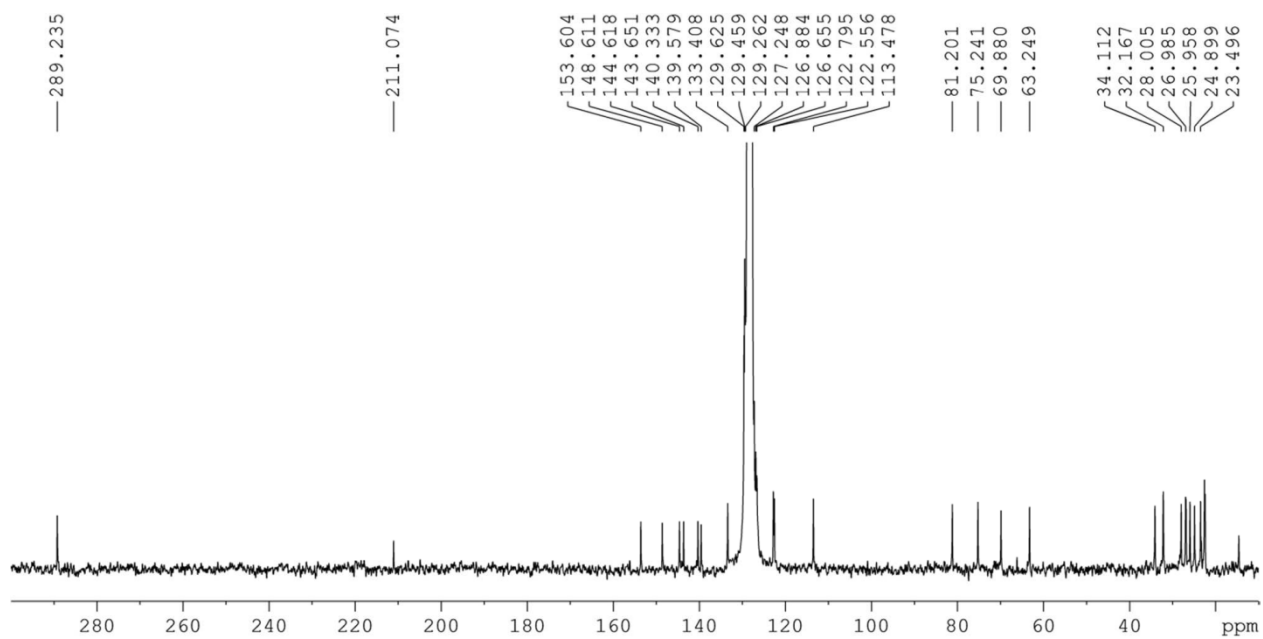
Figure S3.40: ¹³C NMR of **8** (C₆D₆, 100 MHz)
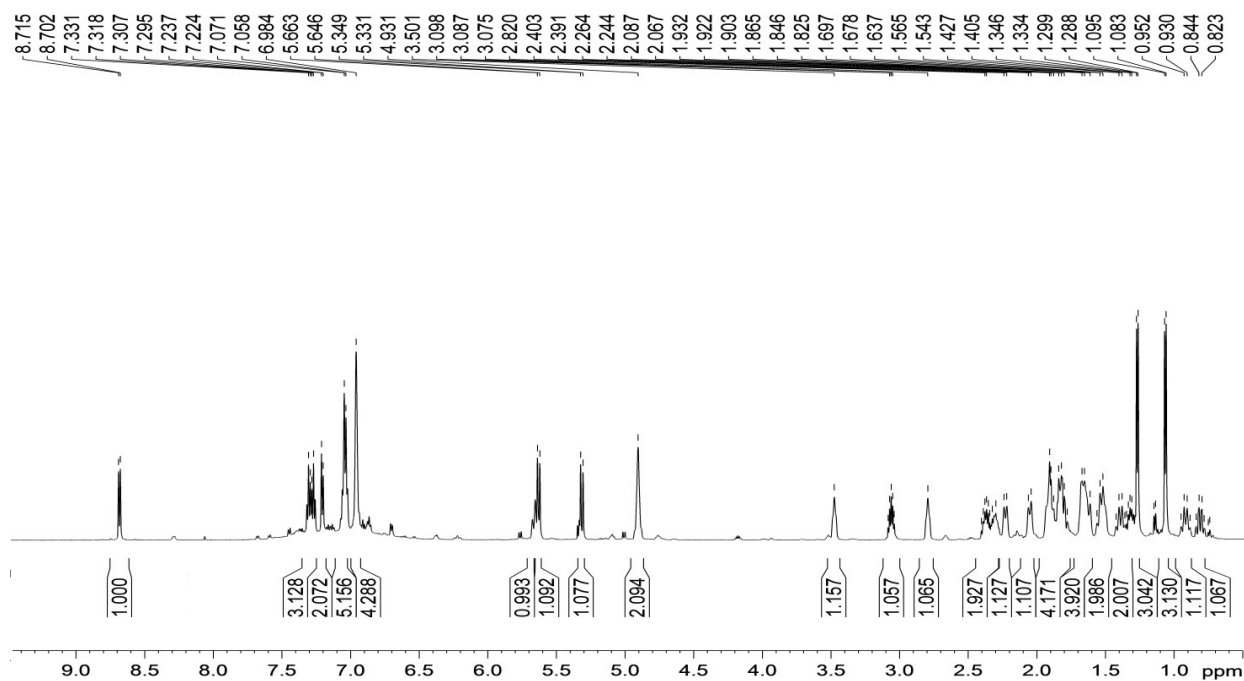
Figure S3.41: ^{1}H NMR of **34** (CD$_2$Cl$_2$, 600 MHz)
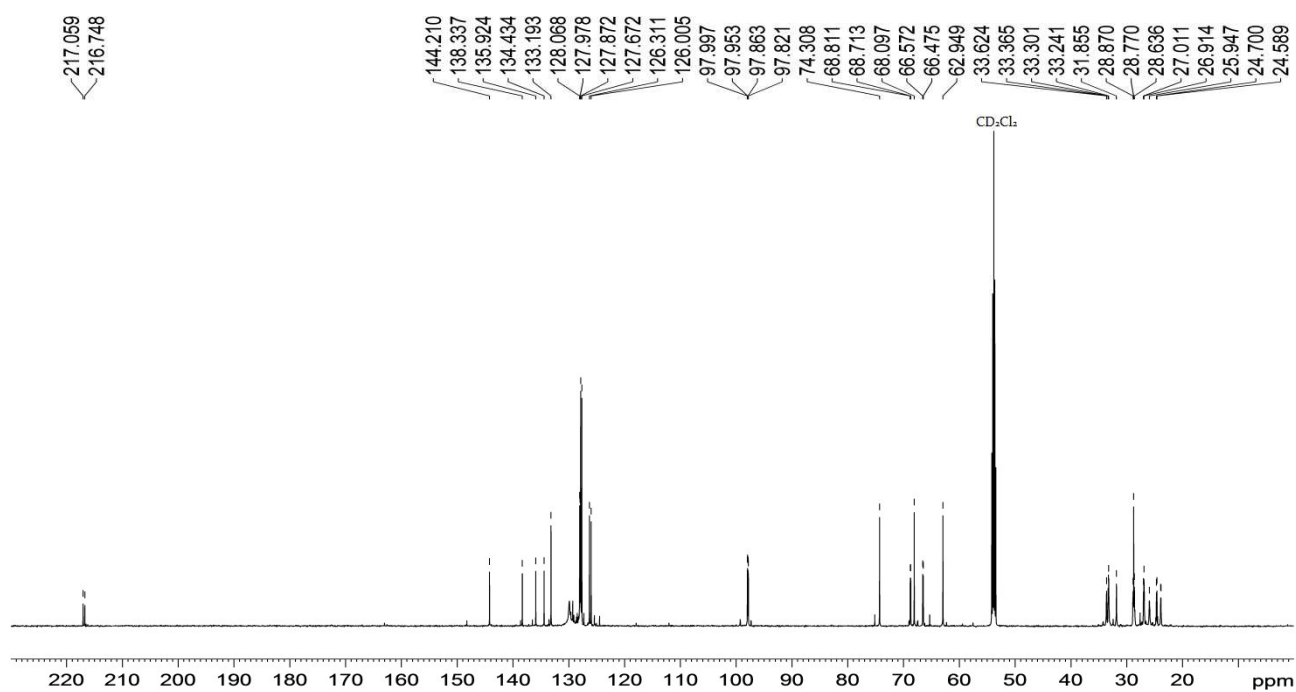
Figure S3.42: ^{13}C NMR of **34** (CD$_2$Cl$_2$, 125 MHz)
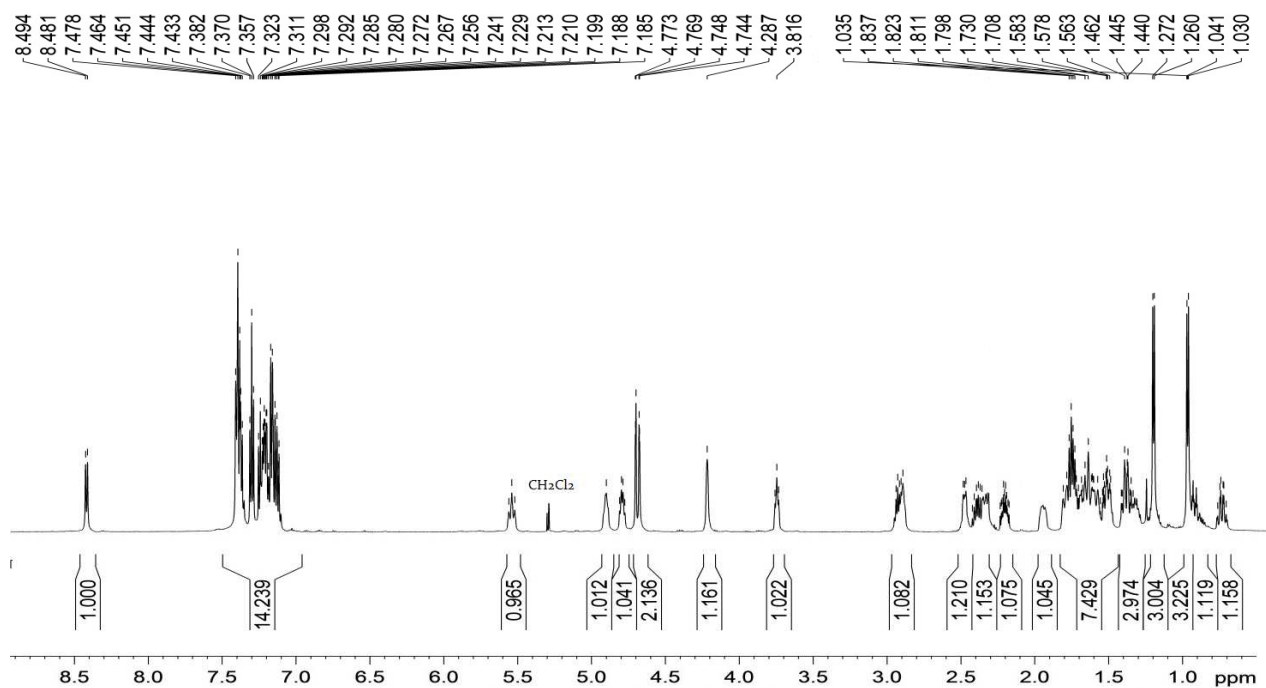
Figure S3.43: ^{1}H NMR of **35** (CD$_2$Cl$_2$, 600 MHz)
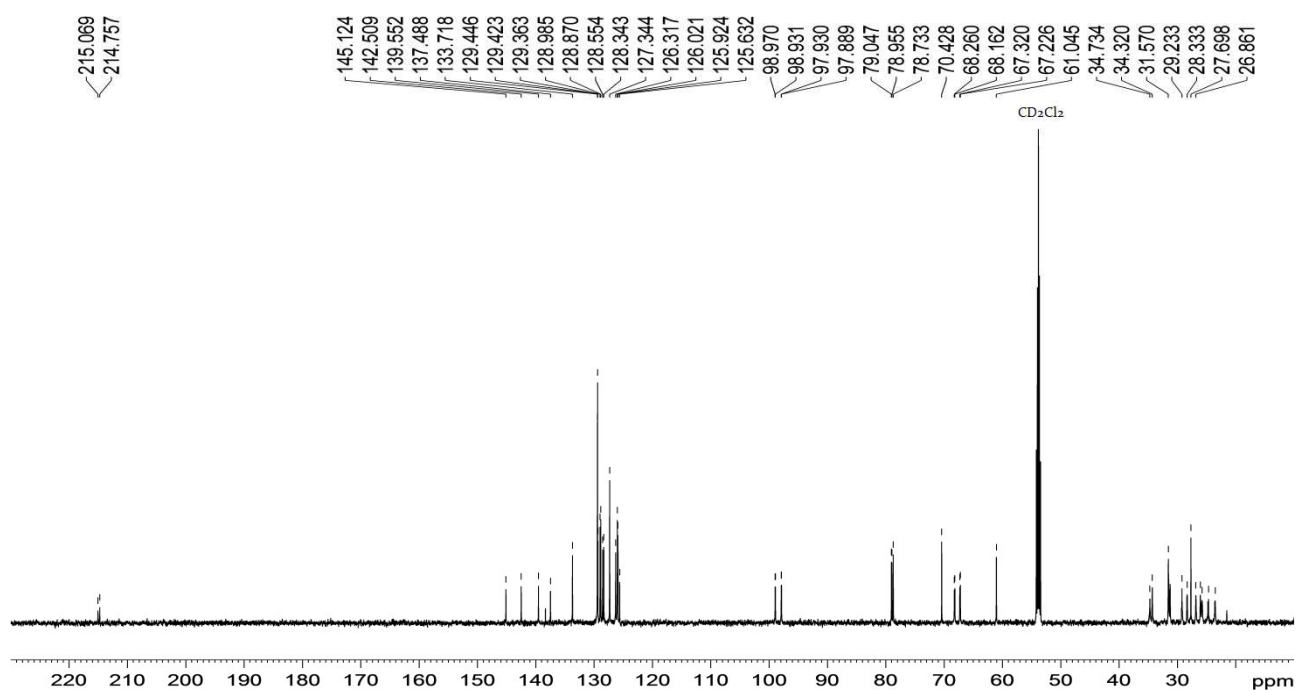
Figure S3.44: ^{13}C NMR of **35** (CD$_2$Cl$_2$, 125 MHz)
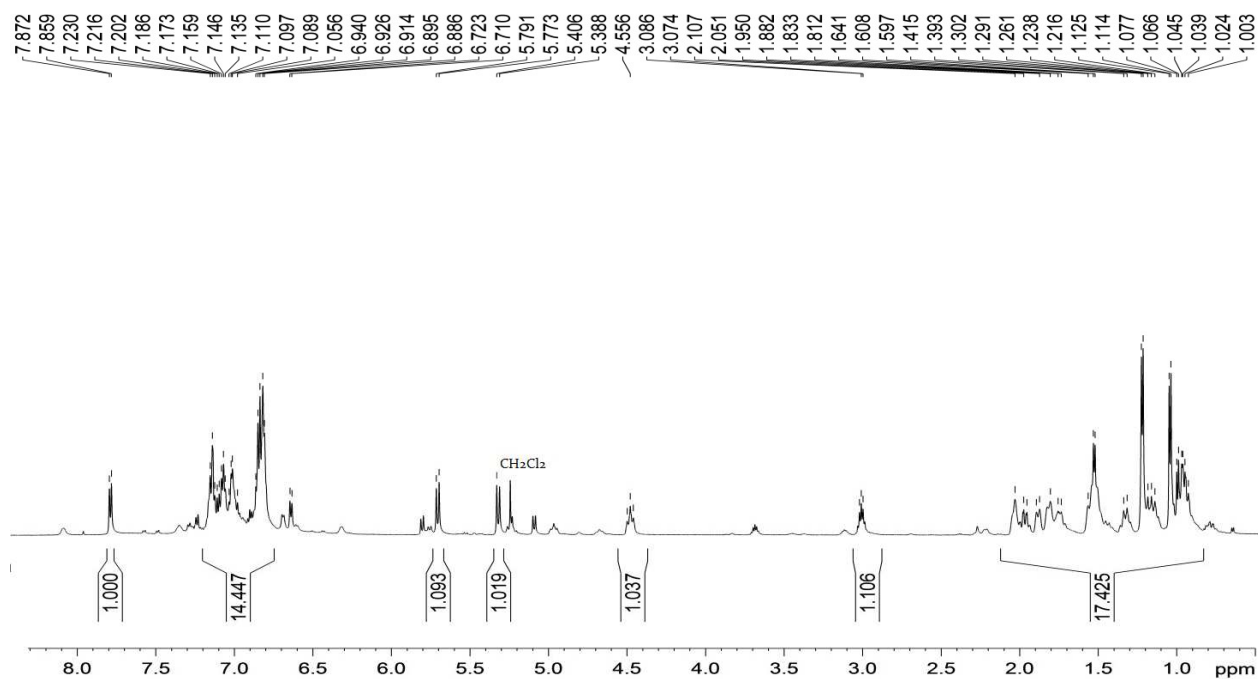
Figure S3.45: ^{1}H NMR of **36** (CD$_2$Cl$_2$, 600 MHz)
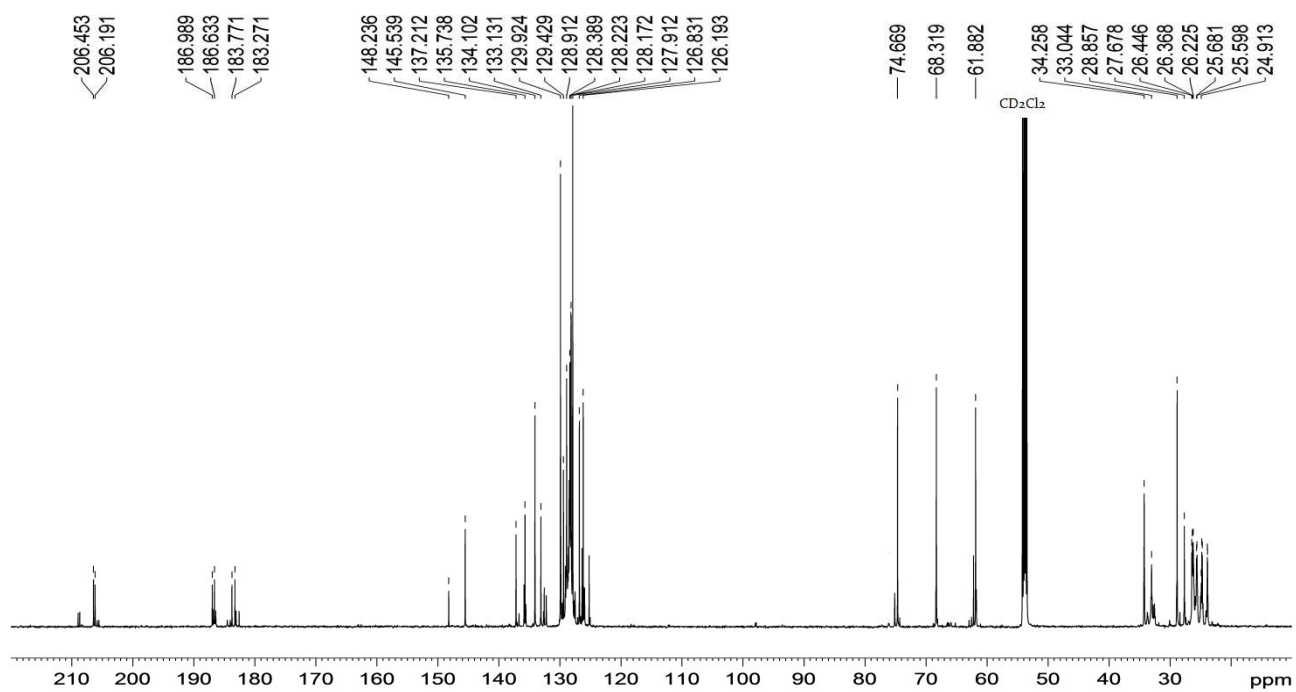
Figure S3.46: ^{13}C NMR of **36** (CD$_2$Cl$_2$, 125 MHz)
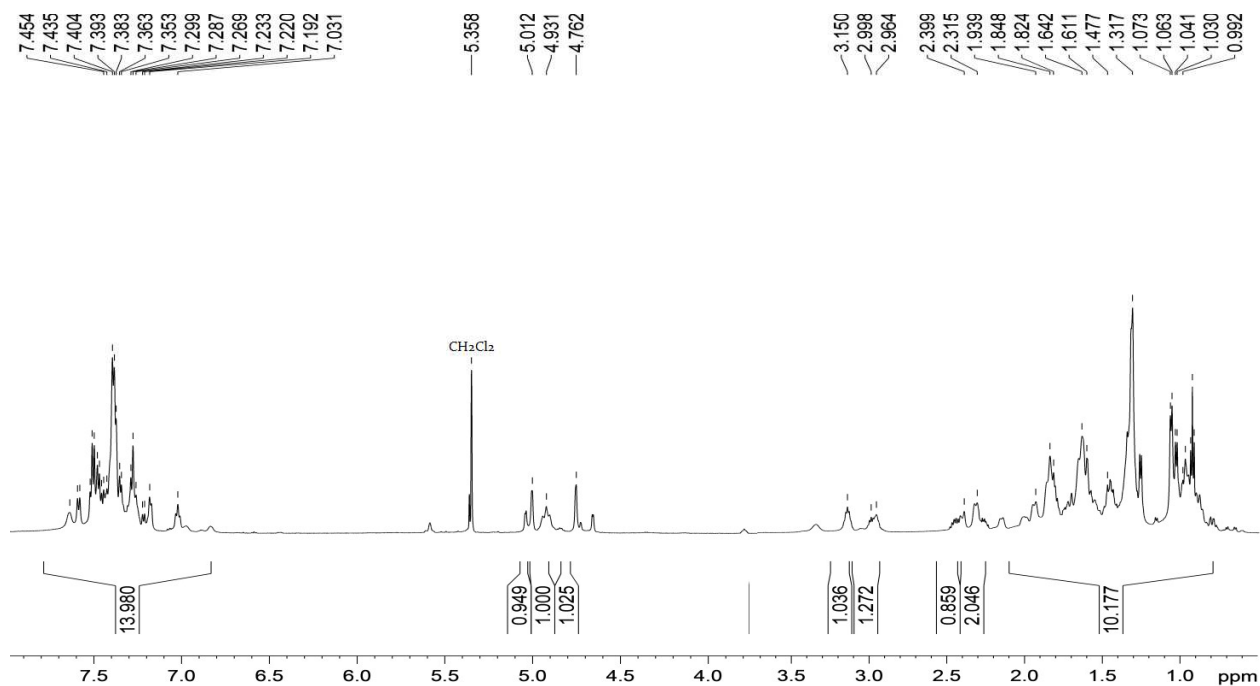
Figure S3.47: ^{1}H NMR of **37** (CD$_2$Cl$_2$, 600 MHz)
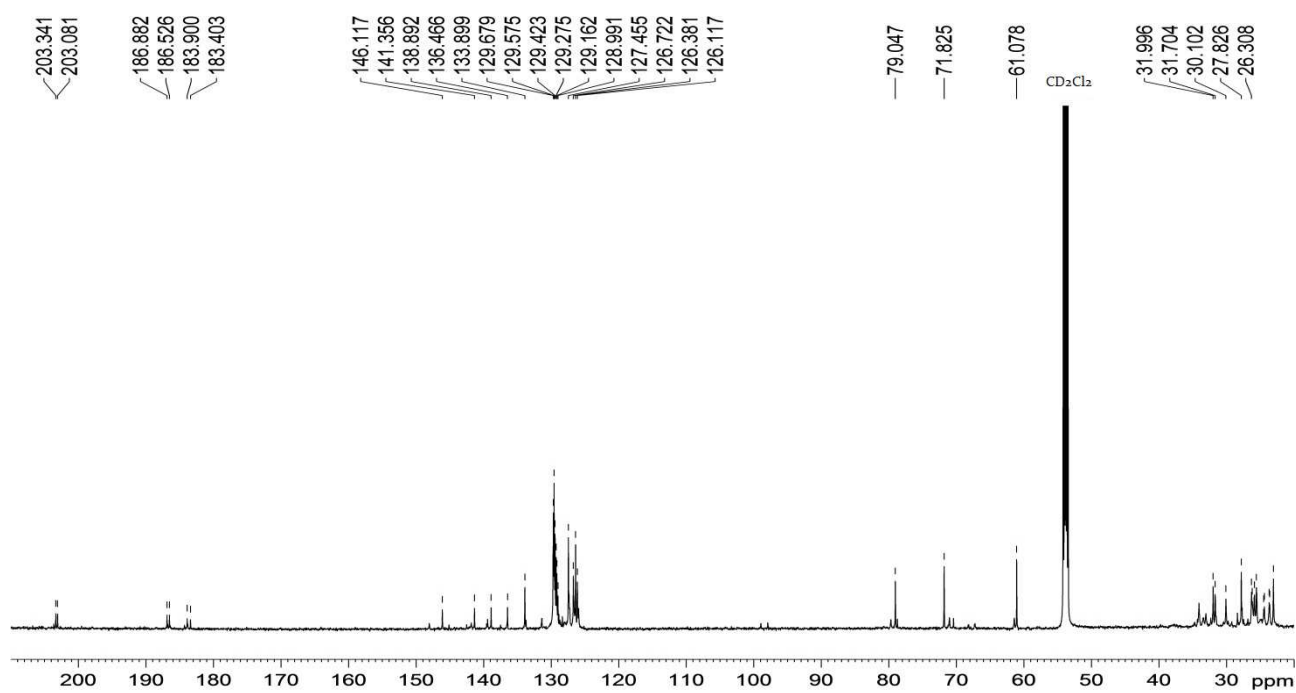
Figure S3.48: ^{1}H NMR of **37** (CD$_2$Cl$_2$, 600 MHz)

3.8.9 Crystal structure determinations[75]

The crystal data of compounds **7**, **8**, **34** and **35** were collected at room temperature using a Nonius Kappa CCD diffractometer with graphite monochromated Mo-K radiation. The data sets were integrated with the Denzo-SMN package[76] and corrected for Lorentz, polarization and absorption effects (SORTAV). The structure was solved by direct methods using SIR97[77] system of programs and refined using full-matrix leastsquares with all non-hydrogen atoms anisotropically and hydrogens included on calculated positions, riding on their carrier atoms. The C7 and C10 atoms of the *COD* alkene molecule in the structure **35** were found disordered and refined isotropically over two independent positions.

All calculations were performed using SHELXL-97[78] and PARST[79] implemented in WINGX[80] system of programs. The crystal data are given in Table S1.

Crystallographic data (excluding structure factors) have been deposited at the Cambridge Crystallographic Data Centre and allocated the deposition numbers CCDC 1414525-1414526. These data can be obtained free of charge via www.ccdc.cam.ac.uk/conts/retrieving.html or on application to CCDC, Union Road, Cambridge, CB2 1EZ, UK [fax: (+44)1223-336033, e-mail: deposit@ccdc.cam.ac.uk].

Table S1: Crystallographic data

Compound	7	8	34	35
Space group	$C2/c$	$P\bar{1}$	$C2/c$	$P2_12_12_1$
Crystal System	Monoclinic	Triclinic	Monoclinic	Orthorhombic
a/Å	24.6791(2)	10.9180(2)	23.2672(6)	15.1213(5)
b/Å	14.5115(2)	11.0325(2)	14.4735(2)	11.1057(3)
c/Å	23.5392(3)	20.8647(4)	22.2443(7)	14.4735(2)
α/°	90.00	76.9799(7)	90.00	90.00
β/°	117.9167(5)	86.9927(8)	114.730(1)	90.00
γ/°	90.00	61.5591(9)	90.00	90.00
U/Å	7449.09(15)	2161.06(7)	6803.9(3)	3419.0(2)
T/K	295	295	295	295
D_c/g cm^{-3}	1.325	1.198	1.306	1.300
F(000)	3088	814	2800	1400
μ(Mo-Kα)/cm^{-1}	5.97	5.18	0.608	0.605
Measured Reflections	34855	27171	27353	14007
Unique Reflections	10795	15697	9786	7166
R_{int}	0.0430	0.0371	0.0500	0.1111
Obs. Refl.ns	8156	13021	6641	5908

[75] X-Ray analysis was carried on by Prof. Valerio Bertolasi at the University of Ferrara

[76] Z. Otwinowski, W. Minor, *Methods in Enzymology*, C.W. Carter, R.M. Sweet Editors, Vol. 276, Part A, Academic Press, London, **1997**, 307-326.

[77] A. Altomare, M. C. Burla, M. Camalli, G. L. Cascarano, C. Giacovazzo, A. Guagliardi, A. G: Moliterni, G. Polidori, R. Spagna, *J. Appl. Crystallogr.* **1999**, *32*, 115-119.

[78] G. Sheldrick, SHELX-97, *Program for Crystal Structure Refinement*, University of Gottingen, Germany, **1997**.

[79] M. Nardelli, *J. Appl. Crystallogr.* **1995**, *28*, 659.

[80] L. J. Farrugia, *J. Appl. Crystallogr.* **1999**, *32*, 837.

Table S1: Crystallographic data

Compound	7	8	34	35
R(F$_2$) (Obs.Refl.ns)	0.0323	0.0440	0.0501	0.0724
wR(F$_2$) (All Refl.ns)	0.0864	0.1117	0.1393	0.1807
No. Variables	419	858	381	379

3.8.10 Cartesian coordinates and energies of calculated structures[81]

[Ru] E(gas)=-3373.4293348 G(gas)=-3372.470993 E(CH$_2$Cl$_2$)=-3373.4437978

---

[81] Theoretical chemistry studies were performed by prof. Chiara Costabile at the University of Salerno

C 3.972346 -1.776102 1.872974
C 4.002205 -0.312258 1.365882
C 5.412935 0.302721 1.501515
C 5.923647 0.190221 2.953624
C 5.891322 -1.258988 3.466800
C 4.486813 -1.866710 3.321234
P 3.074983 -0.154419 -0.273743
Ru 0.602711 -0.293927 0.079652
Cl 0.812409 -0.593016 2.481080
C 3.446815 1.514472 -1.069975
C 3.012010 2.666045 -0.133628
C 3.084618 4.031018 -0.843365
C 4.479767 4.289912 -1.435738
C 4.900639 3.147306 -2.373500
C 4.846884 1.776130 -1.669386
C 3.755341 -1.508722 -1.421151
C 5.285496 -1.743818 -1.449008
C 5.636234 -2.991104 -2.287356
C 5.076568 -2.902006 -3.715690
C 3.562266 -2.636440 -3.698660
C 3.205211 -1.393423 -2.861925
Cl 0.245998 0.395160 -2.231302
C -1.378307 0.073097 0.380410
N -1.850063 1.299531 0.730757
C -3.322619 1.390912 0.642145
C -3.706784 -0.129174 0.730915
N -2.448617 -0.769691 0.235936
C -1.019583 2.373877 1.301187
C -3.810516 2.130208 -0.602548
C -3.102634 2.084476 -1.823050
C -3.608301 2.745113 -2.956805
C -4.818955 3.456820 -2.888758
C -5.525192 3.510557 -1.674221
C -5.021180 2.851981 -0.540273
C -4.998680 -0.540530 0.054873
C -6.147454 -0.727156 0.854686
C -7.385790 -1.056409 0.277719
C -7.489830 -1.214265 -1.114566
C -6.351952 -1.033249 -1.920720
C -5.117711 -0.694637 -1.343079
C -2.396255 -2.152429 -0.151084
C -2.562267 -3.198460 0.798055
C -2.581528 -4.522919 0.303247
C -2.416967 -4.814739 -1.058945
C -2.210731 -3.770656 -1.976971
C -2.205313 -2.446124 -1.520349
C -2.681716 -2.953983 2.303487
C 0.589403 -2.078264 -0.227214
H 0.603005 -2.495906 -1.261509
H 0.589670 -2.823984 0.602748
H -3.730116 1.905456 1.536508
H -3.807504 -0.374050 1.813734

H 3.293763 -2.414572 -0.961749
H 5.800758 -0.859800 -1.882687
H 5.689870 -1.870468 -0.425039
H 6.739345 -3.129800 -2.306366
H 5.218700 -3.894361 -1.784938
H 5.587674 -2.072458 -4.257379
H 5.306591 -3.830891 -4.281892
H 3.175139 -2.513724 -4.733458
H 3.037303 -3.523907 -3.274611
H 3.645169 -0.493916 -3.350371
H 2.109254 -1.222735 -2.853785
H 3.314781 0.247025 2.042423
H 6.129467 -0.207126 0.820844
H 5.403587 1.370479 1.200734
H 6.951702 0.608626 3.022765
H 5.283474 0.822612 3.610904
H 6.620575 -1.870156 2.885060
H 6.227453 -1.300640 4.525805
H 4.484666 -2.927258 3.654815
H 3.772533 -1.328428 3.983835
H 4.606623 -2.420095 1.223473
H 2.934305 -2.163813 1.822073
H 2.713352 1.492977 -1.911703
H 5.623039 1.742268 -0.874435
H 5.107078 0.981664 -2.397415
H 5.923583 3.324697 -2.771368
H 4.220636 3.129794 -3.256037
H 5.221238 4.379339 -0.607851
H 4.497252 5.261961 -1.974719
H 2.807377 4.841675 -0.134842
H 2.327556 4.053987 -1.659886
H 3.659235 2.688720 0.772661
H 1.977203 2.481924 0.231235
H -2.717043 -5.353491 1.014838
H -2.438781 -5.861501 -1.402106
H -2.058239 -3.984011 -3.046581
H -2.021322 -1.608882 -2.210947
C -4.059135 -3.396406 2.843675
H -2.572571 -1.863076 2.474436
C -1.534214 -3.628111 3.086026
H -6.069187 -0.611914 1.948880
H -8.269387 -1.198094 0.920214
H -8.456224 -1.480800 -1.571404
H -6.424736 -1.154429 -3.013106
H -4.238062 -0.547391 -1.984741
H -5.579373 2.898966 0.410029
H -6.470913 4.071821 -1.606873
H -5.209175 3.975322 -3.779220
H -3.042955 2.703381 -3.901633
H -2.140656 1.546207 -1.894434
C -1.183956 2.444097 2.837382
H 0.034351 2.065209 1.103375

C -0.304995 3.544910 3.455306
H -2.252835 2.650344 3.078177
H -0.923127 1.451627 3.260847
C -0.558690 4.912348 2.800815
H -0.480350 3.593726 4.551515
H 0.765585 3.264785 3.327716
C -0.370466 4.835401 1.276445
H -1.598992 5.243315 3.027241
H 0.113849 5.683757 3.234713
C -1.251430 3.745343 0.637597
H -0.591547 5.815840 0.802622
H 0.699034 4.619623 1.052686
H -2.321295 4.031585 0.748641
H -1.060383 3.671177 -0.452998

H -4.158027 -3.140570 3.919898
H -4.893188 -2.915397 2.292842
H -4.192637 -4.495581 2.751519
H -1.647245 -3.430623 4.172896
H -1.530387 -4.730021 2.945361
H -0.549930 -3.221611 2.778227

P1 E(gas)=-2679,1179264 G(gas)=-2678,40223 G(CH2Cl2)=-2679,13256185

C -4.467631 0.771486 -0.807013
C -4.060781 0.708391 0.543223
C -5.031014 0.901573 1.550827
C -6.373828 1.154960 1.223090
C -6.768194 1.207729 -0.124531
C -5.811048 1.013715 -1.136098
C -2.619452 0.501353 0.960334
C -1.675006 1.753482 0.857700
N -0.373145 1.086622 0.641843
C -0.508166 -0.172468 0.154972
N -1.831332 -0.516645 0.195895
C 0.920345 1.693895 1.001418
C 1.139922 3.083824 0.374108
C 2.505072 3.672040 0.776385
C 2.685625 3.713357 2.302705
C 2.485293 2.319140 2.918086
C 1.123718 1.712047 2.533367
C -2.029950 2.766889 -0.228834
C -1.635222 2.590041 -1.572609
C -2.015517 3.527986 -2.548657
C -2.790733 4.647955 -2.199468
C -3.184646 4.830246 -0.862314
C -2.804496 3.895001 0.114586
C -2.409281 -1.722586 -0.326927
C -2.467308 -1.862856 -1.733907
C -3.066837 -2.987760 -2.317152
C -3.623286 -3.977986 -1.490376
C -3.543559 -3.847046 -0.095639
C -2.926562 -2.736424 0.525047
Ru 1.088076 -1.211624 -0.519264
Cl 1.443333 -1.968677 1.750961
C -2.789163 -2.706207 2.048006
C -4.162550 -2.699625 2.752327
Cl 0.730693 -0.134569 -2.677099
C 0.250763 -2.728806 -1.078171
C 2.983152 -2.628950 -1.022988

C 3.273970 -1.303103 -1.313885
C 4.065054 -0.399745 -0.390306
C 5.613131 -0.368299 -0.665131
C 6.232153 -1.760044 -0.431553
C -1.903914 -3.866961 2.553164
C 5.891856 0.096335 -2.110685
C 6.207941 0.653242 0.362491
C 7.695575 0.879539 0.292939
C 8.571655 0.589635 1.273918
H 8.082554 1.334685 -0.638222
H 3.169334 -0.963609 -2.358269
H 0.180227 -2.991730 -2.158385
H -1.681131 2.272657 1.837882
H -2.624184 0.190000 2.030089
H -0.161787 -3.471339 -0.357609
H -3.959262 -4.646493 0.538908
H -4.111597 -4.861712 -1.931076
H -3.102435 -3.083769 -3.413623
H -2.008520 -1.079036 -2.356694
H -2.256601 -1.771743 2.319053
H 7.333494 -1.725753 -0.562319
H 6.027596 -2.125664 0.597349
H 5.827889 -2.508405 -1.143970
H 5.691574 1.628970 0.200135
H 5.935831 0.319558 1.388290
H 6.981383 0.154205 -2.311691
H 5.463584 -0.610319 -2.850747
H 5.453708 1.098291 -2.308818
H 2.705917 -3.325116 -1.830082
H 3.215836 -3.067320 -0.039243
H 3.696404 0.644842 -0.500256
H 3.899265 -0.703869 0.665927
H 9.649552 0.793146 1.165565
H 8.241499 0.141457 2.227574
H -4.728610 0.851911 2.610379
H -7.114776 1.303390 2.024647

H -7.821095 1.397929 -0.386802
H -6.111208 1.053754 -2.195111
H -3.728758 0.631704 -1.608261
H -3.115480 4.044536 1.162267
H -3.787195 5.707170 -0.576311
H -3.082427 5.382315 -2.967280
H -1.694211 3.380429 -3.592150
H -1.006645 1.730014 -1.865022
H 1.690551 1.007369 0.576951
H 0.309489 2.314639 2.999035
H 1.033871 0.672061 2.911572
H 2.577771 2.358957 4.024601
H 3.295894 1.640869 2.566789
H 1.944167 4.421191 2.740982
H 3.689244 4.112777 2.563938
H 2.615095 4.687275 0.338761

H 3.318210 3.054855 0.328900
H 0.332719 3.771340 0.712123
H 1.050970 3.013426 -0.729115
H -1.803225 -3.817971 3.657938
H -2.341340 -4.856211 2.300186
H -0.882830 -3.806804 2.124543
H -4.036038 -2.606058 3.851593
H -4.801312 -1.862638 2.403443
H -4.717896 -3.643322 2.564730

P2 E(gas)=-2679.11768755 G(gas)=-2678.399012 E(CH2Cl2)=-2679.13241863

C 0.912928 3.247009 0.326999
C 0.808893 1.831105 0.925685
C 1.089270 1.827865 2.444980
C 2.435967 2.496999 2.773946
C 2.534787 3.912123 2.180497
C 2.267950 3.895244 0.666089
N -0.457108 1.147696 0.612558
C -1.795460 1.712545 0.883928
C -2.646296 0.390868 0.988843
N -1.805425 -0.559327 0.194396
C -0.516389 -0.113585 0.120625
C -2.259144 2.715740 -0.169669
C -1.905312 2.585999 -1.530324
C -2.389582 3.507550 -2.475375
C -3.227657 4.564605 -2.078335
C -3.580085 4.700545 -0.724220
C -3.096359 3.781316 0.221698
Ru 1.120234 -1.039880 -0.590947
Cl 0.647310 0.013817 -2.729982
C -2.292965 -1.815726 -0.305816
C -2.418424 -1.956466 -1.707635
C -2.942004 -3.130651 -2.265271
C -3.354893 -4.171788 -1.416332
C -3.205576 -4.039329 -0.027932
C -2.660167 -2.876982 0.565346
C -4.106338 0.499324 0.599848
C -5.070851 0.617891 1.624351
C -6.433752 0.775105 1.319940
C -6.853374 0.804976 -0.020657
C -5.901877 0.685003 -1.048835
C -4.539204 0.539237 -0.742993
C -2.451186 -2.829171 2.079372
C -1.506247 -3.953284 2.556464
C -3.791702 -2.863772 2.844759

C 0.519279 -2.652301 -1.209065
C 2.983869 -2.390078 -1.287492
C 3.269728 -1.021605 -1.357323
C 4.106039 -0.293355 -0.321783
C 5.648893 -0.265070 -0.620679
C 5.924411 0.403927 -1.984394
Cl 1.574853 -1.882290 1.628225
C 6.288559 0.572405 0.538159
C 7.783986 0.746227 0.488505
H 8.188754 1.300239 -0.379455
C 6.226633 -1.693403 -0.609985
C 8.648227 0.300101 1.420198
H 3.180826 -0.538142 -2.346136
H 0.293535 -2.819360 -2.286631
H -1.808446 2.211769 1.874587
H -2.608306 0.065908 2.053861
H 0.394177 -3.525163 -0.527242
H -3.508268 -4.875388 0.623139
H -3.783779 -5.095621 -1.836262
H -3.031924 -3.226418 -3.358701
H -2.070263 -1.132200 -2.349483
H -1.937959 -1.873681 2.314210
H 7.326652 -1.673434 -0.753526
H 6.024597 -2.204596 0.355412
H 5.789651 -2.312587 -1.420600
H 5.812208 1.581428 0.523740
H 6.005690 0.106141 1.507713
H 7.012519 0.460748 -2.193230
H 5.465602 -0.168594 -2.816554
H 5.516016 1.436836 -2.020942
H 2.771602 -2.951014 -2.211922
H 3.234407 -2.976058 -0.388564
H 3.768463 0.765990 -0.262480
H 3.940732 -0.746169 0.678835

H 9.733322 0.473267 1.332851
H 8.300551 -0.251672 2.311225
H -4.748154 0.586155 2.678602
H -7.170011 0.865866 2.134313
H -7.921603 0.918877 -0.264538
H -6.222018 0.707263 -2.102514
H -3.805167 0.458097 -1.556579
H -3.374856 3.893779 1.283086
H -4.230701 5.528753 -0.400824
H -3.600692 5.286382 -2.822504
H -2.100862 3.397550 -3.532947
H -1.231518 1.774900 -1.859719
H 1.600665 1.208966 0.440423
H 0.269619 2.378144 2.962843
H 1.071650 0.778023 2.806033
H 2.583822 2.519949 3.874875
H 3.260285 1.867925 2.367420
H 1.788078 4.574372 2.677111

H 3.532084 4.353730 2.393815
H 2.302323 4.924174 0.248539
H 3.081662 3.329333 0.156259
H 0.091924 3.879059 0.733655
H 0.761605 3.201453 -0.770509
H -1.351014 -3.879943 3.653518
H -1.925010 -4.960348 2.345749
H -0.511623 -3.868346 2.074013
H -3.620604 -2.759901 3.937150
H -4.475338 -2.052296 2.521491
H -4.321686 -3.826806 2.683552

P3 E(gas)=-2679.13913821 G(gas)=-2678.417023 E(CH2Cl2)=-2679.15387148

C -2.432143 -2.959650 0.634055
C -2.127709 -1.896093 -0.258289
C -2.170286 -2.088801 -1.657229
C -2.544228 -3.327330 -2.195145
C -2.893864 -4.378046 -1.330251
C -2.830543 -4.188014 0.057848
N -1.765425 -0.583484 0.220444
C -2.677942 0.332098 0.973447
C -1.885376 1.696334 0.887434
N -0.513746 1.205567 0.624410
C -0.514811 -0.057899 0.150980
C -4.121304 0.362313 0.515619
C -4.488358 0.336506 -0.846849
C -5.839769 0.409703 -1.221168
C -6.844032 0.520120 -0.243490
C -6.489897 0.553119 1.115921
C -5.138084 0.468736 1.489675
C -2.383724 2.686227 -0.161811
C -2.015162 2.580833 -1.520608
C -2.529888 3.488929 -2.462498
C -3.413264 4.507731 -2.063722
C -3.780920 4.618910 -0.711446
C -3.266489 3.713422 0.231524
C 0.720916 1.934945 0.963677
C 0.771414 3.363264 0.389698
C 2.094843 4.059301 0.757369
C 2.338470 4.065398 2.275943
C 2.287472 2.639431 2.849660
C 0.975585 1.920396 2.487672
Ru 1.093407 -1.000837 -0.568503
C 3.000714 -0.613697 -1.065544
C 4.058954 -0.267385 -0.031328

C 5.514582 -0.022037 -0.559224
C 6.382640 0.262723 0.714417
C 7.833950 0.586422 0.475758
C 8.875932 -0.153152 0.901971
C -2.319684 -2.842547 2.154501
C -1.366846 -3.905360 2.741567
Cl 1.597096 -1.891206 1.602515
Cl 0.515397 -0.049216 -2.727621
C 1.377671 -2.760659 -1.407873
C 2.831817 -2.144964 -1.478093
C -3.705665 -2.899720 2.834035
C 6.066253 -1.265066 -1.287351
C 5.543860 1.194858 -1.509529
H 8.046799 1.517356 -0.083024
H 3.026488 0.028021 -1.969771
H 0.902957 -2.906750 -2.396101
H -1.931632 2.185554 1.882062
H -2.671059 0.017121 2.041716
H 1.301322 -3.620814 -0.715667
H -3.081126 -5.028802 0.724442
H -3.205541 -5.353639 -1.736412
H -2.567729 -3.465036 -3.287525
H -1.866668 -1.258210 -2.313038
H -1.860195 -1.856931 2.377858
H 7.134138 -1.121540 -1.553315
H 6.003048 -2.171283 -0.647670
H 5.513179 -1.469794 -2.227272
H 5.910719 1.117782 1.253711
H 6.307874 -0.613878 1.395013
H 6.564829 1.380619 -1.902019
H 4.883766 1.040054 -2.387790
H 5.204171 2.119097 -0.993636

H 3.120643 -2.187483 -2.546751
H 3.492499 -2.742973 -0.823228
H 3.744696 0.674312 0.473878
H 4.067425 -1.041651 0.763632
H 9.917967 0.148085 0.705720
H 8.725035 -1.086869 1.471873
H -4.865693 0.484766 2.558391
H -7.268664 0.635790 1.890600
H -7.903100 0.576691 -0.541390
H -6.109467 0.381597 -2.288702
H -3.711975 0.257547 -1.620435
H -3.556046 3.807028 1.291774
H -4.466961 5.417590 -0.387074
H -3.810490 5.219072 -2.805381
H -2.230886 3.398052 -3.518980
H -1.310892 1.796591 -1.850952
H 1.535007 1.344067 0.479733
H 0.126374 2.428270 3.001250
H 0.995563 0.865913 2.835378
H 2.416083 2.652783 3.953117

H 3.143959 2.050159 2.449432
H 1.558862 4.690576 2.770046
H 3.314062 4.543245 2.510442
H 2.094804 5.094881 0.355226
H 2.936580 3.532126 0.251950
H -0.080107 3.954284 0.795820
H 0.635179 3.331082 -0.710469
H -1.268953 -3.763905 3.838672
H -1.745534 -4.935893 2.573409
H -0.355144 -3.816706 2.297453
H -3.610557 -2.743627 3.929598
H -4.398649 -2.132549 2.432006
H -4.185580 -3.890138 2.681394

P4 E(gas)=-2679.11937730 G(gas)=-2678.399405 E(CH2Cl2)=-2679.13384526

C 0.720142 3.536918 0.378768
C 0.812861 2.080408 0.874375
C 1.120779 2.014177 2.389800
C 2.367416 2.836851 2.761660
C 2.267587 4.287309 2.261820
C 1.986515 4.330214 0.750612
N -0.374941 1.274413 0.552143
C -1.752810 1.754554 0.821810
C -2.522919 0.393016 1.001586
N -1.614510 -0.537491 0.270527
C -0.362150 -0.011078 0.132013
C -2.293178 2.671520 -0.272949
C -1.934898 2.506194 -1.628163
C -2.491315 3.344347 -2.610742
C -3.406100 4.351606 -2.256648
C -3.762966 4.522717 -0.907586
C -3.207223 3.687710 0.075895
Ru 1.082639 -1.191819 -0.693867
Cl 1.452326 -2.114226 1.516554
C -1.965311 -1.871386 -0.152962
C -2.014423 -2.111818 -1.546052
C -2.376384 -3.372196 -2.044306
C -2.708282 -4.397724 -1.145334
C -2.650183 -4.158819 0.236791
C -2.269603 -2.909041 0.775098
C -3.978716 0.396738 0.581714
C -4.965867 0.595389 1.572021
C -6.326419 0.673706 1.230375
C -6.720269 0.542546 -0.112229
C -5.746128 0.340709 -1.105324

C -4.385463 0.273376 -0.763793
C -2.193864 -2.736132 2.292481
C -1.348119 -3.838075 2.964183
C -3.603886 -2.671135 2.921715
Cl 0.508790 -0.121738 -2.830500
C 2.590761 -2.901194 -1.379118
C 1.326695 -2.990046 -1.956482
C 2.690266 -0.277793 -0.796773
C 3.833849 -0.231160 0.180117
C 5.232597 0.187186 -0.380020
C 5.184094 1.633771 -0.918193
C 6.228820 0.089991 0.824429
C 7.654628 0.483600 0.540364
H 7.826264 1.535558 0.243354
C 5.679861 -0.774229 -1.500646
C 8.720827 -0.333451 0.638447
H 2.830389 0.292776 -1.747512
H 1.154209 -2.734522 -3.014157
H -1.782404 2.301893 1.786396
H -2.484629 0.130046 2.083537
H 0.545683 -3.596106 -1.457973
H -2.893585 -4.979662 0.929802
H -3.008015 -5.390532 -1.517317
H -2.405384 -3.542194 -3.131932
H -1.739737 -1.296213 -2.232987
H -1.669699 -1.776539 2.485554
H 6.699665 -0.520012 -1.856370
H 5.705828 -1.825132 -1.141795
H 4.996800 -0.723969 -2.374802
H 5.833373 0.742467 1.638913

H 6.205041 -0.949240 1.220326
H 6.156720 1.937565 -1.356919
H 4.420817 1.745272 -1.716282
H 4.936038 2.356319 -0.110656
H 3.443362 -2.546451 -1.978155
H 2.816737 -3.369789 -0.408380
H 3.550177 0.500522 0.975837
H 3.896485 -1.193788 0.730507
H 9.743184 0.022282 0.430535
H 8.611489 -1.390357 0.938919
H -4.662330 0.691127 2.628130
H -7.081070 0.829969 2.017518
H -7.786455 0.594971 -0.384382
H -6.046242 0.237453 -2.160031
H -3.634095 0.124741 -1.551466
H -3.489825 3.827538 1.132931
H -4.473315 5.313416 -0.617763
H -3.836435 5.007431 -3.030360
H -2.200065 3.206235 -3.664294
H -1.207589 1.730067 -1.927177
H 1.643363 1.586050 0.328814
H 0.243491 2.408717 2.953890

H 1.244123 0.949851 2.684445
H 2.524527 2.806346 3.861169
H 3.267688 2.358201 2.311430
H 1.444557 4.808353 2.803872
H 3.198708 4.845233 2.500471
H 1.882759 5.379646 0.401145
H 2.859582 3.907989 0.201873
H -0.165012 4.034946 0.834328
H 0.555758 3.551223 -0.717981
H -1.250364 -3.629248 4.050370
H -1.818890 -4.839269 2.864686
H -0.330012 -3.871961 2.528536
H -3.535377 -2.476474 4.013112
H -4.232479 -1.880199 2.465407
H -4.140078 -3.635205 2.788906

P5 E(gas)=-2679.12778147 G(gas)=-2678.407713 E(CH2Cl2)=-2679,14152059

C -4.327658 -0.017135 -0.888680
C -3.998061 0.128408 0.475484
C -5.044451 0.235860 1.417557
C -6.388518 0.204141 1.010043
C -6.705149 0.053103 -0.350843
C -5.671052 -0.059550 -1.296403
C -2.567178 0.236129 0.963773
C -1.900972 1.662169 0.835746
N -0.487415 1.306288 0.546484
C -0.366032 0.030271 0.129688
N -1.560779 -0.608356 0.258657
C 0.632456 2.200930 0.887336
C 0.453473 3.644057 0.379445
C 1.668756 4.511310 0.758675
C 1.937027 4.494073 2.273060
C 2.112866 3.055272 2.784941
C 0.917582 2.162207 2.407604
C -2.515127 2.582815 -0.215212
C -2.151441 2.505040 -1.576481
C -2.770399 3.343619 -2.520170
C -3.755945 4.263325 -2.120533
C -4.119932 4.346368 -0.765097
C -3.500426 3.511891 0.180037
C -1.755609 -1.974586 -0.161066
C -1.686979 -2.229459 -1.551405
C -1.869249 -3.527614 -2.053269
C -2.142857 -4.576676 -1.162572
C -2.206042 -4.320163 0.216258

C -2.001467 -3.032846 0.760927
Ru 1.184987 -1.066263 -0.696905
C 2.675624 0.000778 -0.610504
C 3.864109 -0.095005 0.301223
C 5.241915 0.294026 -0.330781
C 5.509895 -0.574287 -1.578682
C -2.045731 -2.846629 2.278236
C -3.495511 -2.925460 2.807980
Cl 1.426029 -1.760793 1.640988
Cl 0.539013 0.174508 -2.727376
C 2.113573 -3.056057 -0.981042
C 1.887908 -2.502458 -2.251113
C -1.140453 -3.852707 3.019255
C 5.262954 1.789406 -0.714083
C 6.322824 -0.000561 0.763443
C 7.746901 0.320657 0.392147
C 8.744736 -0.578208 0.290313
H 7.980388 1.385738 0.204076
H 2.720912 0.791848 -1.397415
H 2.697960 -2.036244 -2.832985
H -1.965605 2.165872 1.822134
H -2.556696 -0.042771 2.041508
H 0.995431 -2.777390 -2.835638
H -2.403408 -5.157360 0.904418
H -2.304275 -5.599861 -1.537612
H -1.814390 -3.707328 -3.138432
H -1.484220 -1.388564 -2.233420
H -1.634828 -1.839119 2.496910

H 6.514871 -0.367166 -2.000822
H 5.469402 -1.656193 -1.329676
H 4.759070 -0.378465 -2.372876
H 6.047837 0.585256 1.672332
H 6.250665 -1.072736 1.050745
H 6.225278 2.072660 -1.187987
H 4.462240 2.035416 -1.442153
H 5.120259 2.437234 0.178017
H 3.112661 -3.054497 -0.517397
H 1.404971 -3.781537 -0.546624
H 3.668430 0.583704 1.169116
H 3.918368 -1.105595 0.756262
H 9.771383 -0.275615 0.026711
H 8.572798 -1.653272 0.474422
H -4.802186 0.345751 2.487944
H -7.190724 0.290253 1.760068
H -7.757711 0.020221 -0.674196
H -5.910282 -0.178053 -2.364964
H -3.528154 -0.097560 -1.638376
H -3.787302 3.585069 1.242630
H -4.885978 5.068392 -0.440067
H -4.236504 4.919845 -2.863465
H -2.472924 3.276321 -3.578881
H -1.367129 1.800372 -1.905842

H 1.504758 1.759695 0.362400
H 0.013656 2.513855 2.957840
H 1.098330 1.108556 2.709208
H 2.259913 3.041987 3.886224
H 3.041870 2.622925 2.346579
H 1.080863 4.972028 2.803441
H 2.833061 5.105184 2.515839
H 1.509501 5.550928 0.400815
H 2.569877 4.134528 0.222157
H -0.465056 4.091444 0.821207
H 0.302644 3.640235 -0.719068
H -1.132945 -3.623503 4.105705
H -1.503284 -4.896646 2.908551
H -0.098422 -3.790561 2.648478
H -3.524548 -2.725061 3.900128
H -4.167385 -2.202632 2.303089
H -3.919376 -3.939407 2.643988

P6 E(gas)=-2600.60340065 G(gas)=-2599.927293 E(CH2Cl2)=-2600.61740889

C 1.046691 -2.389730 -1.516474
C 1.149855 -2.090080 -0.138086
C 1.236375 -3.137148 0.825382
C 1.248122 -4.462134 0.335547
C 1.150312 -4.760679 -1.032238
C 1.035672 -3.718864 -1.965360
N 1.172740 -0.696503 0.239702
C 0.055051 0.096418 0.238637
N 0.395769 1.326375 0.704682
C 1.865862 1.489501 0.800425
C 2.336251 -0.011406 0.867192
C -0.538541 2.357107 1.180514
Ru -1.662204 -0.673803 -0.475265
C -2.843348 0.736684 -0.341138
C -4.170889 0.752200 0.350286
C -5.329794 0.149163 -0.523823
C -6.631729 0.174898 0.301429
C 3.696660 -0.305481 0.266655
C 2.452631 2.324087 -0.335990
C 1.324413 -2.893551 2.332537
C -2.731669 -2.500068 -1.243749
C -3.675722 -1.542160 -1.596084
C -4.961626 -1.326335 -0.845504
Cl -2.161919 -1.571914 1.711768
Cl -1.007989 0.088129 -2.699225
C -5.524846 0.972802 -1.815329

H -3.562773 -1.045155 -2.575595
H -2.576899 1.651859 -0.924179
H -4.443484 1.803948 0.599136
H -4.106580 0.162679 1.289894
H -5.786934 -1.747948 -1.468354
H -4.939485 -1.911502 0.098069
H -1.966584 -2.806884 -1.978995
H -2.898508 -3.164249 -0.379269
H 2.373637 -0.295907 1.943824
H 2.131968 1.977724 1.759467
H 1.320167 -5.290836 1.057361
H 1.158218 -5.810703 -1.365821
H 0.950735 -3.931220 -3.042684
H 0.951369 -1.557934 -2.230760
C 0.328196 -3.758812 3.131423
C 2.766241 -3.113652 2.844906
H 1.035905 -1.835750 2.509912
H -7.473397 -0.265203 -0.274834
H -6.524590 -0.402341 1.243692
H -6.915881 1.214467 0.568718
H -6.349765 0.551494 -2.428754
H -5.791975 2.023804 -1.575070
H -4.611914 0.998696 -2.445289
C 3.556555 3.161386 -0.070563
C 4.144805 3.922955 -1.094397
C 3.629907 3.857978 -2.400754

C 2.527809 3.027947 -2.672575
C 1.939297 2.263950 -1.649859
H 3.962278 3.219042 0.953619
H 5.005190 4.573176 -0.868948
H 4.084884 4.457468 -3.205465
H 2.113986 2.973109 -3.692190
H 1.067605 1.627902 -1.884909
C 4.819146 -0.354541 1.122153
C 6.109836 -0.566505 0.608932
C 6.294572 -0.742734 -0.773036
C 5.183704 -0.697554 -1.633313
C 3.895319 -0.476188 -1.119815
H 4.679152 -0.224335 2.208508
H 6.972517 -0.602005 1.293118
H 7.303484 -0.917809 -1.179279
H 5.319458 -0.833369 -2.717928
H 3.035900 -0.434547 -1.803227
C -0.494184 3.670698 0.374218
H -1.540876 1.898929 1.041986
C -1.551897 4.664961 0.888544
H 0.516852 4.127720 0.459476
H -0.646519 3.451934 -0.703410
C -1.402974 4.931054 2.396262
H -1.485394 5.614656 0.315746
H -2.568646 4.254181 0.687944
C -1.432237 3.619771 3.199896

H -0.436226 5.454183 2.581562
H -2.201017 5.619323 2.749364
C -0.375005 2.620761 2.694890
H -1.275993 3.819108 4.281834
H -2.441379 3.155708 3.113841
H 0.638354 3.037682 2.898372
H -0.450480 1.657379 3.242367
H 2.842434 -2.864488 3.924763
H 3.065367 -4.177013 2.725368
H 3.507868 -2.502501 2.292057
H 0.358075 -3.475376 4.204590
H -0.705947 -3.607247 2.764769
H 0.578757 -4.839482 3.072917

P8 E(gas)=-2600.61098419 G(gas)=-2599.935038 E(CH2Cl2)=-2600.62450627

C 1.170443 -2.264073 -1.673864
C 1.239493 -2.081630 -0.274328
C 1.314687 -3.197274 0.604028
C 1.377078 -4.478281 0.009411
C 1.327525 -4.663628 -1.380264
C 1.204671 -3.550761 -2.228599
N 1.227133 -0.725170 0.215292
C 0.142008 0.088322 0.157593
N 0.446298 1.310034 0.641114
C 1.899266 1.454835 0.885478
C 2.342056 -0.061370 0.957749
C -0.571833 2.326798 0.965658
Ru -1.650798 -0.426887 -0.562137
Cl -0.951880 0.439812 -2.713325
C 3.744416 -0.369784 0.476121
C 2.609139 2.298736 -0.169654
C 1.297765 -3.072120 2.127921
C -2.468400 -2.017953 -1.450866
C -3.672775 -1.037067 -1.463173
C -3.381284 0.474672 -0.888293
C -4.464008 0.765196 0.150584
C -5.646543 -0.201996 -0.181978
C -4.887907 -1.483399 -0.625780
C -6.538505 -0.461429 1.043836

C -6.501731 0.361051 -1.338374
Cl -2.181573 -1.291682 1.627175
H -3.300059 1.202836 -1.720959
H -3.888500 -0.837926 -2.533360
H -4.774582 1.831379 0.115189
H -4.095129 0.542091 1.171745
H -5.529258 -2.185558 -1.200627
H -4.516110 -2.017499 0.273692
H -2.053252 -2.254307 -2.447872
H -2.603590 -2.888522 -0.780111
H 2.273195 -0.371040 2.025478
H 2.075354 1.914368 1.879738
H 1.446189 -5.362667 0.662951
H 1.373572 -5.681554 -1.799211
H 1.145332 -3.677679 -3.320892
H 1.061803 -1.377366 -2.317725
C 0.169437 -3.913221 2.761254
C 2.669033 -3.428778 2.743049
H 1.065066 -2.013575 2.367871
H -7.344433 -1.188330 0.804865
H -5.946940 -0.872127 1.888688
H -7.027715 0.473966 1.390496
H -7.294815 -0.359721 -1.631422
H -7.001807 1.306051 -1.037063

H -5.897151 0.580612 -2.243329
C 4.779137 -0.480593 1.430506
C 6.107047 -0.707645 1.031514
C 6.416384 -0.839164 -0.333087
C 5.392539 -0.735468 -1.290963
C 4.067240 -0.497666 -0.891505
H 4.540505 -0.386806 2.503227
H 6.900802 -0.790392 1.790871
H 7.454762 -1.025939 -0.649973
H 5.626088 -0.838726 -2.362364
H 3.276583 -0.411442 -1.649965
C 3.716442 3.084176 0.213471
C 4.421763 3.843028 -0.735436
C 4.023089 3.827005 -2.083295
C 2.917912 3.049489 -2.472156
C 2.212249 2.287802 -1.524447
H 4.031885 3.102864 1.270287
H 5.282756 4.453231 -0.418993
H 4.570601 4.424937 -2.829321
H 2.593603 3.035972 -3.524971
H 1.335393 1.698861 -1.846973
C -0.323441 3.692634 0.298303
H -1.518967 1.909911 0.548521
C -1.449383 4.685564 0.642137
H 0.650184 4.103531 0.648418
H -0.235670 3.561908 -0.799424
C -1.637749 4.834821 2.161073
H -1.232644 5.670190 0.175385

H -2.401795 4.330443 0.185511
C -1.878925 3.469465 2.826999
H -0.725855 5.302709 2.599489
H -2.478703 5.527184 2.381615
C -0.762166 2.463865 2.492216
H -1.968635 3.578820 3.929068
H -2.852447 3.055765 2.477715
H 0.193202 2.810604 2.950551
H -0.992703 1.464834 2.917664
H 2.655690 -3.277299 3.843309
H 2.922169 -4.494565 2.557527
H 3.489852 -2.816275 2.317248
H 0.145420 -3.749335 3.859356
H -0.816882 -3.617827 2.351148
H 0.320401 -5.000752 2.593638

P9 E(gas)=-2600.58390812 G(gas)=-2599.912511 E(CH2Cl2)=-2600.59710554

C -3.886392 -0.951578 -1.588888
C -3.757987 0.407369 -1.260735
C -4.732643 0.765902 -0.142543
C -5.725054 -0.449897 -0.073408
C -4.873730 -1.630730 -0.657665
Ru -1.677032 -0.314984 -0.602501
Cl -0.942070 0.544662 -2.750089
C -6.208679 -0.729757 1.358015
C -6.927596 -0.180376 -1.002711
C 0.149637 0.049973 0.100642
N 0.427688 1.271737 0.618862
C 1.865889 1.452292 0.898758
C 2.327361 -0.053972 0.977065
N 1.269368 -0.727007 0.160320
C -0.624607 2.259322 0.914711
C 1.387627 -2.060843 -0.362386
C 1.433412 -3.198292 0.488102
C 1.621348 -4.457485 -0.128232
C 1.729631 -4.600776 -1.519114
C 1.637554 -3.468748 -2.347094
C 1.472041 -2.204657 -1.766022
C 3.766527 -0.334826 0.597601

C 2.586104 2.313406 -0.136216
C 1.250608 -3.120674 2.004494
C -1.676442 -2.036913 -1.224235
Cl -2.372232 -1.017694 1.605808
H -3.386605 1.143601 -1.993107
H -3.619111 -1.345490 -2.581400
H -5.257030 1.720379 -0.368229
H -4.212883 0.896202 0.829600
H -5.492695 -2.385987 -1.187719
H -4.336919 -2.149033 0.166251
H -1.373697 -2.282258 -2.267618
H -1.993148 -2.889290 -0.579500
H 2.193395 -0.375738 2.035477
H 2.010462 1.910068 1.899281
H 1.669242 -5.357306 0.506136
H 1.874976 -5.600875 -1.957895
H 1.699367 -3.566047 -3.442353
H 1.374633 -1.303246 -2.390798
C 0.022166 -3.931716 2.469908
C 2.527337 -3.555835 2.756291
H 1.038567 -2.062288 2.261786
H -6.878251 -1.615945 1.389613

H -5.346463 -0.919377 2.029890
H -6.781584 0.132958 1.760845
H -7.610909 -1.056000 -1.034368
H -7.515823 0.694285 -0.651450
H -6.599798 0.029533 -2.043916
C 3.679210 3.105693 0.272954
C 4.392965 3.880610 -0.656430
C 4.017501 3.873917 -2.011086
C 2.926191 3.090135 -2.425928
C 2.211659 2.312643 -1.497631
H 3.977158 3.116418 1.334936
H 5.242532 4.495891 -0.319501
H 4.571592 4.484580 -2.741831
H 2.618989 3.084718 -3.483991
H 1.343976 1.721000 -1.840362
C 4.714853 -0.494642 1.631666
C 6.074880 -0.695993 1.341196
C 6.504820 -0.751566 0.004580
C 5.568357 -0.598645 -1.033011
C 4.211145 -0.387304 -0.740963
H 4.380398 -0.460507 2.682232
H 6.798547 -0.817868 2.162779
H 7.568645 -0.916921 -0.228910
H 5.896824 -0.641130 -2.083515
H 3.492208 -0.259818 -1.562122
C -0.390150 3.638116 0.269798
H -1.556656 1.835871 0.456633
C -1.549165 4.601329 0.586024
H 0.562161 4.064765 0.657569
H -0.262820 3.519681 -0.825402

C -1.793575 4.727640 2.098969
H -1.338618 5.595732 0.137656
H -2.477269 4.231093 0.092323
C -2.032213 3.349542 2.738379
H -0.906611 5.206894 2.574741
H -2.654663 5.401600 2.297765
C -0.887574 2.367165 2.432487
H -2.163883 3.441810 3.837737
H -2.985096 2.922474 2.350023
H 0.044390 2.717609 2.933881
H -1.123093 1.355236 2.824099
H -0.099771 -3.841928 3.569953
H -0.906571 -3.550448 1.999825
H 0.128455 -5.011829 2.233239
H 2.397750 -3.430103 3.852120
H 2.757547 -4.626823 2.571178
H 3.413223 -2.967437 2.440891

P10 E(gas)=-2600.58464910 G(gas)=-2599.914959 E(CH2Cl2)=-2600.59775922

C -3.995990 -0.709088 -1.663337
C -3.936760 0.543482 -1.089298
C -4.901615 0.651869 0.077579
C -5.835196 -0.602989 -0.069410
C -4.962994 -1.600243 -0.910623
Ru -1.669205 -0.283905 -0.593402
Cl -1.075848 0.712542 -2.711941
C -6.246995 -1.190578 1.290030
C -7.086995 -0.212262 -0.884135
C 0.151124 0.045224 0.094851
N 0.429935 1.265998 0.626160
C 1.868550 1.451445 0.893151
C 2.332386 -0.051962 0.972585
N 1.281613 -0.723902 0.147176
C -0.616951 2.253363 0.939880
C 1.420247 -2.043472 -0.398657
C 1.514596 -3.193892 0.431922
C 1.718170 -4.437620 -0.208813
C 1.795060 -4.557871 -1.604610
C 1.655675 -3.416770 -2.412295

C 1.474457 -2.165427 -1.807444
C 3.774178 -0.332576 0.603204
C 2.582920 2.308746 -0.149607
C 1.348455 -3.148532 1.951657
C -1.438738 -1.991455 -1.183223
Cl -2.326349 -1.036114 1.606770
H -3.464894 1.407356 -1.586973
H -3.555250 -0.955778 -2.640703
H -5.471082 1.606880 0.042436
H -4.359251 0.624160 1.047533
H -5.573763 -2.223077 -1.600096
H -4.413470 -2.297518 -0.242844
H -1.389870 -2.225906 -2.272332
H -1.390792 -2.861368 -0.488935
H 2.190968 -0.372766 2.030351
H 2.020232 1.912404 1.891234
H 1.801126 -5.346001 0.409632
H 1.953043 -5.547563 -2.062015
H 1.694400 -3.495730 -3.510003
H 1.354491 -1.256406 -2.416999

C 0.109594 -3.951436 2.405448
C 2.622349 -3.620881 2.684861
H 1.154579 -2.094045 2.236377
H -6.876540 -2.097006 1.159643
H -5.352174 -1.469034 1.883988
H -6.839360 -0.457542 1.878705
H -7.736062 -1.095335 -1.067341
H -7.692960 0.546163 -0.343709
H -6.812185 0.216288 -1.872202
C 3.695904 3.079686 0.247042
C 4.408905 3.847577 -0.688561
C 4.013124 3.855220 -2.037473
C 2.901868 3.093418 -2.439794
C 2.187712 2.323111 -1.504943
H 4.010850 3.077960 1.304135
H 5.274132 4.445908 -0.361082
H 4.566686 4.460341 -2.773204
H 2.577963 3.100349 -3.492856
H 1.302440 1.752427 -1.837669
C 4.713742 -0.500911 1.643857
C 6.075288 -0.705971 1.363058
C 6.515505 -0.756761 0.029616
C 5.587975 -0.594225 -1.014563
C 4.229354 -0.378952 -0.732172
H 4.370968 -0.471473 2.691857
H 6.791951 -0.834837 2.189701
H 7.580426 -0.925546 -0.196279
H 5.924779 -0.632196 -2.062594
H 3.517742 -0.242906 -1.558491
C -0.384929 3.637095 0.304808
H -1.553468 1.838509 0.484641
C -1.538698 4.600136 0.640390

H 0.572241 4.058795 0.685905
H -0.270294 3.526395 -0.792621
C -1.770919 4.712385 2.156391
H -1.329569 5.598243 0.199653
H -2.471786 4.236964 0.150760
C -2.009111 3.328854 2.783913
H -0.878675 5.184034 2.629924
H -2.628126 5.387281 2.368352
C -0.869295 2.346581 2.460375
H -2.132766 3.410874 3.885015
H -2.965919 2.908074 2.398160
H 0.067052 2.689296 2.958944
H -1.104834 1.331219 2.842936
H 2.502688 -3.511760 3.783512
H 2.831109 -4.692906 2.481447
H 3.516450 -3.043165 2.373222
H -0.000164 -3.892553 3.508882
H -0.817930 -3.540209 1.957853
H 0.194712 -5.025341 2.134426

NP1 E(gas)=-2679.12037082 G(gas)=-2678.403781 E(CH2Cl2)=-2679.13302907
C -1.396979 -3.329189 0.377426
C -1.310437 -2.113999 -0.356173
C -1.057746 -2.127473 -1.748038
C -0.886963 -3.337960 -2.432969
C -0.988161 -4.549463 -1.728598
C -1.240241 -4.532563 -0.348180
N -1.479143 -0.835882 0.271683
C -2.744952 -0.404680 0.953220
C -2.691575 1.147734 0.737850
N -1.230253 1.334957 0.626867
C -0.574950 0.198132 0.254155
C -4.020585 -1.112300 0.552412
C -4.370088 -1.360530 -0.793413
C -5.588848 -1.981848 -1.109681
C -6.481743 -2.358423 -0.090704
C -6.147007 -2.113092 1.251810
C -4.922634 -1.499761 1.567519
C -3.489051 1.688896 -0.445996

C -2.976906 1.692038 -1.761041
C -3.766577 2.157413 -2.827148
C -5.072928 2.623785 -2.596975
C -5.587941 2.627471 -1.288885
C -4.798859 2.164018 -0.223033
C -0.559651 2.615945 0.918936
C -0.977755 3.774848 -0.007074
C -0.177341 5.049280 0.320581
C -0.306141 5.445643 1.800904
C 0.101887 4.284507 2.722854
C -0.685115 2.999529 2.409548
Ru 1.374594 0.363806 -0.203146
C 3.275607 1.694920 -0.531323
C 3.773413 0.473015 -0.938544
C 4.706249 -0.377393 -0.113824
C 6.230487 -0.210831 -0.445360
C 6.982156 -1.252094 0.451677
C 8.485318 -1.245543 0.359992

C 9.241514 -2.257888 -0.106524
C -1.537542 -3.373712 1.900721
C -0.151894 -3.539445 2.567872
Cl 1.910034 0.435168 2.131343
Cl 0.742365 1.117994 -2.385397
C 1.655367 -1.424182 -0.467880
C -2.526271 -4.451367 2.387004
C 6.502694 -0.515043 -1.933722
C 6.694420 1.221955 -0.110858
H 8.996711 -0.333067 0.720504
H 3.625953 0.190831 -1.996875
H 2.438185 -1.821796 -1.151972
H -3.067527 1.633805 1.660906
H -2.600584 -0.564757 2.046528
H 1.075289 -2.198705 0.074020
H -1.301452 -5.489810 0.192962
H -0.868247 -5.511097 -2.252386
H -0.683391 -3.330612 -3.515231
H -0.975758 -1.165745 -2.278144
H -1.934850 -2.394800 2.234423
H 7.592237 -0.510615 -2.144440
H 6.111904 -1.515639 -2.219550
H 6.028061 0.236718 -2.598028
H 6.686542 -1.056236 1.509123
H 6.603219 -2.268678 0.204085
H 7.765681 1.369174 -0.359736
H 6.116486 1.972724 -0.688333
H 6.559172 1.449864 0.968487
H 2.842603 2.394164 -1.264730
H 3.527559 2.085723 0.469071
H 4.455626 -1.452556 -0.258501
H 4.544775 -0.155755 0.962824
H 10.341602 -2.193433 -0.135007
H 8.786850 -3.195465 -0.472129

H -4.658764 -1.319892 2.623283
H -6.837224 -2.406475 2.058678
H -7.437041 -2.845523 -0.343266
H -5.843219 -2.171574 -2.164381
H -3.684293 -1.068290 -1.600718
H -5.209030 2.171043 0.800884
H -6.607657 2.996848 -1.095282
H -5.686600 2.991270 -3.434907
H -3.349505 2.161280 -3.846909
H -1.943253 1.359560 -1.957239
H 0.526356 2.421775 0.742455
H -1.760303 3.157234 2.658102
H -0.314030 2.154772 3.026134
H -0.039710 4.560508 3.789855
H 1.188813 4.075324 2.599667
H -1.362381 5.732263 2.013184
H 0.309214 6.345778 2.016425
H -0.512458 5.878607 -0.338420
H 0.896917 4.877838 0.078463
H -2.064871 3.976425 0.117648
H -0.823212 3.476736 -1.064174
H -0.252898 -3.566767 3.673557
H 0.333156 -4.485989 2.247352
H 0.527093 -2.699099 2.315820
H -2.670800 -4.370849 3.484722
H -3.517330 -4.345396 1.900373
H -2.154153 -5.478484 2.187082

NP2 E(gas)=-2679.11874502 G(gas)=-2678.40084 E(CH2Cl2)=-2679.13343451

C -4.344254 -1.339441 -1.022120
C -4.088091 -1.138306 0.351142
C -5.074353 -1.520902 1.286538
C -6.290314 -2.085053 0.865000
C -6.532123 -2.284813 -0.504736
C -5.554900 -1.912058 -1.444429
C -2.826280 -0.476830 0.864280
C -2.766769 1.096397 0.762869
N -1.308214 1.294912 0.651545
C -0.664949 0.181651 0.221704
N -1.543273 -0.861499 0.196249
C -0.587550 2.532336 0.996661
C -1.090780 3.783399 0.253000
C -0.259455 5.022431 0.634357
C -0.226895 5.249724 2.155150
C 0.282076 3.999227 2.891085

C -0.533311 2.746654 2.524604
C -3.559128 1.716628 -0.385902
C -3.045975 1.778962 -1.699948
C -3.825410 2.321088 -2.736916
C -5.119850 2.806020 -2.479042
C -5.634720 2.749756 -1.172188
C -4.856847 2.209285 -0.134484
C -1.239996 -2.189600 -0.262145
C -1.099959 -2.381155 -1.655508
C -0.841347 -3.654435 -2.180307
C -0.730189 -4.750168 -1.307011
C -0.846691 -4.552826 0.076633
C -1.086145 -3.277345 0.639157
Ru 1.259341 0.312200 -0.279919
Cl 1.927456 -0.120485 1.998074
C -1.124049 -3.119390 2.159754

C -2.297172 -3.902641 2.787787
Cl 0.595372 0.954077 -2.517516
C 1.810833 -1.337198 -0.850999
C 3.096433 1.559983 -0.549539
C 3.640419 0.371940 -1.058275
C 4.667886 -0.457574 -0.320866
C 6.154099 0.008596 -0.519051
C 6.522494 0.029879 -2.017736
C 0.224332 -3.509090 2.802918
C 6.380126 1.405861 0.093441
C 7.028690 -1.058068 0.225419
C 8.516540 -0.823983 0.213558
C 9.423432 -1.626110 -0.376606
H 8.880077 0.072901 0.749562
H 3.530210 0.206639 -2.144860
H 1.741518 -1.635988 -1.921943
H -3.143631 1.518738 1.717268
H -2.734009 -0.729868 1.945702
H 2.247560 -2.078984 -0.144142
H -0.730779 -5.416687 0.751088
H -0.541260 -5.760696 -1.703167
H -0.733506 -3.788654 -3.268079
H -1.172451 -1.502595 -2.315041
H -1.270840 -2.042311 2.380428
H 7.600799 0.252784 -2.154738
H 6.321959 -0.951711 -2.498888
H 5.946925 0.802773 -2.568790
H 6.678783 -1.096771 1.283409
H 6.812780 -2.057867 -0.212727
H 7.433624 1.730949 -0.030526
H 5.747376 2.171327 -0.400757
H 6.142807 1.417561 1.178795
H 2.707372 2.314251 -1.254108
H 3.377502 1.886723 0.466316
H 4.611386 -1.512696 -0.662958
H 4.420474 -0.450770 0.762786

H 10.503029 -1.407337 -0.336431
H 9.118780 -2.539620 -0.917035
H -4.884665 -1.374725 2.363242
H -7.046927 -2.376717 1.610636
H -7.480563 -2.733775 -0.840126
H -5.736464 -2.065580 -2.519915
H -3.591675 -1.045453 -1.766719
H -5.266352 2.169620 0.889032
H -6.645335 3.132255 -0.957289
H -5.724929 3.233649 -3.294449
H -3.408903 2.369146 -3.755780
H -2.022698 1.427212 -1.921113
H 0.467913 2.356054 0.660788
H -1.574013 2.857474 2.908618
H -0.093408 1.841455 2.993137
H 0.260057 4.152459 3.991289
H 1.349840 3.821966 2.627359
H -1.254319 5.494912 2.511572
H 0.405718 6.129635 2.401666
H -0.663422 5.915885 0.112085
H 0.782225 4.892300 0.259924
H -2.159206 3.958873 0.511847
H -1.052471 3.605072 -0.840943
H 0.172449 -3.380570 3.904758
H 0.483886 -4.570323 2.602428
H 1.043061 -2.861060 2.429716
H -2.344799 -3.722289 3.882594
H -3.271653 -3.611238 2.344644
H -2.177650 -4.997058 2.638744

NP3 E(gas)=-2679.13528894 G(gas)=-2678.414241 E(CH2Cl2)=-2679.14985573

C -0.504025 -3.136253 0.863321
C -0.785720 -2.129413 -0.100318
C -0.490134 -2.331523 -1.467485
C 0.064471 -3.541509 -1.906219
C 0.309125 -4.565283 -0.975938
C 0.028632 -4.354124 0.382146
N -1.374321 -0.865439 0.269595
C -2.741228 -0.679902 0.845723
C -2.927797 0.882828 0.691357
N -1.517237 1.325961 0.607086
C -0.699131 0.312445 0.257845
C -3.833459 -1.551159 0.261534
C -3.921324 -1.835909 -1.117942
C -4.976530 -2.615860 -1.617956

C -5.964937 -3.114686 -0.751403
C -5.890485 -2.832876 0.623352
C -4.828156 -2.061537 1.124052
C -3.771893 1.330788 -0.498877
C -3.228494 1.440296 -1.797316
C -4.049751 1.811960 -2.875986
C -5.415687 2.078160 -2.674553
C -5.961137 1.974652 -1.382982
C -5.141871 1.604126 -0.303493
C -1.029129 2.668021 0.978113
C -1.768570 3.814918 0.264738
C -1.190555 5.181612 0.677478
C -1.207593 5.375613 2.203156
C -0.468380 4.229788 2.913914

C -1.024096 2.851712 2.512123
Ru 1.217509 0.524260 -0.238570
C 2.683097 -0.632158 -0.891918
C 3.420120 0.770270 -0.928806
C 4.747307 0.755545 -0.128541
C 5.981185 0.061115 -0.784394
C 7.147012 0.221972 0.254588
C 8.494160 -0.305206 -0.164727
C 9.156736 -1.313337 0.434179
C -0.723802 -2.953888 2.365658
C 0.573846 -3.184062 3.169509
Cl 1.857593 0.181709 2.046985
Cl 0.521690 0.948404 -2.514700
C 2.517157 1.994742 -0.424696
C -1.868479 -3.854247 2.880926
C 5.750378 -1.439781 -1.054201
C 6.349507 0.771625 -2.106686
H 8.974484 0.197218 -1.025699
H 3.554398 0.987145 -2.008024
H 2.877797 2.428219 0.529099
H -3.393950 1.268967 1.621104
H -2.685266 -0.896010 1.936949
H 2.312188 2.728778 -1.227383
H 0.247189 -5.157590 1.103738
H 0.728938 -5.529118 -1.305445
H 0.294296 -3.682923 -2.973872
H -0.676645 -1.510464 -2.176887
H -1.008944 -1.894611 2.534858
H 6.686946 -1.916645 -1.411380
H 5.435030 -1.974952 -0.133793
H 4.974428 -1.605307 -1.829259
H 7.247572 1.309880 0.479267
H 6.839505 -0.266637 1.205271
H 7.240183 0.310437 -2.580741
H 5.525209 0.705904 -2.847281
H 6.569914 1.848564 -1.942286
H 2.518901 -1.076782 -1.891137
H 3.078975 -1.325876 -0.127251

H 4.538316 0.306773 0.867225
H 5.042504 1.809683 0.065975
H 10.150260 -1.639869 0.085720
H 8.732201 -1.846678 1.302816
H -4.768082 -1.852444 2.205349
H -6.657344 -3.221882 1.311885
H -6.791115 -3.726592 -1.147060
H -5.026409 -2.834418 -2.696310
H -3.157506 -1.447325 -1.805901
H -5.574428 1.526109 0.708164
H -7.028426 2.188483 -1.212932
H -6.054288 2.372686 -3.522670
H -3.611773 1.897663 -3.883254
H -2.154973 1.250943 -1.973774
H 0.031519 2.682785 0.634346
H -2.067133 2.749041 2.892612
H -0.419229 2.038655 2.966078
H -0.523133 4.349199 4.017206
H 0.613861 4.271565 2.653672
H -2.264108 5.410244 2.557145
H -0.756972 6.354774 2.473940
H -1.757278 5.992712 0.172248
H -0.141943 5.261554 0.308862
H -2.850429 3.778792 0.525103
H -1.703957 3.676172 -0.833654
H 0.387510 -3.006049 4.249746
H 0.944153 -4.226135 3.065437
H 1.370024 -2.485213 2.842889
H -2.059412 -3.666604 3.958867
H -2.812816 -3.683376 2.324531
H -1.610253 -4.929303 2.771724

pcy3 E(gas)=-1046.56037777 G(gas)=-1046.141425 E(CH2Cl2)=-1046.56258699

P 0.004987 -0.006533 -1.260465
C 1.627679 -0.695914 -0.547442
C -0.210394 1.744249 -0.548571
C -1.411423 -1.056601 -0.552105
H -2.276604 -0.663782 -1.140523
H 0.559675 2.303679 -1.134185
H 1.730371 -1.638805 -1.138698
C -1.816305 -0.981538 0.935503
C -1.219992 -2.527649 -0.999782
C 1.777967 -1.090395 0.939638
C 2.792284 0.222427 -0.993549
C -1.583373 2.300945 -1.000094

C 0.047979 2.063643 0.941058
C -3.056549 -1.851069 1.228034
H -0.973282 -1.316493 1.578035
H -2.027504 0.069019 1.223607
C -2.855569 -3.309149 0.784403
H -3.307989 -1.802736 2.310262
H -3.933239 -1.425041 0.686527
C -2.462851 -3.386884 -0.700760
H -2.049040 -3.771662 1.399999
H -3.774058 -3.905228 0.977196
H -2.279304 -4.441455 -1.002154
H -3.313419 -3.027462 -1.325156

H -0.345849 -2.966160 -0.464538
H -0.971849 -2.563238 -2.083335
C -0.094132 3.573126 1.226921
H -0.666503 1.500538 1.580880
H 1.062901 1.726842 1.236912
C -1.460439 4.116720 0.777541
H 0.069367 3.772831 2.308668
H 0.711170 4.121624 0.684709
C -1.719669 3.806564 -0.706538
H -2.261996 3.647052 1.394377
H -1.525347 5.210671 0.965042
H -2.727472 4.165093 -1.010482
H -0.987085 4.367292 -1.332118
H -2.396369 1.758002 -0.464079

H -1.734768 2.099929 -2.083441
C 3.160200 -1.716145 1.220499
H 1.643596 -0.197225 1.588097
H 0.983594 -1.808421 1.231053
C 4.308962 -0.795461 0.776351
H 3.253002 -1.963504 2.300779
H 3.238053 -2.684261 0.672826
C 4.167296 -0.407604 -0.705008
H 4.298196 0.129620 1.398919
H 5.291520 -1.282219 0.960112
H 4.978259 0.291385 -1.005564
H 4.290272 -1.318174 -1.336065
H 2.723987 1.194402 -0.451793
H 2.692880 0.460291 -2.075474

Model of substrate E(gas)=-352.27643243 G(gas)=-352.094685 E(CH2Cl2)=-352.277946504

C -3.637620 -0.273775 -0.184025
C -2.544741 0.512529 -0.147514
C -1.235316 0.217103 -0.830423
C 0.000000 0.000019 0.106813
C -0.235193 -1.240921 0.993340
H -2.602242 1.463176 0.415531
C 1.235314 -0.217143 -0.830410
C 2.544731 -0.512563 -0.147483
H 2.602208 -1.463179 0.415615
C 0.235195 1.241028 0.993242
C 3.637629 0.273712 -0.184039
H 1.170334 1.132703 1.580605
H 0.331908 2.163367 0.380360

H -0.596827 1.394877 1.711129
H 0.990555 -1.064558 -1.513356
H 1.351486 0.682229 -1.475460
H 0.596829 -1.394713 1.711238
H -1.170332 -1.132550 1.580694
H -0.331906 -2.163308 0.380529
H -4.571139 0.008724 0.329572
H -3.641974 -1.229593 -0.737064
H -1.351468 -0.682308 -1.475423
H -0.990576 1.064486 -1.513415
H 4.571141 -0.008781 0.329573
H 3.642008 1.229497 -0.737134

ethylene E(gas)=-78.5245851448 G(gas)=-78.496235 E(CH2Cl2)=-78.5254875623

C 0.000000 0.000000 0.670834
C 0.000000 0.000000 -0.670834
H 0.000000 0.938061 -1.251855

H 0.000000 -0.938061 -1.251855
H 0.000000 -0.938061 1.251855
H 0.000000 0.938061 1.251855

Anti Rh (37) E(gas)=-2071.27094193

C -3.145075 0.173677 1.678504
C -2.616056 -0.011805 0.249031
C -3.549065 0.636448 -0.782105
C -4.969965 0.071558 -0.649400
C -5.516852 0.244209 0.771418
C -4.572038 -0.376142 1.805781
N -1.204898 0.414078 0.123776
C -0.735274 1.789708 0.405917
C 0.803648 1.572662 0.596481
N 0.977112 0.198423 0.053475
C -0.196803 -0.440237 -0.076619
H -1.166862 2.134403 1.344554
Rh -0.414743 -2.492647 -0.414306
C -0.254449 -2.243187 -2.243667
C 2.279536 -0.403102 -0.072857
C 2.642406 -1.391879 0.844141
C 3.894264 -1.985191 0.780593
C 4.797943 -1.576379 -0.194091
C 4.432434 -0.594622 -1.104585
C 3.169177 0.008595 -1.078442
C 1.274105 1.728630 2.028448
C 2.044159 2.838708 2.376911
C 2.442918 3.041887 3.695464
C 2.077037 2.129845 4.679213
C 1.312599 1.016100 4.338179
C 0.911038 0.815074 3.022484
C 2.808716 1.039558 -2.139364
C 2.879057 0.447570 -3.557961
C 3.679296 2.303204 -2.030508
C -0.656565 -4.399106 -0.529269
Cl -0.667280 -2.692613 1.977593
C -1.055425 2.806451 -0.674721
H 1.348948 2.279930 -0.026124
H 5.142071 -0.296982 -1.867398
H 5.782835 -2.024559 -0.249975
H 4.160687 -2.755819 1.493187
H 1.930369 -1.697067 1.598112
H 1.772869 1.336084 -1.975525
H 2.336047 3.550431 1.612202
H 3.043601 3.906910 3.949916
H 2.389888 2.281289 5.705325
H 1.030678 0.296855 5.097667
H 0.328116 -0.065018 2.773685
H -2.582504 -1.085003 0.045331
H -3.576158 1.719850 -0.635682
H -3.164356 0.463768 -1.789789
H -5.626744 0.558641 -1.374843
H -4.960487 -0.993758 -0.906267
H -5.637911 1.313031 0.983952
H -6.511537 -0.202591 0.851144
H -4.943543 -0.200102 2.818589

H -4.546082 -1.462640 1.671680
H -3.148112 1.238106 1.939811
H -2.479954 -0.339437 2.374728
H 2.558581 1.190175 -4.292801
H 3.896249 0.145710 -3.816154
H 2.235438 -0.427606 -3.657048
H 3.354160 3.054890 -2.753545
H 3.625972 2.744278 -1.033008
H 4.728980 2.078923 -2.232711
O -0.153443 -2.074752 -3.374575
O -0.785206 -5.528156 -0.555239
C -0.930235 2.507064 -2.032982
C -1.170085 3.480228 -2.996602
C -1.536332 4.769222 -2.616450
C -1.662975 5.077140 -1.266109
C -1.424254 4.100241 -0.303120
H -0.665245 1.503213 -2.341643
H -1.076363 3.230501 -4.046662
H -1.726516 5.525359 -3.368386
H -1.953589 6.074938 -0.960160
H -1.529935 4.345815 0.748025

Syn Rh (36) E(gas)=-2071.26262662 A.U.

C 2.287884 2.907692 0.171172
C 1.975840 1.654065 0.996521
C 2.104448 1.926135 2.502980
C 3.495979 2.474739 2.846298
C 3.831099 3.718912 2.018575
C 3.683779 3.441673 0.519580
N 0.680561 1.017252 0.677838
C -0.638781 1.646601 0.924400
C -1.575153 0.384656 0.914839
N -0.713121 -0.612762 0.213862
C 0.572526 -0.219302 0.187882
C -0.989457 2.748553 -0.059136
C -0.646500 2.676978 -1.410116
C -1.014012 3.696752 -2.280688
C -1.729479 4.796829 -1.816880
C -2.072968 4.875726 -0.471659
C -1.701590 3.857179 0.399650
Rh 2.163507 -1.300094 -0.642343
C 2.424966 -2.229243 0.938143
C -1.179581 -1.886495 -0.270762
C -1.157013 -2.092937 -1.651691
C -1.613601 -3.282226 -2.197417
C -2.115911 -4.269577 -1.357744
C -2.119831 -4.069161 0.014820
C -1.638815 -2.890712 0.597398
C -2.969981 0.578617 0.371053
C -4.008889 0.794050 1.279177
C -5.307744 1.026303 0.840123
C -5.587819 1.032717 -0.521540
C -4.561550 0.812134 -1.434597
C -3.262515 0.590761 -0.993290
C -1.604007 -2.772459 2.115499
C -0.820870 -3.925521 2.766458
C -3.018862 -2.679500 2.712827
C 3.607713 -2.183429 -1.565692
Cl 1.798858 -0.016554 -2.650644
H -0.658506 2.071852 1.927220
H -1.677777 0.056887 1.952892
H -2.491482 -4.858124 0.657017
H -2.490491 -5.199405 -1.768306
H -1.581693 -3.430765 -3.269339
H -0.754811 -1.317037 -2.288988
H -1.069175 -1.854802 2.365104
H -3.800933 0.779313 2.343612
H -6.098929 1.192630 1.560960
H -6.598868 1.205204 -0.869541
H -4.771156 0.813383 -2.497152
H -2.476633 0.427519 -1.715911
H -1.969212 3.927574 1.448543
H -2.624317 5.730245 -0.098539

H -2.011207 5.590440 -2.498182
H -0.733154 3.631664 -3.324866
H -0.068316 1.840362 -1.784764
H 2.710584 0.891291 0.725401
H 1.348993 2.656742 2.813420
H 1.910360 1.004700 3.059290
H 3.549487 2.698263 3.915086
H 4.244943 1.698641 2.653029
H 3.158668 4.536414 2.304388
H 4.845938 4.057452 2.244242
H 3.879837 4.349333 -0.056645
H 4.437968 2.709593 0.209592
H 1.544010 3.683781 0.369744
H 2.228759 2.663421 -0.890079
H -0.744990 -3.764355 3.844490
H -1.318699 -4.885064 2.612852
H 0.189540 -4.002070 2.365289
H -2.969265 -2.516039 3.792356
H -3.594209 -1.867792 2.266475
H -3.572730 -3.605880 2.544134
O 2.598348 -2.791635 1.923349
O 4.454297 -2.683887 -2.136530

NHC-anti E(gas)=-1273.55138855 A.U.

C -3.091388 -2.056227 -0.714379
C -2.573666 -0.766420 -1.370744
C -3.647450 0.330651 -1.338086
C -4.941506 -0.151422 -2.007999
C -5.463150 -1.442771 -1.370259
C -4.389659 -2.535300 -1.376357
N -1.268327 -0.355490 -0.833074
C -1.026685 -0.050579 0.603204
C 0.530632 -0.134964 0.682399
N 0.885281 -0.164392 -0.770076
C -0.161321 -0.400664 -1.589838
H -1.465298 -0.828050 1.229111
C 2.245731 -0.221948 -1.213232
C 2.703650 -1.412143 -1.783530
C 4.012244 -1.536900 -2.222288
C 4.885939 -0.463925 -2.080384
C 4.428485 0.723693 -1.528438
C 3.105864 0.882244 -1.098490
C 1.048372 -1.327636 1.460589
C 1.753081 -1.130503 2.647768
C 2.206220 -2.212072 3.398481
C 1.959129 -3.509749 2.967277
C 1.258173 -3.718642 1.781740
C 0.808522 -2.637212 1.034885
C 2.640251 2.239122 -0.590880
C 2.745692 3.311513 -1.689088
C 3.389226 2.676314 0.678225
C -1.559049 1.293168 1.065418
H 0.920274 0.769430 1.148172
H 5.112146 1.560480 -1.447208
H 5.915187 -0.547774 -2.407886
H 4.349170 -2.466762 -2.663784
H 2.008287 -2.233777 -1.885429
H 1.583215 2.153655 -0.342262
H 1.949463 -0.120603 2.990128
H 2.755552 -2.038689 4.315955
H 2.313407 -4.353811 3.546286
H 1.066955 -4.727629 1.436453
H 0.275029 -2.809454 0.107874
H -2.350784 -0.987759 -2.416572
H -3.861515 0.615933 -0.303963
H -3.268833 1.223450 -1.840439
H -5.700191 0.633784 -1.951778
H -4.753480 -0.325857 -3.073788
H -5.765907 -1.238591 -0.336490
H -6.358144 -1.789736 -1.894155
H -4.755213 -3.432512 -0.869368
H -4.178004 -2.827508 -2.411223
H -3.279880 -1.882718 0.351036
H -2.322699 -2.830531 -0.781758
H 2.335605 4.260621 -1.334420

H 3.783944 3.486615 -1.980057
H 2.194075 3.013195 -2.582296
H 2.986619 3.619173 1.056446
H 3.304987 1.929011 1.469921
H 4.453311 2.825528 0.480505
C -1.411399 2.444785 0.288723
C -1.853200 3.675910 0.758461
C -2.451784 3.776394 2.012172
C -2.606238 2.635629 2.791404
C -2.161856 1.403812 2.318922
H -0.965702 2.370534 -0.695843
H -1.735489 4.559487 0.142565
H -2.798900 4.736082 2.375056
H -3.075287 2.701407 3.765789
H -2.287747 0.517602 2.931413

NHC-syn E(gas)=-1273.54399617 A.U.
C 3.789923 -0.810861 -0.697067
C 2.547147 -1.634348 -0.332965
C 2.763694 -2.397775 0.985308
C 4.019974 -3.275126 0.930589
C 5.260904 -2.460295 0.554031
C 5.040626 -1.697701 -0.755826
N 1.293196 -0.869054 -0.307918
C 1.066580 0.325580 0.549362
C -0.491609 0.280769 0.661659
N -0.822854 -0.503521 -0.570094
C 0.207755 -1.281172 -0.981022
C 1.657293 1.603109 -0.023467
C 1.719635 1.838094 -1.397942
C 2.241752 3.029239 -1.889756
C 2.713006 4.004122 -1.014995
C 2.658792 3.778235 0.356077
C 2.135162 2.585586 0.844320
C -2.180920 -0.801260 -0.932767
C -2.767595 -0.053293 -1.953153
C -4.075417 -0.287197 -2.352158
C -4.811561 -1.282581 -1.719846
C -4.225374 -2.037787 -0.713889
C -2.905519 -1.825399 -0.300727
C -1.227469 1.581492 0.871946
C -1.752806 1.853845 2.137327
C -2.418522 3.046969 2.399427
C -2.578588 3.988006 1.389225
C -2.068001 3.725200 0.121346
C -1.398696 2.534965 -0.134257
C -2.295379 -2.728735 0.760679
C -2.151143 -4.169740 0.242629
C -3.077733 -2.686046 2.083013
H 1.491754 0.170654 1.541598

H -0.724554 -0.355214 1.523885
H -4.805027 -2.823874 -0.244474
H -5.835558 -1.477535 -2.015194
H -4.513827 0.300706 -3.149065
H -2.175093 0.708291 -2.441164
H -1.286391 -2.369946 0.961507
H -1.642726 1.119851 2.928249
H -2.817329 3.235545 3.388873
H -3.101409 4.916199 1.585352
H -2.191441 4.450854 -0.673489
H -1.002303 2.347915 -1.121642
H 2.096573 2.417763 1.915170
H 3.026847 4.527784 1.046268
H 3.123759 4.929692 -1.399653
H 2.285296 3.194965 -2.959707
H 1.367651 1.078066 -2.084275
H 2.378559 -2.369485 -1.122982
H 2.862200 -1.683695 1.811468
H 1.880196 -3.007299 1.191353
H 4.166979 -3.773825 1.892601
H 3.871240 -4.068856 0.189481
H 5.482474 -1.745915 1.355866
H 6.132753 -3.115066 0.470182
H 5.914552 -1.084282 -0.990987
H 4.935929 -2.416182 -1.577203
H 3.944290 -0.019308 0.043038
H 3.633839 -0.314813 -1.656626
H -1.666687 -4.798470 0.994350
H -3.124698 -4.611023 0.015925
H -1.546492 -4.193067 -0.664839
H -2.571464 -3.284787 2.844339
H -3.170991 -1.664734 2.458464
H -4.086768 -3.088252 1.966814

Rh-CO-relax E(gas)=-797.629609638 A.U.
Rh 0.021873 -0.291625 -0.000283
C -1.837303 -0.620817 -0.000068
C -0.285986 1.505252 -0.000025

Cl 2.292279 -0.377045 0.000399
O -2.952526 -0.854275 0.000657
O -0.449136 2.632559 0.000157

3.8.11 Catalysis

RCM of Diethyldiallyl malonate (23)
An NMR tube with a screw-cap septum top was charged with 0.8 mL of a CD_2Cl_2 or C_6D_6 solution of catalyst (0.8 µmol) and then was equilibrated at the appropriate temperature (30°C for Grubbs-type catalyst and 60°C for Hoveyda-type catalysts) in the NMR probe. After that, 19.3 µL (0.080 mmol) of **23** were injected and the reaction was controlled as a function of time. The conversion to the cyclic product **23a** was determined by integrating themethylene protons in the starting material, δ 2.61 (dt) in CD_2Cl_2 or 2.84 (dt) in C_6D_6, and those in the product, δ 2.98 (s) in CD_2Cl_2 or 3.14 (s) in C_6D_6.

RCM of Diethyldiallylmethallylmalonate (25)
An NMR tube with a screw-cap septum top was charged with 0.8 mL of a CD_2Cl_2 or C_6D_6 solution of catalyst (0.8 µmol) and then was equilibrated at the appropriate temperature (30°C for Grubbs-type catalyst and 60°C for Hoveyda-type catalysts) in the NMR probe. After that, 20.5 µL (0.080 mmol) of **25** were injected and the reaction was controlled as a function of time. The conversion to the cyclic product **25a** was determined by integrating the methylene protons in the starting material, δ 2.67 (s), 2.64 (dt) in CD_2Cl_2 or 2.96 (d), 2.93 (s) in C_6D_6, and those in the product, δ 2.93 (s), 2.88 (m) in CD_2Cl_2 or 3.18 (m), 3.07 (s) in C_6D_6.

RCM of Diethyldimethallylmalonate (27)
An NMR tube with a screw-cap septum top was charged with 0.8 mL of a CD_2Cl_2 or C_6D_6 solution of catalyst (0.8 µmol) and then was equilibrated at the appropriate temperature (30°C for Grubbs-type catalyst and 60°C for Hoveyda-type catalysts) in the NMR probe. After that, 21.6 µL (0.080 mmol) of **27** was injected and the reaction was controlled as a function of time. The conversion to the cyclic product **27a** was determined by integrating the methylene protons in the starting material, δ 2.71 (s) in CD_2Cl_2 or 2.98 (s) in C_6D_6, and those in theproduct, δ 2.89 (s) in CD_2Cl_2 or 3.15 (s) in C_6D_6.

RCM of N-Tosyl diallylamine (24)
An NMR tube with a screw-cap septum top was charged with 0.8 mL of a CD_2Cl_2 or C_6D_6 solution of catalyst (0.8 µmol) and then was equilibrated at the appropriate temperature (30°C for Grubbs-type catalyst and 60°C for Hoveyda-type catalysts) in the NMR probe. After that, 17.2 µL (0.080 mmol) of **24** was injected and the reaction was monitored as a function of time, determining the conversion to the cyclic product **24a** by integrating the methyleneprotons in the starting material, δ 3.70 (dt) in CD_2Cl_2 or 3.71 (d) in C_6D_6, and those in the product, δ 4.00 (s) in CD_2Cl_2 or 3.90 (s) in C_6D_6.

RCM of N-tosyl allylmethallylamine (26)
An NMR tube with a screw-cap septum top was charged with 0.8 mL of a CD_2Cl_2 or C_6D_6 solution of catalyst (0.8 µmol) and then was equilibrated at the appropriate temperature (30°C for Grubbs-type catalyst and 60°C for Hoveyda-type catalysts) in the NMR probe. After that, 19.4 µL (0.080 mmol) of **26** was injected and the reaction was monitored as a function of time, determining the conversion to the cyclic product **26a** by integrating the methylene protons in the starting material, δ 3.63 (s), 2.64 (dt) in CD_2Cl_2 or 3.70 (d), 3.67 (s) in C_6D_6, and those in the product, δ 3.91 (s), 2.88 (m) in $CD2Cl2$ or 3.96 (m), 3.82 (s) in C_6D_6.

RCM of N-tosyl dimethallylamine (28)

An NMR tube with a screw-cap septum top was charged with 0.8 mL of a CD_2Cl_2 or C_6D_6 solution of catalyst (0.8 μmol) and then was equilibrated at the appropriate temperature (30°C for Grubbs-type catalyst and 60°C for Hoveyda-type catalysts) in the NMR probe. After that, 20.2 μL (0.080 mmol) of **24** was injected and the reaction was monitored as a function of time, determining the conversion to the cyclic product **26** by integrating the methylene protons in the starting material, δ 3.61 (s) in CD_2Cl_2 or 3.69 (s) in C_6D_6, and those in the product, δ 3.87 (s) in CD_2Cl_2 or 3.90 (s) in C_6D_6.

Table S3.2: RCM of **23** and **24**

Entry[a]	Substrate	Product	Catalyst	Time (min)	Yield[b] (%)
1			1	60	78
2			2	22	>97
3	EtOOC COOEt 1%mol [Ru] 0.1M -C₂H₄ **23**	EtOOC COOEt **23a**	5	60	52
4			6	20	>97
5			GII tol	35	97
6			3	5	>99
7			4	3	>99
8			7	20	>99
9			8	4	>99
10			HII tol	4	>99
11			1	60	65
12			2	35	94
13	Tos N 1%mol [Ru] 0.1M -C₂H₄ **24**	Tos N **24a**	5	60	32
14			6	35	94
15			GII tol	27	>99
16			3	60	>99
17			4	2	>99
18			7	4	93
19			8	3	>99
20			HII tol(0.1%mol)	6	>99

[a] All runs were carried out in C_6D_6 at 60°C. [b] Yields based on NMR analysis.

Table S3.3: RCM of **25** and **26**

Entry[a]	Substrate	Product	Catalyst (mol%)	Time (min)	Yield[b] (%)
1			1	60	72
2			2	60	91
3	EtOOC COOEt 1%mol [Ru] 0.1M -C₂H₄ **25**	EtOOC COOEt **25a**	5	60	45
4			6	60	84
5			**GII tol**	60	79
6			3	60	94
7			4	8	>99
8			7	11	99
9			8	9	>99
10			**HII tol**	8	>99
11			1	60	84
12			2	24	98
13	Tos N 1%mol [Ru] 0.1M -C₂H₄ **26**	Tos N **26a**	5	60	66
14			6	30	96
15			**GII tol**	45	99
16			3	14	99
17			4	4	>99
18			7	7	>99
19			8	5	>99
20			**HII tol**(0.1%mol)	11	>99

[a] All runs were carried out in C_6D_6 at 60°C. [b]Yields based on NMR analysis.

Table S3.3: RCM of **27** and **28**

Entry[a]	Substrate	Product	Catalyst (mol%)	Time (min)	Yield[b] (%)
1			1	60	22
2			2	60	57
3			5	60	9
4			6	60	30
5			**GII tol**	60	70
6			3	60	45
7			4	60	>97
8			7	60	37
9			8	60	34
10			**HII tol**	60	97
11			1	60	33
12			2	60	64
13			5	60	29
14			6	60	31
15			**GII tol**	60	92
16			3	60	77
17			4	60	97
18			7	60	76
19			8	60	77
20			**HII tol**(1%mol)	23	>99

For entries 1–10, the substrate is **27** (EtOOC, COOEt bearing cyclohexane with two exocyclic methylenes) reacting with 5%mol [Ru], 0.1M -C_2H_4, to give product **27a** (EtOOC, COOEt cyclopentene with two methyl groups).

For entries 11–20, the substrate is **28** (N-Tos piperidine with two exocyclic methylenes) reacting with 5%mol [Ru], 0.1M -C_2H_4, to give product **28a** (N-Tos pyrroline with two methyl groups).

[a] All runs were carried out in C_6D_6 at 60°C. [b]Yields based on NMR analysis.

ROMP of 1,5-cyclooctadiene (29)

An NMR tube with a screw-cap septum top was charged with 0.8 mL of a CD_2Cl_2 or C_6D_6 solution of catalyst (0.8 μmol) and then was equilibrated at the appropriate temperature (30°C for Grubbs-type catalyst and 60°C for Hoveyda-type catalysts) in the NMR probe.
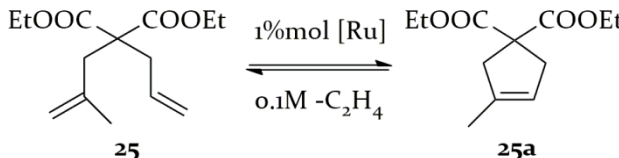
After that, 49.1 μL (0.40 mmol) of **29** was injected and the reaction was monitored as a function of time, determining the conversion by integrating the protons in the monomer at δ =2.36 (s) in CD_2Cl_2 or 2.22 (s) in C_6D_6, and those in the polymer, δ=2.09 (s) and 2.04 (s) in CD_2Cl_2 or 2.14 (s) and 2.11 (s) in C_6D_6. Those signals of the polymer are also used to determine the *E/Z* ratio.

When the conversion is complete, the polymerization is quenched with a solution of ethylvinyl ether in methanol.

CM of Allylbenzene (30) and cis-(1,4)-Diacetoxy-2-butene (31)

In an oven-dried 4-ml vial (equipped with a magnetic stirrer) a 66 μL amount of **30** (0.5 mmol) and160 μL amount of **31** (1.0 mmol) were added simultaneously to a 2.5 mL solution of the catalyst(0.0013 mmol) in methylene chloride. The reaction mixture was refluxed under nitrogen overnight.

Crude reaction product was purified on column chromatography eluting with hexane:ethyl acetate 9:1.

33 was obtained as a pale oil. The *E/Z* ratio was determined by ^{1}HNMR spectroscopy.

Chapter 4

Applications of u-NHC Catalysts
in Metathesis Polymerisations

In the middle of the last century polymer materials were overwhelmingly coming into people houses and were significantly improving the quality of life. The development of new polymerisation reactions were strongly promoted and industries were motivated to invest in the applications of new processes.

In these favourable context ROMP, the oldest metathesis-based transformation, was discovered. The novelty of this polymerisation contributed to the progresses of all the metathesis transformations up to the consecration of metathesis as a one of the most important reactions of the twentieth century.

The mechanism of ROMP of course traces those proposed by Chauvin, with some interesting peculiarities (scheme 4.1).[82]

The initiation step (kinetic constant k_I) consists in the formation of a coordination vacancy with the consequent formation of the metallacyclobutane intermediate. The subsequent opening of the cycle is irreversible when the monomer is a highly strained olefin.

The propagation step (kinetic constant k_P) includes the coordination of other monomer units and determines the growth of the polymer chain.

The introduction of an appropriate terminating agent (usually ethyl vinyl ether, which irreversibly generates the metathesis inactive $Ru=CH-O-CH_2CH_3$ Fisher carbene) stops the polymerisation.

Above these fundamental phases of polymerisation, other side reactions can occur, including intra- and intermolecular chain transfer.

The use of a single type of monomer is the simplest possibility for ROMP reactions and gives homopolymers. This is the case of the most relevant ROMP macromolecules like Norsorex® and Telene® (see chapter 1).

The involvement of different kinds of monomers with a k_I significantly higher than k_P and their judicious addition in the reaction mixture allows for the synthesis of block copolymers. More complex is the case of the synthesis of alternated copolymers. Indeed, for this scope, a precise circumstance has to occur: the insertion of the monomer **A** should be favoured when monomer **B** was the previously inserted and strongly disfavoured when another molecule of **A** was just inserted. This particular condition is not limited to olefin metathesis but regards also other polymers synthetic strategies and pushed the research towards the development of catalysts selective towards the formation of alternated copolymers.

---

[82] A. C. Knall, C. Slugovic, *Olefin Metathesis Polymerisation,* chapter of *Olefin Metathesis: Theory and Practice,* Edited by K. Grela, John Wiley and Sons, Hoboken **2014**
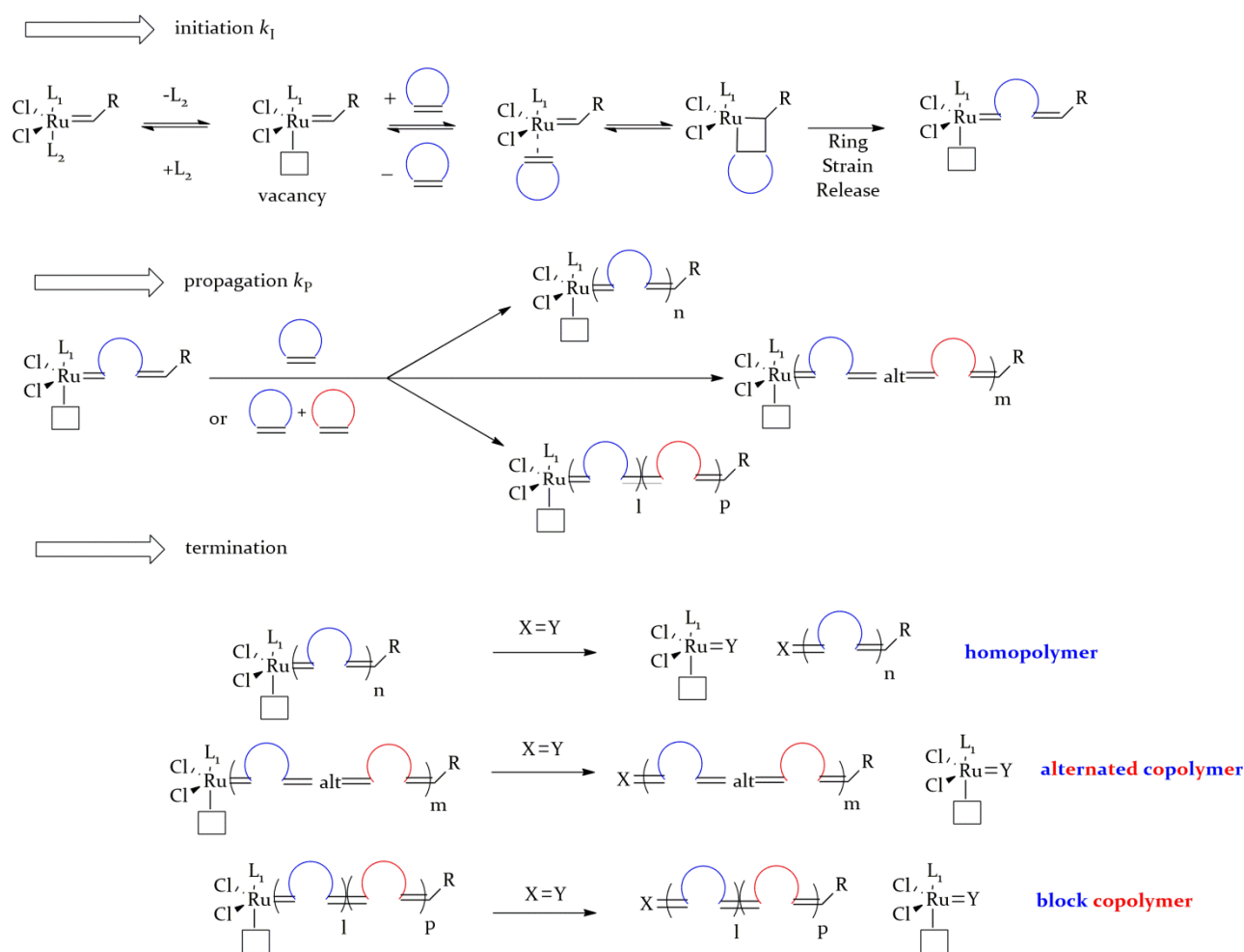
Scheme 4.1: A simplified ROMP mechanism

Unfortunately, the achievement of alternated copolymers is still a tricky question.

In this context, very promising is the application of u-NHC ruthenium catalysts. To illustrate the potentialities of these systems, a representative ROMP propagating cycle is reported in scheme 4.2.[83] In this representative scheme, norbornene (**NBE**) is the more active monomer while the less strained cyclooctene (**COE**) is the less active olefin.

Addition to **COE** or **NBE** to the active species generates **4** (**COE** addition) or **2** (**NBE** addition). **2** is a considerably hindered species and favours only **COE** coordination. This is because a further **NBE** coordination to **2** would result or in a ruthenacyclobutane trans to the NHC (that would give the very hindered species **2a**, that is avoided) or in a ruthenacyclobutene side-on to the NHC (that would result in the encumbered species **2b**). Since the formation of **2b** is slow but is not avoided, an excess of **COE** is necessary.

The active species **4** is less hindered and there is no steric obstacle in the coordination of both **NBE** and **COE**. However, **4** is more prone to incorporate **NBE**, the more active monomer.

---

[83] a) K. Vehlow, D. Wang, M. R. Buchmeiser, S. Blechert, *Angew. Chem. Int. Ed.* **2008**, *47*, 2615.; b) Study of alternated ROMP with catalysts bearing unsymmetrical phosphine ligands were published in: M. Bornand, S. Torker, P. Chen, *Organometallics* **2007**, *26*, 3585.

These coordination preferences of the propagating species **2** and **4** generate the alternated junctions.

According to this mechanism, ROMP alternated copolymerisation can occur if:

- There are two different propagating species and one of them has a consistent steric hindrance;
- Monomers involved have a different ring strains;
- The less strained monomer is in excess

P = growing polymer chain
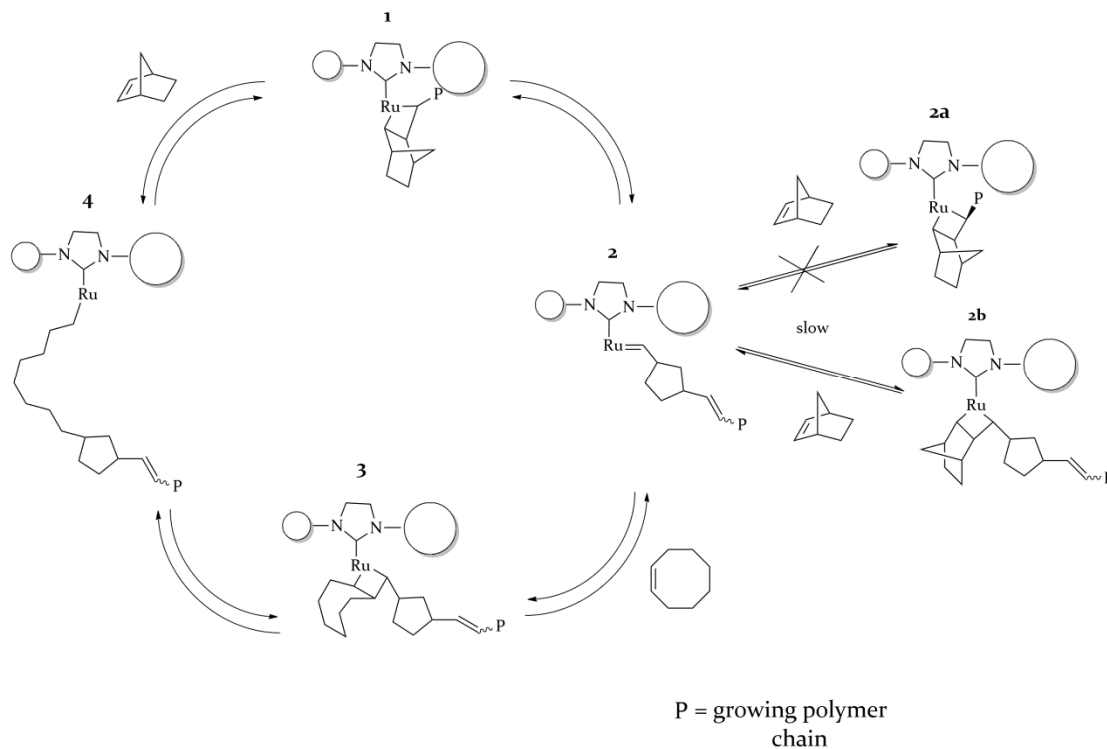
Scheme 4.2: Representative propagation of ROMP catalysed by u-NHC ruthenium catalysts (chloride atoms have been omitted for clarity)
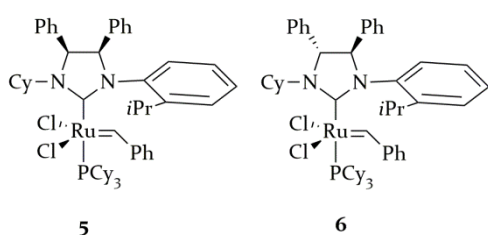
Figure 4.1: Catalysts **5** and **6**

Between all the u-NHC catalysts discussed in the previous chapter, **5** and **6** (figure 4.1) were the most promising since they combined the facility of synthesis, an intriguing activity and a pronounced backbone effect.

Inspired by the interesting results obtained in standard metathesis reactions, we decided to first investigate the behaviours of these catalysts in the homopolymerisation of norbornene (**NBE**) and of exo,exo-5,6-dicarbometoxy-7-oxa-2-norbornene (**ONBE**), in order to to have an overview of their ROMP activity in comparison with the symmetrical commercial catalyst **GII**.

Then, the potentialities of **5** and **6** were evaluated in the alternating copolymerisation of norbornene (**NBE**) with cyclopentene (**CPE**) or cis-cyclooctene (**COE**) and very preliminary copolimerisation results are discussed.

4.1 Homopolimerisation of NBE
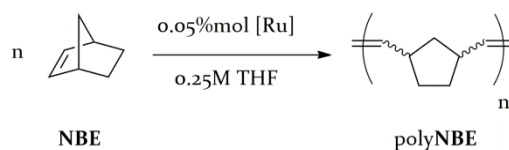
Scheme4.3: Polymerisation of **NBE**

Bicyclo[2.2.1] hept-2-ene, also known as norbornene (**NBE**), is a white, deliquescent solid, with a typical intense smell. It is a 'classic' monomer for ROMP, due to its high ring strain energy (27.2 kcal/mol)[1b] and to the properties of the corresponding homopolymer poly**NBE**. It can be also considered as a very useful olefin in a preliminary and explorative evaluation of ROMP activity of new catalysts . Moreover, due to the monomer symmetry, NMR spectra of poly**NBE** are very comprehensive and extensively studied in the literature.[84]

In this polymer, the tacticity and the cis or trans geometry of the chain double bonds make in principle four different regular structures possible (figure 4.2):

- cis-isotactic: m diad and cis double bond;
- cis-syndiotactic: r diad and cis double bond;
- trans-isotactic: m diad and trans double bond;
- trans-syndiotactic: r diad and trans double bond.
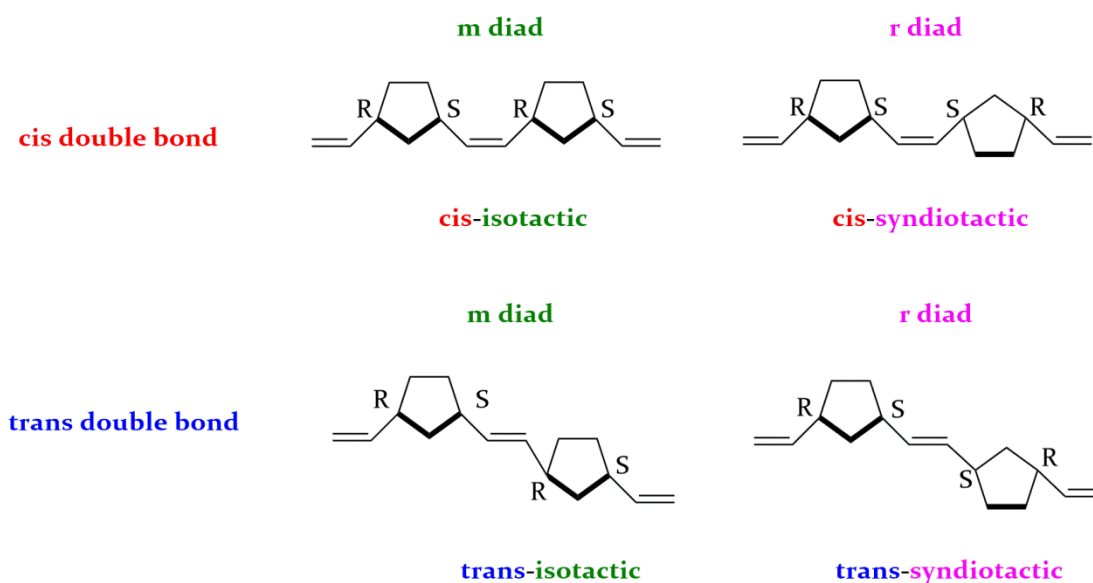
Figure 4.2: The four regular diads possible in poly**NBE**

Cis and trans double bonds can be quantified by the integration of olefins proton in the ^{1}H NMR spectra. Even more informative is the ^{13}C NMR analysis, in which the relative proportions of trans-trans (tt), cis-cis (cc), trans-cis (tc) and cis-trans (ct) junctions in the polymer chain can be esteemed.

---

[84] K. J. Ivin, D. T. Laverty, J. H. O'Donnell, J. J. Rooney, C. D. Stewart, *Makromol. Chem.* **1979**, *180*, 1989.
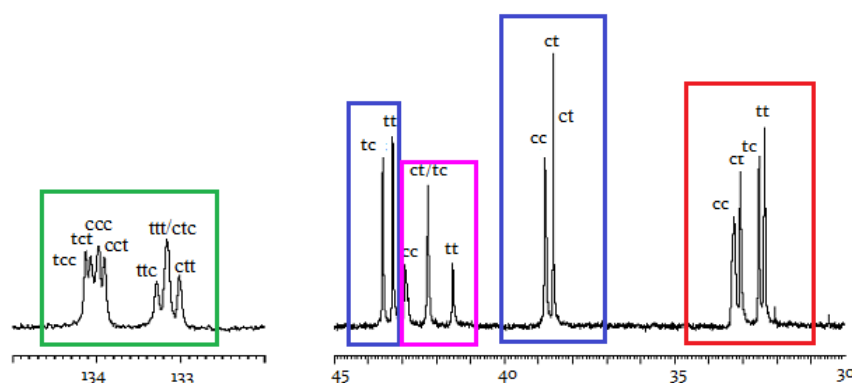
Figure 4.3: Representative regions of the poly**NBE** carbon spectrum.

Distribution of double bonds can be thus calculated using the parameters rt and r_c, defined as follows:

$$rt = \frac{tt}{tc} \qquad rc = \frac{cc}{ct}$$

Equation 4.1   **Equation 4.2**

When the formation of a cis double bond is statistic, $rt*r_c \leq 1$ and the fraction of cis double bond σ_c is lower than 0.35.[85]
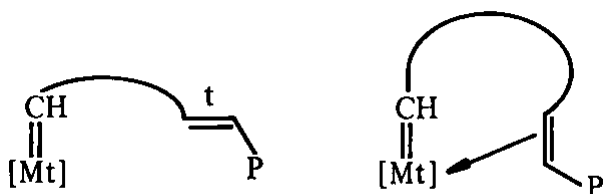
Figure 4.4: Proposed propagating species for the chain controlled configuration in polymerisation of **NBE**[86]

Differently, a higher cis content ($rt*r_c > 1$) indicates a chain end control through the presence of two propagating species differing for the configuration of the last double bond (figure 4.4). In the cis hypothesized structure (figure 4.4, right), double bond has the tendency to remain in the proximity of the metal centre until the next coordination step.[86]

Catalyst **5**, **6** and **GII** were tested in the polymerisation of **NBE** (scheme 4.3) in dry THF with a loading of 0.5% mol. The amount of cis double bonds was evaluated with ^{1}H and ^{13}C NMR spectroscopy and molecular weights were determined using gel permeation chromatography. Results are summarised in table 4.1. u-NHC catalysts **5** and **6** in this reaction were less efficient than **GII** and led to obtain a very similar σ_c. Calculated values of $r_t r_c$ of all tested complexes were slightly higher than 1, indicating a very modest chain end control. Differently, $r_t r_c$ values up to eight were reported in the literature for first generation ruthenium systems.[84]

Determination of polymer tacticity would require NMR analysis of the hydrogenated samples and was not investigated yet.[87]

---

[85] Calculated by dividing the integrated area of cis carbons by the area of all carbons (cis+trans) and then by four (the number of non equivalent carbons in poly**NBE** monomeric unit).

[86] R. M. E. Greene, J. G. Hamilton, K. J. Ruin, J. J. Rooney, *Makromol. Chem.* **1986**, *187*, 619.

[87] K. J. Ivin, D. T. Laverty, J. J. Rooney, *Makromol. Chem.* **1978**, *179*, 253.

Table 4.1: ROMP of **NBE** with **5**, **6** and **GII**

catalyst	yield (%)	σ_c[a]	rt[a]	r_c[a]	$r_t r_c$[a]	M_n (KDa)[b]	$M_{theoric}$(KDa)	PDI[b]
5	84	0.54	0.98	1.19	1.16	37	16	1.57
6	55	0.54	1.07	1.24	1.33	41	10	1.40
GII[c]	92	0.58	0.77	1.52	1.17	865	17	1.63

Norbornene was always full converted, reactions were carried out at room temperature for two hours in methylene chloride ([NBE]=0.3 M); [a]Determined via NMR spectroscopy; [b]Determined through GPC analysis; [c]After 35 s gelification was observed

With all catalysts, the number average molecular weights (Mn) were significantly higher with respect to the calculated, thus suggesting an incomplete catalytic site activation.

The broad polidispersity indexes (PDI) observed were probably caused by chain transfer side reactions.

4.2 Homopolymerisation of ONBE

exo,exo-5,6-dicarbometoxy-7-oxa-2-norbornene (**ONBE**) is a functionalized monomers containing two ester groups.
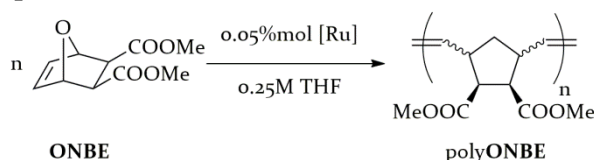
Scheme 4.4: Polymerisation of **ONBE**

Analogously to poly**NBE**, four regular structures are possible (figure 4.5):

- exo,exo-cis-isotactic;
- exo,exo-cis-syndiotactic;
- exo,exo-trans-isotactic;
- exo,exo-trans-syndiotactic.
-

Ruthenium compounds **5**, **6** and **GII** were investigated in the polymerisation of this functionalised monomer in the same reaction conditions chosen for poly**NBE** (table 4.2).

All complexes were efficient in this reaction and **5** displayed the highest reactivity. Analogously to poly**NBE**, NMR analysis was very useful in the determination of cis/trans amount of double bonds in the polymer chain. In fact, for poly**ONBE** both ¹H and ¹³C NMR spectra allow for an accurate evaluation of σ_c.

GII showed a significant cis content (σ_c =0.64), differently from **5** and **6** which exhibited a lower σ_c that is unusual for catalysts bearing NHC ligands.[88]

---

[88] L. E. Rosebrugh, T. S. Ahmed, V. M. Marx and R. H. Grubbs, *J. Am. Chem. Soc.* **2016**, *138*, 1394.
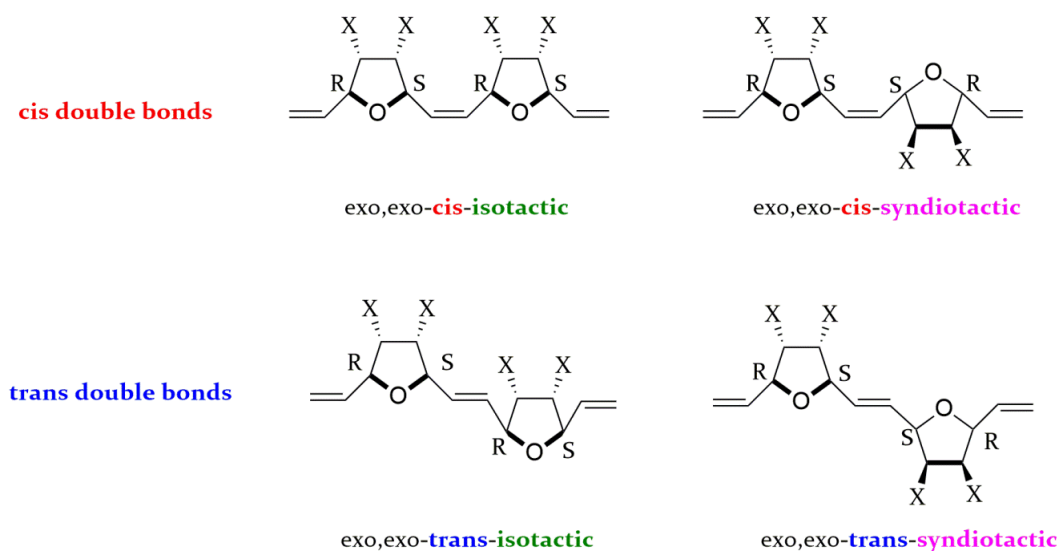
Figure 4.5: The four regular diads possible in poly**ONBE**

Table 4.2: ROMP of **ONBE** with **5**, **6** and **GII**

catalyst	yield (%)	$\sigma_c{}^a$	M_n (KDa)[b]	$M_{theoric}$(KDa)	PDI[b]
5	92	0.31	75	39	1.21
6	82	0.22	83	35	1.22
GII	80	0.64	256	34	1.52

Norbornene was always full converted, reactions were carried out at room temperature for two hours; [a] Evaluated via NMR spectroscopy; [b] Determined through GPC analysis;
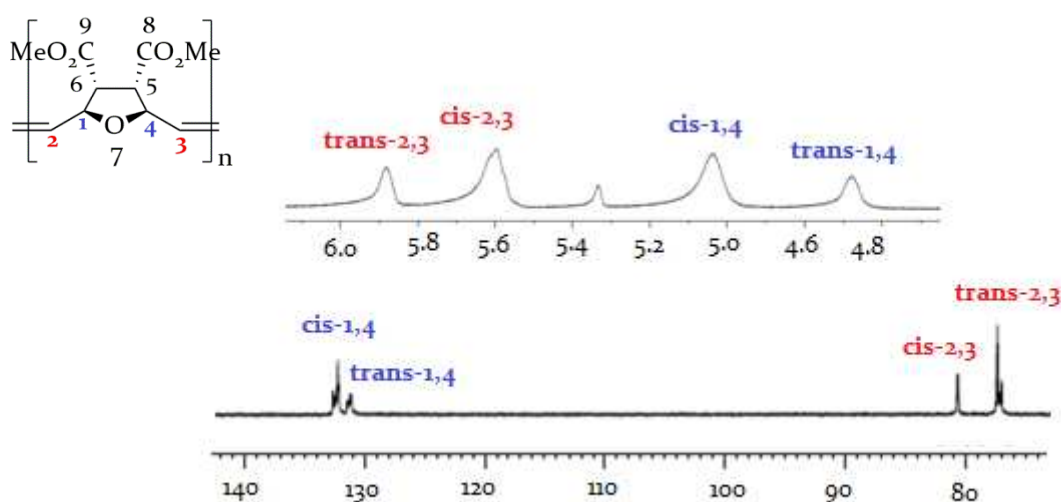
Figure 4.6: Representative regions of the poly**ONBE** proton and carbon spectra

In the case of poly**ONBE**, NMR analysis of the polymer provides also an evaluation of the tacticity. Indeed, signals of trans C_1 and C_4 carbons have an adequate resolution to consent a quantification of the r and the m diads (figure 4.7).[89] Examination of tacticity of the cis

---

[89] V. Amir-Ebrahimi, D. A. K. Corry, J. G. Hamilton, J. J. Rooney, *J. Mol. Catal. A: Chem.* **1998**, *133*, 115.

sequences is even informative albeit more difficult, particularly if samples have a low degree of stereoregularity.

Commercial **GII** led to obtain a polymer with atactic trans diads and mainly syndiotactic cis diads, in agreement with literature results.[90]

With **5** and **6** polymers with highly syndiotactic trans sequences (>99%) and mainly syndiotactic cis diads were obtained. An analogue stereoregularity was observed in ROMP of **ONBE** promoted by other u-NHC ruthenium systems.[88]

Similarly to ROMP of **NBE**, GPC analysis showed number average molecular weights significantly higher than the theoric thus suggesting a non complete activation of catalytic sites.

PDIs of poly**ONBE**s, in particular with **5** and **6**, were lower respect to those of poly**NBE**. This was probably due to the presence of ester functionalities, which disfavoured chain transfer processes. However, they were still higher than 1, excluding a living nature of the polymerisation.

Figure 4.7: Selected region of carbon spectra of the poly**ONBE**s obtained with **5**, **6** and **GII**

4.3 Copolymerisation of NBE with COE or CPE

As mentioned at the beginning of the chapter, the synthesis of alternated copolymers is still challenging. To investigate the potentialities of **5** and **6** in this transformation, copolymerisations of highly strained **NBE** with the less strained cyclooctene (**COE**, ring strain 7.4 Kcal/mol)[91] and cyclopentene (**CPE**, ring strain 6.8 Kcal/mol)[91] were studied.

For these reactions, a comparison with **GII** was not possible, due to its symmetric nature that makes alternated polymers inaccessible[83].

4.3.1 Poly(NBE-*alt*-COE)

Copolymerisations of **NBE** and **COE** (scheme 4.5) with **5** and **6** were carried out in dry methylene chloride with a loading of 0.1% mol.
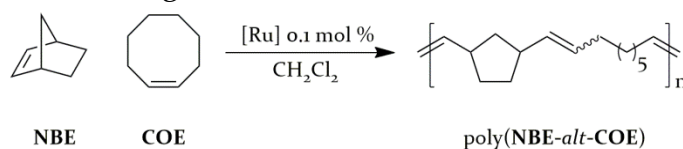
Scheme 4.5: Copolymerisation of **NBE** and **COE**

[90] M. A. Tallon, Y. Rogan, B. Marie, *Journal of Polymer Science, Part A: Polymer Chemistry* **2014**, *52*, 2477.

[91] P. R. Schleyer, J. E. Williams, K. R. Blanchard, *J. Am. Chem. Soc.* **1970**, *92*, 2377.

The copolymer was characterised through ^{13}C NMR analysis and the abundance of the homosequence and eterosequence was evaluated (figure 4.8).

Vinylic signals of the heterosequences can be observed at 135.0 ppm (C_a) and 128.5 ppm (C_b). In the case of the lower field signal, an accurate evaluation of the cis/trans content is possible. Olefinic carbons of the homosequences have their signals at 133-134 ppm (C_c and C_d, **NBE** homosequence) and 130 ppm (C_e and C_f, **COE** homosequence). Also in this case, signals of cis and trans vinylic carbons are splitted and their integration allows for the calculation of the cis/trans content.
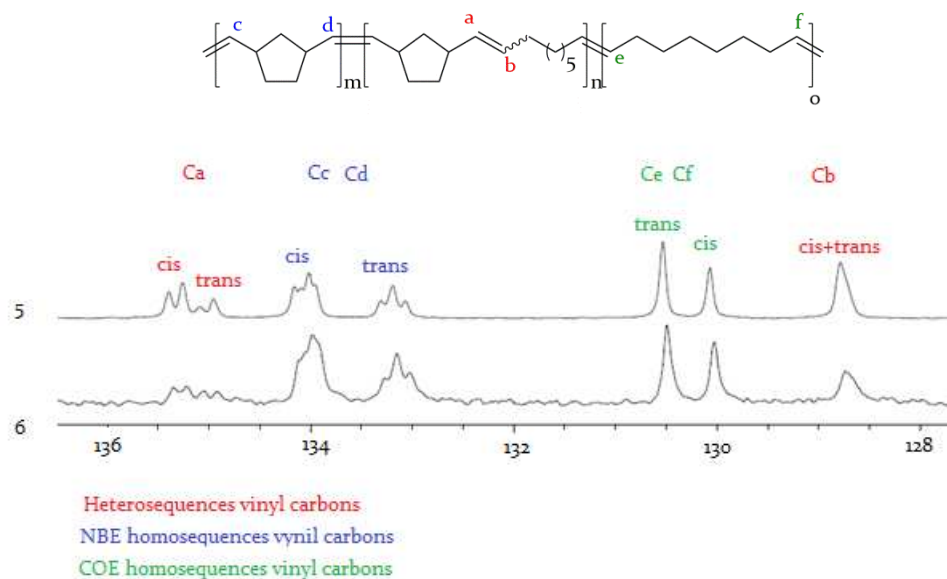
Figure 4.8: ^{13}C spectra of Poly(**NBE**-*alt*-**COE**)obtained with catalysts **5** and **6**

The average lengths of homosequences for both **COE** (L_{COE}) and **NBE** (L_{NBE}) were also calculated, for copolymers with a content of heterosequences less of 50%, using the following equations:

$$L_{NBE} = \frac{I(C_{c,d}) + I(C_a)}{I(C_a)} \qquad L_{COE} = \frac{I(C_{e,f}) + I(C_b)}{I(C_b)}$$

Equation 4.3   **Equation 4.4**

Results of copolymerisations with a **NBE:COE** monomer ratio of 1 and 2 are reported in tables 4.3 and 4.4.

Due to the very different monomers reactivity, an **NBE:COE** ratio of 1 and 2 are not favourable for the obtainment of an alternated copolymer, since higher concentrations of the less strained monomer are required. However these reaction conditions were chosen to have a preliminary estimation of **5** and **6** catalytic activity and to reveal potential differences in their behaviours.

Interestingly, for both complexes, percentages of alternated heterosequences (table 4.3) were quite promising and comparable with those reported in the literature for u-NHC

systems under analogues reaction conditions.[92] Moreover, by doubling the concentration of **COE** (table 4.4) the amount of alternated heterosequences further increased of about twenty percentage points.

Table 4.3: Poly(**NBE**-*alt*-**COE**) with catalysts **5** and 6, **NBE:COE 1:1**

catalyst	poli(NBE)[a]		poli(COE)[a]		poli(NBE-*alt*-COE)[a]		t[b]	L$_{NBE}$[a]	L$_{COE}$[a]	M$_n$[c]	PDI[c]
	(%)cis/trans		(%) cis/trans		(%) cis/trans		(s)			(kD)	
5	36	64/36	27	38/62	37	68/32	12	3.0	2.4	227	1.77
6	50	60/40	31	43/57	19	61/19	80	6.2	3.9	352	2.22

Norbornene was always full converted, reactions were carried out in methylene chloride ([NBE]=0.3 M); [a] Determined via NMR spectroscopy; [b]At those times reaction mixture gelified; [c] Evaluated through GPC analysis

Table 4.4: Poly(**NBE**-*alt*-**COE**) with catalysts **5** and 6, **NBE:COE 1:2**

catalyst	poli(NBE)[a]		poli(COE)[a]		poli(NBE-*alt*-COE)[a]		t[b]	L$_{NBE}$[a]	L$_{COE}$[a]	M$_n$[c]	PDI[c]
	(%)cis/trans		(%) cis/trans		(%) cis/trans		(s)			(kD)	
5	31	60/40	14	34/66	55	68/32	9	–	–	585	2.30
6	28	63/37	32	48/52	40	63/37	8	2.44	2.61	382	1.60

Norbornene was always full converted, reactions were carried out in methylene chloride ([NBE]=0.3 M); [a]Determined via NMR spectroscopy; [b] At those times reaction mixture gelified; [c] Evaluated through GPC analysis.

The homosequences lengths were between 2.4 and 6.2 and lower values were related to a higher amount of heterosequences. A L$_{COE}$ and L$_{NBE}$ value of 2 would indicate a perfectly alternated copolymers.

PDI obtained were lower with respect to those reported in the literature.[94]

Between the two investigated u-NHC ruthenium complexes, **5** showed an higher prominence towards the formation of alternated sequences. Analogously to standard reaction, ROMP copolymerization behavior of these complexes is significantly influenced by backbone relative configuration.

Catalyst **5** was tested in ROMP involving a higher NBE:COE ratios (table 4.5)

This complex showed to be particularly competent in the copolymerization of **NBE** and **COE** (yields were always quantitative) also when the loading was reduced to 0.5%mol. A certain preference towards the formation of cis double bond was displayed both in hetero- and in homosequences.
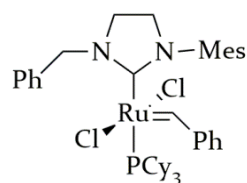
Figure 4.9: The complex reported by Buchmeiser

GPC characterization of these samples is underway.

Interestingly, by increasing the **COE** concentration, the percentage of alternate diads raised without any improvement of the amount of cyclooctene sequences. Up to 84% of alternate diads were obtained with just eight equivalent of **COE**. This is a considerable advancement with respect to the literature results obtained with the catalyst reported by Buchmeiser (figure 4.9).[14] This complex, bearing an N= benzyl, N'=

[92] M. R. Buchmeiser, I. Ahmad, V. Gurram, P. S. Kumar, *Macromolecules* **2011**, *44*, 4098-4106.

mesityl NHC ligand, led to obtain up to 97% of alternate diads but with a very larger cyclooctene excess (50 equivalents).

Table 4.5: Poly(**NBE**-*alt*-**COE**) with catalysts **5** at various monomer ratios

Cat:NBE:COE	poli(NBE)[a]		poli(COE)[a]		poli(NBE-*alt*-COE)[a]		t[b]	M_n[c]	PDI[c]
	(%)cis/trans		(%) cis/trans		(%) cis/trans		(s)	(kD)	
1:1000:4000	18	59/41	18	68/32	64	72/28	1.75	254	1.89
1:1000:8000	7	61/39	14	54/46	79	74/26	5.5	321	1.54
1:2000:16000	16	70/30	-	-	84	72/28	4.2	316	2.06

Norbornene was always full converted, reactions were carried out in methylene chloride ([NBE]=0.3 M); [a]Determined via NMR spectroscopy; [b] At those times reaction mixture gelified; [c] Evaluated through GPC analysis.

4.3.2 Poly(NBE-*alt*-CPE)

Due to the promising results obtained in the ROMP of **NBE** and **COE**, unsymmetrical catalysts **5** and **6** were also tested in the copolymerisation of **NBE** and **CPE** (scheme 4.6).
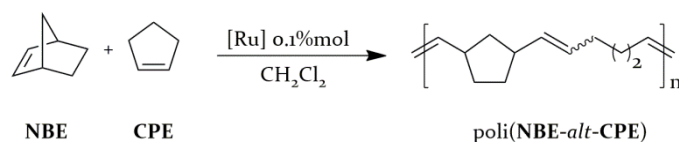
Scheme 4.6: Copolymerisation of **NBE** and **CPE**

CPE is less reactive than **COE**.[93] In its homopolymerisation cyclic oligomers and low molecular weight are achieved, as a consequences of the frequent intramolecular chain transfers.[94]

Also in the case of poly(**NBE**-*alt*-**CPE**), an accurate carbon-13 NMR spectrum analysis makes possible the quantification of hererosequences, homodiads and percentages of cis/trans double bonds (figure 4.10).

Vinylic signals of the heterosequences can be observed at 135.1 ppm (C_a) and 128.3 ppm (C_b). Similarly to copolymerisation of NBE and COE, activity of complexes was evaluated at low monomers ratio first. Results of copolymerisations with a **NBE:CPE** monomer ratio of 1 and 2 are reported in tables 4.6 and 4.7.

Also in this copolymerisation, **5** was the more efficient in the formation of heterodiads.

Using a monomer ratio of 1 (table 4.6), polymers with a significative amounts of alternated diads were obtained. As expected, homodiads of CPE were almost totally absent. At double concentration of **CPE** (table 4.7), the percentage of heterosequences substantially raised until 76% when complex **5** was used. This latter data is very interesting since, in the same reaction conditions, a maximum amount of 55% of heterodiads is reported in the literature.[14]

---

[93] P. R. Schleyer, J. E. Williams, K. R. Blanchard, *J. Am. Chem. Soc.* **1970**, *92*, 2377.

[94] L. B. W. Lee, R. A. Register, *Polymer* **2004**, *45*, 6479.
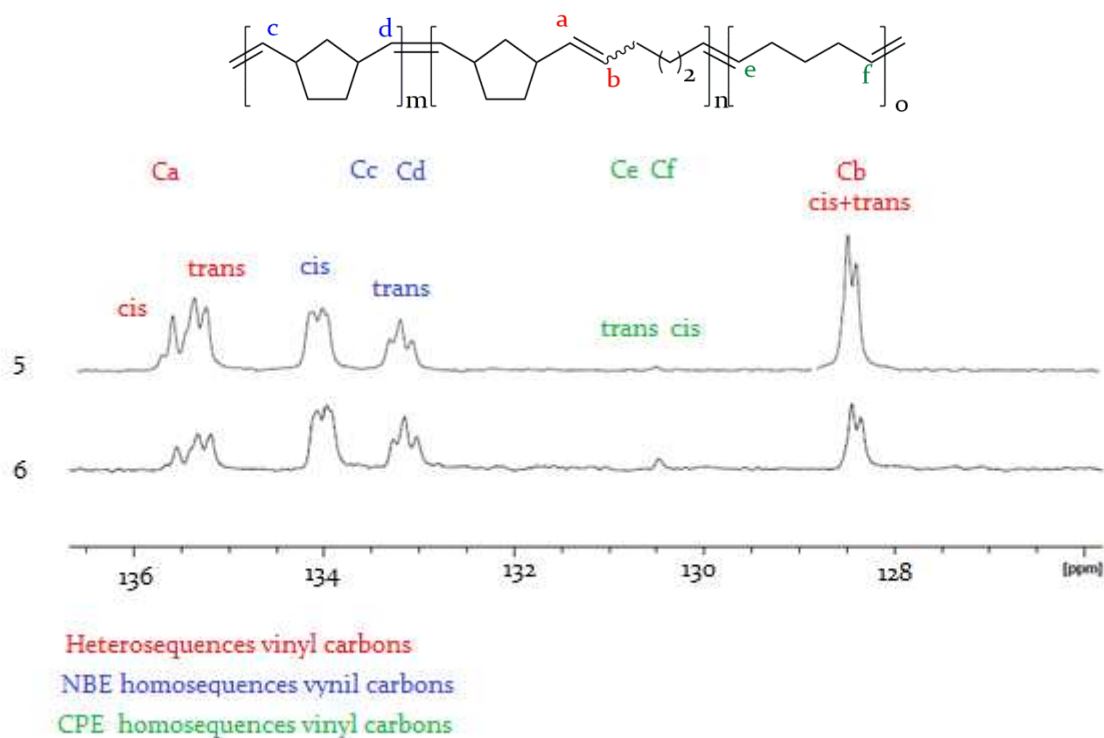
Figure 4.10: ^{13}C spectra of Poly(**NBE**-*alt*-**CPE**)obtained with catalysts **5** and **6**

Table 4.6: Poly(**NBE**-*alt*-**CPE**) with catalysts **5** and **6**, **NBE:CPE 1:1**

catalyst	poli(NBE)[a]		poli(CPE)[a]		poli(NBE-*alt*-CPE)[a]		t[b]	M$_n$[c]	PDI[c]
	(%)cis/trans		(%) cis/trans		(%) cis/trans		(s)	(kD)	
5	37	62/38	-	-	63	21/79	110	100	1.70
6	54	59/41	2	-	44	18/82	110	77	1.64

Norbornene were always full converted, reactions were carried out in methylene chloride ([NBE]=0.3 M); [a] Determined via NMR spectroscopy; [b]At those times reaction mixture gelified; [c] Evaluated through GPC analysis

Table 4.7: Poly(**NBE**-*alt*-**CPE**) with catalysts **5** and **6**, **NBE:CPE 1:2**

catalyst	poli(NBE)[a]		poli(CPE)[a]		poli(NBE-*alt*-CPE)[a]		t	M$_n$[b]	PDI[b]
	(%)cis/trans		(%) cis/trans		(%) cis/trans		(min)	(kD)	
5	18	62/38	6	19/81	76	29/71	15	55	1.56
6	35	62/38	9	22/78	56	25/75	15	52	1.60

Norbornene were always full converted, reactions were carried out in methylene chloride ([NBE]=0.3 M); [a] Determined via NMR spectroscopy; [b] Evaluated through GPC analysis.

For these polymers, due to the higher alternated diads content, the average length of the homosequence was not calculated.

The high amount of heterodiads in the polymer, despite of the low monomers ratio, can be rationalised by assuming that the propagating species, once inserted the **NBE**, is less prone to coordinate again the same monomer (due to strong steric constrictions) and this can

favour the subsequent insertion of **CPE**. Only at this point, due to the improved flexibility of the growing chain, norbornene can be inserted again.

Gel permeation chromatography of these polymers showed low number average molecular weights and PDIs in the 1.56-1.70 range.

Also in the case of poly(**NBE**-*alt*-**CPE**), the behaviour of **5** were tested at higher **NBE:CPE** ratios and results are reported in table 4.8.

Table 4.8: Poly(**NBE**-*alt*-**CPE**) with catalysts **5** at various monomer ratios

NBE:CPE	poli(NBE)[a]		poli(CPE)[a]		poli(NBE-*alt*-CPE)[a]		t	M_n[b]	PDI[b]
	(%)cis/trans		(%) cis/trans		(%) cis/trans		(min)	(kD)	
1:1000:4000	8	63/37	9	24/76	83	28/72	15	39	1.72
1:1000:6000	15	60/40	4	-	90	29/71	15	63	1.59

Norbornene was always full converted, reactions were carried out in methylene chloride ([NBE]=0.3 M); [a] Determined via NMR spectroscopy; [b] Evaluated through GPC analysis.

Very interestingly and coherently with results showed in table 4.5, ruthenium compound **5** led to obtain a very appreciable amount of alternated diads (up to 90%).

The pronounced selectivity of **5** towards the formation of heterosequences is very interesting. Further studies to determine the 'optimal' monomers ratio and the ideal reaction conditions are ongoing. In fact monomer concentrations, solvents, as well as temperature and time, can play a very important role.

A complete characterisation of copolymers obtained, which would be very informative, is in progress.

4.4 Conclusion

Catalytic behaviors of GII-type catalysts **5** and **6** were evaluated in the homopolymerisation of NBE and ONBE as well as in the copolymerization of **NBE** with the less reactive monomers **COE** and **CPE**.

In the ROMP of **NBE**, **5** and **6** were less efficient than commercial **GII** and gave a very similar σ_c. The number average molecular weights (Mn) were higher with respect to the theoric, thus suggesting an incomplete catalytic site activation. Broad PDIs were observed.

In the homopolymerisation of **ONBE**, both u-NHC catalysts reached polymers with a lower σ_c respect to **GII**. Interestingly, **5** and **6**, gave polymers with very stereoregular trans regions (>99% isotactic).

u-NHC catalysts displayed very intriguing performances in the copolymerisations of **NBE** with **COE** and **CPE**. Both reactions were first investigated at low monomers ratio (1 and 2) and **5** and **6** showed an overall tendency to form alternated diads. **5**, the most promising catalysts, was further tested in reactions with higher concentrations of the less reactive monomers. As expected, the percentages of alternated diads further increased, with no appreciable improvement in the amount of homosequences.

These very valuable results nominate **5** as a one of the best u-NHC catalysts for the copolymerisation of these monomers via ROMP. The complete copolymers characterisation and the optimisation of reaction conditions are in progress.

4.5 Supporting Information

For the general information regarding manipulation of solvents and reagents see paragraph 3.8.

4.5.1. Representative Polymerisation procedure

In a Schlenk tube, under nitrogen atmosphere, the monomer (0.53 mmol, 1 equiv.) and the dry THF (2 mL) were added. After that, a THF solution of the catalyst was injected (2.65 μmol in 0.25 mL, 0.5% mol).

After two hours at room temperature, polymerisation was quenched with a solution of THF (2 mL), ethyl vinyl ether (0.1 mL) and butylated hydroxytoluene (BHT). The viscous solution was filtered through a small plug of silica gel and then precipitated in an ethyl vinyl ether solution of methanol. The polymer obtained was filtered and dried under vacuum.

4.5.2. Representative Copolymerisation procedure

To a methylene chloride solution of **NBE** (2.65 mmol, 1 equiv.) and **COE** or **CPE**, a methylene chloride solution of the catalyst (2.65 μmol in 0.25 mL) was injected. The polymerisation was quenched with an ethyl vinyl ether solution of methanol. The polymer obtained was filtered and dried under vacuum.

4.5.3 NMR spectra
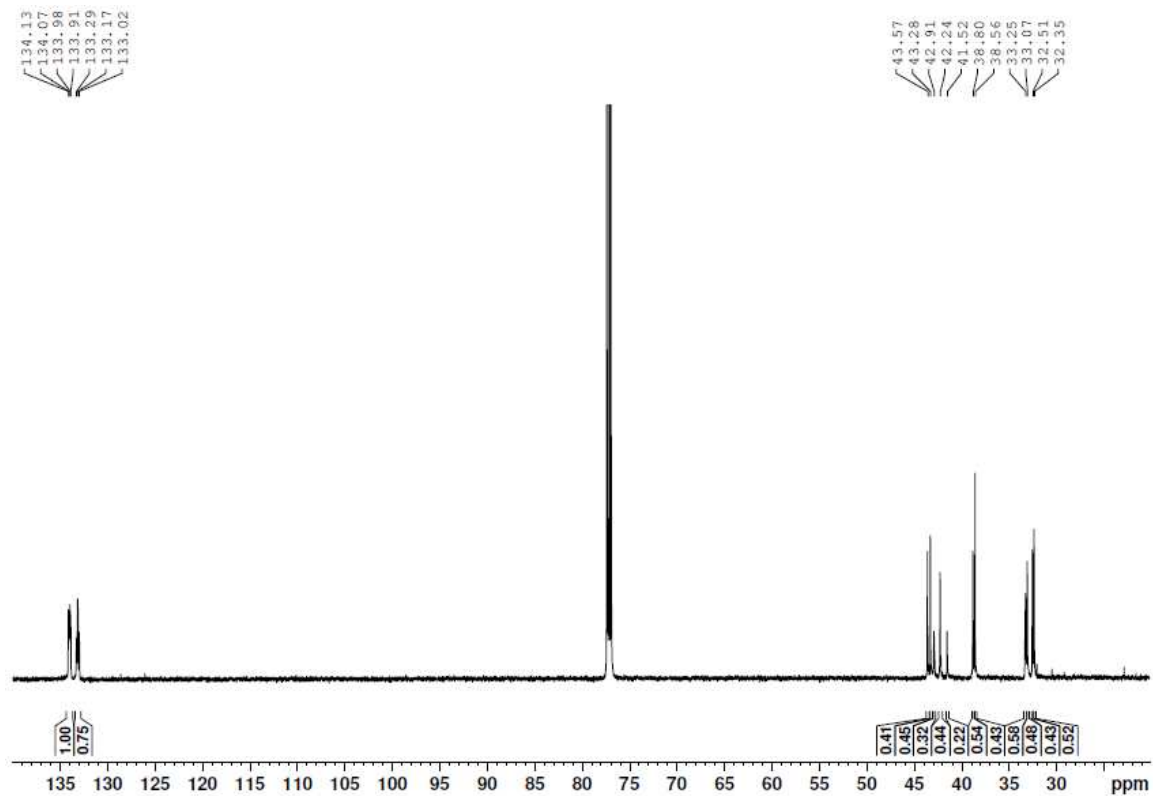
Figure S4.1: Representative ¹³C NMR of poly**NBE**
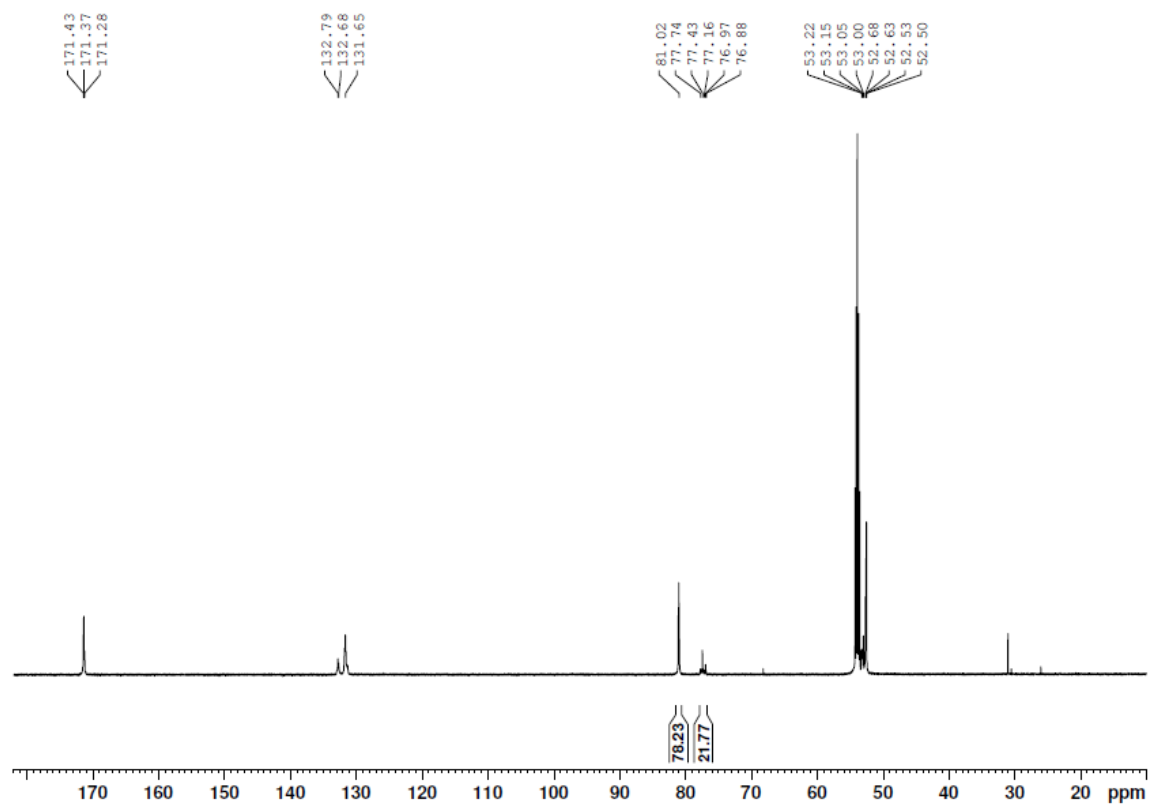
Figure S4.2: Representative ¹³C NMR of poly**ONBE**
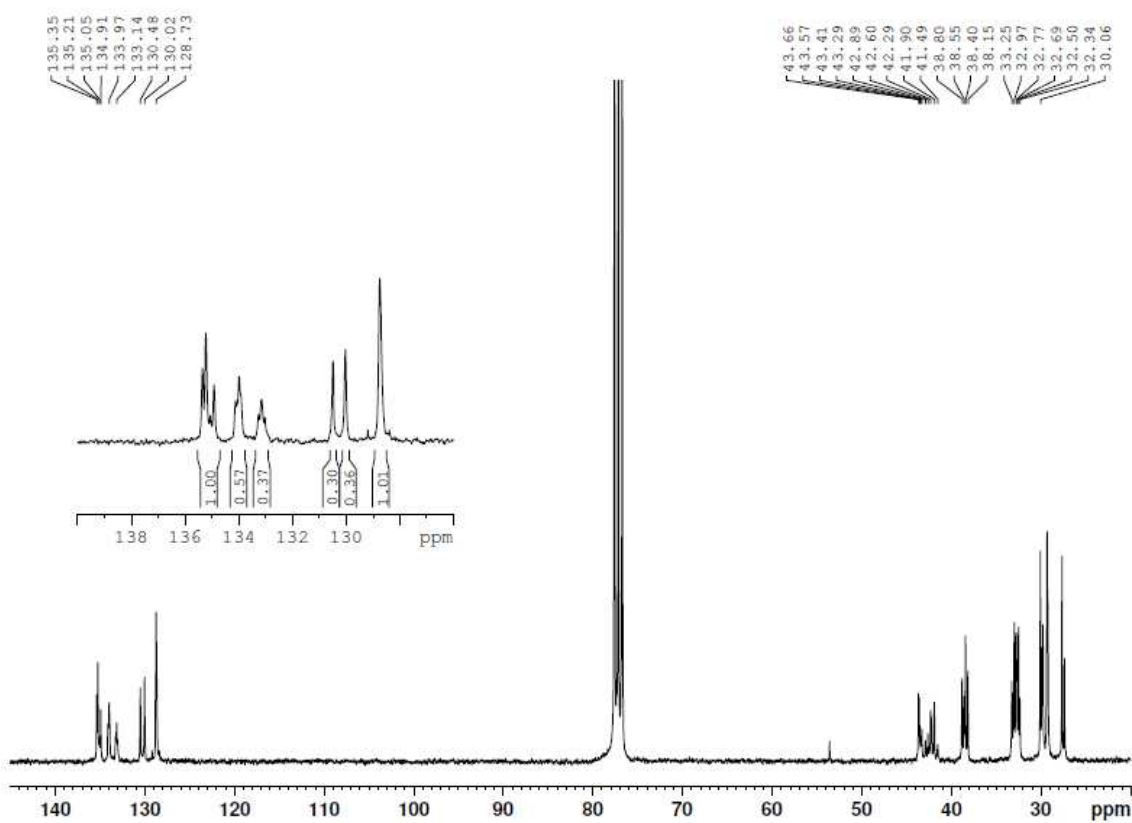
Figure S4.3: Representative ¹³C NMR of poly(**NBE**-*alt*-**COE**)
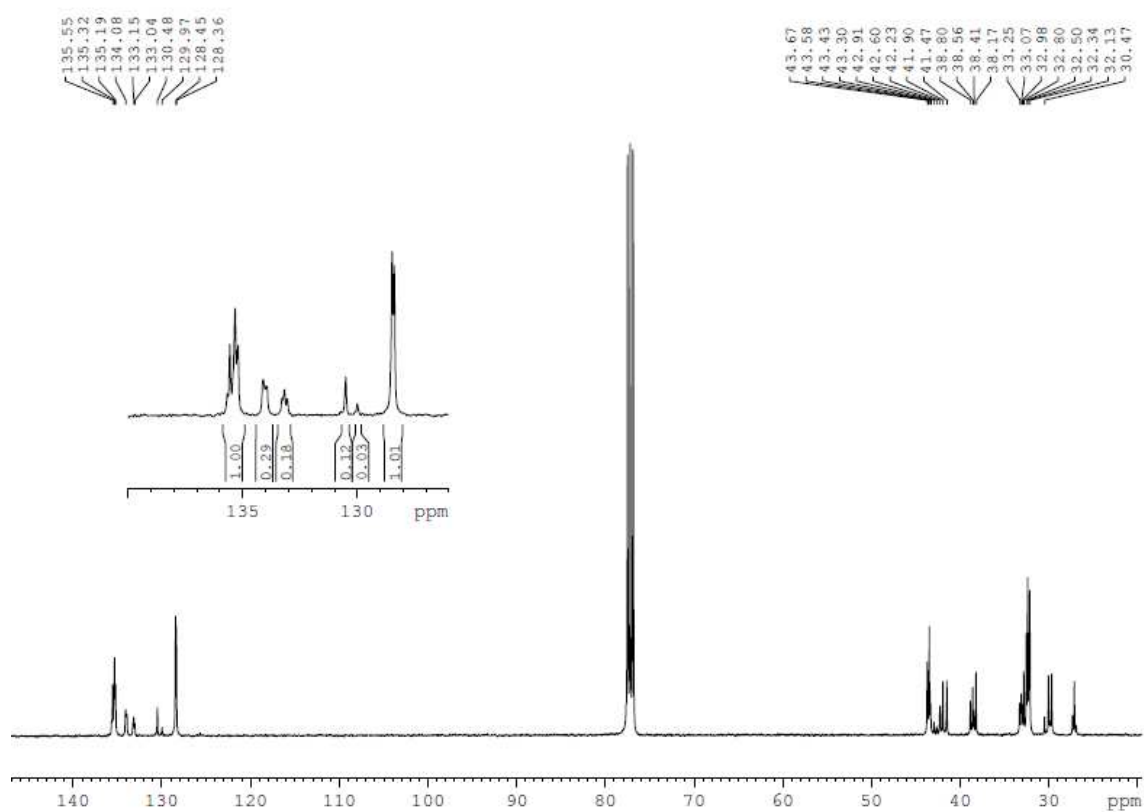
Figure S4.3: Representative ¹³C NMR of poly(**NBE**-*alt*-**CPE**)

Chapter 5

Expanding the Family of Hoveyda Catalysts Containing Unsymmetrical NHC Ligands

The possibility to fine differentiate the hindrance around the metal centre, as well as the surprising backbone effect and the enhanced stability, increased the awareness of the potentialities of backbone substituted u-NHC Ru catalysts and nurtured our interest in this field.

In reactions promoted by **1-8**, discussed in chapter 3, beyond a pronounced efficiency of catalysts with anti backbone configuration, a significant reactivity differences were observed between complexes with methyl or cyclohexyl as the alkyl group. However, in those preliminary study, no other alkyl groups were tested and a possible influence on reactivity of the N'-aryl substituents was not investigated.

With the aim to enlarge our knowledge of this family of catalysts, we extended our study to the synthesis of six new ruthenium complexes **36-37**, **38-39** and **40-41** bearing backbone substituted u-NHC ligands (figure 5.1)
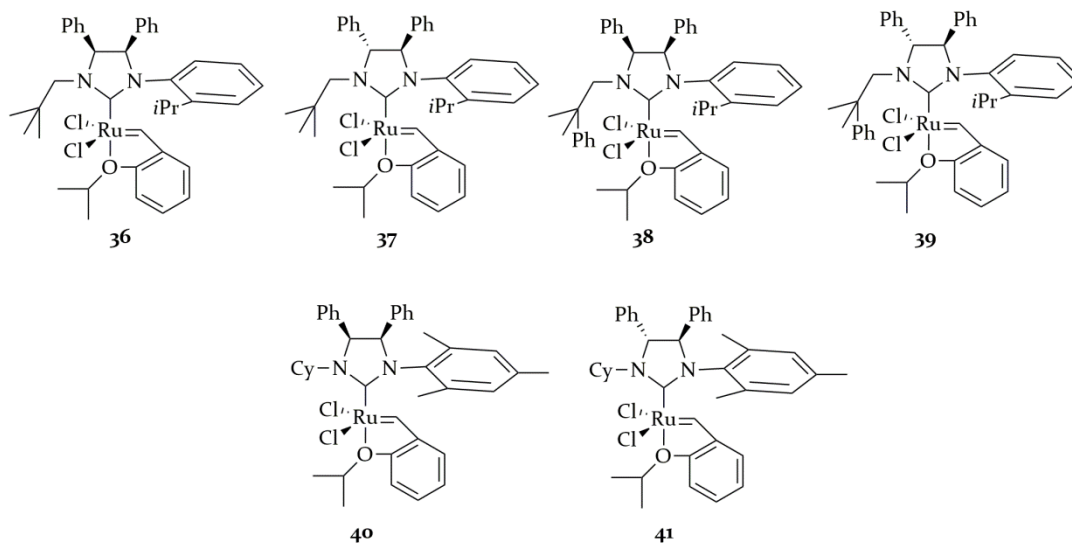
Figure 5.1: Complexes 36-41

36 and **37** differ from **1-8** for neopentyl as the N-alkyl group, chosen in order to explore the influence of a different bulky and ramified group.

The further substitution of a methyl with a phenyl led to compounds **38** and **39**, thus allowing to investigate the potential influence of the neophyl group which combined slightly different steric hindrance and electronic properties.

Compounds **40** and **41**, with N'-mesityl NHC ligand, were prepared in order to explore the effect of the N'-aryl group which had not been studied so far for this group of compounds. The alkyl group chosen was cyclohexyl because of the easy synthesis, interesting reactivity and pronounced backbone effect observed with catalysts **5-8**.

Since for **1-8** reactivity trends shown by Grubbs-type and Hoveyda-type catalysts were similar, we decided to synthesize all the new catalysts as phosphine-free compounds, in order to take advantage of their stability and ease to handle.

Respect to the previous work, we decided to keep the nature of the backbone substituents unchanged. Electronic and steric properties of backbone groups would very likely influence catalytic performances of complexes. This interesting aspect, which unfortunately complicates synthetic pathways, will be the content of future studies.

These six complexes **36-41** were tested in standard metathesis reactions as well as in more 'green' applications involving renewable substrates. Their solution stabilities were also investigated and electronic and steric properties were studied using, respectively, cyclic voltammetry and topographic steric maps.[95]

## 5.1 Synthesis of 36-41 and X-Ray characterisation

Synthesis of **36-41** are depicted in schemes 5.1 and 5.2.

For the synthesis of salts **44**, **45**, **48** and **49**, (*meso*)- or (*1R,2R*)-diphenylethylendiamine underwent palladium-catalysed Buchwald-Hartwig arylation and then alkylation with 2,2-dimethylpropanaldehyde (**42** and **46**) or with 2-methyl-2-phenylpropanaldehyde (**43** and **47**) followed by reduction with sodium borohydride. Tetrafluoroborate salts were obtained through treatment of the N-alkyl, N'-aryl diamine with triethylortoformate and ammonium tetrafluoroborate.

Salts **52** and **54** were prepared through synthetic pathways analogues to those described for **19** and **22** in chapter 3.

Ligand precursors **44-45**, **48-49**, **52** and **54**, treated with $(CF_3)_2CH_3COK$, gave in situ the corresponding free carbenes that reacted with **HI** to form the desired complexes **36-41** in moderate-good yields (45-70%).

It should be noted that ruthenium complexes **37**, **39** and **41** are enantiopure while **36**, **38** and **40** are racemic compounds. Enantiomerically pure catalysts were tested in asymmetric metathesis transformations and data will be discussed in chapter 6.

Ruthenium complexes and all intermediates were characterised with 1D and 2D NMR spectroscopy.

36, **40** and **41** gave good quality crystals for X-Ray analysis (figure 5.2). In both complexes the metal is pentacoordinated and adopted a distorted square-pyramidal coordination geometry. Chlorine atoms are trans-oriented in the basal plane and the carbene C1 atom is in a trans position with respect to the O1 oxygen of the 2-*i*PrO substituent at the

---

benzylidene ligand, which is almost coplanar with the NHC ring, being rotated by only 8.80(8), 11.20(13), and 3.13(8)° for **36, 40** and **41** respectively.
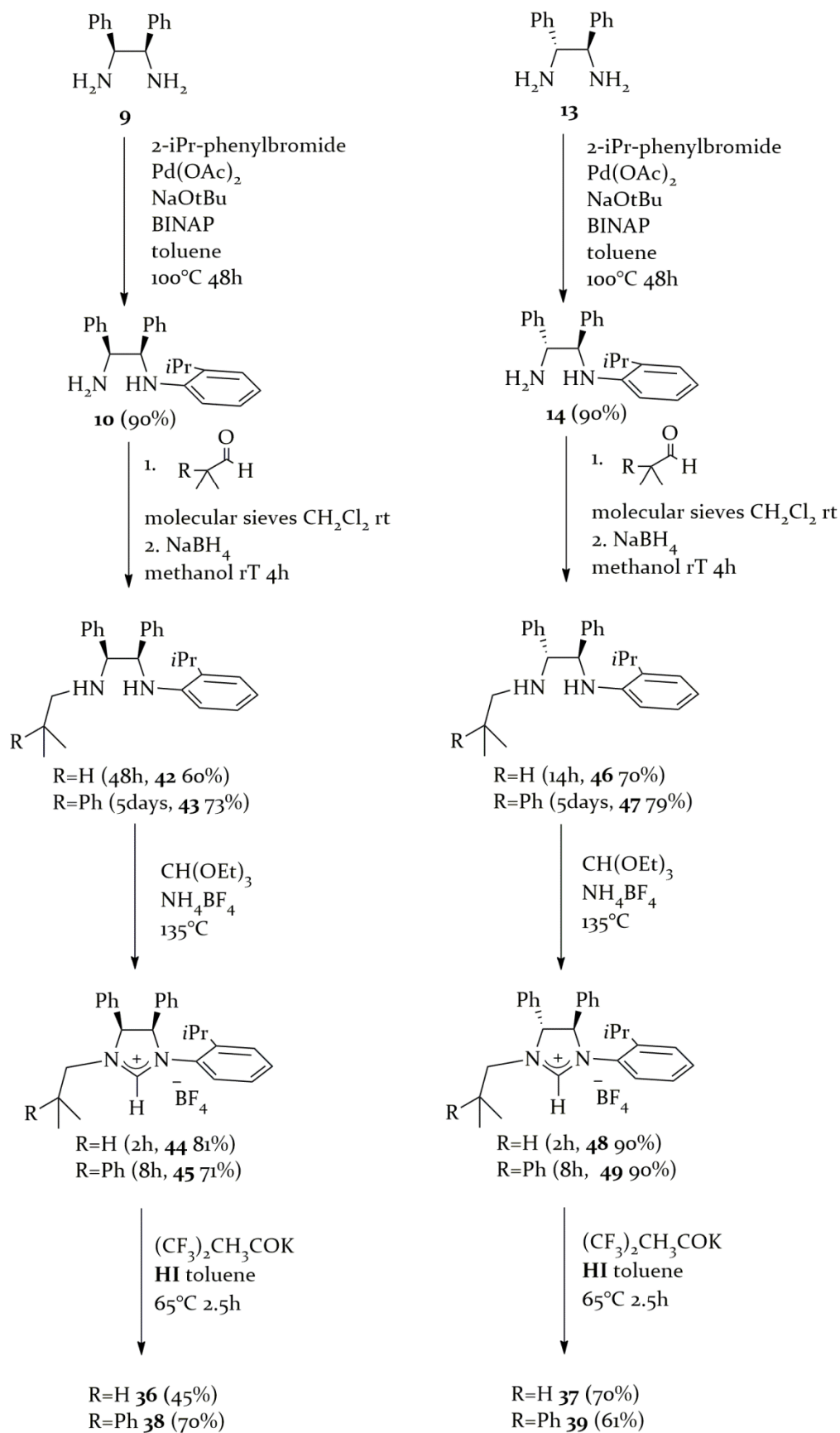
Scheme 5.1: Synthesis of **36-39**
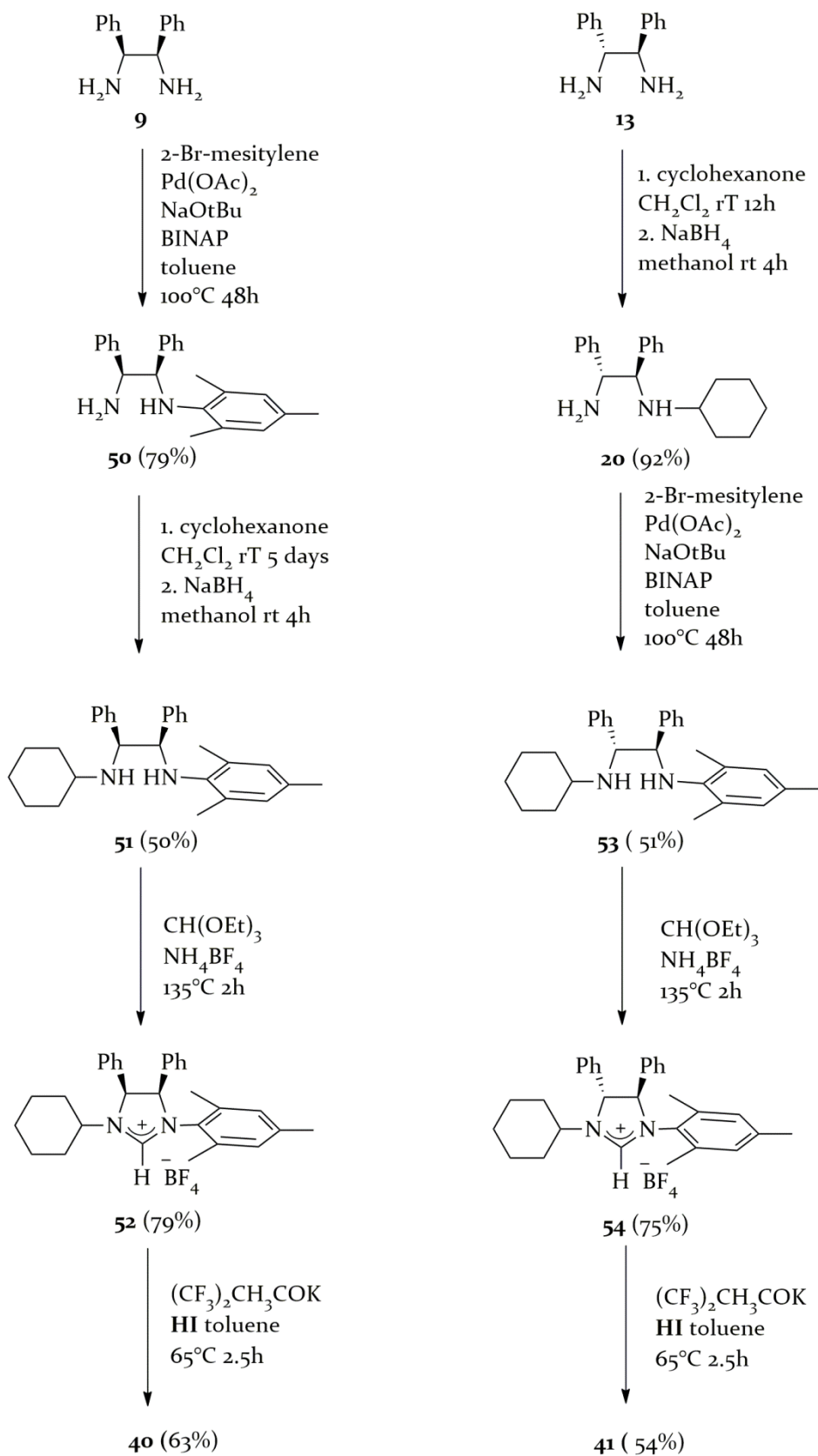
Scheme 5.2: Synthesis of **40** and **41**
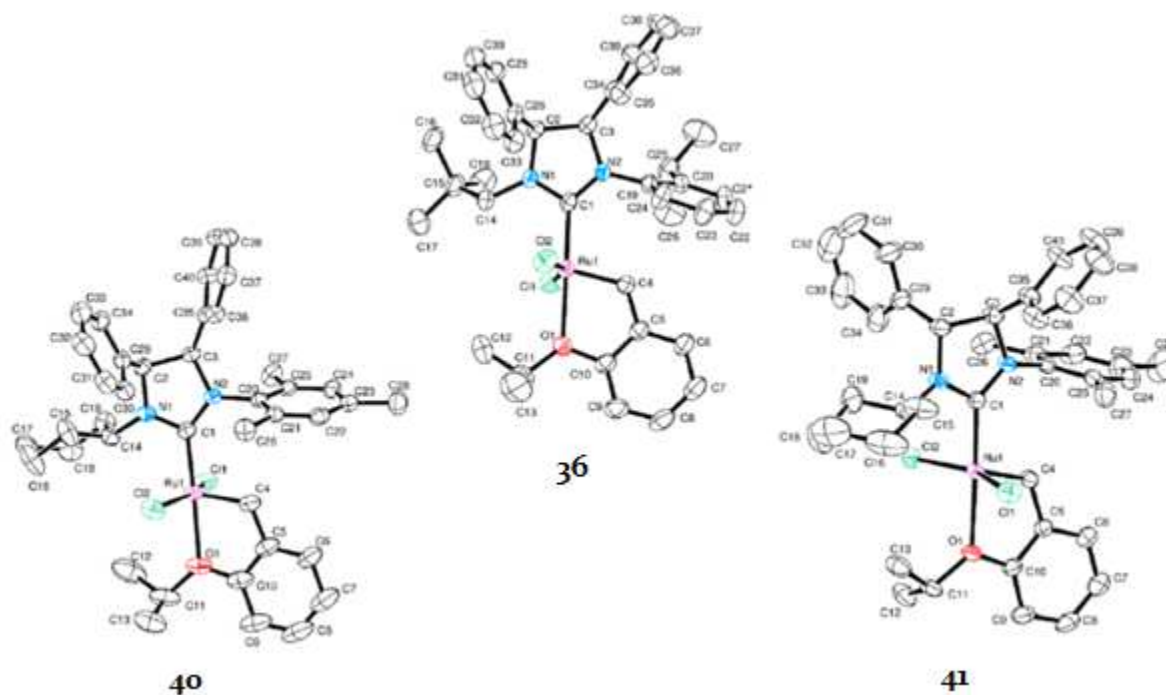
Figure 5.2: ORTEP view of complexes **36** and **40-41** with the thermal ellipsoids at 40% probability

36 crystallizes in the centrosymmetric P2₁/n space group with the NHC phenyl groups in cis positions with respect to the C2–C3 bond. Crystal contains a racemic mixture of (*SR* or *RS*) enantiomers at the C2 and C3 asymmetric carbon atoms. The conformations of the substituents at the N1 and N2 NHC atoms are mainly determined by short intramolecular interactions: H14b⋯Ru1 = 2.54 Å and H4⋯(centroid of C19/ C24 phenyl ring) = 2.40 Å. **40** and **41** are isomers with different relative configurations at the C2 and C3 atoms of NHC group. Both crystallize in the noncentrosymmetric C2 space group. In **40** the phenyl substituents, bonded to C2 and C3 of the NHC ring, are in cis positions. Accordingly, the C2 and C3 carbons display *S* and *R* configurations, respectively. Contrarily, in **41** phenyl substituents at C2 and C3 are in trans positions and the C2 and C3 carbon atoms of NHC display the same *R* chirality. The absolute configurations could be determined reliably from the crystallographic data, using the calculated Flack parameters[96] of 0.00(2) and –0.03(2) for complexes **40** and **41**, respectively The conformations of the substituents at the N1 and N2 of the NHC rings are controlled by short intramolecular interactions between the C4–H4 group of the benzylidene moiety and the centroid of the C20/C25 phenyl ring, as well as by interactions between the C14–H14 group of the cyclohexyl substituent and the Ru atom. The C–H⋯π interactions between the C4–H4 group and the centroids C of the C20/ C25 phenyl rings are characterized by the following parameters H4⋯C(C20/C25) = 2.70 and 2.58 Å and C4–H4⋯C = 162 and 168°, for **40** and **41**. Furthermore, the short C–H⋯Ru interactions display H14⋯Ru1 distances of 2.51 and 2.50 Å and C14–H14⋯Ru1 angles of 122 and 123° for complexes **40** and **41**, respectively.

---

96 S. Parsons, H. Flack, T. Wagner, *Acta Crystallogr., Sect. B: Struct. Sci., Cryst. Eng. Mater.* **2013**, *69*, 249.

It should be underlined that nor NMR analysis neither X-Ray spectroscopy (**36**) evidenced any N-alkyl-ruthenium C-H activation for catalysts precursors bearing neopentyl or neophyl alkyl groups.

5.2 Thermal stability tests

Thermal stability of new u-NHC complexes was investigated in solution of deuterated benzene (0.01 M) at 60°C (figure 5.3). Decomposition was monitored via ¹H NMR spectroscopy comparing the signals of the carbene proton with protons of the internal standard (tetrakis(trimethylsilyl)silane). Thermal decomposition of **7**, **8** and **HII** are also plotted for comparison.
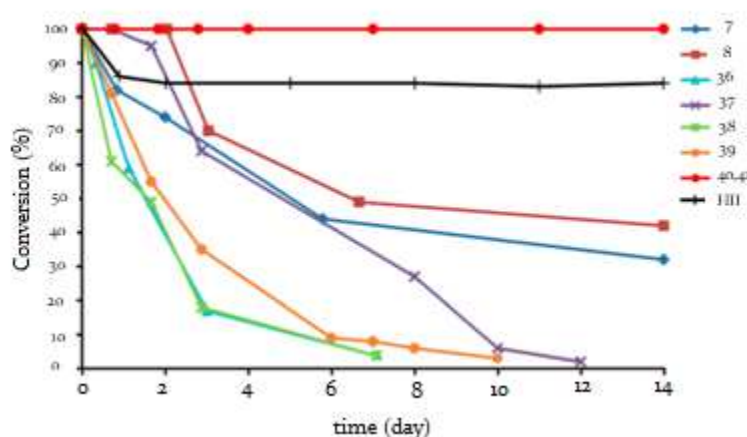
Figure 5.3: Thermal stability plots of new complexes **36-41** and of **HII, 7** and **8**

N-neopentyl, N'-isopropylphenyl ruthenium complexes **36-37** were both almost totally decomposed within one week. N-neophyl congeners **38** and **39** were more stable and decomposed later, respectively after 12 and 10 days. An exceptional thermal stability was shown by N-cyclohexyl, N'-mesityl compounds **40** and **41** which were still intact after one month, thus exhibiting an enhanced robustness respect to **HII** and to the N'-isopropylphenyl analogues **7** and **8** (respectively 79%, 8% and 26% of residual complex after one month).

5.3 Evaluation of steric and electronic properties

The stability of unsymmetrical catalysts is related with the nature of the NHC nitrogens' substituents[55, 97] and, in a recent study on NHC aluminium complexes,[98] it was attributed to steric factors with the use of topographic maps and %Vbur .[99]

---

[97] P. Małecki, K. Gajda, O. Ablialimov, M. Malińska, R. Gajda, K. Woźniak, A. Kajetanowicz, K. Grela, *Organometallics* **2017**, *36*, 2153.

[98] M. Wu, A. M. Gill, L. Yunpeng, L. Falivene, L. Yongxin, R. Ganguly, L. Cavallo, F. Garcìa, *Dalton Trans.* **2015**, *44*, 15166.

[99] L. Falivene, R. Credendino, A. Poater, A. Petta, L. Serra, R. Oliva, V. Scarano, L. Cavallo, Organometallics 2016, 35, 2286.

%V*bur,* discussed in paragraph 3.8, gives an estimation of the hindrance of a ligand calculating the volume it occupies in a sphere centred on the metal. However, it does not give an exhaustive description of the metal environment since, especially for unsymmetrical ligands, it is reasonable that the volume in the surroundings of the metal centre is not homogeneously occupied.[68] To give a better estimation of how the hindrance is distributed throughout the space, Cavallo et al. have developed the topographic steric maps (figure 5.3).[100] Steric maps are divided into quadrants and, for each quadrant, the calculated %V*bur* is reported. Moreover, the coloured contours let to immediately visualise the hindrance.
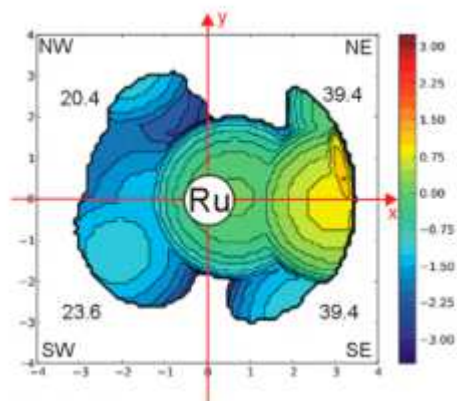
Figure 5.3: A representative topographic steric maps (complex **36**)

%V*bur* and topographic steric maps can be both calculated with the program SambVca 2.0 starting from CIF files or DFT data.

In order to relate the observed thermal stability data with steric properties of the NHC ligands, topographic steric maps and %V$_{bur}$ of **36**-**41** were investigated.

Since X-Ray structures were not available for all complexes, DFT minimum Energy optimised structures were used to calculate both %V*bur* and topographic steric maps.

Minimum energy structures of **38** and **39** showed a partial

π-stacking interaction between the aryls on the backbone and of the neophyl group (figure 5.4). Other possible structures, in which such interaction was not present, had higher internal energies and did not involve a significant variations in steric maps and %V$_{bur}$.[101]

Evaluations of minimum energy structures of N-neopentyl and of N-cyclohexyl complexes was easier, since the alkyl mobility is related to C-N bond and N-neopentyl orientation is imposed by groups on the backbone.

Topographic steric maps are reported in figure 5.5.

Figure 5.4: Minimum Energy Structures of **38** and **39**

According to them, the higher hindrance is located on the alkyl side on the NHC. Comparing %V$_{bur}$ of the most encumbered quadrant (%V$_{bur}$ max), a higher hindrance of N-cyclohexyl catalysts **40** and **41** was observed. Less encumbered alkyl quadrants were characteristic of, in decreasing order, N-neophyl **38** and **39** and N-neopentyl **36** and **37**.

---

[100] A. Poater, F. Ragone, R. Mariz, R. Dorta and L. Cavallo, *Chem. Eur. J.* **2010**, *16*, 14348.
[101] These additional minimum energy structures can be found in the experimental part.

Since complexes with higher $\%V_{bur}$ max displayed also a more pronounced thermal stability, this seemed to suggest that this two properties could be somehow linked. Unfortunately, the absence in the literature of any investigation of the decomposition mechanism of u-NHC compounds makes difficult any further rationalisation.
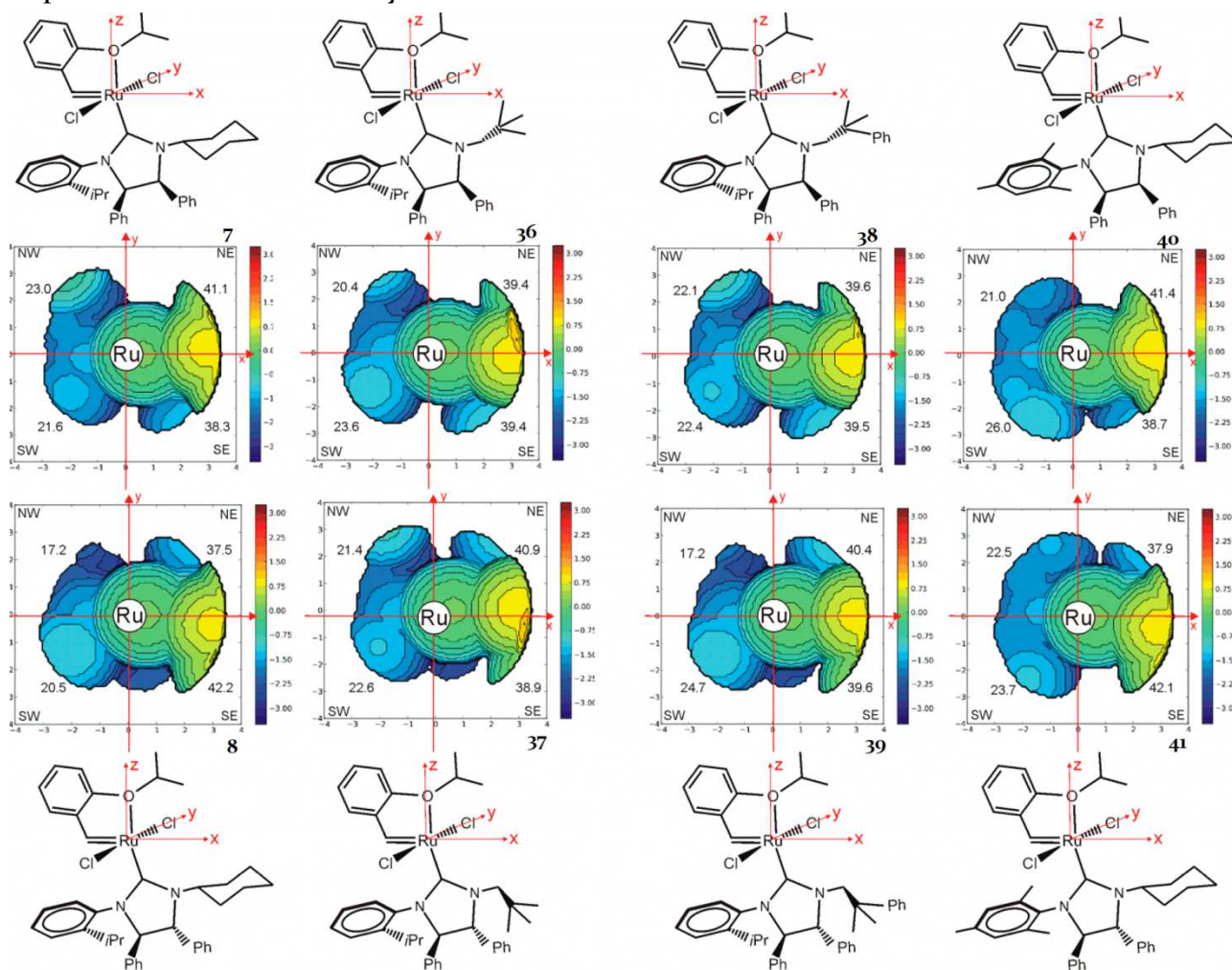
Figure 5.5: Topographic steric maps of **7**, **8** and **36-41**. The iso-contour curves of steric maps are given in Å. The complexes are oriented according to the complex scheme of the corresponding map. $\%VBur$ representative of each single quadrant is reported for each map.

In order to study the influence of the NHC nitrogens substituents on the overall electronic properties of the ligand, cyclic voltammetry experiments were performed.

Grubbs type and Hoveyda type complexes are very suitable for cyclic voltammetry analysis, due to the reversible nature of the Ru(II)-Ru(III) redox couple. For this reason, several systematic studies correlating $\Delta E_{1/2}$ and NHC groups were published in the literature.[102]

For example, the significant cathodic shift observed by analysing the $\Delta E_{1/2}$ of **GII** and **GI** (0.585 V and 0.455 V, respectively) indicates a higher electron density at the metal center due to the enhanced σ-donor properties of the NHC with respect to the tricyclohexylphosphine.

---

[102] a) M. Sussner, H. Plenio, *Chem. Comm.* **2015**, 5417; b) S. Leuthausser, V. Schmidts, C. M. Thiele, H. Penio, *Chem. Eur. J.* **2008**, *14*, 5465.

Measured $\Delta E_{1/2}$ of the u-NHC complexes were higher with respect to those of **HII**, consistently with a less electron-donating character of the NHC ligand (table 5.1).

Redox potentials of N-neopentyl catalysts **36**-**37** and of their N-neophyl akins **38**-**39** were all very similar, demonstrating a scarce influence of nature and configuration on the NHC substituents on electronic properties of these complexes.

Complex	$\Delta E_{1/2}$(V)	Ea-Ec(mV)
7	0.947	73
8	0.960	102
36	0.969	102
37	0.978	112
38	0.972	98
39	0.976	112
40	0.961	98
41	0.950	83
HII	0.860[a]	60

Conditions: 1 mM analyte, 0.1 M NBu$_4$PF$_6$ as supporting electrolyte
and 1 mM octamethylferrocene as an internal standard. Scan rate: 100 mV/s.
[a]Data from ref 8a is 0.850 V

Analogously, comparable redox potentials were detected for N-cyclohexyl catalysts **7**, **8**, **40** and **41**. Indeed, for these compounds, very little (3-13 MV) potential difference were observed and no unambiguous backbone configuration or N-aryl effect was displayed.

5.4 RCM of malonate and tosyl derivatives

The catalytic behaviours of the new catalysts were investigated in the RCM of malonate and tosyl derivatives **23**-**28**. Each reaction was performed in an NMR tube in deuterated benzene at 60°C and conversions were monitored over time. Kinetic profiles of **7**, **8** and **HII** were also plotted for comparison.

In the RCM of **23** (figure 5.6 a), the most efficient catalyst is **HII** which exhibited a reactivity comparable to the best u-NHC catalyst despite of a ten times lower catalytic loading (0.1% mol). Catalyst **8**, bearing an anti N=Cyclohexyl N'=isopropylphenyl NHC ligand, outperformed all the other u-NHC catalysts **36**-**37** and **38**-**39**, bearing respectively neopentyl and neophyl as N-alkyl group. No substantial influence of backbone configurations was showed by these compounds, in fact anti catalysts **37** and **39** were slightly more performing than their syn congeners **36** and **38**.

Compounds **40** and **41** were the less efficient. Anti **41** was less performing than **7** while its syn isomer **40** proved to be the less active overall.

In this ring closing the replacement of an N=cyclohexyl group (**7**, **8**) with an N=neopentyl (**36**, **37**) or an N=neophyl (**38**, **39**) substituent slightly reduced efficiency and smoothed over the backbone configuration influence. Differently, the change of the aryl group, from N'=isopropylphenyl in **7**-**8** to N'=mesityl in **40**-**41**, significantly decreased the reactivity of the corresponding complexes and accentuated the backbone configuration effect.

A similar reactivity order was observed in the RCM of **24** (figure 5.6 b). Analogously to what observed with **1**-**8**, these new catalysts displayed a lower efficiency in the ring closure of this

substrate with respect to the RCM of **23**, the malonate derivative with a comparable steric hindrance. This confirmed the tendency of u-NHC catalyst to undergo unproductive metathesis events.
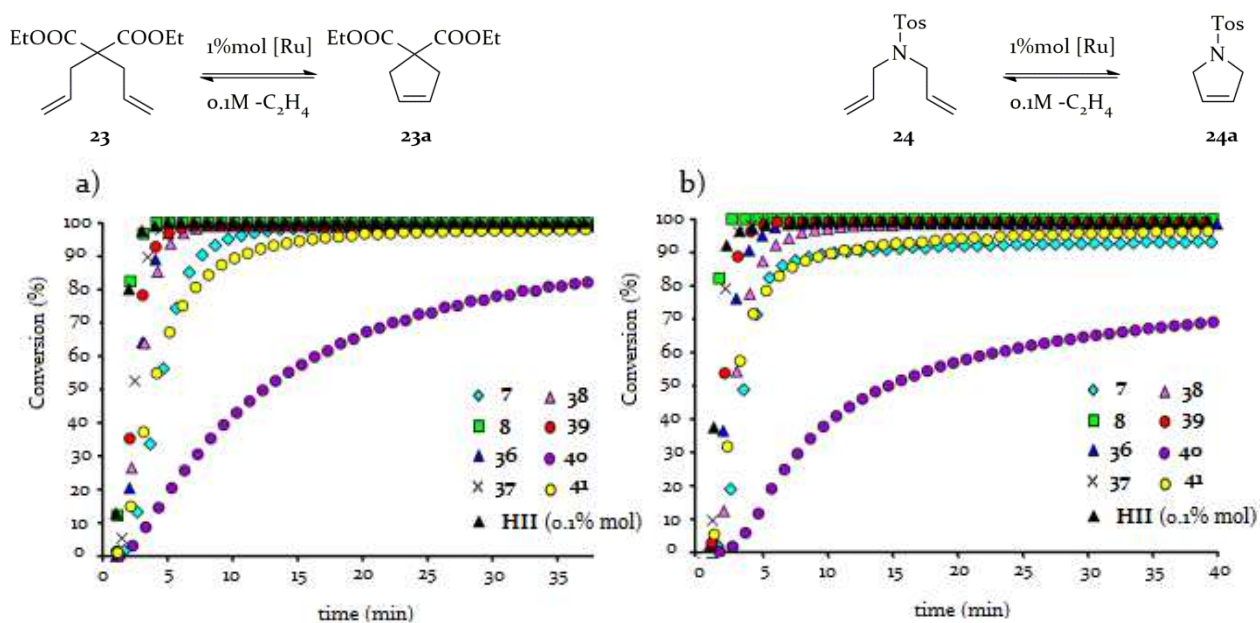
Figure 5.6: RCM of **23** (left) and **24** (right) with **7**, **8**, **36-41** and **HII**

Also in the RCM of **25** (figure 5.7 a), **HII** proved its superior efficiency in comparison with the u-NHC catalysts. **38** and **39** surpassed their syn analogues and, coherently with the ring closure of **23**, the activity gap was less pronounced with respect to those observed between **7** and **8**. The influence of backbone configuration on the catalytic behaviours of **40** and **41** was again quite marked.

In the RCM to achieve **26a** (figure 5.7 b), complexes **36-39** and **41** were all able to full convert the substrate. N-neophyl NHC ruthenium compounds **38-39** were less active than N-cyclohexyl **8** and displayed kinetic plots very similar to those of their N-neopentyl analogues **36-37.**

For this particular reaction the backbone configuration effect for **36-37** and **38-39** was almost totally flattened. Also in this transformation, **41** was the worst anti complex and **40** demonstrated to be the less performing catalyst.

In the RCM to form the tetrasubstituted malonate derivative **27a** (figure 5.8 a), all new u-NHC compounds were surpassed by **8**. **37** showed a pronounced reactivity, outperforming its syn analogue and all other new catalysts. This is the first RCM in which an u-NHC syn catalyst displayed reactivity significantly larger respect to its anti isomer.

Syn catalysts **36** and **38** showed very comparable kinetic plots. Very similar is also the behaviours of **37** and **8**, albeit displaying a slower initiation. **HII** was not very efficient in this reaction, reaching a conversion of 20% in 60 minutes. Almost no conversion was observed in the reactions promoted by **40** and **41**.
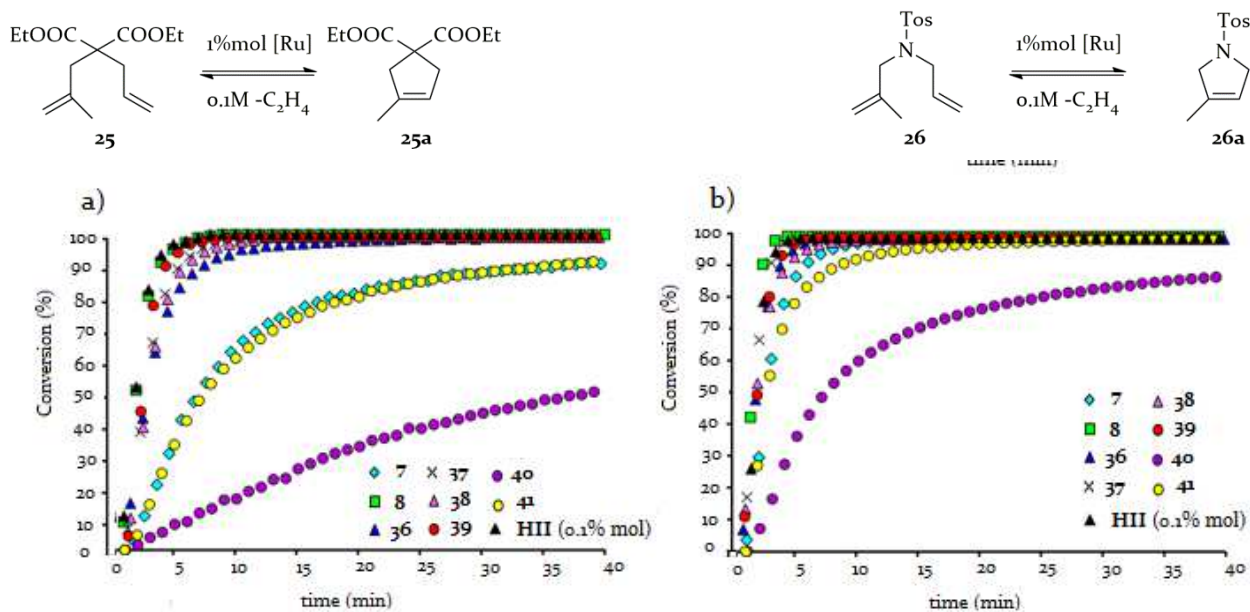
Figure 5.7: RCM of **25** (left) and **26** (right) with **7**, **8**, **36-41** and **HII**
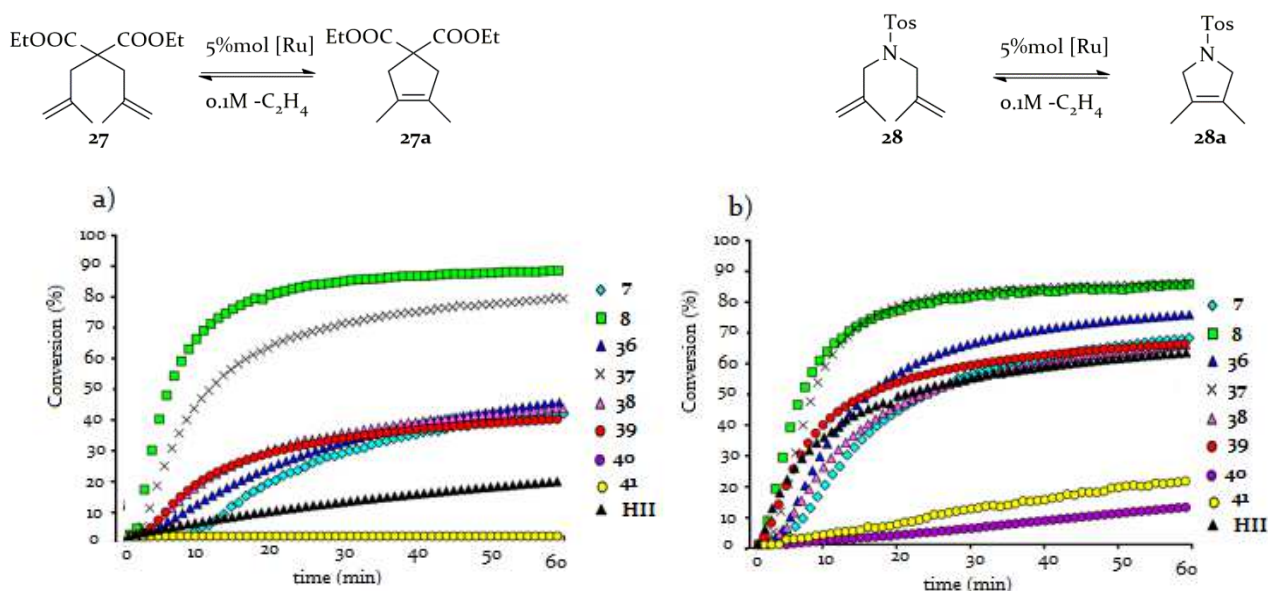
Figure 5.8: RCM of **27** (left) and **28** (right) with **36-41** and **HII**

In the RCM of **28** (figure 5.8 b) a different trend was observed. **8** and **37** were the most performing catalysts and exhibited very similar kinetic plots. **7**, **38**, **39** and **HII** reached very similar conversions (74-77%, 1h) although with different initiation times. Coherently with what previously noticed, **40** and **41** were found to be the less performing complexes.

In summary, these RCM of malonate and tosyl derivatives highlighted several aspects of the catalytic behaviours of these new catalysts. A general overview of the RCM of **23-28** showed an overall low efficiency of **36-41** with respect to **7** and **8**. In the RCM performed with **36-39**, the pronounced backbone effect observed in RCM promoted by **7** and **8** was appreciable just in transformations involving the hindered olefins **27** and **28** and with an opposite reactivity trend (syn **36** and **38** were more performing than their anti congeners). Comparison of behaviours of N-neopentyl **36-37** with their N-neophyl analogues **38-39** is not easy to

rationalise, since the reactivity trend changes considerably on the base of the substrate involved. The introduction of an N'-mesityl group adversely affect catalytic performances. In fact, **41** showed an overall lower activity with respect to the other anti catalysts and the syn isomer **40** exhibited the poorest efficiency in all the examined RCM. Nevertheless, interestingly, these two catalysts displayed a very important backbone configuration effect, with anti catalyst always more performing than the syn, coherently with the behaviour observed for **7** and **8**.

5.5 Cross Metathesis Transformations
5.5.1 CM of 30 and 31
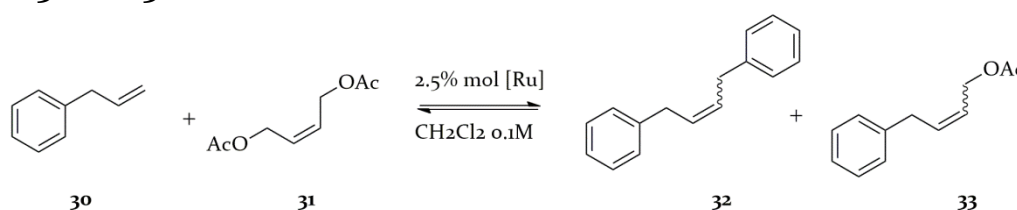
Scheme 5.3: CM of **30** and **31**

New u-NHC catalysts were tested in the 'standard' CM of **30** and **31** (scheme 5.3). Results are summarised in table 5.2 and data obtained with **HII** and **7** and **8** are also reported.

All catalysts were competent in the examined CM. Syn and anti complexes with N-neopentyl group (**11a** and **12a**) displayed a very comparable activity and a quite pronounced backbone induced Z-selectivity difference. In fact, similarly to the N-cyclohexyl congeners **7** and **8**, syn compound reached **33** with a lower E/Z ratio with respect to the anti analogue.

N-neophyl ruthenium catalysts **38** and **39** exhibited the same Z-selectivity trend and, conversely, a little reactivity difference (**39** was less efficient than the syn analogue **38**).

Ruthenium compounds **40** and **41**, analogously to what previously observed in RCM reactions , exhibited a pronounced backbone influenced reactivity. In fact anti **41** was more performing than the anti isomer **40**. Interestingly, albeit this substantial activity difference, comparable Z-selectivities were showed by the two complexes.

Table 5.2: CM of **30** and **31** catalysed by u-NHC catalysts and **HII**

catalyst	yield 33 (%)[a]	E/Z 33[b]
7	72	2.6
8	67	7.6
36	78	3.0
37	80	7.6
38	80	4.2
39	69	7.7
40	50	3.9
41	89	4.4
HII	69	8.6

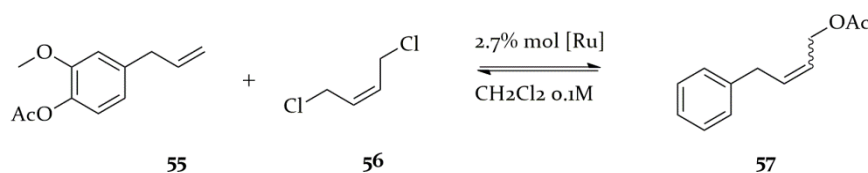a)isolated yield; b)evaluated with NMR spectroscopy

5.5.2 CM involving renewable substrates

The gradual exhaustion of the petroleum-based feedstock, as well as the environmental issues concerned with their use, encouraged chemists to discover more sustainable transformations and also to develop a 'green' version of the most important reactions. In this context olefin metathesis, in the last decades, has been extended to alkenes of plant origin which can nowadays successfully undergo CM, ROMP, ADMET and RCM.[103]

Today, the 'green' metathesis field has an increasing importance, particularly for transformations mediated by ruthenium catalysts. In fact, robustness makes their application possible also with natural substrates which often present protic functional groups as well as several impurities (such as acids, epoxides, esthers).

Eugenol is a phenolyc allylbenzene compound that can be extracted from lignocellulosic biomass. Its acetate analogue, a constituent of clove oil, can undergo cross metathesis with electron-poor olefins to reach new polyfunctional phenol frameworks.[104]

7 and **8**, the catalysts that showed a more prominent backbone influenced Z-selectivity in CM of **30** and **31**, were tested in the renewable CM involving eugenol acetate (**55**) and cis-2,4-dichloro-2-butene (**56**) (scheme 5.4). Results are summarised in table 5.3

Scheme 5.4: CM of **55** and **56**

Table 5.3: CM of **30** and **31** catalysed by u-NHC catalysts and **HII**

catalyst	yield 57[a]	E/Z 57[b]
7	60	2
8	77	9
HII	50	7.4

a) isolated yield; b)evaluated with NMR spectroscopy

7 and **8** both showed an higher efficiency with respect commercial **HII.** Very interestingly in this transformation the backbone configuration effect, already observed in standard CM and RCM reactions, was even more emphasized and had consequences both on yields (anti **8** was more efficient than syn **7**) and on Z-selectivity (**7** was more Z-selective if compared with **8**). These results encourage further study on an unclear point of olefin metathesis: the role of backbone configuration in the induction of Z-selectivity.

Ethenolysis (the cross metathesis involving ethylene as a cross partner) is the only industrially relevant cross metathesis (see chapter 1). Ruthenium catalysts bearing u-NHC ligands have been successfully applied in this reaction, due to their preference to propagate

[103] A. Nickel, R. L. Pederson, *Commercial Potential of Olefin Metathesis of Renewable Feedstocks,* chapter of *Olefin Metathesis: Theory and Practise*, Edited by K. Grela, John Wiley and Sons, Hoboken **2014**

[104] H. Bilel, N. Hamdi, F. Zagrouba, C. Fishmeister, C. Bruneau, *RSC Adv.* **2012**, *2*, 9584.

as Ru-methylidene species which determines high selectivity for ethenolysis products over self metathesis products.[105]

7, **8** and **36-41** were tested in the ethenolysis of ethyl oleate **EO** (scheme 5.5). and results are summarised in table 5.4. Data of the same reaction catalysed by **HII** are reported for comparison as well as ethenolysis performed with **BertEt** catalyst (figure 5.9),[106] presenting a cyclic alkylaminocarbene (CAAC) ligand, since catalysts bearing the CAAC (cyclic alkylaminocarbene) ligands are the most efficient known so far for this transformation.[107]
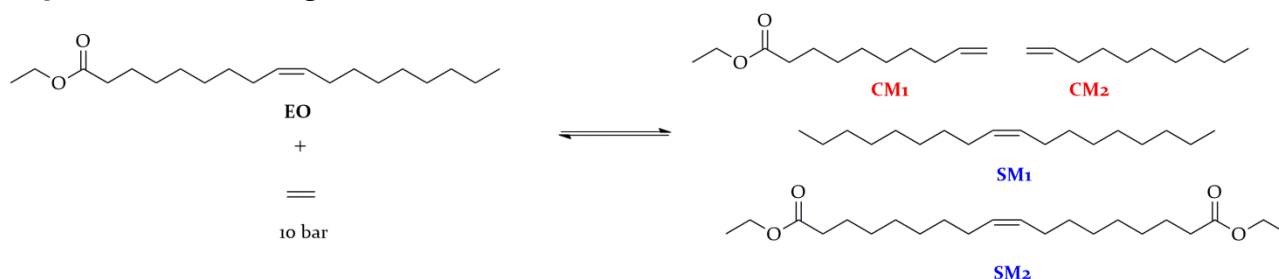
Scheme 5.5: Ethenolysis of **EO**

Table 5.4: Ethenolysis of **EO** with u-NHC catalyst, **HII** and **BertEt**

catalyst	loading (ppm)	temperature (°C)	time (h)	conversion[a] (%)	selectivity[a] (%)	yield[b] (%)	TON[c]
7	500	50	3	38	77	29	580
8	500	50	3	63	58	36	720
36	500	50	3	53	60	32	640
37	500	50	3	70	64	45	900
38	500	50	3	53	43	23	460
39	500	50	3	71	57	40	800
40	500	50	3	75	81	61	1220
41	500	50	3	81	83	67	1340
BertEt	500	50	3	85	83	70	1400
HII	500	50	3	71	43	30	600
41	100	50	3	48	86	41	4100
41	100	50	2	49	90	44	4400
41	100	40	3	39	88	34	3400
41	20	50	3	18	83	15	7500

[a] Determined via GC analysis of the crude reaction mixture after determination of the response factors

$$\text{Conversion } (\%) = 100 * \left(1 - \frac{\text{Area } (\textbf{EO})\text{sample} * \text{Area (dodecane)t0}}{\text{Area } (\textbf{EO})\text{t0} * \text{Area (dodecane)sample}} \right) ; \text{Selectivity } (\%) = 100 * \left(\frac{n(\textbf{CM1}) + n(\textbf{CM2})}{n(\textbf{CM1}) + n(\textbf{CM2}) + 2(n(\textbf{SM1}) + n(\textbf{SM2}))} \right)$$

[b] Conversion x Selectivity/100, [c] (Yield x (mol **EO**/mol catalyst))/100 (see Supporting Information)

[105] R. M. Thomas, B. K. Keitz, T. M. Champagne, R. H. Grubbs, *J. Am. Chem. Soc* **2011**, *19*, 7490.

[106] D. Anderson, V. Lavallo, D. J. O'Leary, G. Bertrand, R. H. Grubbs, Angew. Chem., Int. Ed. 2007, 46, 7262.

[107] a) D. R. Anderson, T. Ung, G. Mkrtumyan, G. Bertrand, R. H. Grubbs, *Organometallics* **2008**, *27*, 563; b) Y. Schrodi, T. Ung, A. Vargas, G. Mkrtumyan, W. C. Lee, T. M. Champagne, R. L. Pederson, S. H. Hong, *Clean: Soil, Air, Water* **2008**, *8*, 669; c) J. Zhang, S. Song, X. Wang, J. Jiao, M. Shi, Chem. Commun. 2013, 49, 9491; d) V. M. Marx, A. H. Sullivan, M. Melaimi, S. C. Virgil, B. K: Keitz, D. S. Weinberger, G. Bertrand, R. H. Grubbs, *Angew. Chem., Int. Ed.* **2015**, *6*, 1919. e) R. Gawin, A. Kozakiewicz, P. A. Guńka, P. Dąbrowski, K. Skowerski, *Angew. Chem., Int. Ed.* **2017**, *4*, 981.
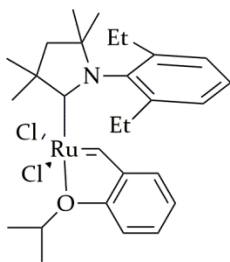
Figure 5.9:
BertEt catalyst

Catalysts' efficiency were firstly tested at a loading of 500 ppm. N-cyclohexyl, N'=isopropylphenyl compounds **7** and **8** again displayed a behaviour influenced by backbone configuration. In fact **7** exhibited an interesting selectivity albeit with a low conversion while **8** showed moderate conversion and selectivity.

The analogous compounds with a ramified N-neopentyl and N-neophyl group on the NHC exhibited moderate conversions and selectivity. Both for **36-37** and for **38-39** it was observed a reduced efficiency and selectivity of the syn catalyst with respect to the anti. Comparable results, in term of the overall yield, were obtained with the commercial **HII**.

More interesting are the catalytic performances of N-cyclohexyl, N'-mesityl catalysts **40** and **41**. In fact they both showed good conversions (75-81%) and very good selectivities (81-83%) in line with what observed with **BertEt** (conversion 85%, selectivity 83%), tested in the same reaction conditions. If we compare data of N'-mesityl **40-41** with those of their N'=isopropylphenyl congeners **7-8**, the significant role of the NHC aryl substituent is evident.

The behaviour of **41**, the most promising among the u-NHC compounds tested, was thus further investigated.

The catalyst, tested at 100 ppm, preserved its very good selectivity albeit with a decreased activity. The promising TON and the high degree of the desired ethenolysis product (**CM1** and **CM2** in scheme 5.5) encouraged us to test different reaction conditions maintaining the same catalyst loading. Reducing the reaction time from three to two hours slightly increased selectivity without affecting conversion. On the contrary, a decrease in the reaction temperature (from 50°C to 40°C) reduced the conversion but gained comparable selectivity.

Finally, we decided to decrease again the loading down to 20 ppm. At such catalyst quantity, twenty-five times lower with respect to the one chosen for the explorative screening of catalysts, **12c** preserved its selectivity, albeit conversion was significantly affected. Results at 20 ppm of catalyst were very interesting, since the TON obtained (7500) is the highest published for the ethenolysis promoted by u-NHC ruthenium catalysts up to now.

At this point it should be underlined that **BertEt**, and more in general CAAC ruthenium catalysts, have largely demonstrated their superior competence with respect to the NHC complexes in the ethenolysis of fatty acid methyl esthers.[11] However, it is very well known that the great performances of these catalysts are strictly tied to the high purity of oil. In this study, commercially available ethyl oleate underwent just a filtration on neutral alumina before use while it is more than reasonable to think that, in the case of CAAC catalysts, more expensive and complex purification treatment were used. This consideration derives by the fact that ethenolysis promoted by CAAC-Ru complexes were realised in collaboration with industrial partners (Materia® or Apeiron®) working intensively on methods of oil purification and, of course, their cleaning strategies are covered by the industrial secret.

For this reason, the only rational comparison between these u-NHC catalysts and CAAC complexes is the one reported in table 5.3 and it is realistic to expect that TON's of new catalysts, using an appropriately purified oil, could be several times higher.

5.6 Conclusion

In order to better understand the role of NHC substitution and backbone configuration in olefin metathesis, six new u-NHC ruthenium complexes were synthesized and characterised. Their thermal stability in solution was investigated and complexes **40**-**41**, bearing N-cyclohexyl, N'=mesityl ligands, showed an excellent behaviour, bearing unaltered after one month at 60°C. Topographic steric maps, calculated on the base of DFT minimum energy structures, showed that these two complexes have the most encumbered alkyl quadrant (%V$_{bur}$ max) and thus suggested a relation between steric hindrance and thermal stability. New catalysts were tested in representative metathesis transformations and compared with **HII** and our previously reported catalysts **7** and **8**.

In the RCM, the introduction of a branched alkyl group (neopentyl or neophyl, **36**-**37** or **38**-**39**, respectively) reduced the backbone configuration influence while the presence of an N'-mesityl substituent (**40**-**41**) accentuated this effect in the RCM with less hindered substrates. Unfortunately, the nature of the aryl group gave to **40**-**41** also an overall lower activity.

Very promising results were obtained in the CM involving renewable substrates **7** and **8** showed a pronounced backbone effect in the CM of **55** and **56**. All new catalysts were tested in the ethenolysis of ethyl oleate, and **41** displayed the most intriguing performances, giving, at 20 ppm, the highest TON so far reported for u-NHC catalysts in the ethenolysis of fatty acid methyl esthers.

5.7 Supporting Information

For all the general information please see paragraph 3.8.

Electrochemical measurements were conducted with an AUTOLAB PG STAT 302N potentiostat. A three-electrode configuration was employed. The working electrode was a Pt disk (diameter 2 mm), the counter-electrode a Pt bar and the reference a quasi-reference electrode (PtQRE)1, calibrated vs. octamethylferrocene as internal standard. All cyclic voltammograms were recorded in dry CH_2Cl_2 under a nitrogen atmosphere using NBu_4PF_6 (0.1 M) as supporting electrolyte at a scan rate of 100 mV/s. Potentials were referenced against the potential of octamethylferrocene. ESI-MS of organic compounds were performed on a Waters Quattro Micro triple quadrupole mass spectrometer equipped with an electrospray ion source. ESI-FT-ICR of complexes were performed on a Bruker Solaris XR. Optical activity was determined using a JASCO P2000 polarimeter.

The DFT calculations were performed with the Gaussian09 set of programs,[108] using the BP86 functional of Becke and Perdew.[109] The electronic configuration of the molecular

---

[108]M. J. Frisch, G. W. Trucks, H. B. Schlegel, G. E. Scuseria, M. A. Robb, J. R. Cheeseman, G. Scalmani, V. Barone, B. Mennucci, G. A. Petersson, H. Nakatsuji, M. Caricato, X. Li, H. P. Hratchian, A. F. Izmaylov, J. Bloino, G. Zheng, J. L. Sonnenberg, M. Hada, M. Ehara, K. Toyota, R. Fukuda, J. Hasegawa, M. Ishida, T. Nakajima, Y. Honda, O. Kitao, H. Nakai, T. Vreven, J. Jr Montgomery, J. E. Peralta, F. Ogliaro, M. Bearpark, J. J. Heyd, E. N. Brothers, K. Kudin, V. N. Staroverov, R. Kobayashi, J. Normand, K. Raghavachari, A. Rendell, J. C. Burant, S. S. Iyengar, J. Tomasi, M. Cossi, N. Rega, J. M. Millam, M. Klene, J. E. Knox, J. B. Cross, V. Bakken, C. Adamo, J. Jaramillo, R. Gomperts, R. E. Stratmann, O. Yazyev, A. J. Austin, R. Cammi, C. Pomelli, J. W.

systems was described with the standard split-valence basis set with a polarization function of Ahlrichs and co-workers for H, C, N, O, and Cl (SVP keyword in Gaussian).[110] For Ru we used the small-core, quasi-relativistic Stuttgart/Dresden effective core potential, with an associated (8s7p6d)/[6s5p3d] valence basis set contracted according to a (311111/22111/411) scheme (standard SDD keywords in gaussian09).[111] The geometry optimizations were performed without symmetry constraints, and the characterization of the located stationary points was performed by analytical frequency calculations.

5.7.1 General Procedure for the arylation of diamines.

Under a nitrogen atmosphere, in a roundbottom flask equipped with a magnetic stirrer and a condenser, 2,2-bis(diphenylphosphino)-1,1-binaphthyl (BINAP) (0.2 equiv), palladiumacetate (0.1 equiv), sodium tert-butoxide (2 equiv), and toluene (C = 0.05 M) were introduced. The orange solution was stirred for few minutes. Then the diamine (1 equiv.) and mesityl bromide (1 equiv.) were added and the reaction mixture was heated to 100 °C for 48 h. After this time the purple mixture was cooled to room temperature, diluted with hexane, and then filtered through a plug of silica gel with methanol as eluent. The crude yellow oil was purified by flash column chromatography on silica gel (hexane/ethyl acetate 9/1 to 6/4) to give the desired product as a yellow oil.

50 (MW = 330.5 g/mol. Yield: 79%).
^{1}H NMR (300 MHz, CDCl$_3$): δ 7.29–7.27 (m, 3H); 7.23–7.20 (m, 3H); 7.10–7.07 (m, 2H); 7.02–6.98 (m, 2H); 6.75 (s, 2H); 4.43 (d, ^3J = 4.9 Hz, 1H); 4.35 (d, ^3J = 5.2 Hz, 1H); 2.21 (s, 3H); 2.16 (s, 6H).
^{13}C NMR (75 MHz, CDCl$_3$): δ 143.8; 142.8; 139.8; 130.1; 129.7 (overlapped); 128.5; 128.2; 128.1;127.8; 127.2; 127.1; 67.7; 60.2; 20.6; 19.3.
ESI$^+$MS: m/z 353.2 (MNa$^+$).

53 (MW = 412.6 g/mol. Yield: 51%).
^{1}H NMR (400 MHz, CDCl$_3$): δ 7.20–7.15 (m, 5H); 7.09 (br s, 3H); 7.01–6.99(m, 2H, Ar-H); 6.67 (s, 2H); 4.41 (d, ^3J = 7.2 Hz); 4.21 (d, ^3J = 7.2 Hz, 1H); 2.33–2.28 (m, 1H); 2.15 (s, 3H); 2.13 (s, 6H); 2.01–1.98 (br d, 1H); 1.67 (br t, 3H); 1.54 (br s, 1H); 1.17–1.10 (m, 5H).
^{13}C NMR (100 MHz, CDCl$_3$) δ: 142.4; 142.3; 141.9; 129.8; 128.3; 128.0; 127.9 (overlapped); 127.8; 126.9; 67.1; 65.5; 53.7; 35.0; 32.8; 26.3; 25.2, 24.8, 20.5, 19.6.
ESI$^+$MS: m/z 413.9 (MH$^+$).
$[\alpha]^D$ = −45.3° (c = 0.5, CH$_2$Cl$_2$).

Ochterski, R. L. Martin, K. Morokuma, V. G. Zakrzewski, G. A. Voth, P. Salvador, J. J. Dannenberg, S. Dapprich, A. D. Daniels, O. Farkas, J. B. Foresman, J. V. Ortiz, J. Cioslowski, D. J. Fox *Gaussian 09, Revision A.02; Gaussian*, Inc., Wallingford, CT, **2009**.
[109] a) A. D. Becke, *Phys. Rev. A: At., Mol., Opt. Phys.* **1988**, *6*, 3098; b) J. P. Perdew, *Phys. Rev. B: Condens. Matter Mater. Phys.* **1986**, *12*, 8822; c) J. P. Perdew, *Phys. Rev. B: Condens. Matter Mater. Phys.* **1986**, *13*, 7406.
[110] A. Schaefer, H. Horn, R. J. Ahlrichs, *J. Chem. Phys.* **1992**, *4*, 2571.
[111] a) U. Haussermann, M. Dolg, H. Stoll, H. Preuss, *Mol. Phys.* **1993**, *5*, 1211; b)W. Kuechle, M. Dolg, H. Stoll, H. J. Preuss, *J. Chem. Phys.* **1994**, *10*, 7535; c) T. Leininger, A. Nicklass, H. Stoll, M. Dolg, P. Schwerdtfeger, *Chem. Phys.* **1996**, *3*, 1052.

5.7.2 General procedure for the alkylation of diamines (devo correggere numeri)
A round bottom flask was charged with the diamine (1 eq.), the carbonylic compound (3 eq. of pivalaldehyde for **42** and **46**, 6 eq. of 2-methyl-2-phenylpropanaldehyde for **43** and **47** and 7 eq. of cyclohexanone **51**) and anhydrous methylene chloride (C = 0.1 M). The reaction mixture was stirred at room temperature over activated molecular sieves 4Å for 48 hours (**42**) or 14hours (**46**) or 5 days (**43**, **47** and **51**) and then filtered. Then, the solvent was removed under reduced pressure, anhydrous MeOH was added (C=0.1 M) followed by a portionwise addition of $NaBH_4$ (4 eq.) under nitrogen atmosphere. The reaction mixture was stirred for 3.5 h, diluted with methylene chloride and extracted with water. The organic layer was dried over anhydrous Na_2SO_4 and then the solvent was removed under vacuum to afford a yellowish oil which was then purified by flash column chromatography on silica gel (hexane: ethyl acetate 9:1)

42 (MW=400.6 g/mol, Yield=60%)
^{1}H NMR (300 MHz, $CDCl_3$): δ 7.31-7.30 (o m, 3H); 7.25-7.23 (o m, 3H); 7.19-7.16 (o m, 1H); 7.08-7.01 (o m, 3H); 6.91 (t, ^3J=8.0 Hz, ^3J=7.2 Hz, 1H), 6.68 (t, ^3J=7.4 Hz, ^3J=7.4 Hz, 1H); 6.31 (d, ^3J=8.2 Hz, 1H); 5.42 (br s, 1H); 4.63 (t, ^3J=4.7 Hz, ^3J=4.7 Hz, 1H); 4.15 (d, ^3J=4.7 Hz , 1H); 3.12-2.99 (m, 1H); 2.37 (d, ^3J=11.4 Hz, 1H); 2.20 (d, ^3J=11.4 Hz, 1H); 1.41 (d, ^3J=6.6 Hz, 3H); 1.35 (d, ^3J=6.8 Hz, 3H); 0.97 (s, 9H).
^{13}C NMR (75 MHz, $CDCl_3$) δ: 143.9; 140.2; 139.8; 132.2; 128.2; 128.1; 127.9; 127.8; 127.4; 127.2; 126.6; 124.8; 116.9; 111.7; 68.7; 62.8; 59.8; 31.8; 27.8; 27.7; 22.5; 22.4.
ESI$^+$MS: m/z = 401.4 (MH$^+$).

46 (MW=400.6 g/mol, Yield=70%)
^{1}H NMR (300 MHz, CD_2Cl_2) δ: 7.33-7.22 (o m, 10H); 7.15 (dd, ^3J=7.7 Hz, , ^3J=1.3 Hz, 1H); 6.83 (dt, ^3J=7.6 Hz, ^3J=1.5 Hz, 1H); 6.64 (dt, ^3J=7.0 Hz, 1H); 6.21 (d, ^3J=8.1 Hz, 1H); 5.82 (br s, 1H); 4.42 (d, ^3J=6.9 Hz, 1H); 3.86 (d, ^3J=6.8 Hz, 1H); 3.25-3.16 (m, 1H); 2.28 (d, ^3J=11.3 Hz, 1H); 2.09 (d, ^3J=11.3 Hz, 1H); 1.42 (d, ^3J=6.8 Hz, 3H); 1.38 (d, ^3J=6.7 Hz, 3H); 0.95 (s, 9H).
^{13}C NMR (75 MHz, CD_2Cl_2) δ: 144.7; 142.4; 141.7; 133.2; 128.6; 128.5; 128.1; 127.5; 127.3; 126.5; 125.0; 117.2; 111.9; 70.4; 64.4; 60.1; 31.8; 27.8; 27.7; 23.0; 22.4.
ESI$^+$MS: m/z = 401.4 (MH$^+$).
$[\alpha]_D^{20}$ = +49.1 (c=0.5, CH_2Cl_2).

43 (MW=462.7 g/mol, Yield=73%)
^{1}H NMR (250 MHz, $CDCl_3$) δ: 7.28 (d, ^3J=4.4 Hz, 4H); 7.21-7.20 (o m, 4H); 7.09-7.07 (o m, 4H);6.86 (d, ^3J=7.3 Hz, 2H); 6.82-6.77 (o m, 3H); 6.60 (t, ^3J=7.5 Hz, ^3J=7.3 Hz, 1H); 6.19 (d, ^3J=7.9 Hz, 1H); 5.12 (d, ^3J=5.1 Hz, 1H); 4.43 (t, ^3J=5.2 Hz, ^3J=5.1 Hz, 1H); 3.99 (d, ^3J=4.9 Hz, 1H); 2.90-2.82 (m, 1H); 2.62 (d, ^3J=11.3 Hz, 1H); 2.51 (d, ^3J=11.3 Hz, 1H); 1.37 (s, 3H); 1.31-1.29 (o m, 6H); 1.24-1.22 (d, ^3J=6.8 Hz, 3H).

^{13}C NMR (100 MHz, CDCl$_3$) δ: 147.7; 143.8; 140.0; 139.7; 132.2; 128.3; 128.1; 128.0; 127.9; 127.7; 127.5; 127.1; 126.5; 126.0; 125.9; 124.7; 116.9; 111.7; 68.4; 62.8; 59.8; 38.9; 27.6; 27.4; 27.0; 22.5; 22.3.

ESI$^+$MS: m/z = 463.2 (MH$^+$).

47 (MW=462.7 g/mol, Yield=79%)

^{1}H NMR (300 MHz, CDCl$_3$) δ:7.32-7.26 (o m, 8H); 7.17-7.16 (o m 8H); 6.83 (br t, 1H); 6.64 (br t, 1H); 6.14 (d, ^3J=7.6 Hz, 1H); 5.61 (br s, 1H); 4.24 (br s, 1H); 3.76 (br d, 1H); 3.05 (br t, 1H); 2.64 (d, ^3J=10.9 Hz, 1H); 2.48 (d, ^3J=10.9 Hz, 1H); 1.41-1.33 (o m, 12H).

^{13}C NMR (75 MHz, CDCl$_3$) δ:147.4; 144.3; 141.8; 141.1; 132.7; 128.4; 128.2; 127.7; 127.3; 127.0; 126.4; 126.0; 124.7; 116.9; 111.7; 69.7; 64.2; 59.8; 38.8; 27.7; 27.6; 27.1; 22.8; 22.4.

ESI+MS: m/z = 463.1 (MH$^+$).

$[\alpha]_D^{20}$ =+65.8 (c=0.5, CH$_2$Cl$_2$).

51 (MW=412.6 g/mol, Yield=50%)

^{1}H NMR (300 MHz, CDCl$_3$) δ: 7.26-7.25 (o m, 3H); 7.16-7.13 (o m, 3H); 6.93-6.90 (o m, 2H); 6.85-6.82 (o m, 2H); 6.71 (s, 2H); 4.91 (br s, 1H); 4.49 (br s, 1H); 4.38 (d, ^3J=4.5 Hz, 1H); 2.33 (br s, 1H); 2.18 (br s, 9H); 1.99 (br s, 1H); 1.71-1.57 (o m, 4H); 1.38 (br s, 1H); 1.18-1.13 (o m, 5H).

^{13}C NMR (75 MHz, CDCl$_3$) δ: 142.8; 141.5; 139.7; 129.7; 129.1; 128.4; 128.0; 127.8; 127.5; 127.1; 127.0; 126.9; 66.8; 63.7; 53.2; 35.1; 33.0; 26.3; 25.1; 24.7; 20.5; 19.8.

ESI+MS: m/z = 413.2 (MH$^+$).

5.7.3 General procedure for the synthesis of tetrafluoroborate salts

Diamine (1 eq.) and triethyl orthoformate (8 eq.) were introduced in a flask equipped with a magnetic stir and a condenser. The reaction mixture was stirred at room temperature for few minutes. Then ammonium tetrafluoroborate (1.2 eq.) was added and the solution was heated at 130°C for 2 hours(**44**, **48**, **52**, **54**) or 8 hours (**45**, **49**). After that, the condenser was removed in order to facilitate the evaporation of the ethanol produced during the reaction. The crude brownish oil was washed with diethyl ether and purified by flash column chromatography on silica gel (hexane:ethyl acetate 9:1 to 1:1) to obtain the product as a white solid.

44 (MW=498.4 g/mol, Yield=81%)

^{1}H NMR (400 MHz, CD$_2$Cl$_2$) δ: 8.70 (s, 1H); 7.50-7.48 (o m, 2H); 7.36-7.35 (o m, 2H); 7.25-7.18 (o m, 4H); 7.11-6.97 (o m, 6H); 6.19 (br t, 1H); 5.98 (br t, 1H); 4.01 (d, ^3J=14.2 Hz, 1H); 3.21-3.11 (o m, 2H); 1.34-1.29 (o m, 6H); 1.08 (s, 9H).

^{13}C NMR (100 MHz, CD$_2$Cl$_2$) δ:160.6; 145.6; 131.8; 130.9; 130.5; 130.4; 129.8; 129.5; 129.4; 128.8; 128.7; 127.9; 127.7; 73.6; 72.2; 58.7; 33.2; 29.0; 27.7; 24.5; 24.1.

ESI$^+$MS: m/z = 411.4 (M-BF$_4^-$).

48 (MW=498.4 g/mol, Yield=90%)

^{1}H NMR (400 MHz, CD$_2$Cl$_2$) δ: 8.58 (s, 1H); 7.58-7.56 (o m, 3H); 7.45-7.34 (o m, 7H); 7.27-7.25 (o m, 2H); 7.21-7.18 (o m, 2H); 5.53 (d, ^3J=8.0 Hz, 1H); 5.37 (d, ^3J=8.0 Hz, 1H); 3.82 (d, ^3J=14.9 Hz, 1H); 3.06 (d, ^3J=14.9 Hz, 1H); 2.96-2.89 (m, 1H); 1.23 (d, ^3J=6.8 Hz, 3H); 1.09 (s, 9H); 1.02 (d, ^3J=6.8 Hz, 3H).

^{13}C NMR (100 MHz, CD$_2$Cl$_2$) δ 159.3; 145.9; 135.1; 134.7; 131.4; 131.0; 130.9; 130.8; 130.7; 130.3; 130.2; 128.8; 128.0; 127.9; 127.7; 127.6; 127.5; 127.0; 78.1; 75.4; 57.6; 33.6; 28.7; 28.0; 24.5; 23.8.

ESI$^+$MS: m/z = 411.5 (M-BF$_4^-$).

$[\alpha]_D^{20}$ =+313.0 (c=0.5, CH$_2$Cl$_2$).

45 (MW=560.5 g/mol, Yield=71%)
^{1}H NMR (400 MHz, CD$_2$Cl$_2$) δ: 8.36 (s, 1H); 7.41-7.32 (o m, 9H); 7.20-7.19 (o m, 4H); 7.00-6.98 (m, 3H); 6.83 (d, ^3J=6.8 Hz, 3H); 5.73 (d, ^3J=12.4 Hz, 1H); 4.91 (d, ^3J=11.6 Hz, 1H); 4.33 (d, ^3J=14.4 Hz, 1H); 3.57 (d, ^3J=14.4 Hz, 1H); 3.02-2.92 (m, 1H); 1.54 (s, 3H); 1.45 (s, 3H); 1.29-1.27 (o m, 6H).

^{13}C NMR (100 MHz, CD$_2$Cl$_2$) δ 160.1; 145.4; 145.2; 131.6; 130.9; 130.2; 129.6; 129.5; 129.2; 128.6; 127.8; 127.6; 126.4; 73.3; 71.1; 59.1; 39.8; 28.9; 27.7; 25.6; 24.5; 24.1.

ESI$^+$MS: m/z = 474.9 (M-BF$_4^-$).

49 (MW=560.5 g/mol, Yield=90%)
^{1}H NMR (300 MHz, CDCl$_3$) δ: 8.46 (s, 1H); 7.50-7.45 (o m, 7H); 7.37-7.09 (o m, 9H); 6.97 (d, ^3J=8.3 Hz, 1H); 6.81 (d, ^3J=7.6 Hz, 2H); 5.00 (d, ^3J=8.3 Hz, 1H); 4.60 (d, ^3J=8.0 Hz, 1H); 4.30 (d, ^3J=14.8 Hz, 1H); 3.55 (d, ^3J=14.8 Hz, 1H); 2.67-2.56 (m, 1H); 1.57 (s, 3H); 1.40 (s, 3H); 1.15 (d, ^3J=6.7 Hz, 3H); 0.86 (d, ^3J=6.9 Hz, 3H).

^{13}C NMR (100 MHz, CD$_2$Cl$_2$) δ 158.9; 145.5; 145.2; 134.9; 134.2; 130.9; 130.7; 130.4; 130.3; 129.6; 129.3; 127.9; 127.5; 127.4; 127.2; 126.8; 126.5; 73.6; 57.7; 39.6; 28.4; 28.2; 25.9; 24.7; 23.6.

ESI$^+$MS: m/z = 474.9 (M-BF$_4^-$).

$[\alpha]_D^{20}$ =+210.6 (c=0.5, CH$_2$Cl$_2$).

52 (MW=510.4 g/mol, Yield=79%)
^{1}H NMR (300 MHz, CDCl$_3$) δ: 8.45 (s, 1H); 7.24-7.23 (o m, 4H); 7.03-6.92 (o m, 4H); 6.85-6.72 (o m, 4H); 6.61 (d, ^3J=11.8 Hz, 1H); 5.95 (d, ^3J=11.8 Hz, 1H); 3.63 (t, 1H); 2.48 (s, 3H); 2.33-2.20 (o m, 4H); 2.17 (s, 3H); 1.94-1.77 (o m, 3H); 1.63-1.55 (o m, 3H); 1.38-1.21 (o m, 3H).

^{13}C NMR (100 MHz, CDCl$_3$) δ: 157.4; 139.4; 135.2; 133.9; 131.9; 131.1; 130.3; 129.9; 129.3; 129.0; 128.9; 128.2; 127.5; 72.6; 67.8; 58.6; 32.3; 31.8; 25.3; 25.0; 24.9; 20.9; 19.7; 19.5.

ESI$^+$MS: m/z = 425.2 (M-BF$_4^-$).

54 (MW=510.4 g/mol, Yield=75%)
^{1}H NMR (250 MHz, CDCl$_3$) δ:8.62 (s, 1H); 7.52-7.32 (o m, 7H); 7.18-7.15 (o m, 3H); 6.86 (br s, 1H); 6.69 (br s, 1H); 5.66 (d, ^3J=8.1 Hz, 1H); 5.12 (d, ^3J=7.9 Hz, 1H); 3.75-3.66 (br t, 1H); 2.35 (s, 3H); 2.19-2.11 (o m, 5H); 1.92-1.84 (o m, 1H); 1.75 (s, 3H); 1.63 (s, 3H); 1.45-1.20 (o m, 4H).

^{13}C NMR (100 MHz, CDCl$_3$) δ:156.8; 140.2; 136.3; 134.8; 133.7; 130.7; 130.3; 130.2; 129.5; 129.0; 128.6; 127.0; 75.6; 70.4; 58.5; 32.3; 31.5; 25.1; 24.8; 21.0; 18.8; 18.0.

ESI+MS: m/z = 424.5 (M-BF$_4^-$).

$[\alpha]_D^{20}$ =+309.8 (*c*=0.5, CH$_2$Cl$_2$).

5.7.4 General procedure for the synthesis of catalysts

In a glove box, potassium hexafluorotbutoxide (1 eq.) was added to a suspension of tetrafluoroborate salt (1 eq.) in toluene (C = 0.1 M). The reaction mixture was stirred for few minutes at RT and then (PCy$_3$)Ru(=CH-*o*-OiPrC$_6$H$_4$)Cl$_2$ (0.5 eq.) was added. The flask was removed from the glove box and stirred at 65°C for 2.0 hours. The reaction mixture was cooled at room temperature and purified by flash column chromatography on silica gel (hexane:diethyl ether 5:1 to 1:1).

36 (MW=730.8 g/mol, Yield=45%)

^{1}H NMR (600 MHz, C$_6$D$_6$) δ: 16.29 (major isomer, s, 1H, Ru=CH–*o*OiPrC$_6$H$_4$); 16.22 (minor isomer, s, 0.3H); (mixed signals of both isomers) 8.96 (d, ^3J=7.3 Hz, 1H); 7.99 (br s, 1H); 7.94 (br s, 1H); 7.85 (d, ^3J=6.8 Hz, 1H); 7.20 (d. ^3J=7.8 Hz, 1H); 7.53-7.50 (o m, 3H); 7.37 (br t, 1H); 7.31-7.28 (o m, 1H); 7.25-7.23 (br t, 1H); 7.09-7.03 (o m, 3H); 6.98 (br s, 3H); 6.93-6.90 (o m, 1H); 6.82-6.65 (o m, 5H); 6.48 (d, ^3J=9.1 Hz, 1H); 6.22 (d, ^3J=7.3 Hz, 1H); (only major isomer signals are shown below) 5.99 (t, ^3J=10.0 Hz, 1H); 5.56 (d, ^3J=14.6 Hz, 1H); 5.41 (d, ^3J=10.0 Hz, 1H); 4.70(br s, 1H); 4.13 (d, ^3J=13.7 Hz, 1H); 3.41 (m, 1H); 1.77 (s, 6H); 1.24 (s, 9H); 1.18 (br s, 3H).

^{13}C NMR (125 MHz, C$_6$D$_6$) δ: (only major isomer signals are shown below) 291.8 (Ru=CH–*o*OiPrC$_6$H$_4$); 291.2; 216.1; 163.7; 163.5; 153.2; 149.1; 148.9; 148.4; 147.3; 144.5; 143.5; 142.4; 141.3; 139.7; 139.2; 138.9; 138.5; 133.8; 133.3; 133.2; 131.2; 130.7; 130.5; 130.4; 130.2; 129.6; 129.4; 129.3; 129.3; 129.0; 128.9; 128.8; 127.7; 128.6; 127.5; 127.2; 127.0; 126.9; 126.8; 126.1; 122.5; 113.2; 78.3; 77.4; 75.5; 75.2; 70.8; 69.8; 68.6; 65.2; 62.5; 62.0; 61.1; 60.2; 59.8; 32.8; 32.7; 31.3; 30.2; 29.4; 29.3; 29.2; 28.8; 27.7; 27.6; 27.3; 25.6; 24.8; 24.5; 24.4; 24.3; 24.2; 23.6; 22.8; 22.2; 22.1.

ESI-FT-ICR (11a-Cl).: m/z = calc. 695.2342 found 695.2339 .

37 (MW=730.8 g/mol, Yield=70%)

^{1}H NMR (600 MHz, C$_6$D$_6$) δ: 16.38 (minor isomer, s, 0.1H, Ru=CH–*o*OiPrC$_6$H$_4$); 16.38 (major isomer, s, 1H); (only major isomer signals are shown below) 7.75 (br s, 1H); 7.56 (d, ^3J=6.8 Hz, 2H); 7.43 (d. ^3J=8.1 Hz, 1H); 7.30 (t, ^3J=7.5 Hz, ^3J=7.5 Hz, 1H); 7.19-7.08 (o m, 5H); 7.02-6.98 (m, 3H); 6.67 (t, ^3J=7.4 Hz, ^3J=7.4 Hz, 1H); 6.57 (t, ^3J=7.4 Hz, ^3J=7.4 Hz, 1H); 6.47 (d, ^3J=8.3 Hz, 1H); 5.42 (d, ^3J=13.5 Hz, 1H); 5.26 (d, ^3J=2.7 Hz, 1H); 4.71-4.67 (m, 1H); 4.16 (d, ^3J=14.8 Hz, 1H); 3.47-3.43 (m, 1H); 1.78 (d, ^3J=6.0 Hz, 3H); 1.72 (d, ^3J=6.0 Hz, 3H); 1.28 (d, ^3J=7.0 Hz, 3H); 1.10 (s, 9H); 0.97 (d, ^3J=7.0 Hz, 3H).

^{13}C NMR (125 MHz, C$_6$D$_6$) δ: (only major isomer signals are shown below) 291.7 (Ru=CH–*o*OiPrC$_6$H$_4$); 214.4; 153.6; 148.5; 144.7; 140.3; 139.6; 139.4; 133.3; 129.9; 129.7; 129.6; 129.5; 129.4; 129.0; 127.3; 127.2; 127.1; 122.8; 122.6; 113.5; 80.7; 75.4; 73.9; 63.3; 63.2; 33.9; 32.2; 29.8; 28.0; 27.9; 24.9; 24.8; 23.8; 23.7; 23.3; 22.6; 22.6; 22.4; 14.7; 14.5.

ESI-FT-ICR (12a-Cl).: m/z = calc. 695.2342 found 695.2344 .

38 (MW=792.8 g/mol, Yield=70%)

^{1}H NMR (600 MHz, C_6D_6) δ: 16.31 (major isomer, s, 1H, Ru=CH–oOiPrC$_6$H$_4$); 16.36 (minor isomer, s, 0.2H); (only major isomer signals are shown below) 8.88 (d, ^3J=8.3 Hz, 1H); 7.50-7.47 (o m, 2H); 7.28-7.23 (o m, 1H); 7.18-7.17 (o m, 1H); 7.09-7.03 (o m, 3H); 7.01-6.95 (o m, 4H); 6.93-6.91 (o m, 1H); 6.86-6.85 (o m, 3H); 6.73-6.67 (o m, 1H); 6.59-6.56 (o m, 5H); 6.50 (d, ^3J=8.5 Hz, 1H); 6.47-6.44 (o m, 1H); 5.90 (d, ^3J=9.7 Hz, 1H); 5.82 (d, ^3J=13.6 Hz, 1H); 5.35 (d, ^3J=7.8 Hz, 1H); 4.91 (d, ^3J=9.7 Hz, 1H); 4.80 (d, ^3J=13.6 Hz, 1H); 4.75-4.71 (m, 1H); 3.42-3.38 (m, 1H); 2.09 (s, 3H); 1.82-1.80 (o m, 6H); 1.45 (s, 3H); 1.20 (d, ^3J=7.2 Hz, 3H); 1.15 (d, ^3J=7.2 Hz, 3H).

^{13}C NMR (125 MHz, C_6D_6) δ: (mixed signals of both isomers) 292.1; 291.6; 220.6; 215.9; 163.9; 163.7; 153.6; 149.1; 148.5; 148.3; 144.8; 144.5; 141.7; 139.5; 134.1; 133.4; 133.2; 131.4; 130.5; 130.2; 129.8; 129.7; 129.5; 129.3; 129.1; 129.0; 128.8; 128.0; 127.9; 127.9; 127.7; 127.5; 127.1; 127.0; 126.3; 126.3; 126.2; 122.8; 113.5; 78.6; 77.5; 77.4; 75.8; 75.5; 75.4; 70.2; 69.1; 68.7; 65.2; 62.7; 62.2; 61.2; 60.5; 60.1; 39.6; 39.5; 38.9; 34.0; 32.0; 30.5; 29.1; 29.0; 28.6; 28.5; 27.9; 24.8; 24.6; 24.5; 24.5; 24.4; 22.6; 22.5.

ESI-FT-ICR (11b-Cl).: m/z = calc. 757.2499 found 757.2494 .

39 (MW=792.8 g/mol, Yield=61%)

^{1}H NMR (600 MHz, C_6D_6) δ: 16.39 (minor isomer, s, 0.1H, Ru=CH–oOiPrC$_6$H$_4$); 16.36 (major isomer, s, 1H); (only major isomer signals are shown below) 7.50 (d, ^3J=7.6 Hz, 4H); 7.19-7.15 (o m, 5H); 7.11-7.08 (o m, 3H); 7.02-6.98 (o m, 3H); 6.91 (d, ^3J=8.1 Hz, 2H); 6.84 (t, ^3J=7.6 Hz, ^3J=7.1 Hz, 1H); 6.75 (t, ^3J=7.6 Hz, 2H); 6.68 (t, ^3J=7.6 Hz, ^3J=7.1 Hz, 1H); 6.50 (d, ^3J=8.1 Hz, 1H); 5.64 (d, ^3J=14.2 Hz, 1H); 4.79 (d, ^3J=14.2 Hz, 1H); 4.74-4.71 (m, 1H); 4.70 (d, ^3J=1.9 Hz, 1H); 4.60 (d, ^3J=1.9 Hz, 1H); 3.36-3.31 (m, 1H); 2.06 (s, 3H); 1.82 (d, ^3J=6.2 Hz, 3H); 1.78 (d, ^3J=6.2 Hz, 3H); 1.41 (s, 3H); 1.27 (d, ^3J=6.6 Hz, 3H); 0.89 (d, ^3J=6.6 Hz, 3H).

^{13}C NMR (125 MHz, C_6D_6) δ: (only major isomer signals are shown below) 291.6 (Ru=CH–oOiPrC$_6$H$_4$); 213.8; 153.6; 148.5; 147.7; 144.7; 139.8; 139.7; 139.5; 133.2; 129.6; 129.5; 129.5; 129.3; 129.2; 127.9; 127.3; 127.1; 126.5; 126.4; 126.2; 122.9; 122.6; 113.5; 80.4; 75.5; 72.8; 63.4; 40.0; 32.3; 32.2; 27.9; 27.8; 25.7; 24.9; 24.8; 23.6; 23.4; 22.6; 22.6; 22.5; 22.4.

ESI-FT-ICR (12b-Cl).: m/z = calc. 757.2499 found 757.2505 .

40 (MW=742.8 g/mol, Yield=63%)

^{1}H NMR (600 MHz, C_6D_6) δ: 16.56 (major isomer, s, 1H, Ru=CH–oOiPrC$_6$H$_4$); 16.44 (minor isomer, s, 0.1H); (only major isomer signals are shown below) 8.78 (br s, 1H); 7.37 (br s, 1H); 7.15-7.12 (o m, 2H); 7.00 (t, ^3J=7.5 Hz, ^3J=7.5 Hz, 1H); 6.78 (br s, 1H); 6.70-6.67 (o m, 5H); 6.62-6.60 (o m, 3H); 6.56 (br s, 1H); 6.47 (d, ^3J=8.3 Hz, 1H); 6.27 (br s, 1H); 6.04 (d, ^3J=9.3 Hz, 1H); 5.72 (t t, ^3J=3.1 Hz, ^3J=3.4 Hz, 1H); 5.04 (d, ^3J=9.0 Hz, 1H); 4.73-4.68 (m, 1H); 3.07 (d, ^3J=11.5 Hz, 1H); 2.86 (d, ^3J=12.4 Hz, 1H); 2.63 (s, 3H); 2.43 (s, 3H); 1.95 (s, 3H); 1.88-1.84 (o m, 2H); 1.81 (d, ^3J=6.1 Hz, 3H); 1.78 (d, ^3J=6.1 Hz, 3H); 1.76-1.73 (o m, 1H); 1.67-1.59 (o m, 3H); 1.12-1.06 (o m, 1H); 0.97-0.87 (o m, 1H).

^{13}C NMR (125 MHz, C$_6$D$_6$) δ: (only major isomer signals are shown below) 290.9 (Ru=CH–oOiPrC$_6$H$_4$); 214.0; 152.9; 145.0; 139.9; 138.1; 138.0; 137.5; 136.8; 133.1; 130.6; 129.6; 129.5; 129.2; 122.6; 122.5; 113.2; 75.6; 74.9; 64.9; 63.7; 33.7; 33.4; 33.3; 26.8; 26.6; 22.3; 20.8; 20.8; 20.3; 20.2. ESI-FT-ICR (11c-Cl).: m/z = calc. 707.2342 found 707.2339 .
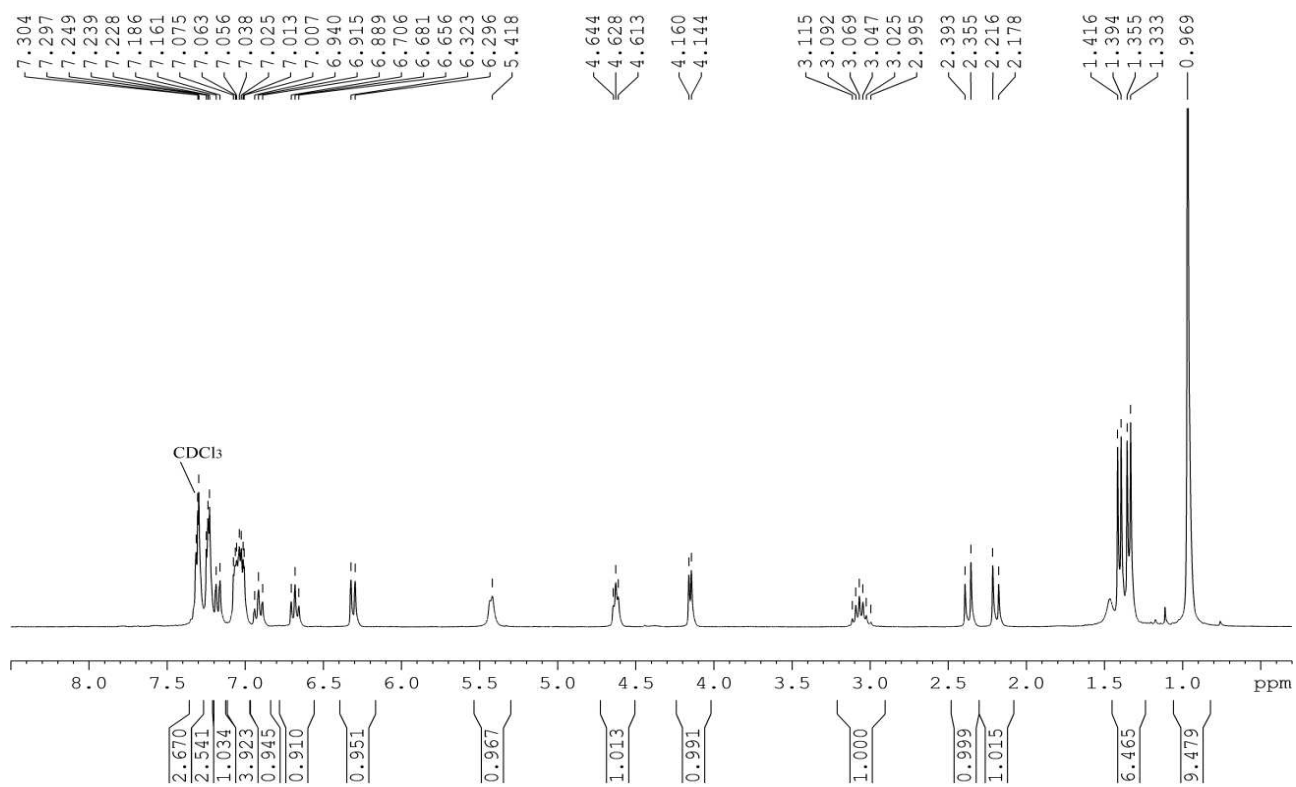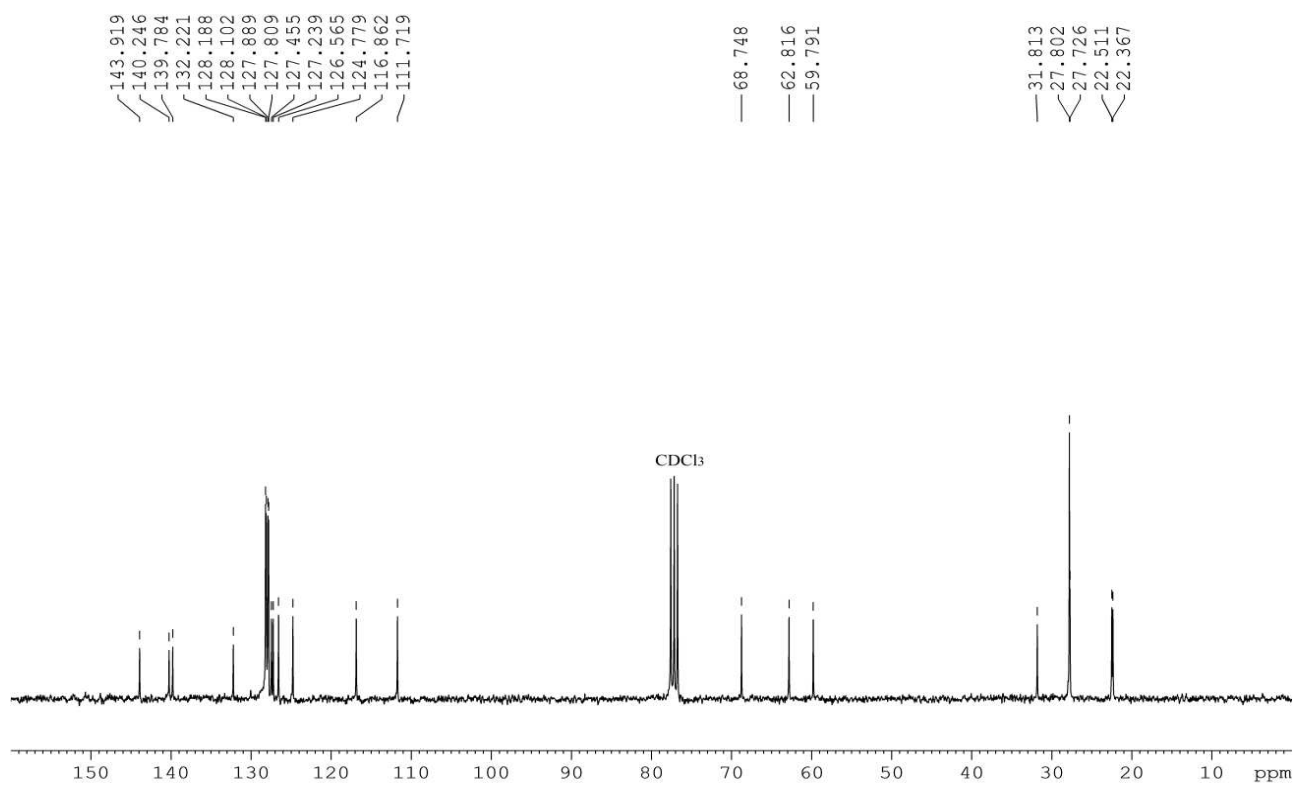
41 (MW=742.8 g/mol, Yield=54%)

^{1}H NMR (600 MHz, C$_6$D$_6$) δ: 16.44 (s, 1H, Ru=CH–oOiPrC$_6$H$_4$); 7.14-7.08 (o m, 6H); 7.05 (t, ^3J=7.3 Hz, ^3J=7.3 Hz, 1H); 7.00-6.94 (o m, 5H); 6.78 (br s, 1H); 6.68 (t, ^3J=7.3 Hz, ^3J=7.5 Hz 1H); 6.57 (br s, 1H); 6.46 (d, ^3J=8.2 Hz, 1H); 5.70 (t t, ^3J=3.1 Hz, ^3J=3.0 Hz, 1H); 5.48 (d, ^3J=6.4 Hz, 1H); 4.78 (d, ^3J=6.8 Hz, 1H); 4.71-4.67 (m, 1H); 3.10 (d, ^3J=11.1 Hz, 1H); 2.85 (d, ^3J=12.4 Hz, 1H); 2.54 (s, 3H); 2.07 (s, 3H); 1.96-1.88 (o m, 2H); 1.79-1.77 (o m, 9H); 1.63-1.58 (o m, 3H); 1.00-0.86 (o m, 3H).
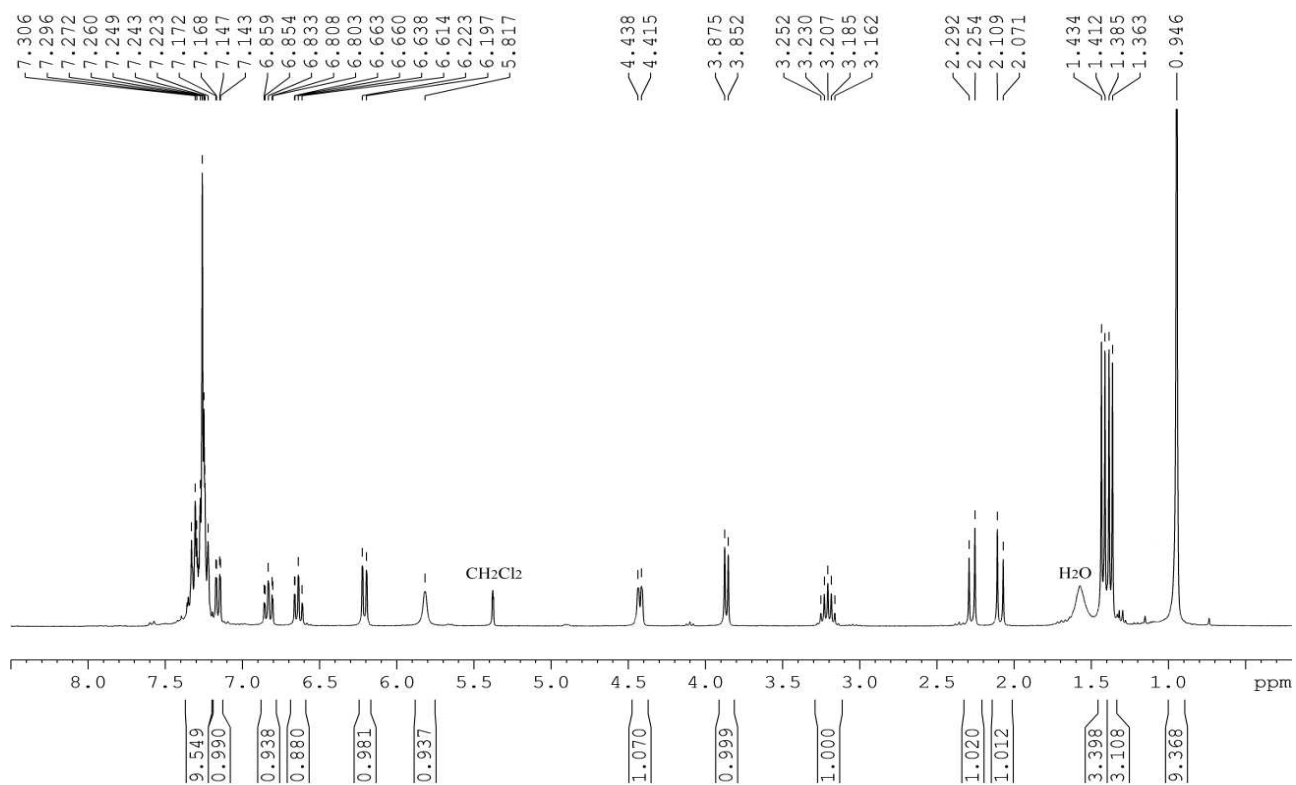
^{13}C NMR (125 MHz, C$_6$D$_6$) δ: 290.2 (Ru=CH–oOiPrC$_6$H$_4$); 211.8; 153.3; 145.2; 143.3; 141.0; 139.2; 138.8; 137.5; 130.4; 130.2; 129.7; 129.4; 129.3; 129.3; 129.1; 128.9; 122.8; 122.7; 113.5; 79.3; 75.2; 69.6; 64.2; 34.5; 34.3; 32.3; 32.2; 27.4; 26.9; 26.2; 26.1; 22.7; 22.6; 21.3; 21.2; 21.2; 21.1; 20.0; 19.9; 19.5. ESI-FT-ICR (12c-Cl).: m/z = calc. 707.2342 found 707.2362.

5.7.5 NMR spectra
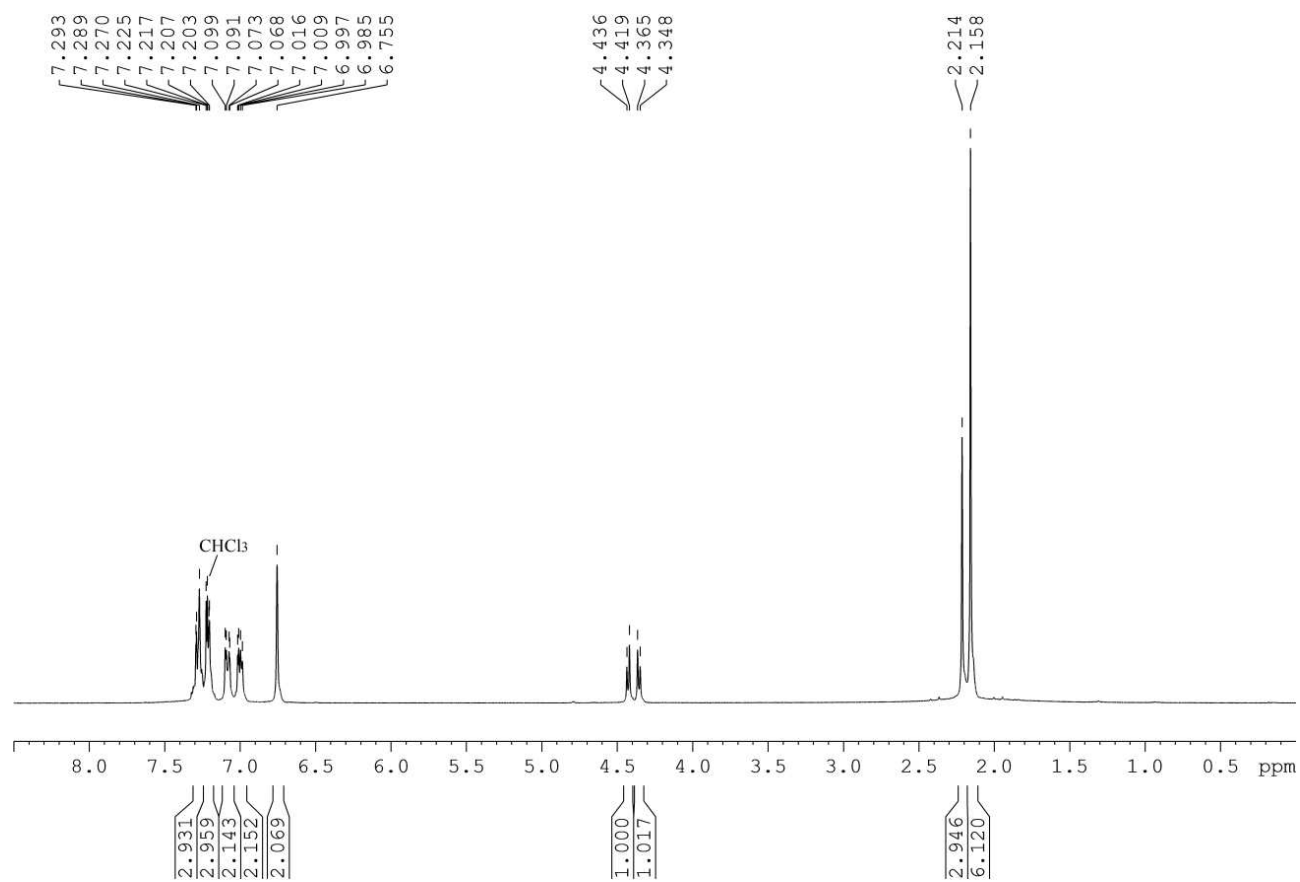
Figure S5.1: ¹H NMR of **50** (CDCl3, 300 MHz)
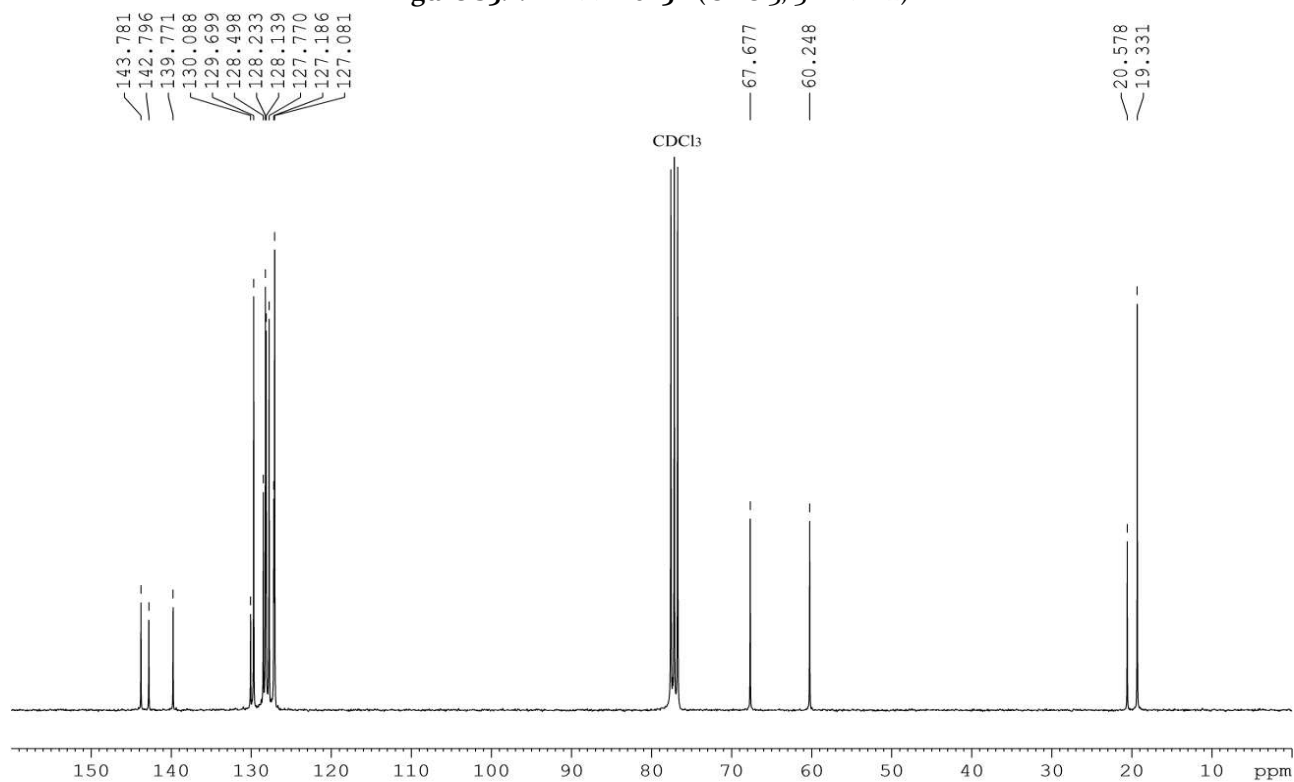
Figure S5.2: ¹³C NMR of **50** (75 MHz, CDCl₃)
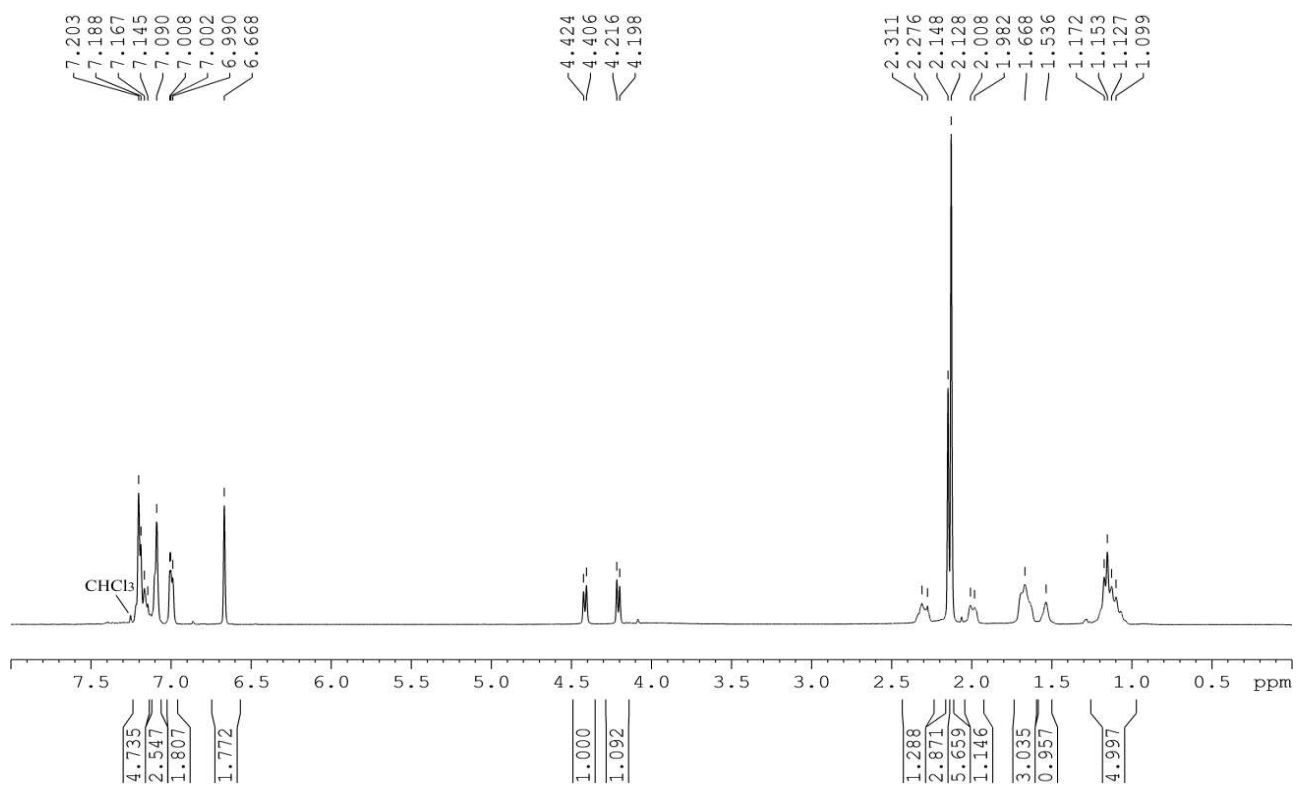
Figure S5.3: ¹HNMR of **53** (400 MHz, CDCl₃)
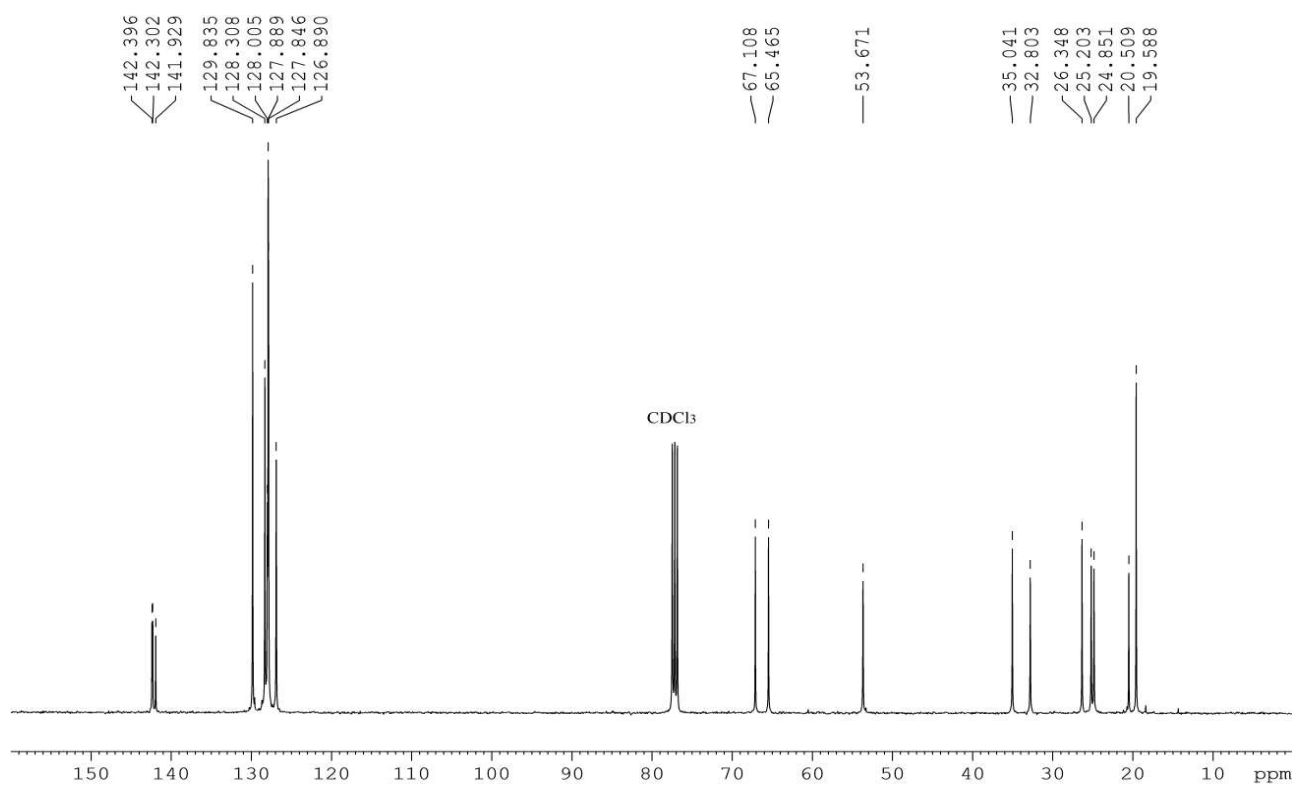
Figure S5.4: ¹³C NMR of **53** (100 MHz, CDCl₃)
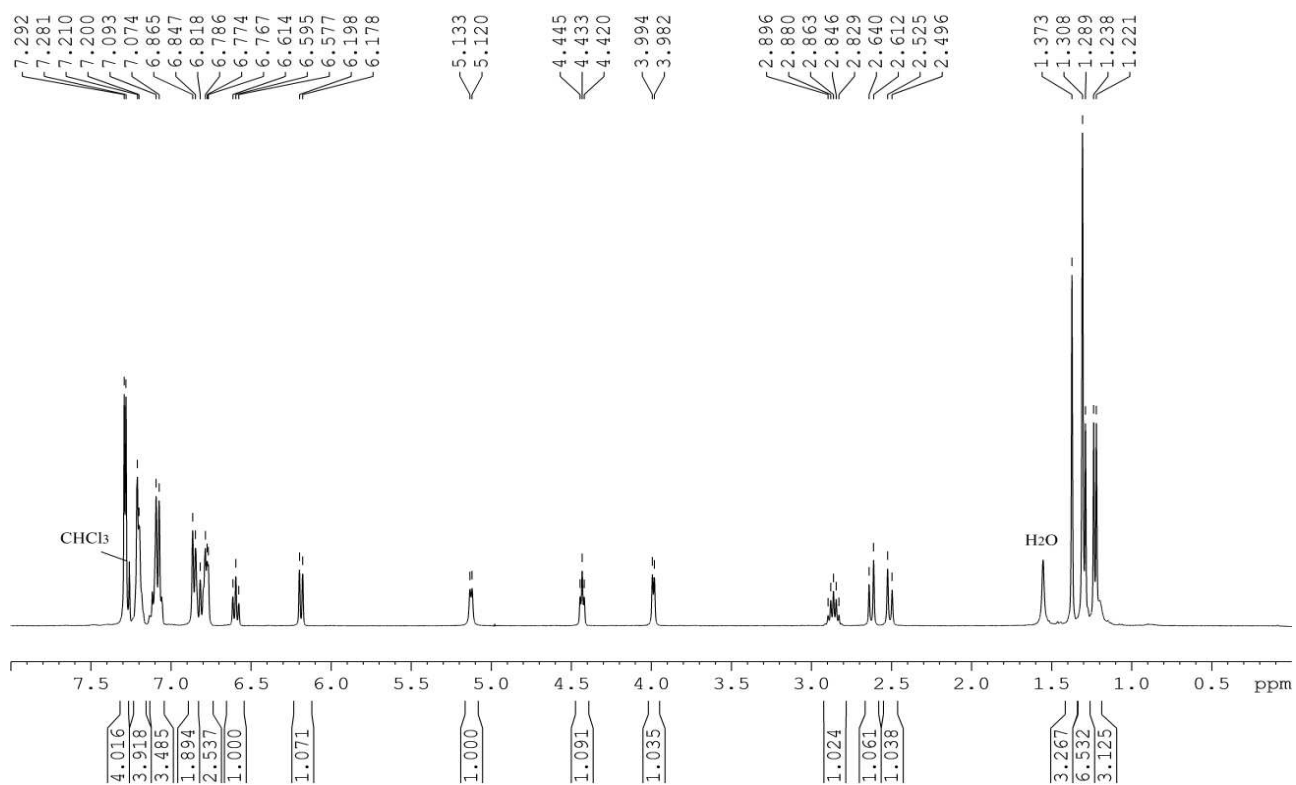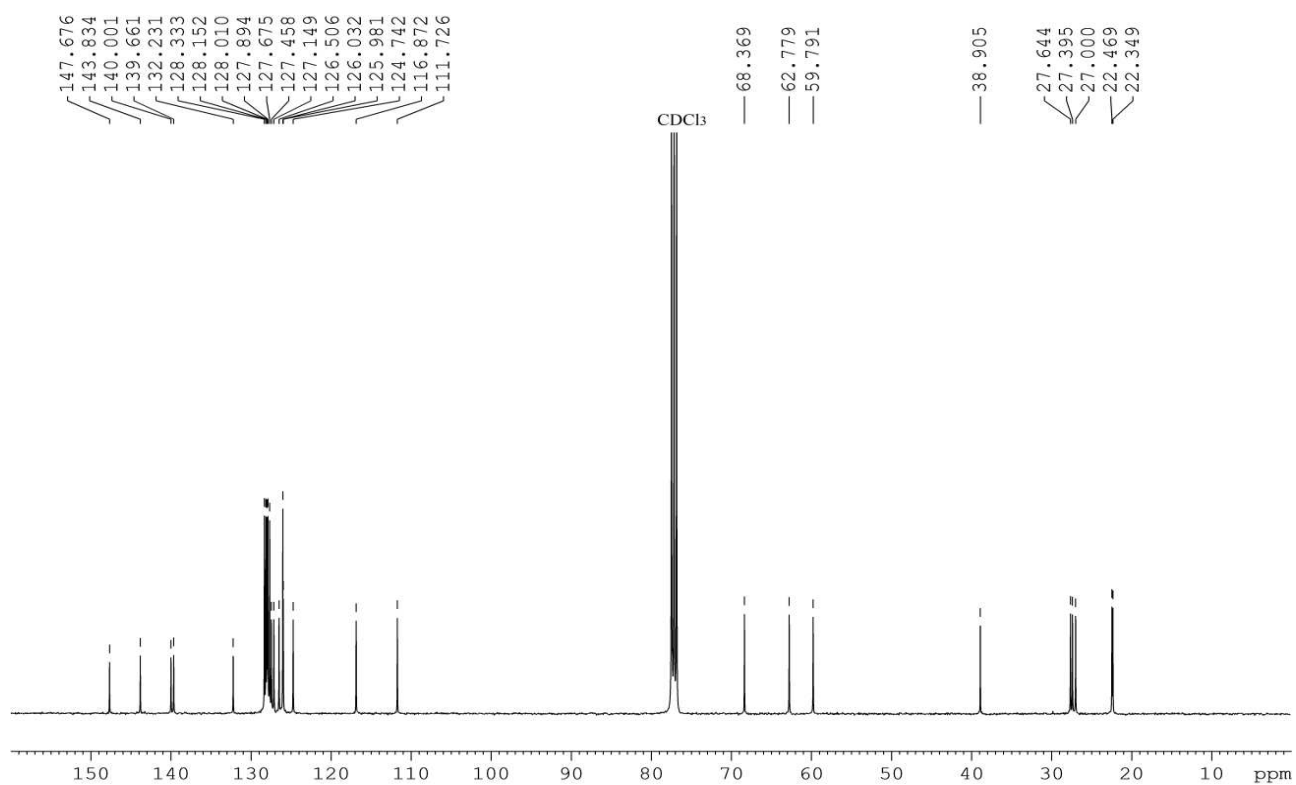
Figure S5.5: ¹HNMR of **42** (300 MHz, CDCl₃)

Figure S5.66: ¹³C NMR of **42** (75 MHz, CDCl₃)

7.306
7.296
7.272
7.260
7.249
7.243
7.223
7.172
7.168
7.147
7.143
6.859
6.854
6.833
6.808
6.803
6.663
6.660
6.638
6.614
6.223
6.197
5.817

4.438
4.415

3.875
3.852

3.252
3.230
3.207
3.185
3.162

2.292
2.254
2.109
2.071

1.434
1.412
1.385
1.363

0.946

CH2Cl2

H2O

9.549
0.990
0.938
0.880
0.981
0.937
1.070
0.999
1.000
1.020
1.012
3.398
3.108
9.368

Figure S5.7: ¹HNMR of **46** (300 MHz, CD₂Cl₂)

144.661
142.422
141.695
133.236
128.568
128.507
128.072
127.530
127.347
126.495
125.044
117.241
111.938

70.360
64.366
60.074

31.808
27.784
27.743
22.974
22.435
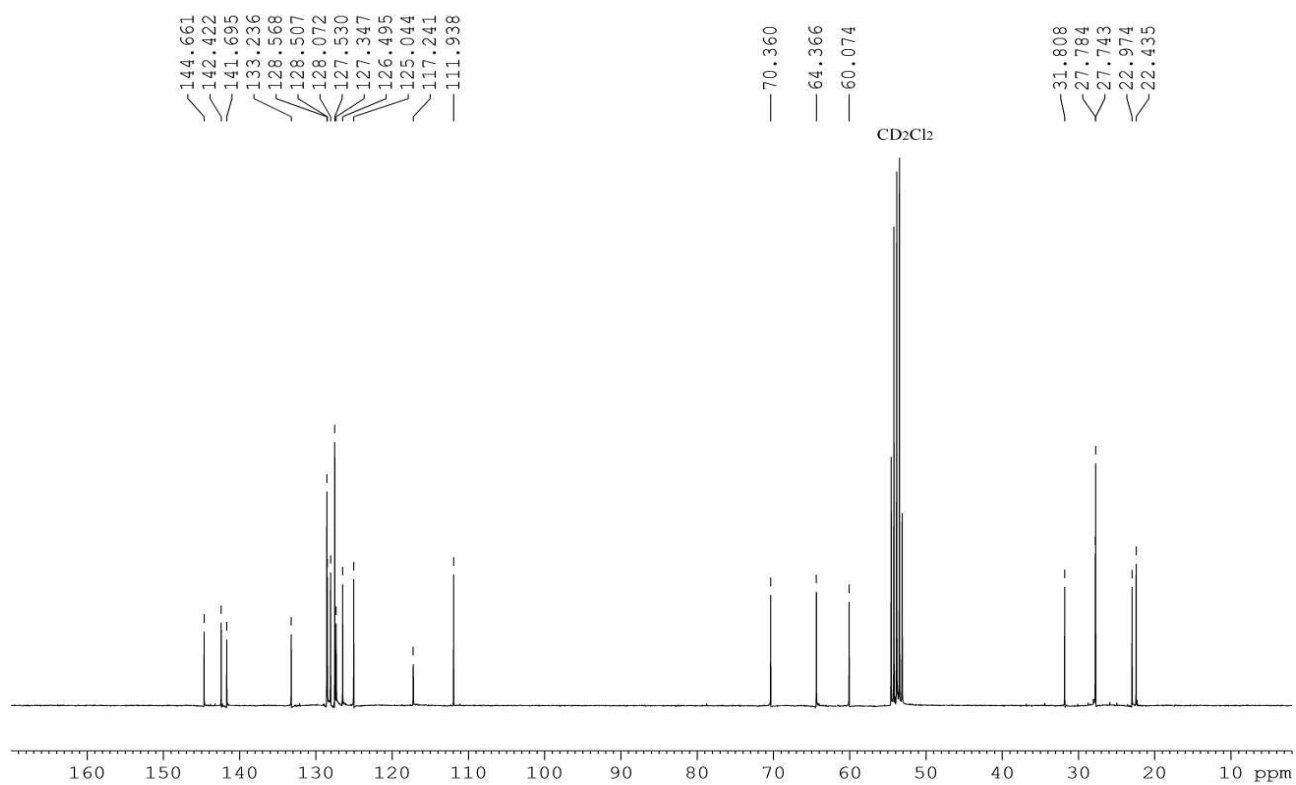
CD2Cl2

Figure S5.8: ¹³C NMR of **46** (75 MHz, CD₂Cl₂)

7.292
7.281
7.210
7.200
7.093
7.074
6.865
6.847
6.818
6.786
6.774
6.767
6.614
6.595
6.577
6.198
6.178

5.133
5.120

4.445
4.433
4.420

3.994
3.982

2.896
2.880
2.863
2.829
2.846
2.640
2.612
2.525
2.496

1.373
1.308
1.289
1.238
1.221

CHCl3

H2O

7.5   7.0   6.5   6.0   5.5   5.0   4.5   4.0   3.5   3.0   2.5   2.0   1.5   1.0   0.5   ppm

4.016
3.918
3.485
1.894
2.537
1.000

1.071

1.000

1.091

1.035

1.024
1.061
1.038

3.267
6.532
3.125

Figure S5.9: ^{1}HNMR of **43** (250 MHz, CDCl$_3$)

147.676
143.834
140.001
139.661
132.231
128.333
128.152
128.010
127.894
127.675
127.458
127.149
126.506
126.032
125.981
124.742
116.872
111.726

68.369

62.779
59.791

38.905

27.644
27.395
27.000
22.469
22.349

CDCl3

150   140   130   120   110   100   90   80   70   60   50   40   30   20   10   ppm

Figure S5.10: ^{13}C NMR of **43** (100 MHz, CDCl$_3$)

7.322
7.305
7.262
7.172
7.134
7.094
7.063
6.826
6.641

6.146
6.126

5.605

4.244

3.774
3.763

3.048
3.035

2.674
2.646
2.493
2.465

1.413
1.411
1.396
1.365
1.353
1.335

CHCl₃

7.749
8.108
0.944
0.895
0.985
1.036
1.045
1.035
1.000
1.072
1.059
12.447
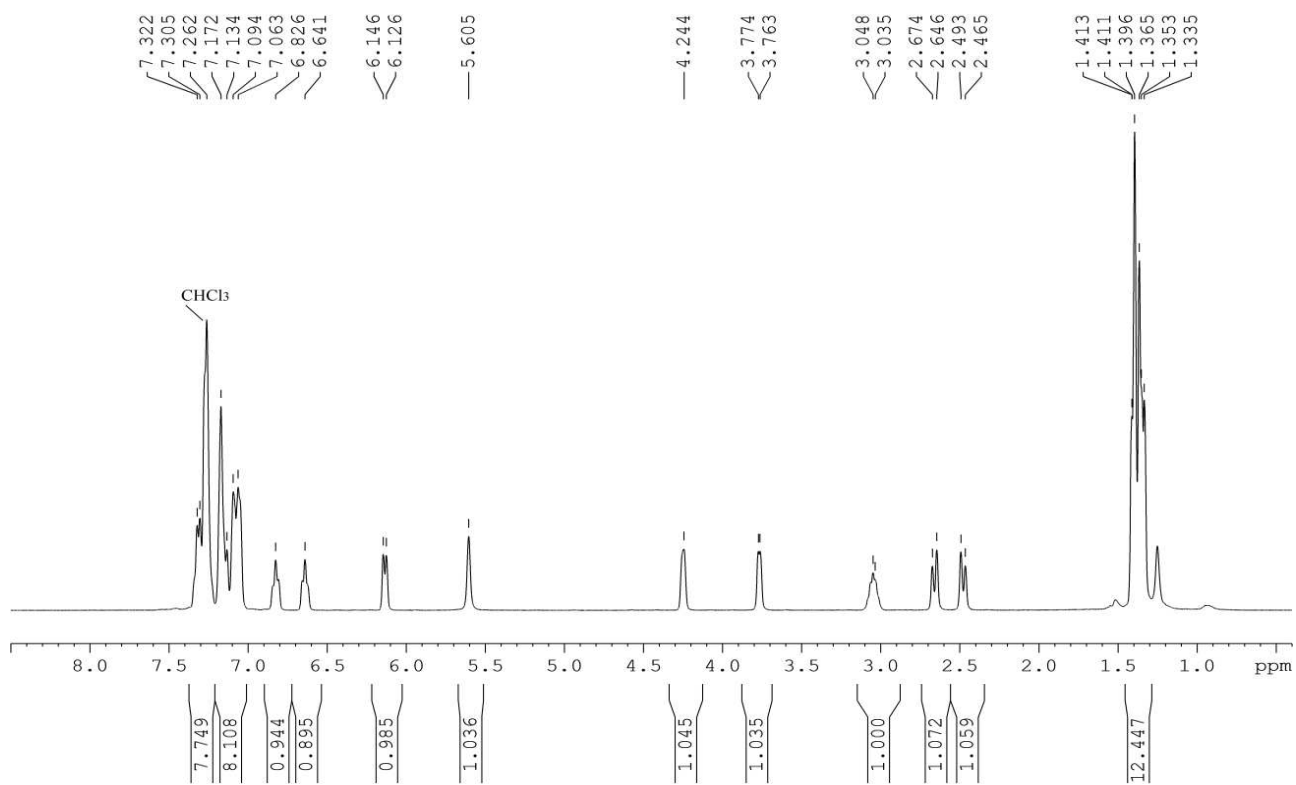
Figure S5.11: ¹HNMR of **47** (300 MHz, CDCl₃)

147.402
144.309
141.842
141.073
132.654
128.387
128.254
127.740
127.349
127.009
126.423
126.000
124.730
116.899
111.855

69.660
64.212
59.766

38.846

27.715
27.570
27.113
22.821
22.429
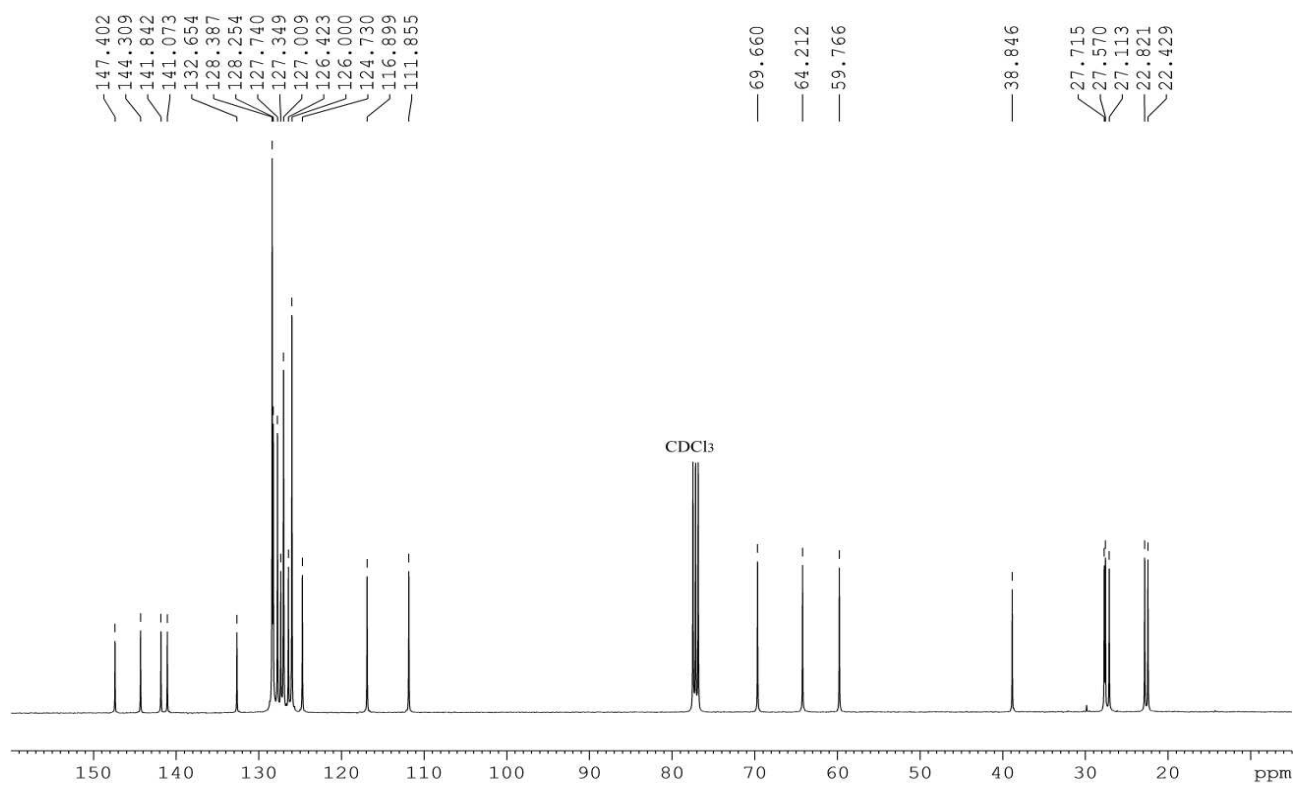
CDCl₃

Figure S5.12: ¹³C NMR of **47** (75 MHz, CDCl₃)

7.263
7.253
7.247
7.158
7.134
6.931
6.918
6.907
6.901
6.829
6.823
6.709

4.907

4.495
4.389
4.375

2.330
2.184
2.177
1.994
1.701
1.679
1.648
1.603
1.384
1.184
1.155
1.126

CHCl₃

2.797
2.727
1.967
1.932
1.843

0.720

1.000
0.977

1.172
8.833
0.976

3.872
0.978

4.510
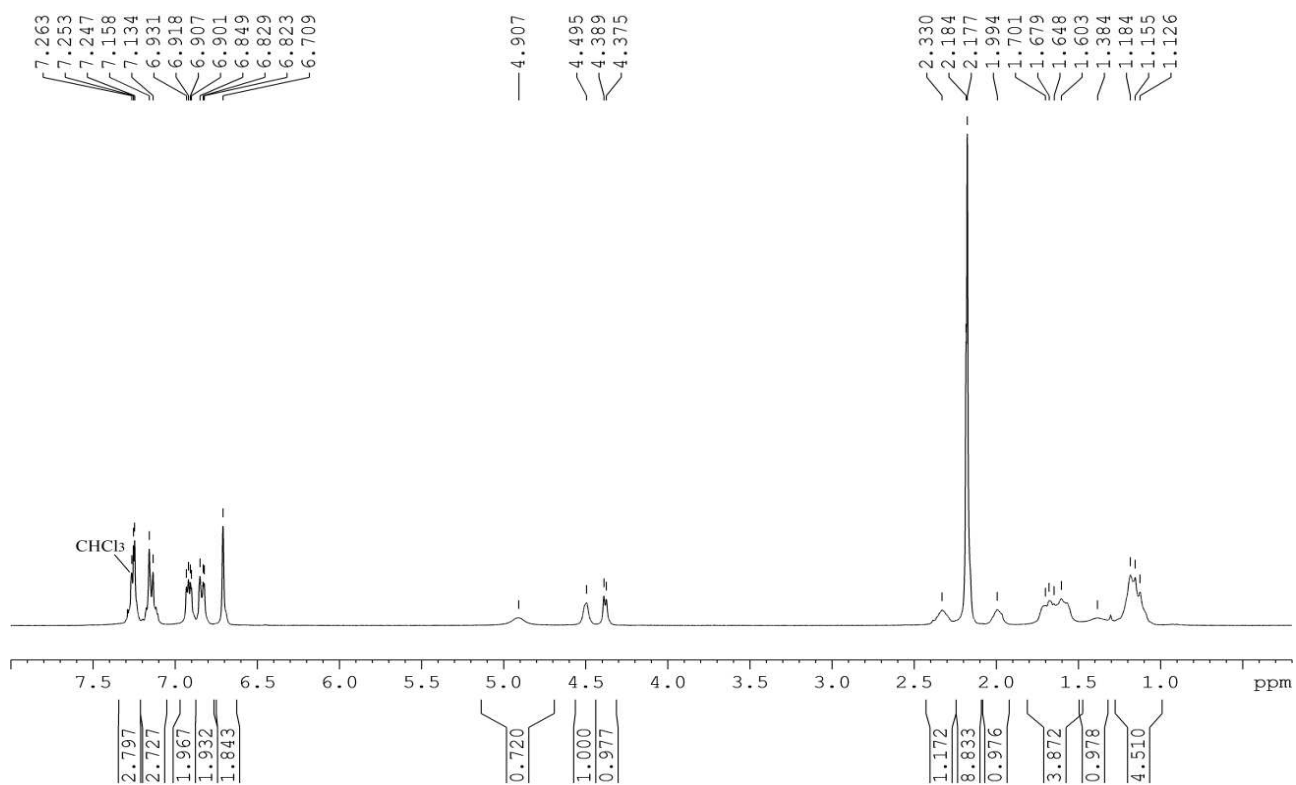
Figure S5.13. ¹HNMR of **51** (300 MHz, CDCl₃)

142.786
141.479
139.674
129.714
129.115
128.427
127.995
127.812
127.522
127.125
127.028
126.905

66.761
63.665

53.162

35.096
33.042
26.278
25.137
24.671
20.506
19.757
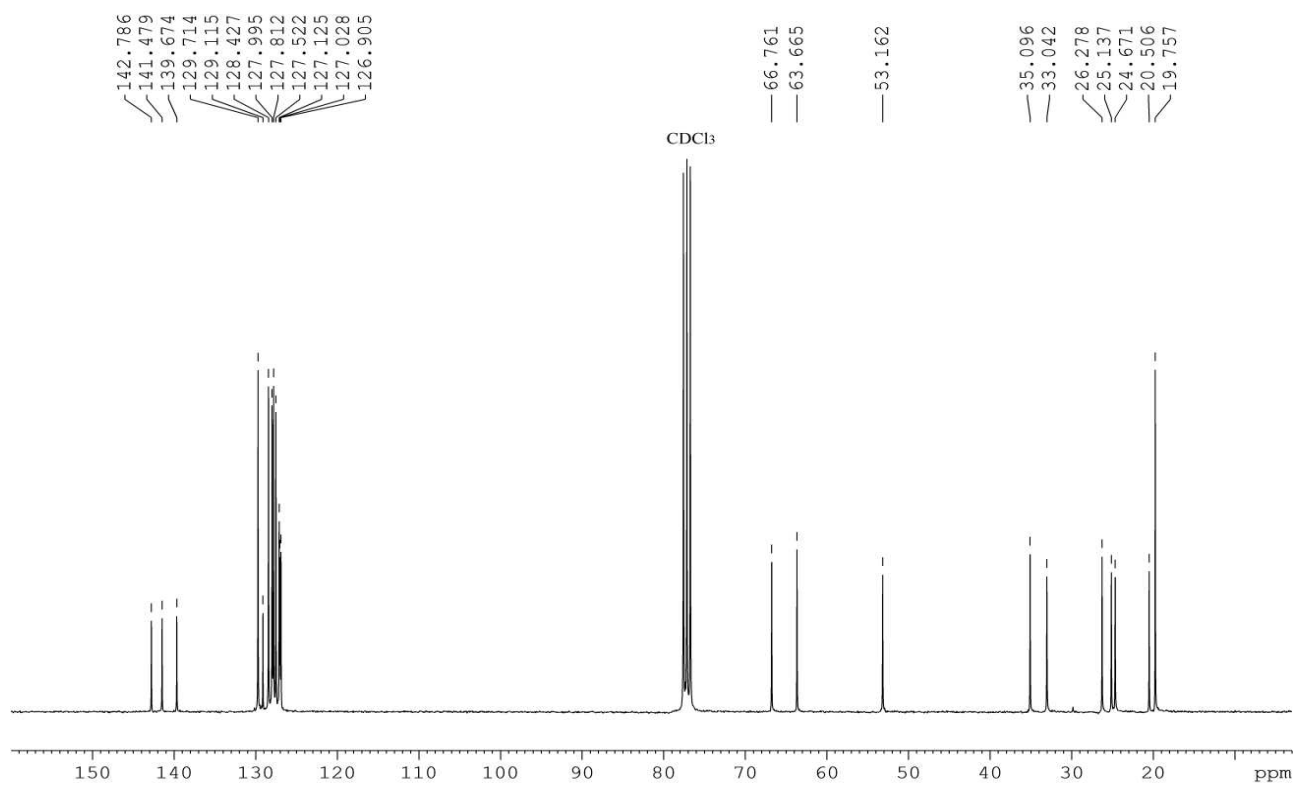
CDCl₃

Figure S14: ¹³C NMR spectrum of **51** (75 MHz, CDCl₃)
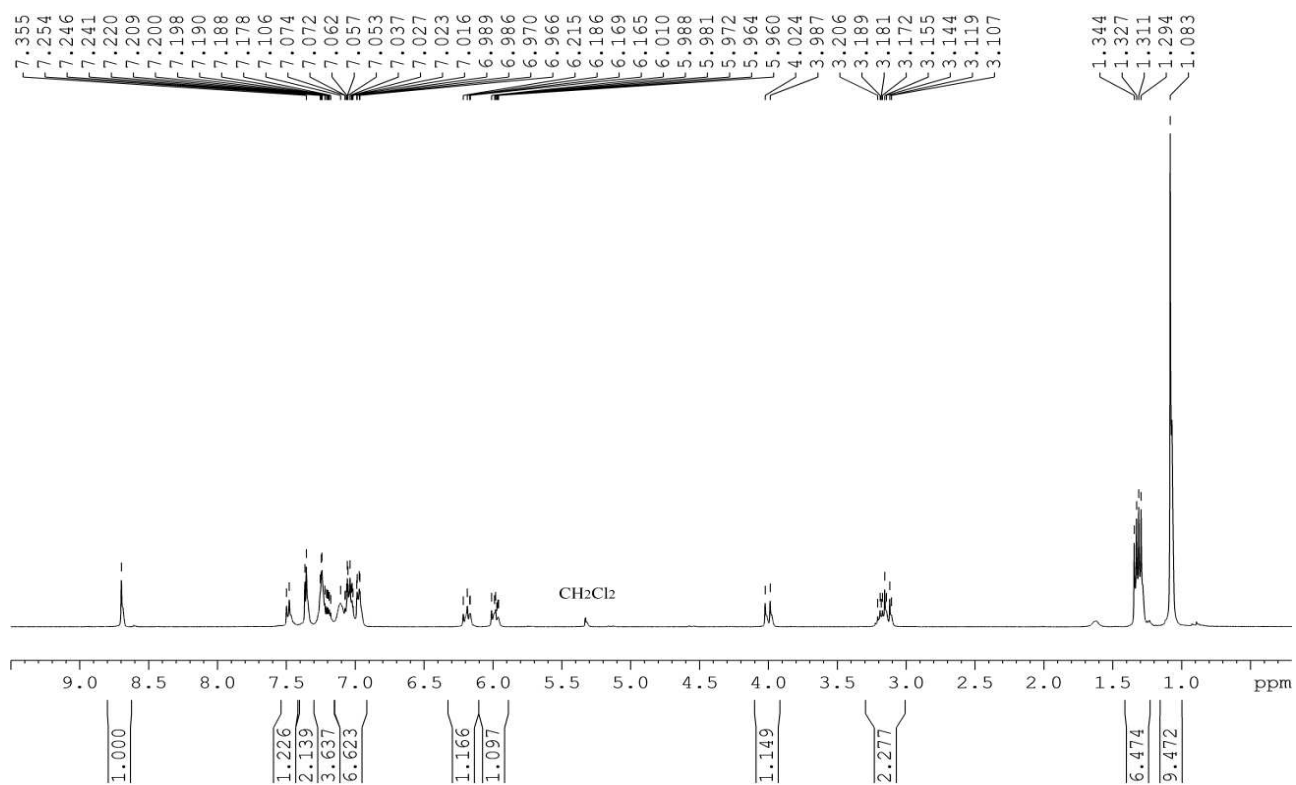
Figure S5.15: ¹HNMR of **44** (400 MHz, CD₂Cl₂)
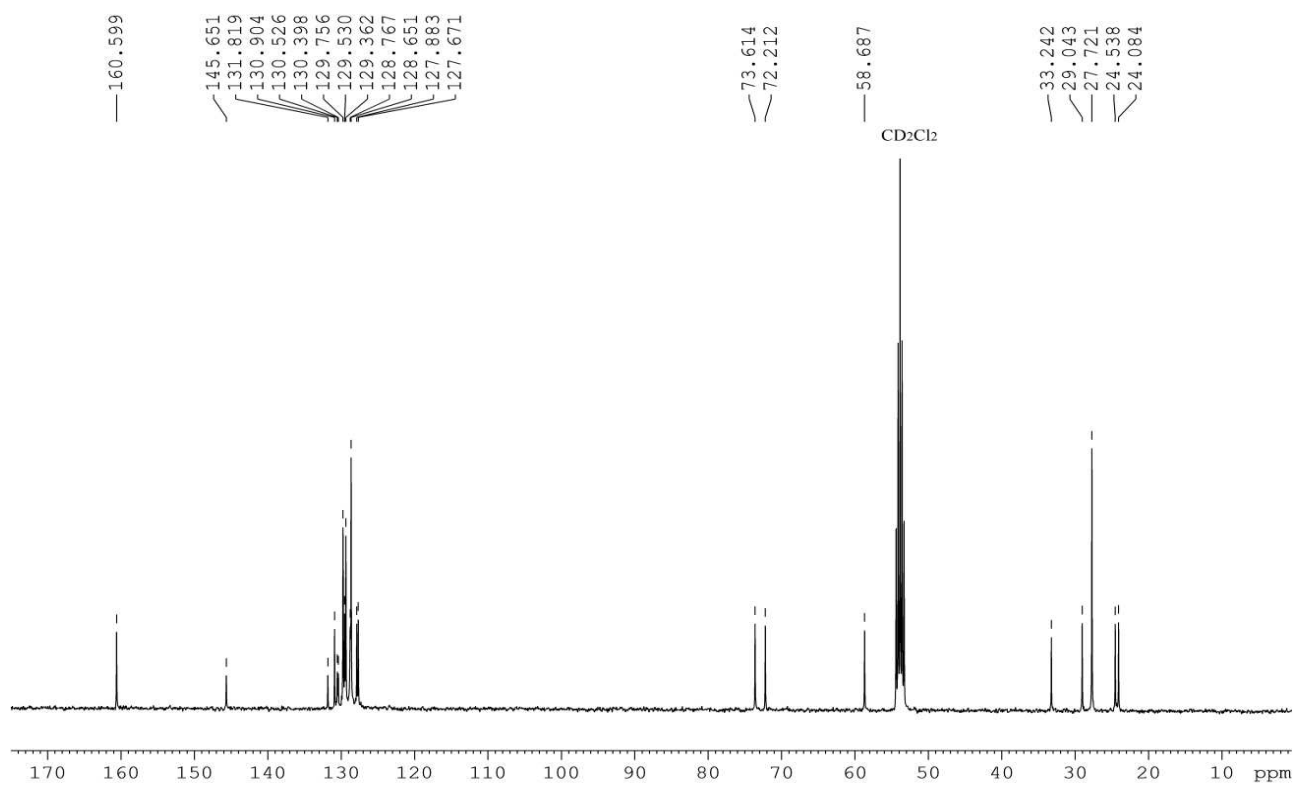
Figure S5.16: ¹³C NMR of **44** (100 MHz, CD₂Cl₂)

8.579

7.576
7.558
7.453
7.430
7.423
7.414
7.379
7.359
7.343
7.253
7.206
7.182

5.535
5.515
5.383
5.363

3.833
3.797

3.077
3.040
2.927

1.240
1.223
1.095
1.031
1.015

CH₂Cl₂

H₂O

| | | | | | | | | | | | | | | | | | |
8.5 8.0 7.5 7.0 6.5 6.0 5.5 5.0 4.5 4.0 3.5 3.0 2.5 2.0 1.5 1.0 0.5 ppm
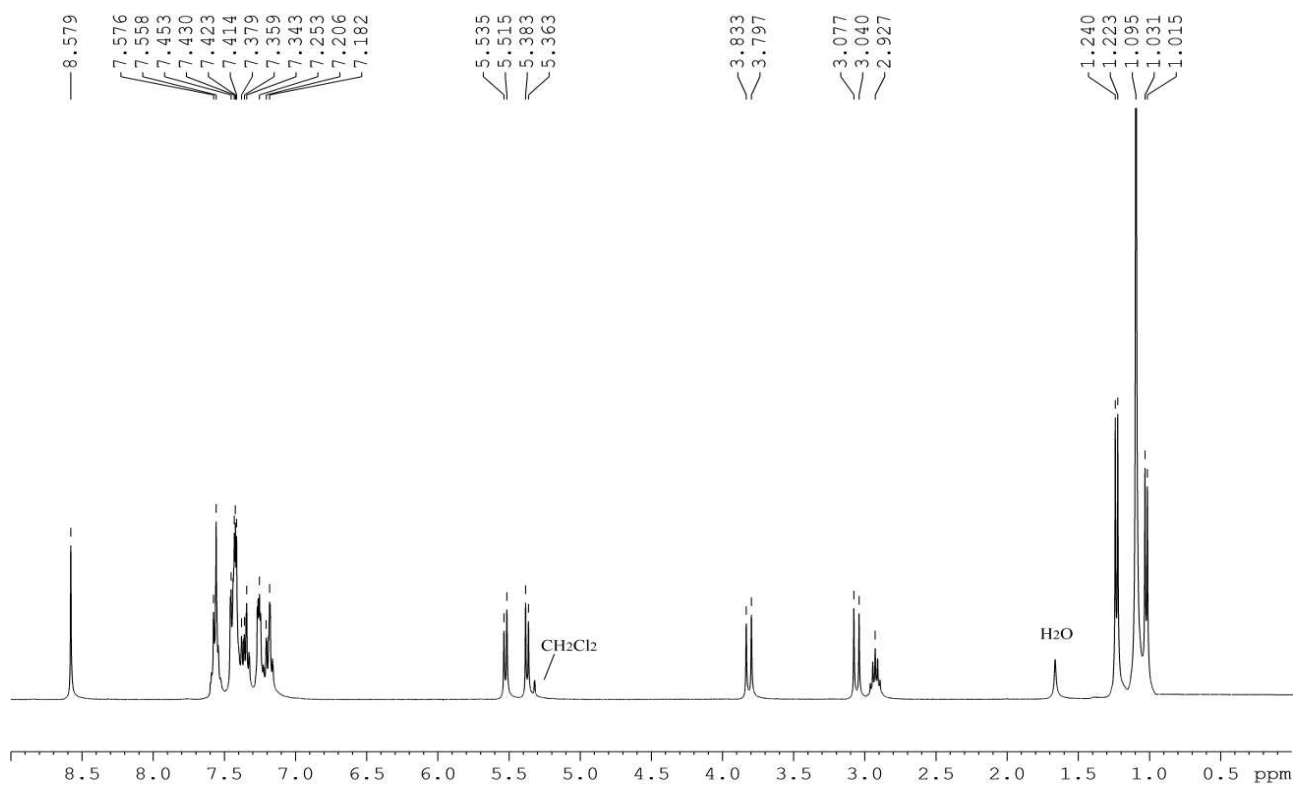
Figure S5.17: ¹H NMR of **48** (400 MHz, CD₂Cl₂)

159.269

145.872
135.120
134.679
131.406
130.994
130.908
130.876
130.667
130.275
130.257
128.203
128.034
128.017
127.754
127.604
127.589
127.045

78.096
75.436

57.616

33.578
28.704
27.961
24.532
23.820

CD₂Cl₂

| | | | | | | | | | | | | | | | |
160 150 140 130 120 110 100 90 80 70 60 50 40 30 20 10 ppm
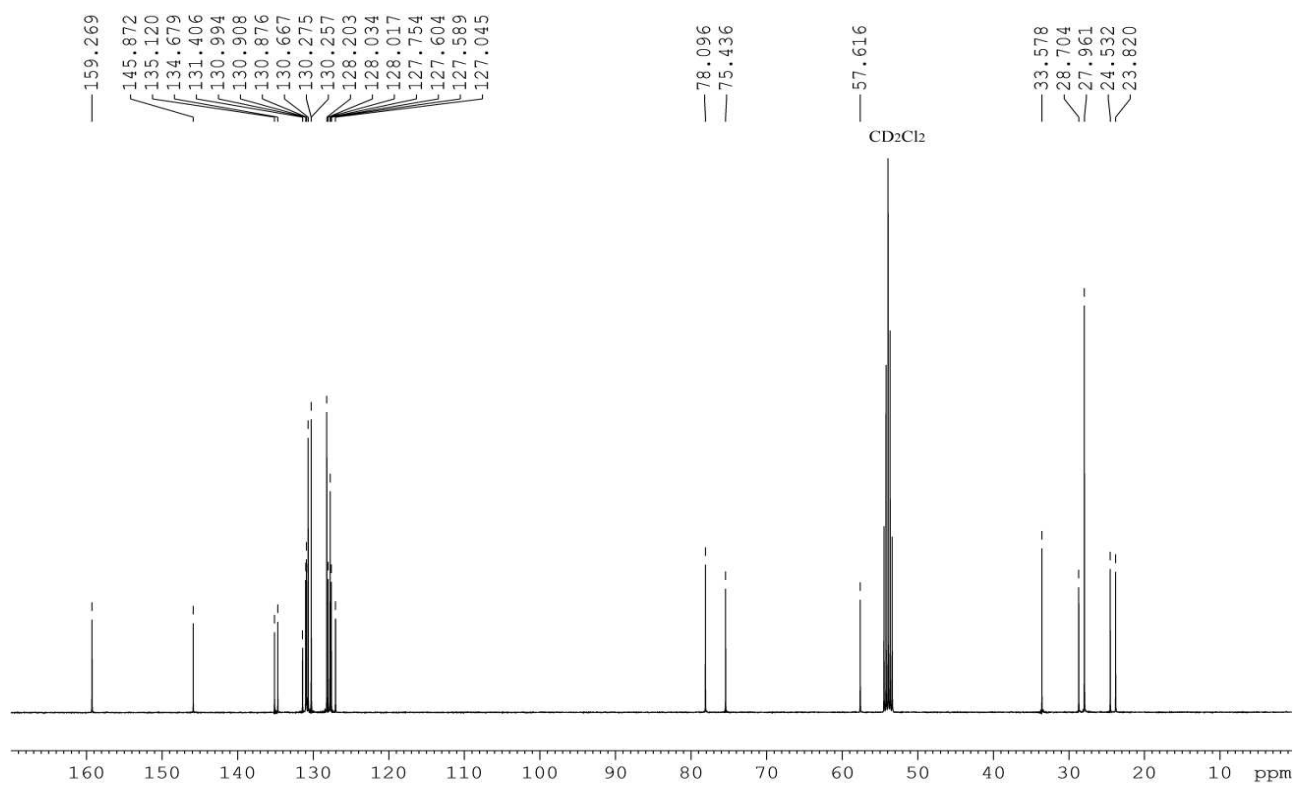
Figure S5.18: ¹³C NMR of **48** (100 MHz, CD₂Cl₂)

153
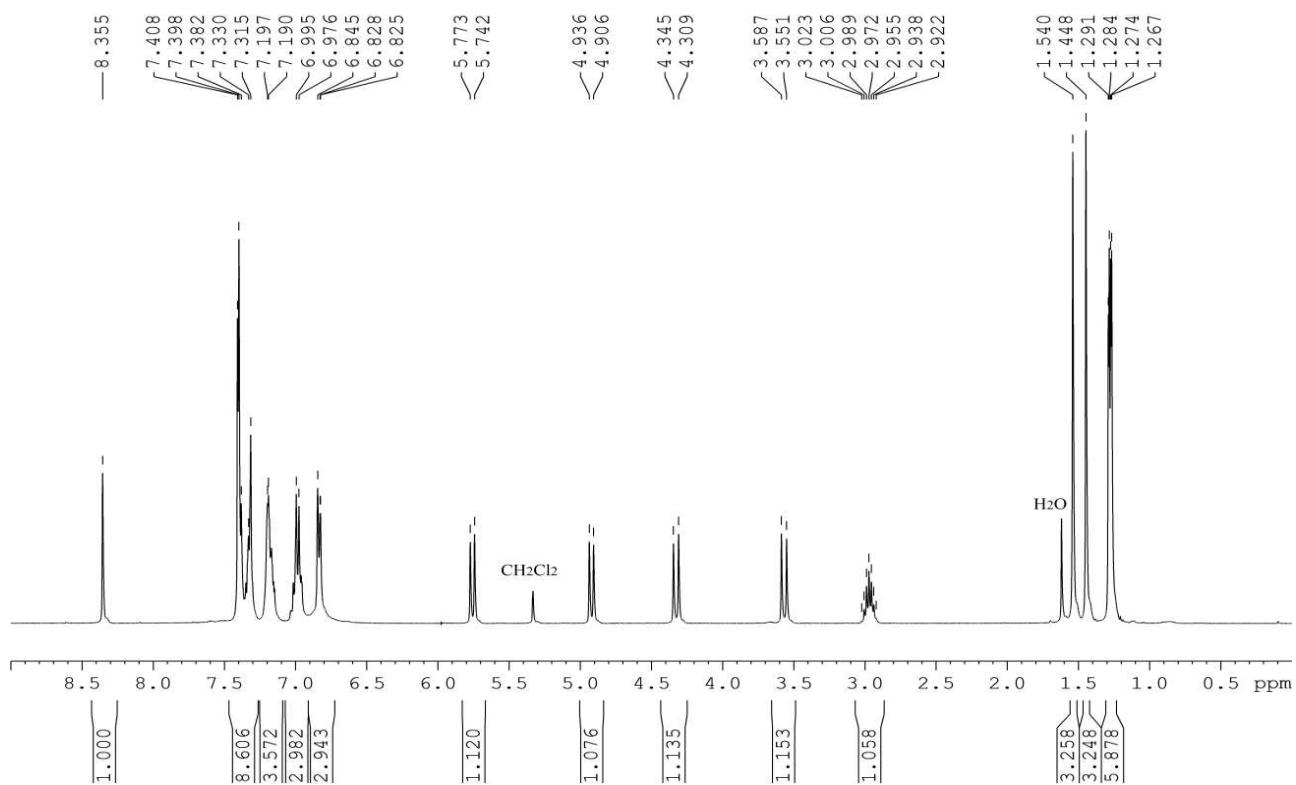
Figure S5.19: ¹HNMR of **45** (400 MHz, CD₂Cl₂)
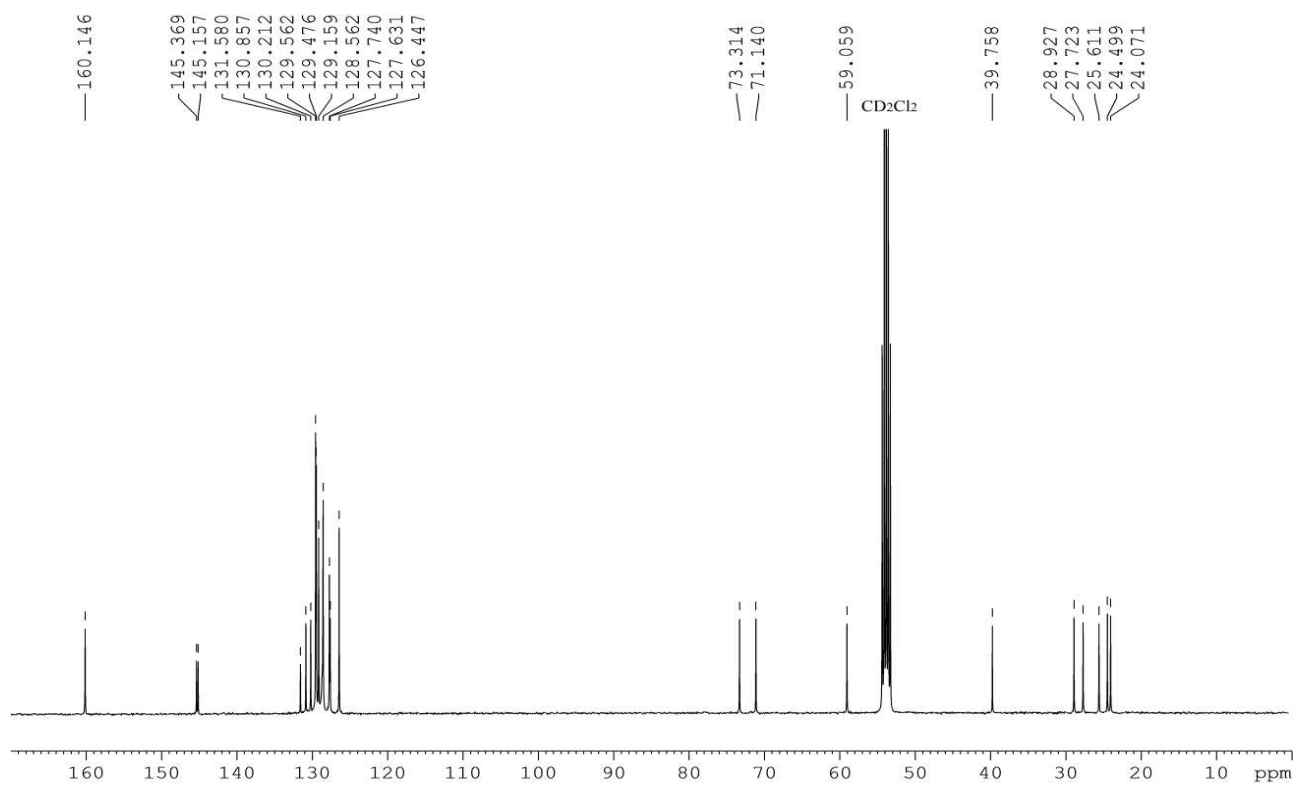
Figure S5.20: ¹³C NMR of **45** (100 MHz, CD₂Cl₂)
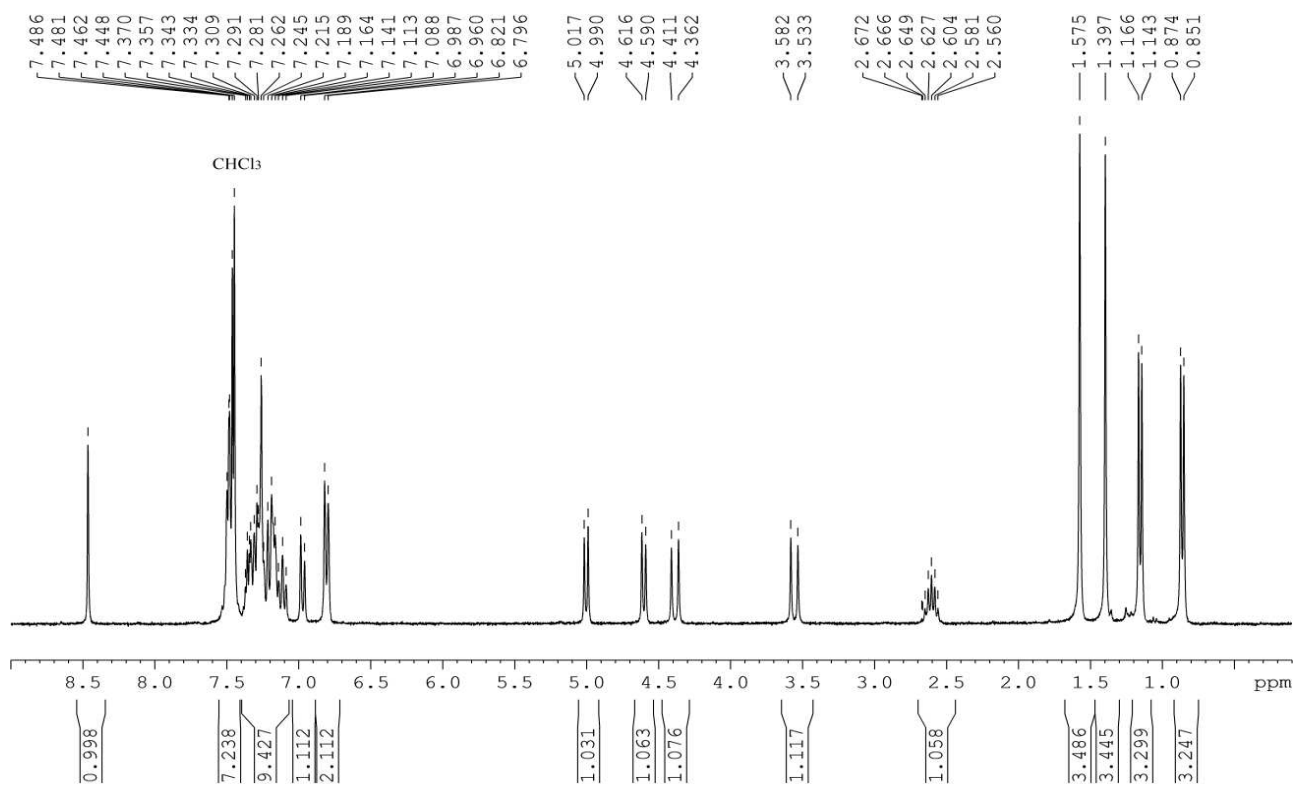
Figure S5.21: ^{1}HNMR of **49** (300 MHz, CDCl$_3$)
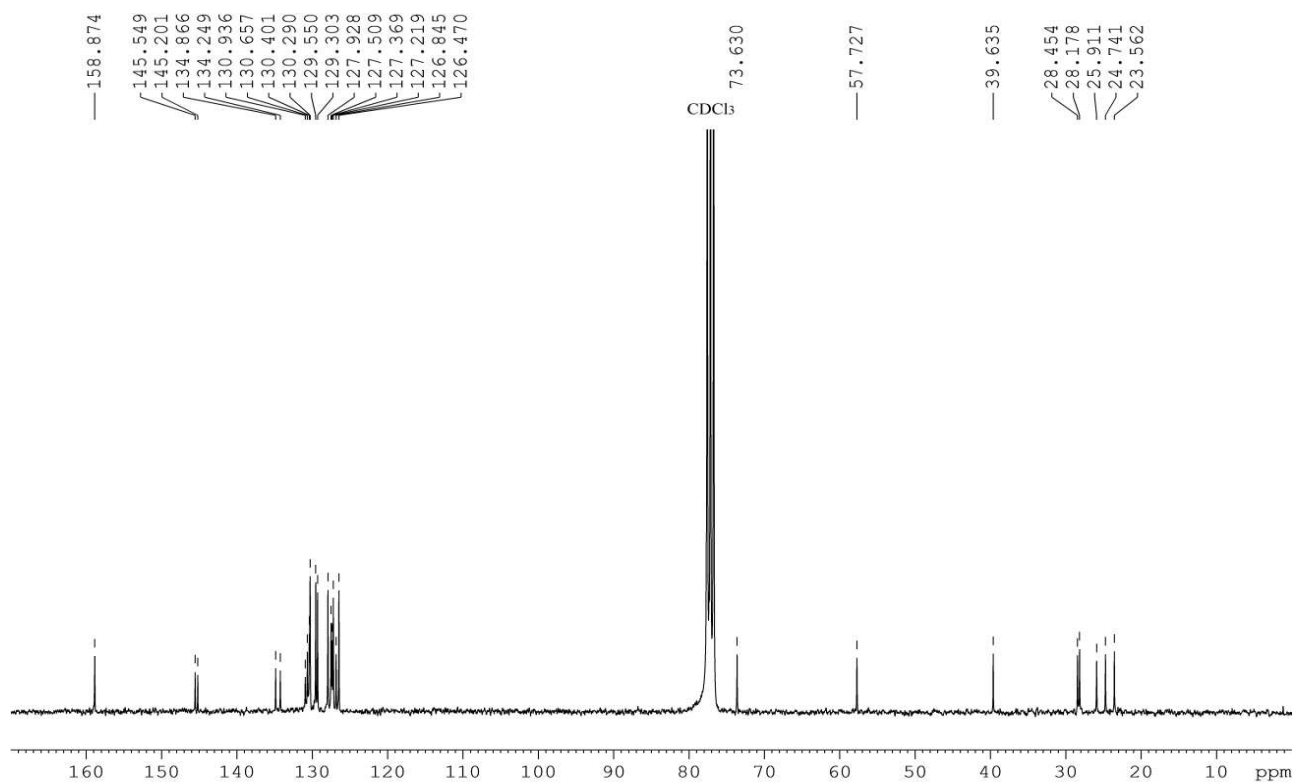
Figure S5.22: ^{13}C NMR of **49** (100 MHz, CDCl$_3$)
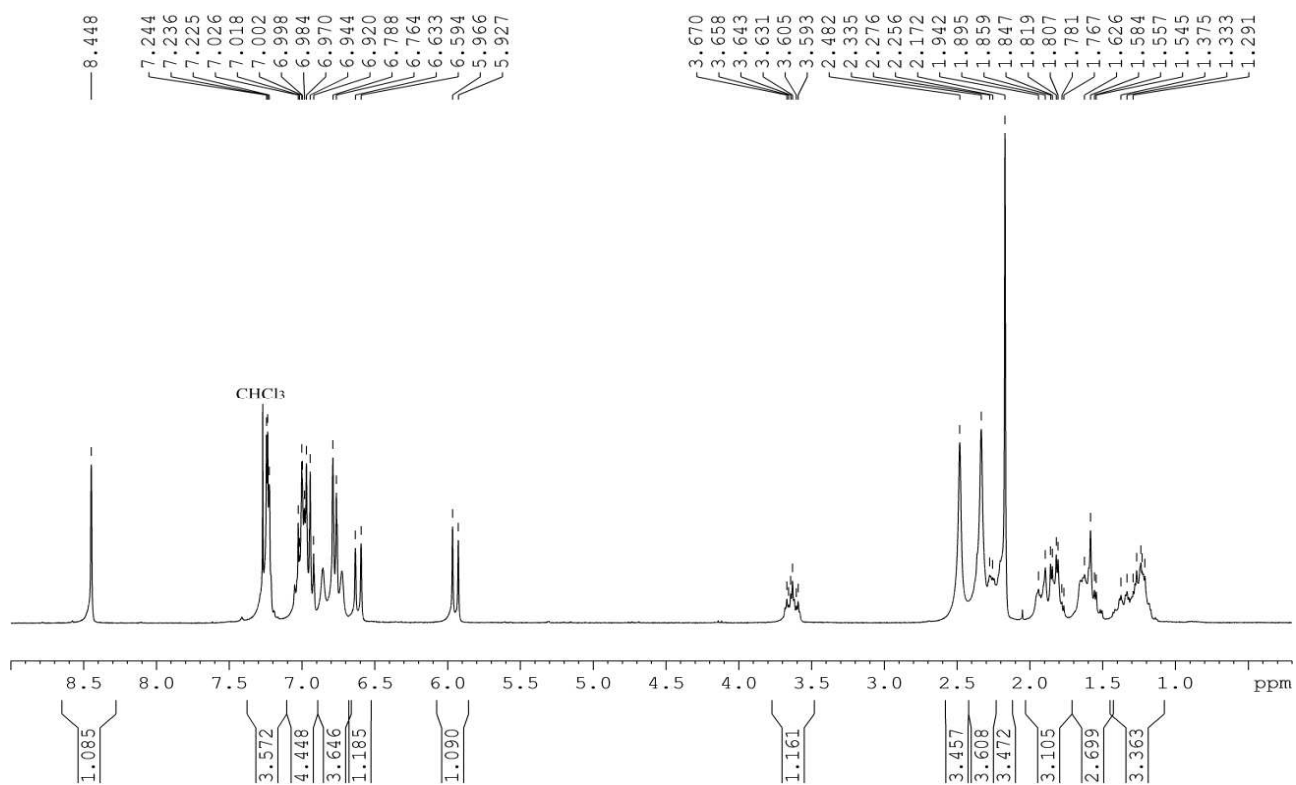
Figure S5.23: ¹HNMR of **52** (300 MHz, CDCl₃)
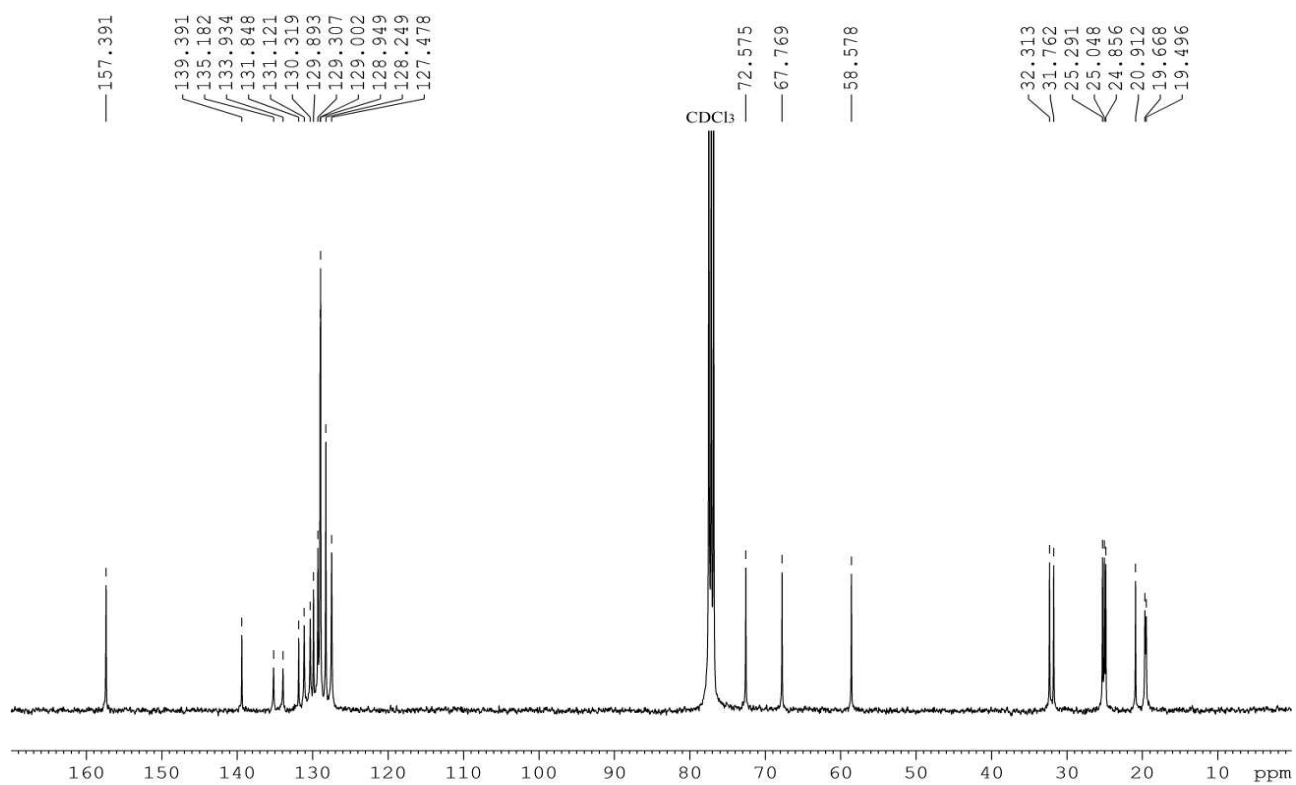
Figure S5.24: ¹³C NMR of **52** (100 MHz, CDCl₃)

Figure S5.25: ¹HNMR of **54** (300 MHz, CDCl₃)
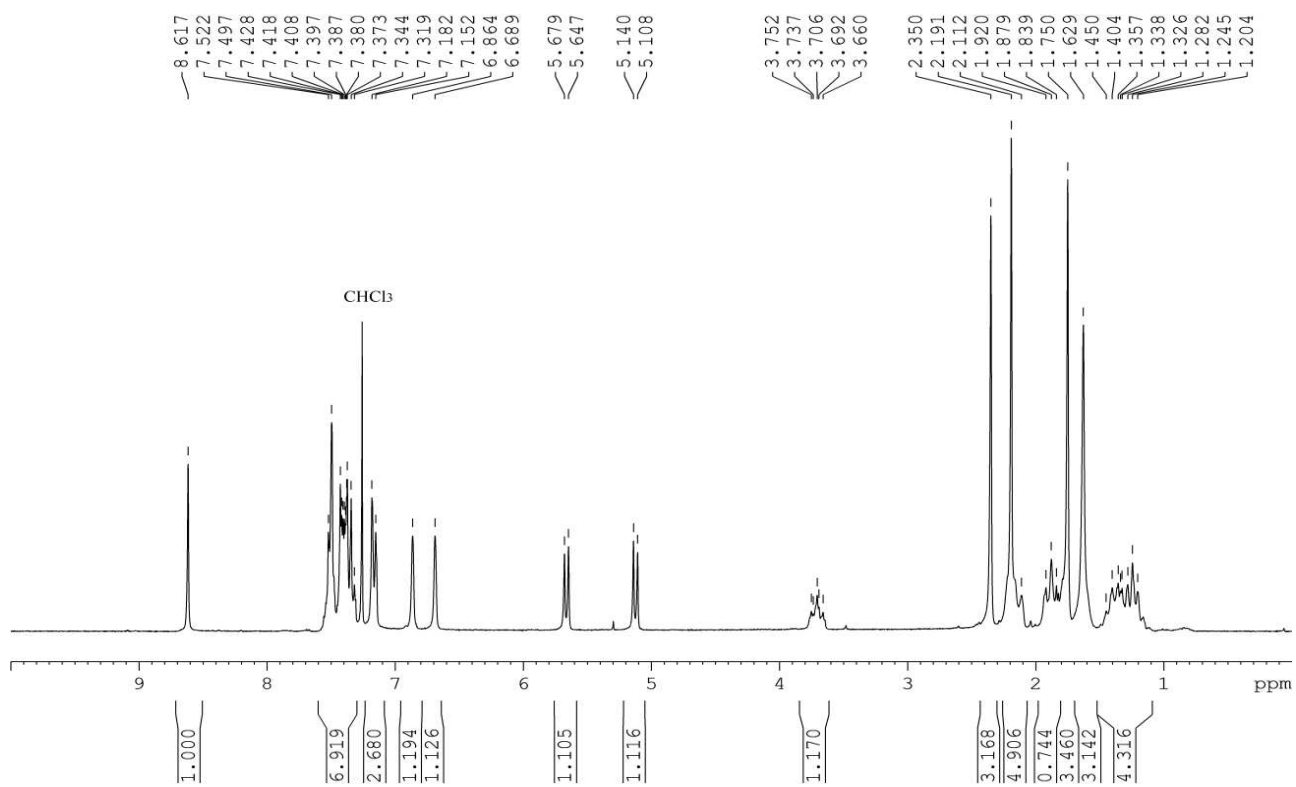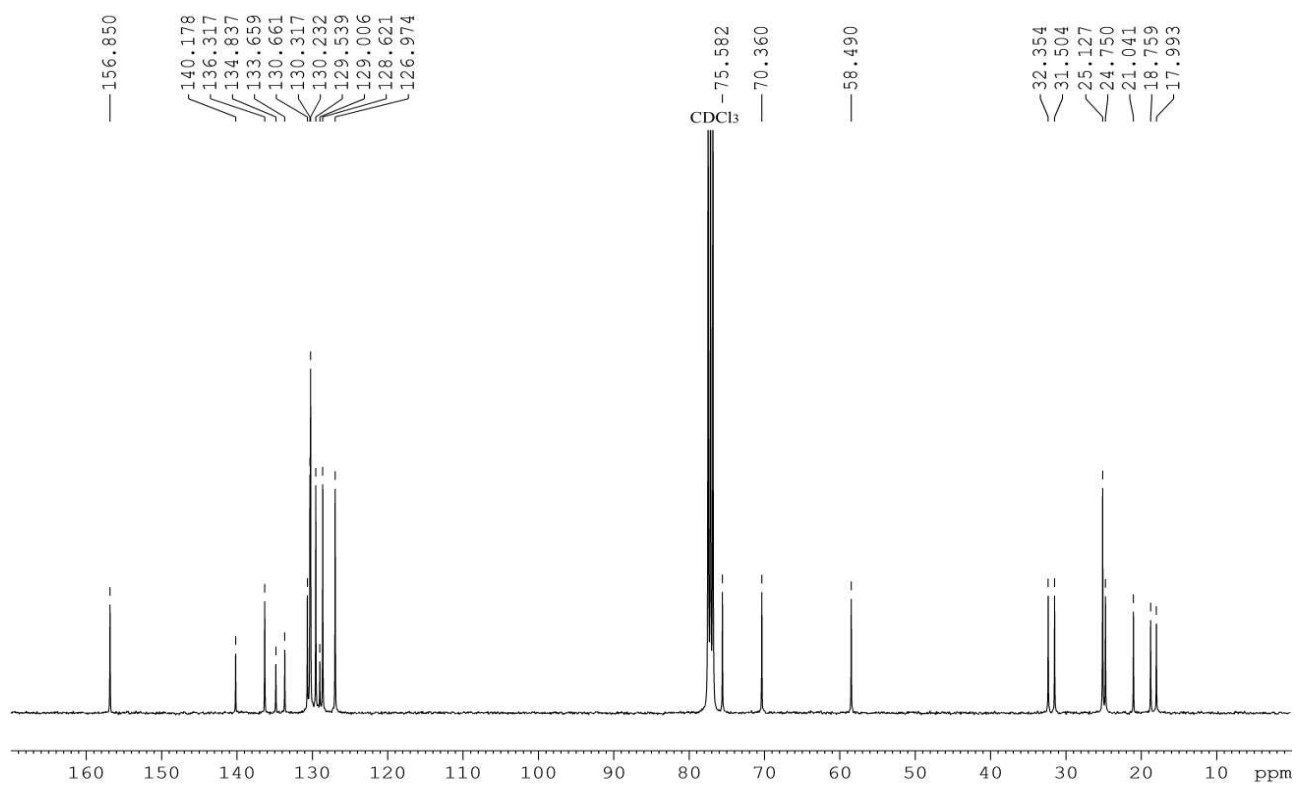

Figure S5.26: ¹³C NMR of **54** (100 MHz, CDCl₃)
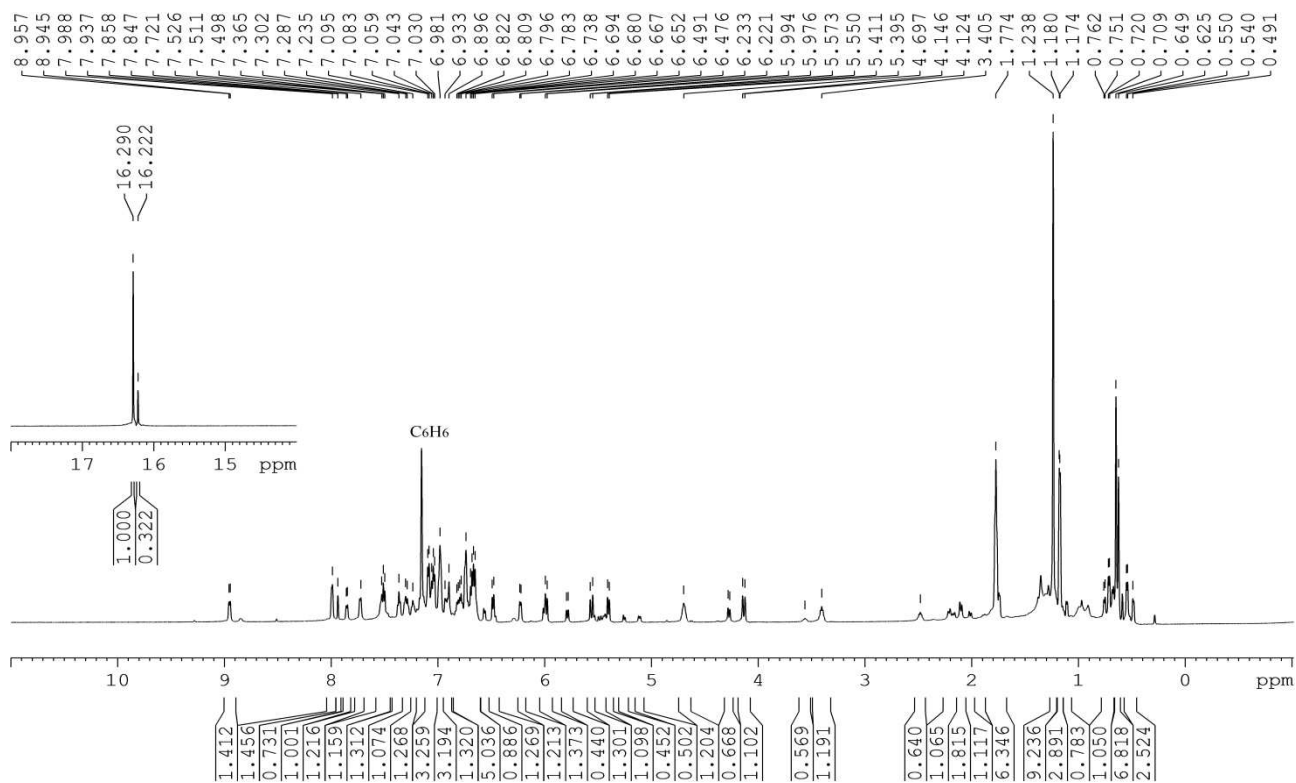
Figure S5.27: ¹HNMR spectrum of **36** (600 MHz, C₆D₆)
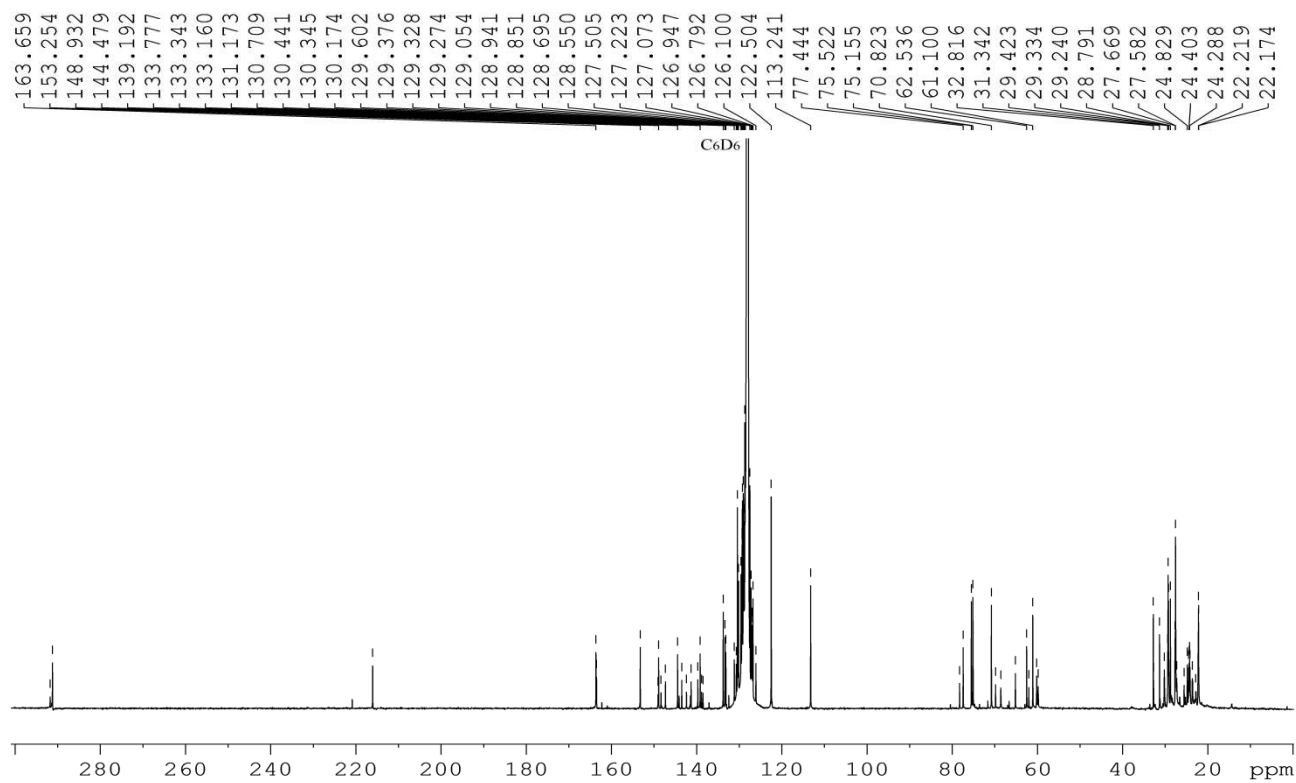
Figure S5.28: ¹³C NMR of **36** (125 MHz, C₆D₆)
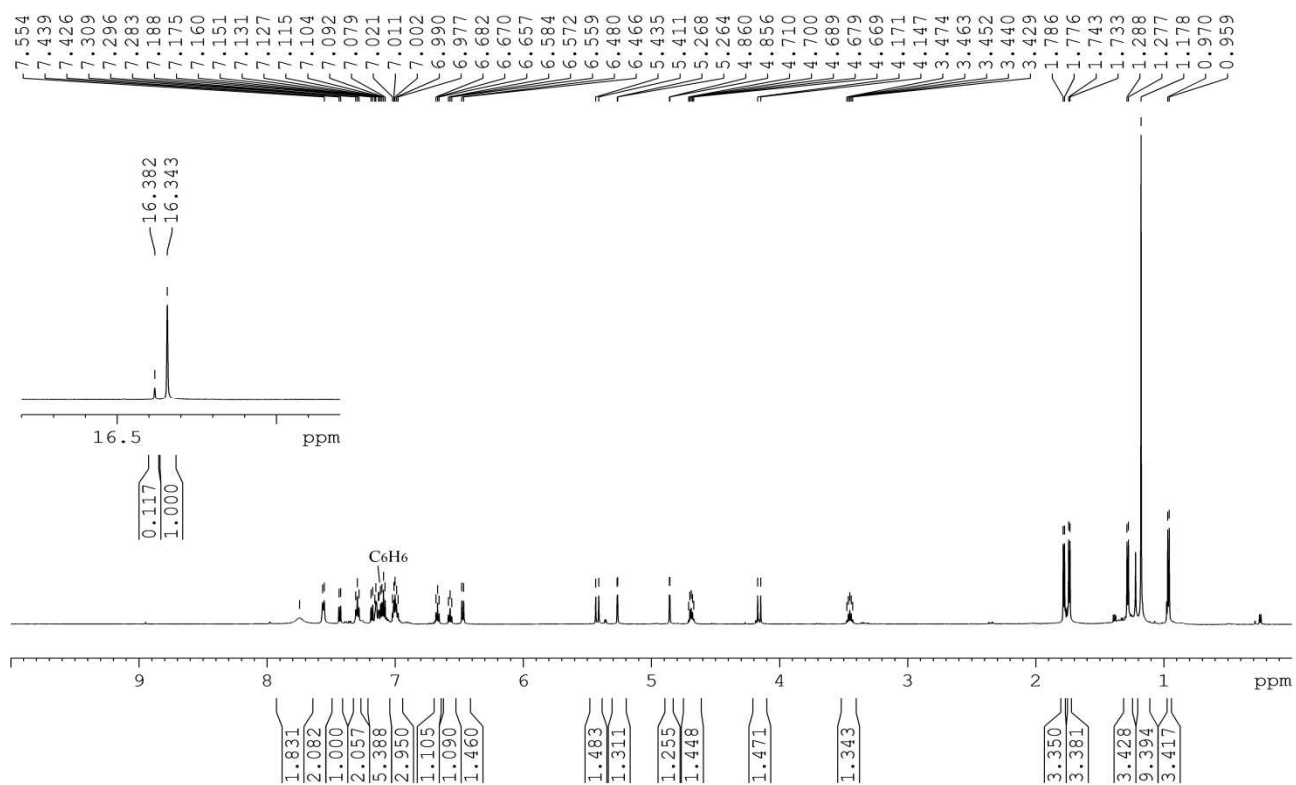
Figure S5.29: ¹HNMR of **37** (600 MHz, C₆D₆)
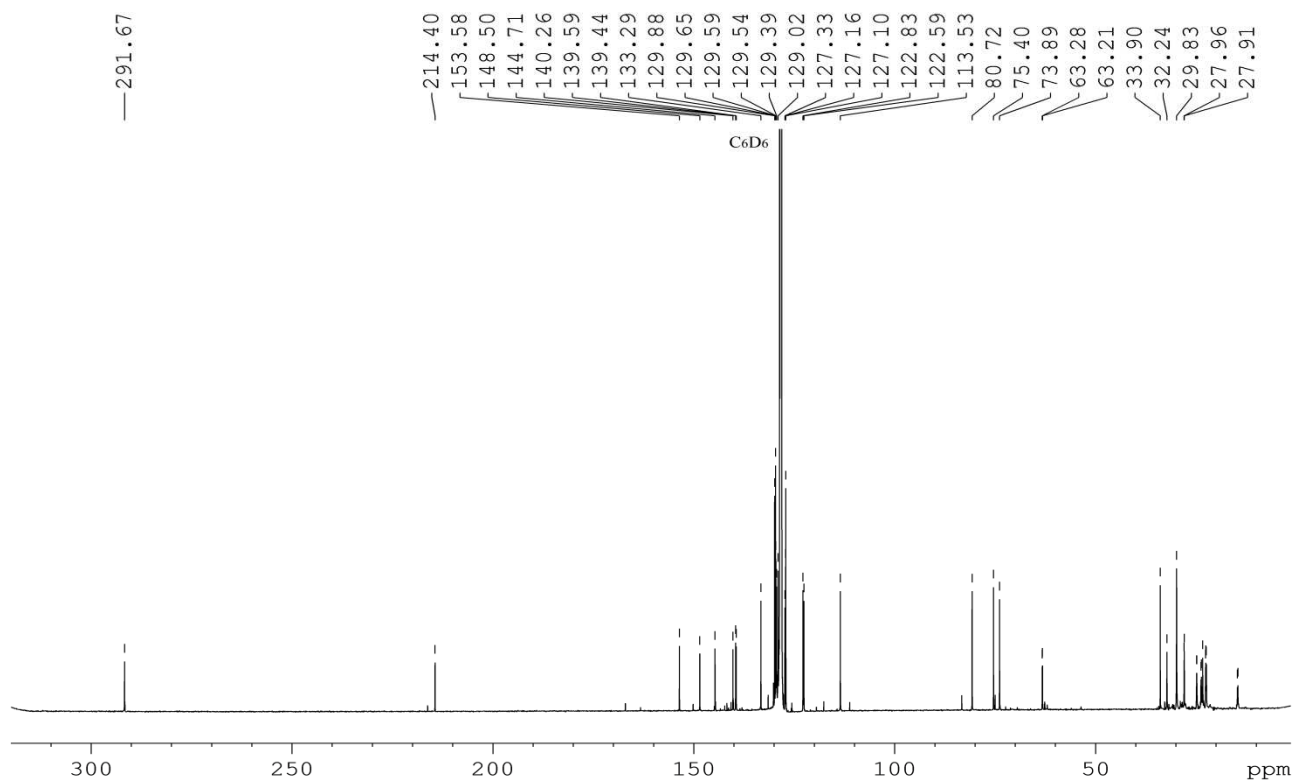
Figure S5.30: ¹³C NMR of **37** (125 MHz, C₆D₆)
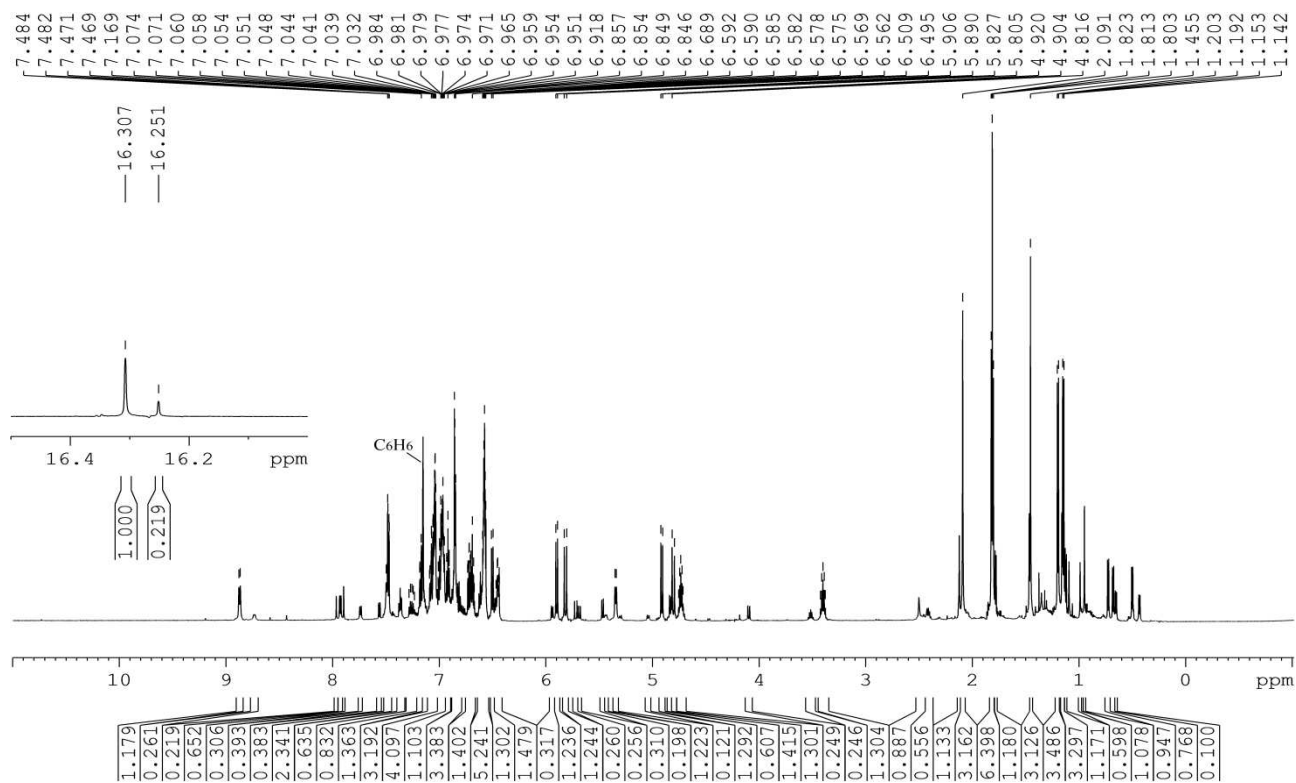
Figure S5.31: ¹HNMR of **38** (600 MHz, C₆D₆)
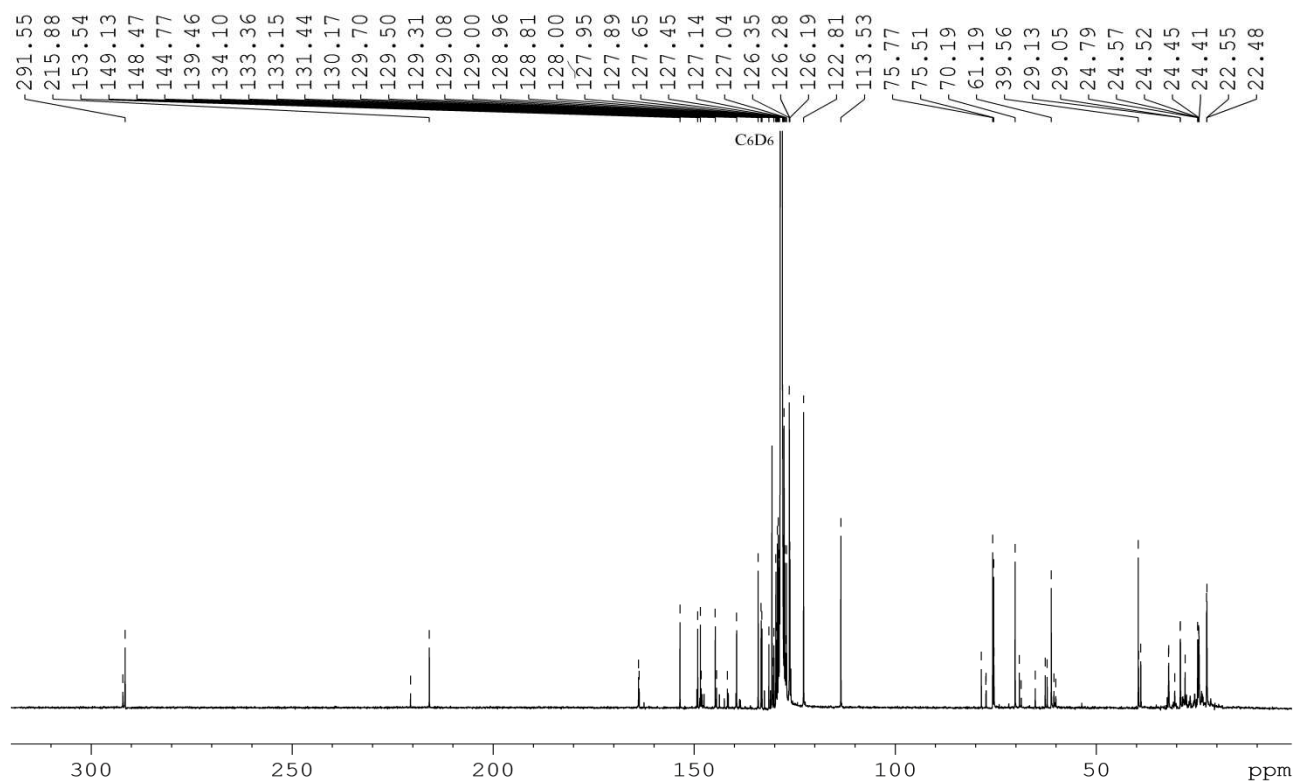
Figure S5.32: ¹³C NMR spectrum of **38** (125 MHz, C₆D₆)
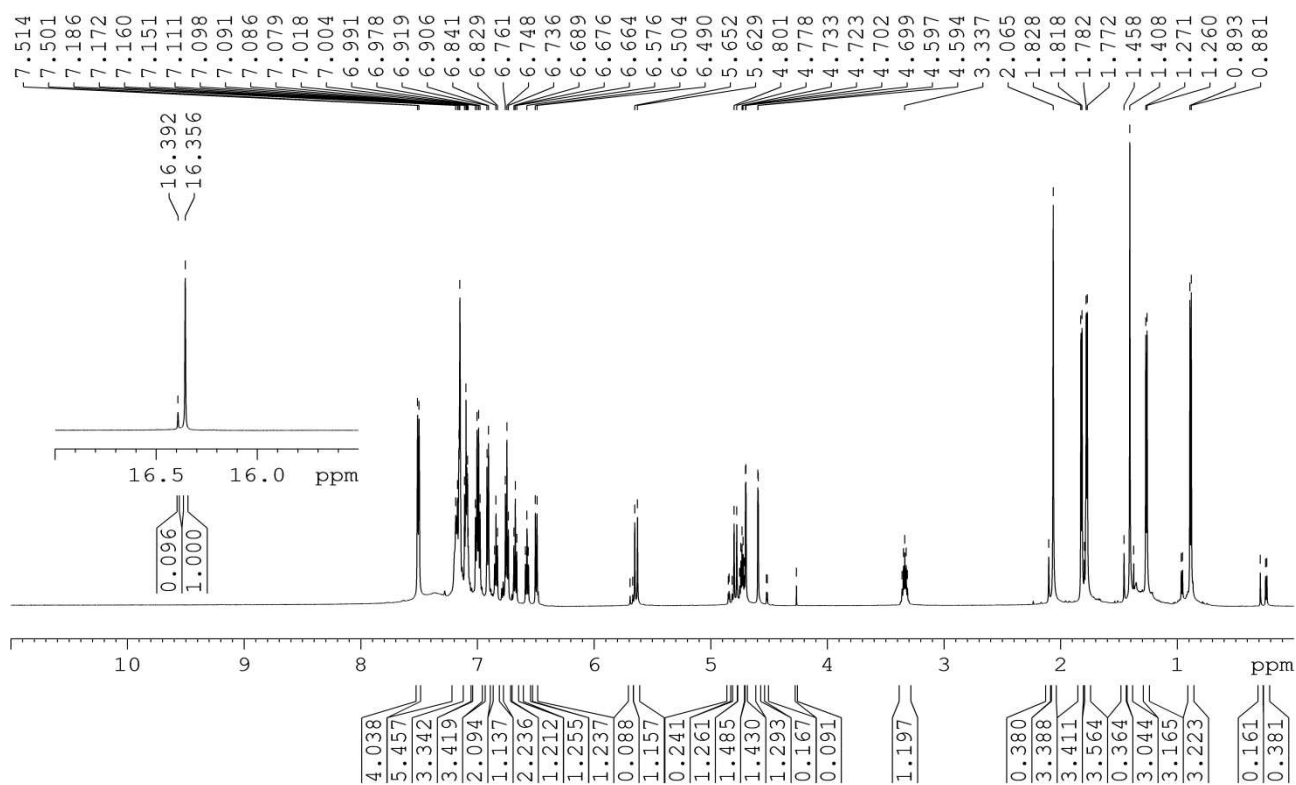
Figure S5.33: ¹HNMR of **39** (600 MHz, C₆D₆)
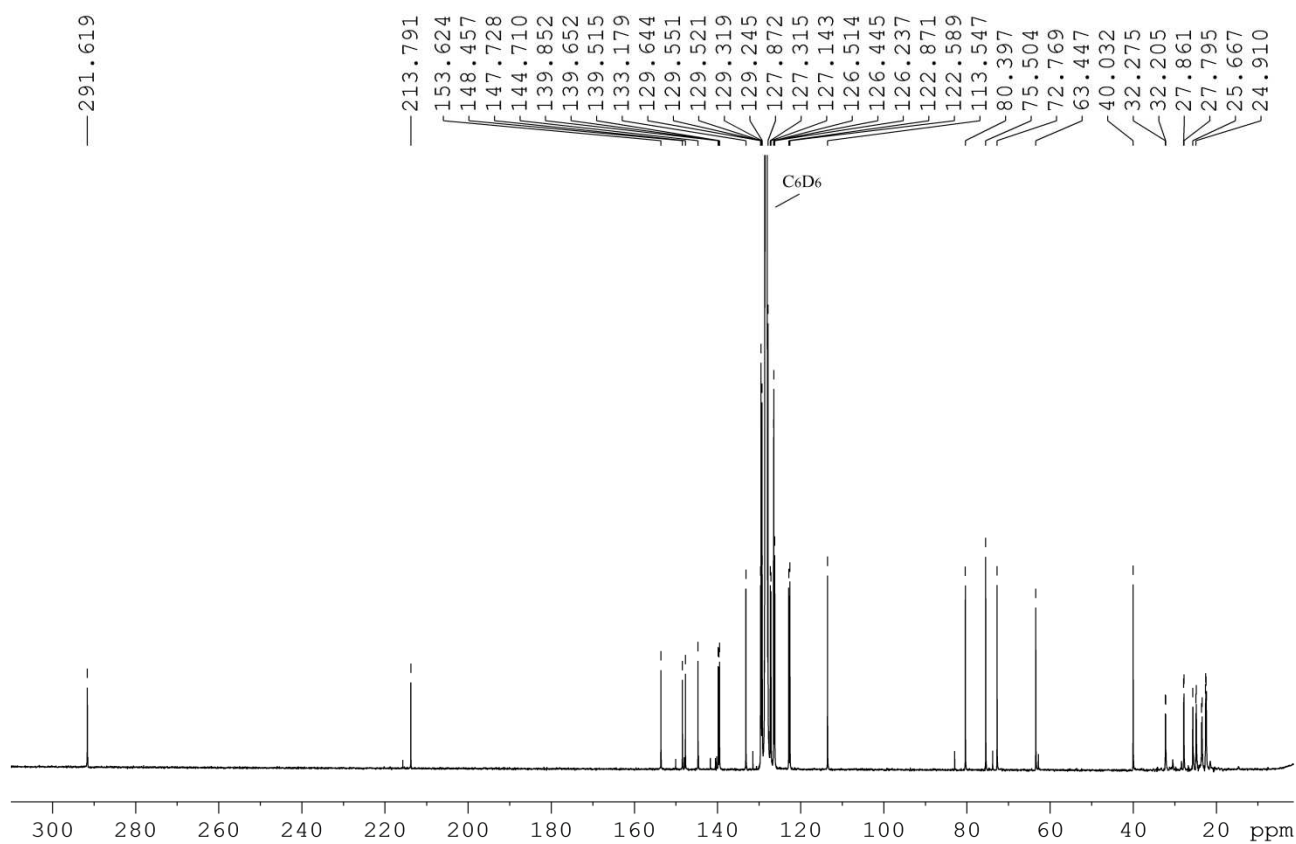
Figure S34: ¹³C NMR of **39** (125 MHz, C₆D₆)
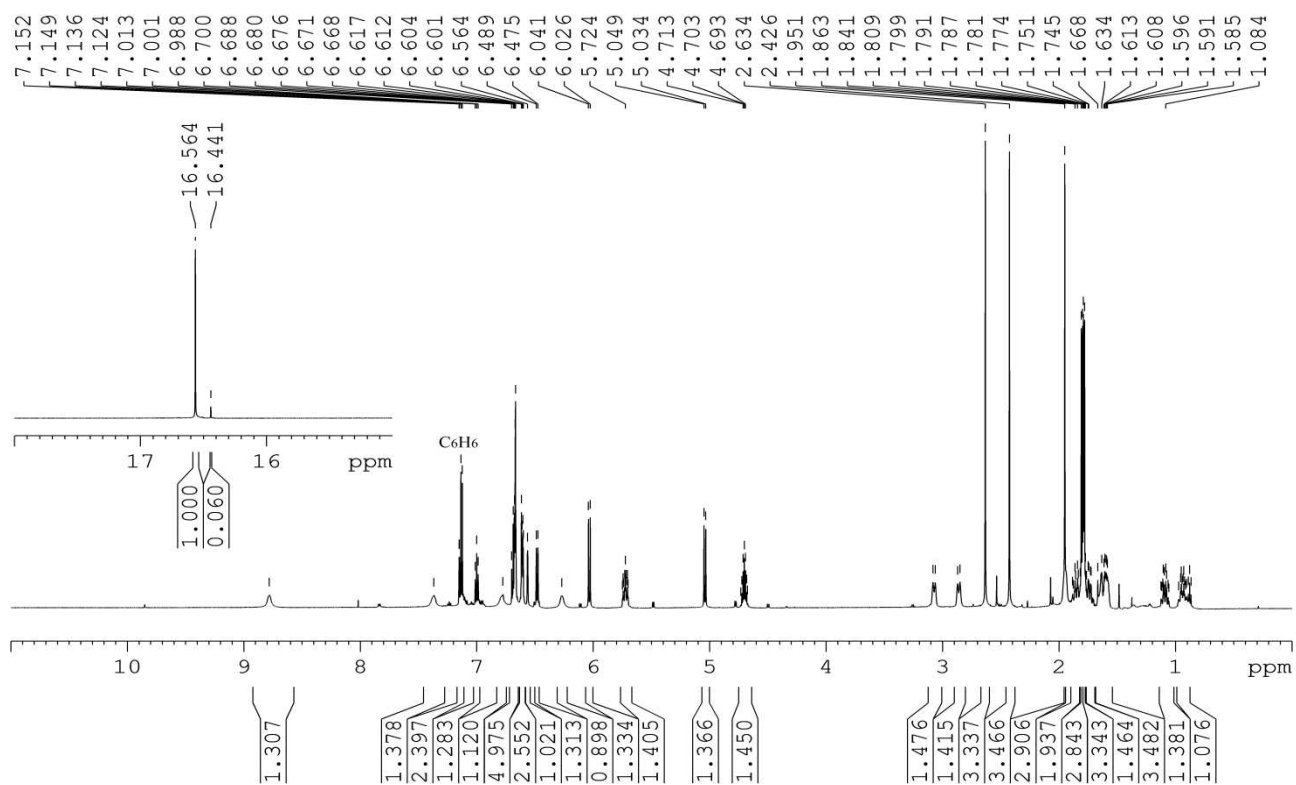
Figure S5.35: ¹HNMR of **4o** (600 MHz, C₆D₆)
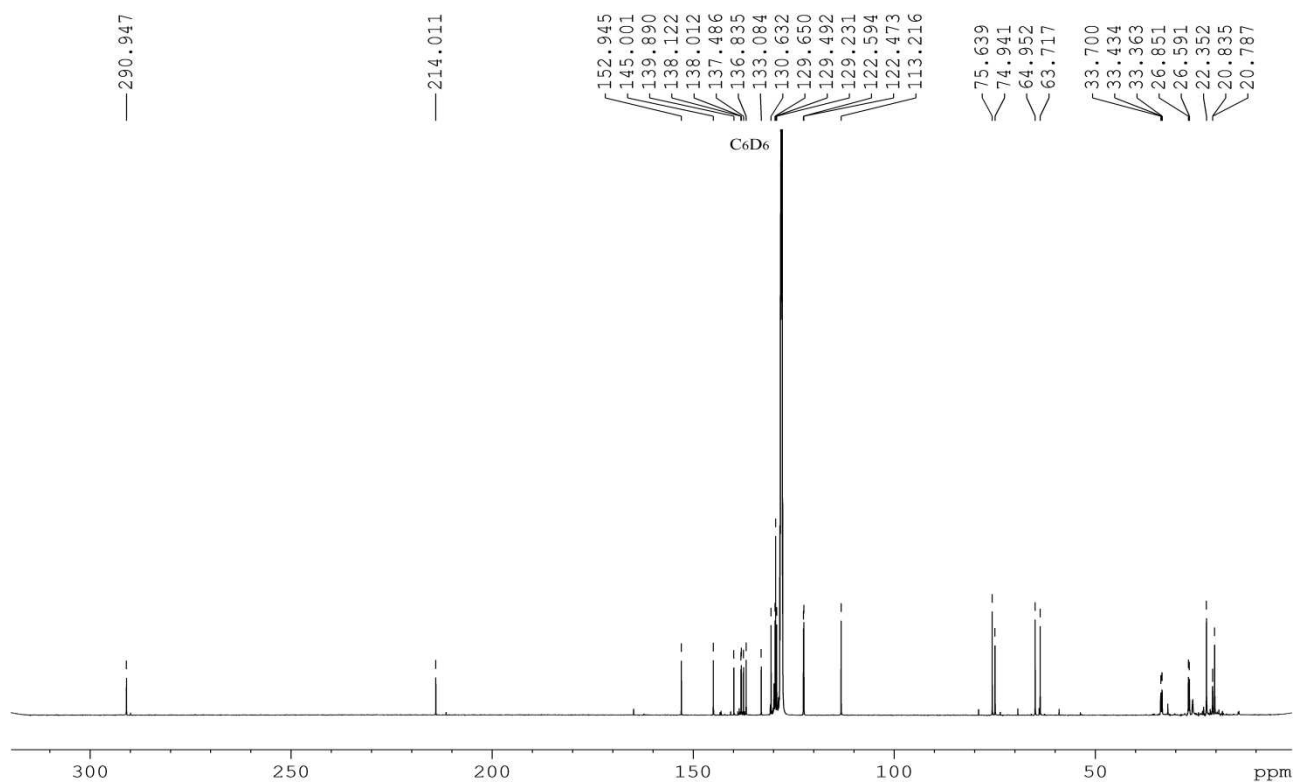
Figure S5.36: ¹³C NMR of **4o** (125 MHz, C₆D₆)
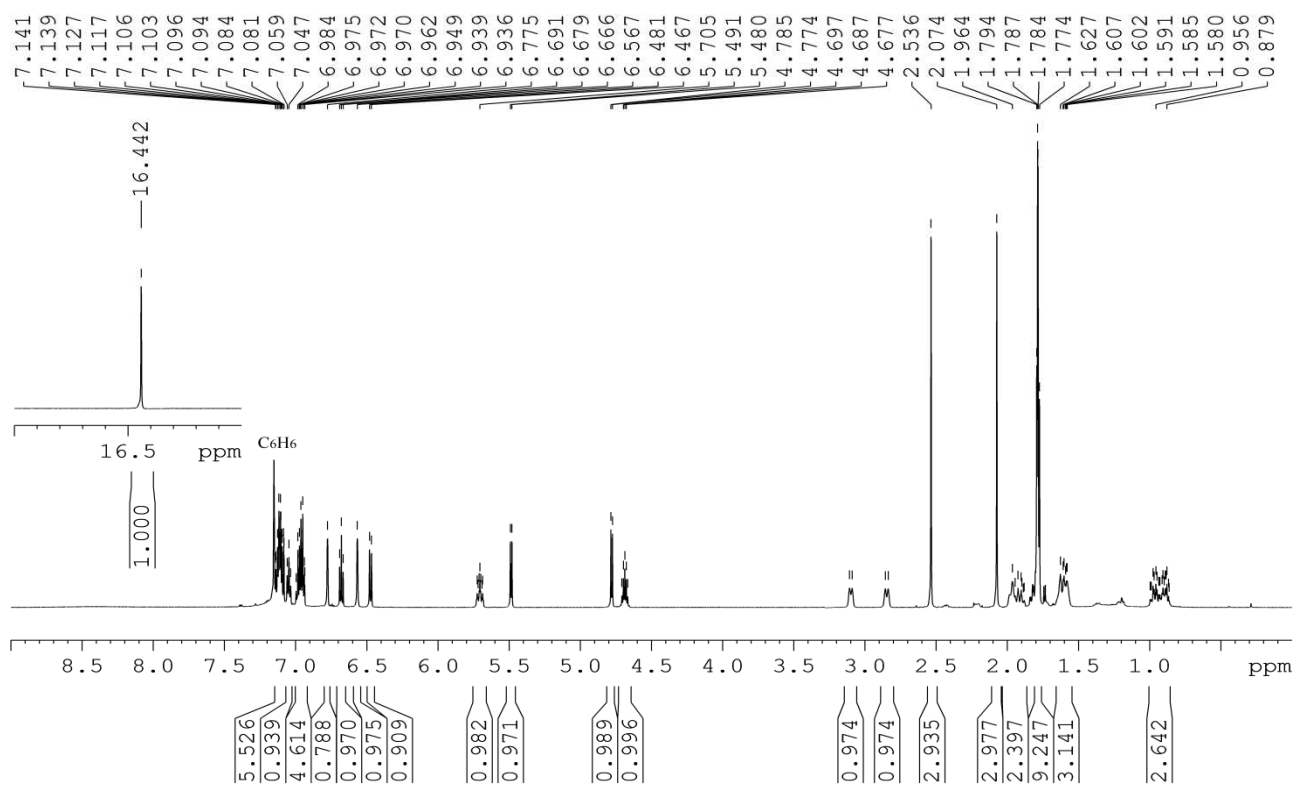
Figure S5.37: ¹HNMR of **41** (600 MHz, C₆D₆)
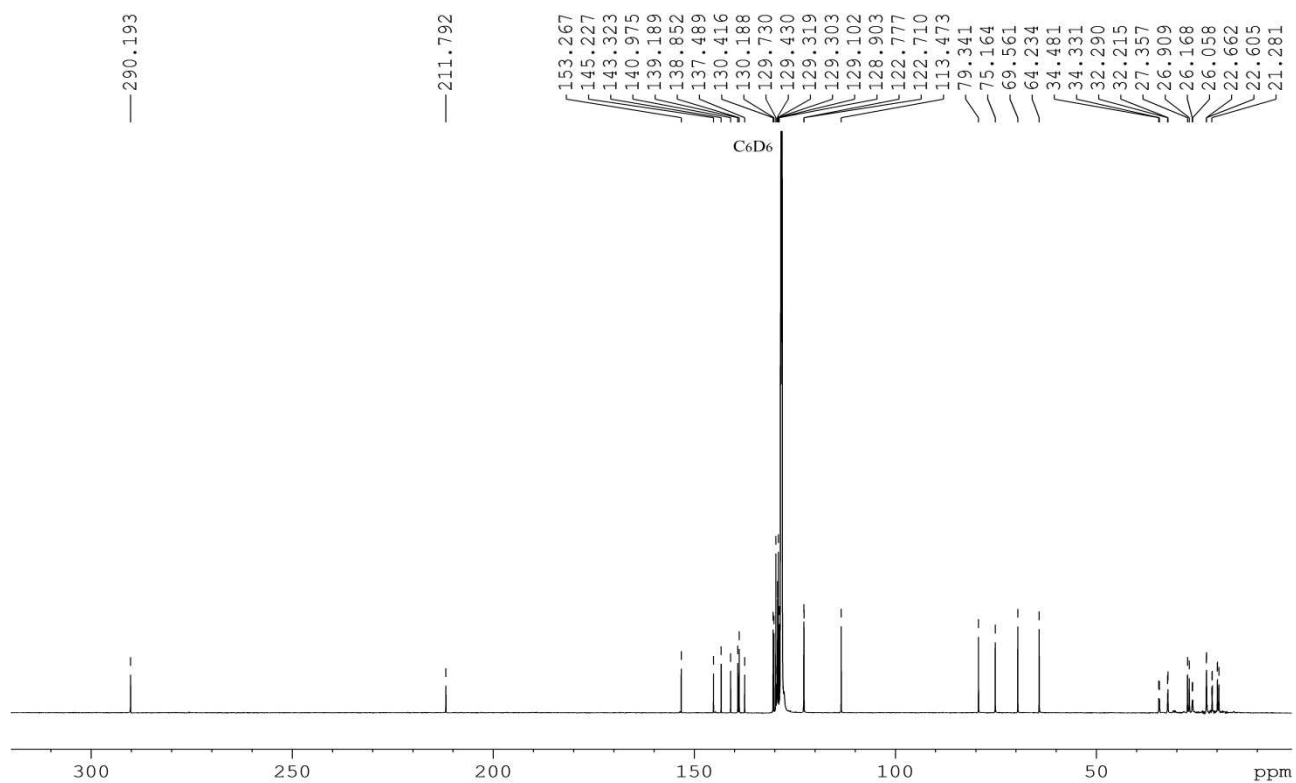
Figure S5.38: ¹³C NMR of **41** (125 MHz, C₆D₆)

5.7.6 ESI-FT-ICR spectra
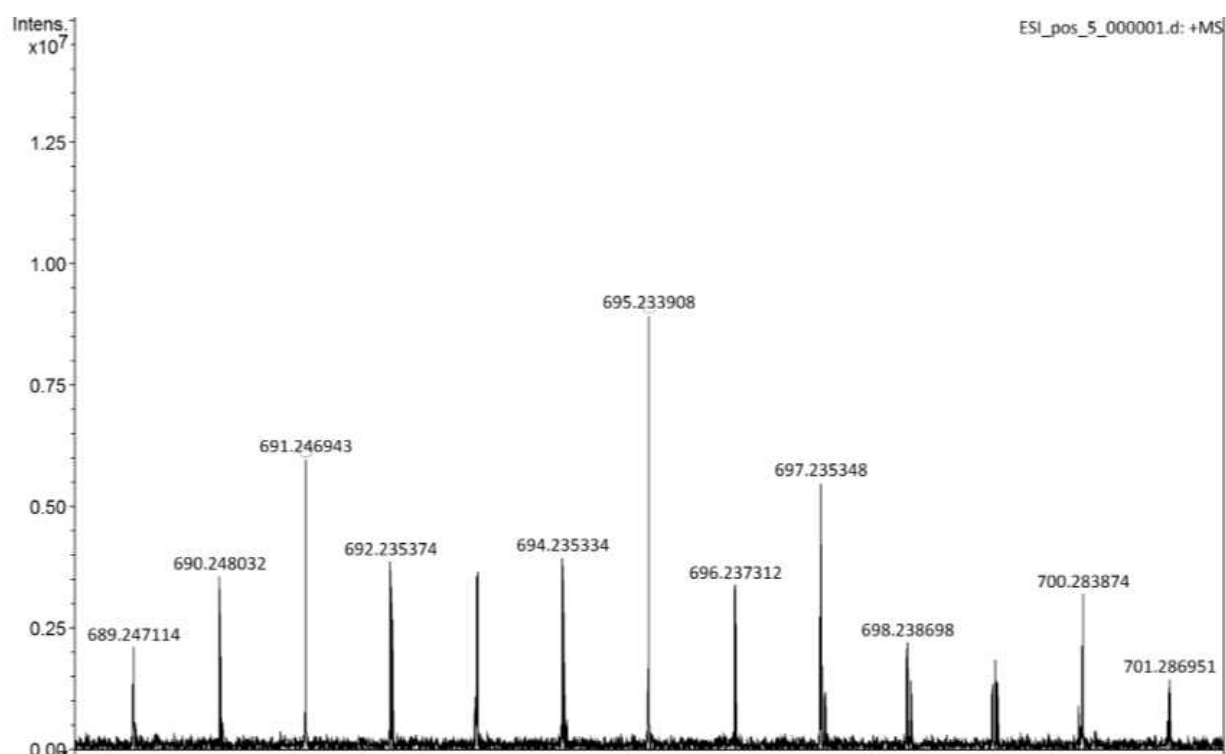
Figure S5.39: ESI-FT-ICR of **36**
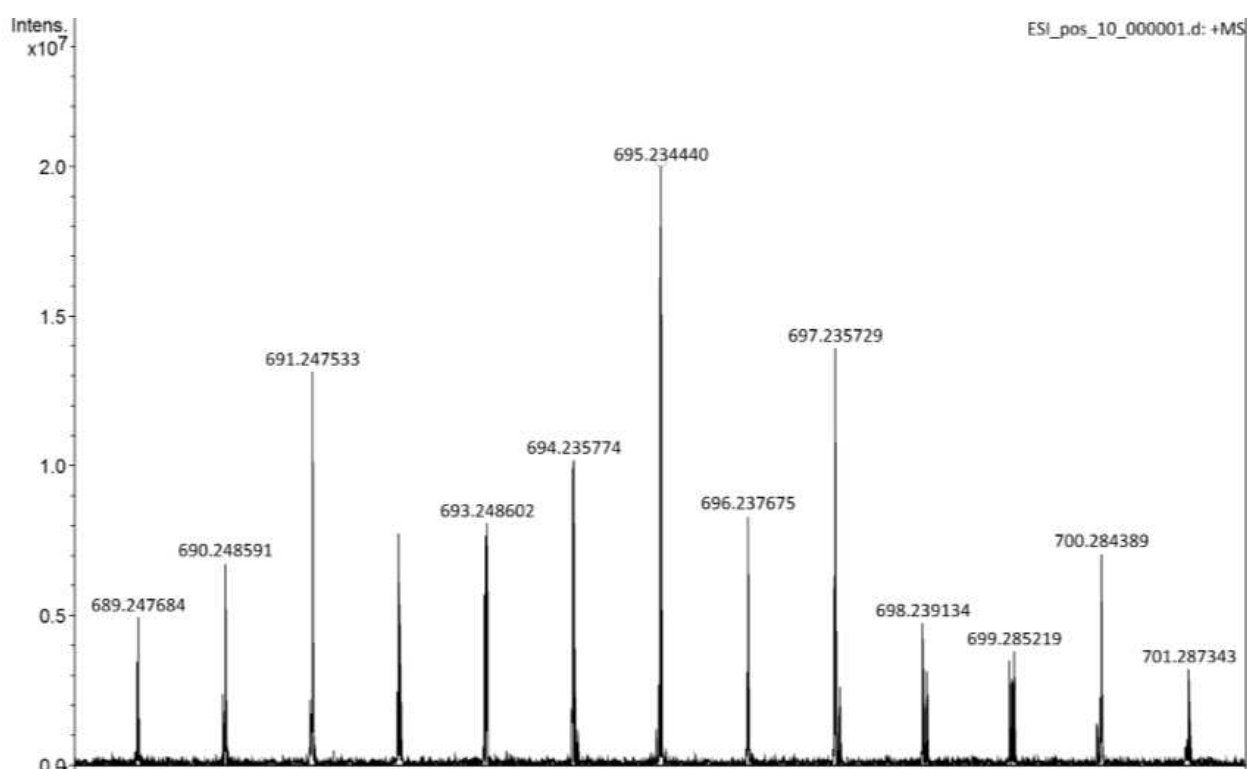
Figure S5.40: ESI-FT-ICR of **37**
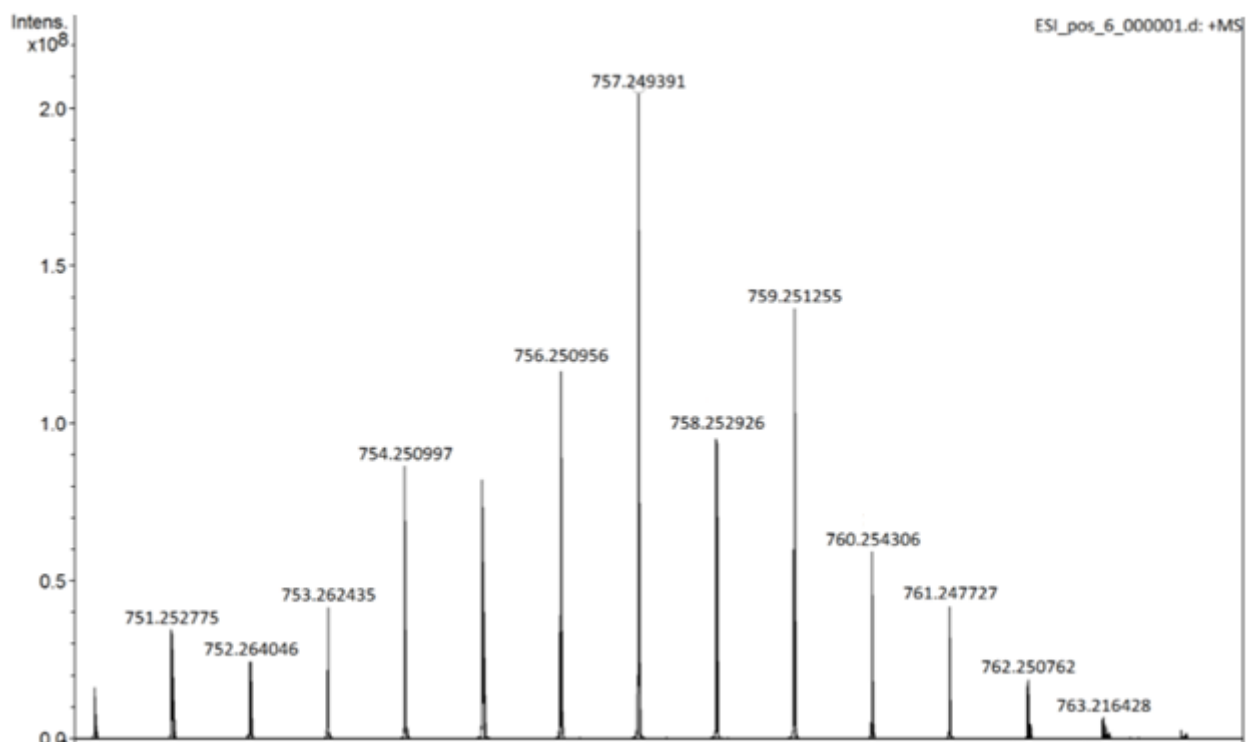
Figure S5.41. ESI-FT-ICR of **38**
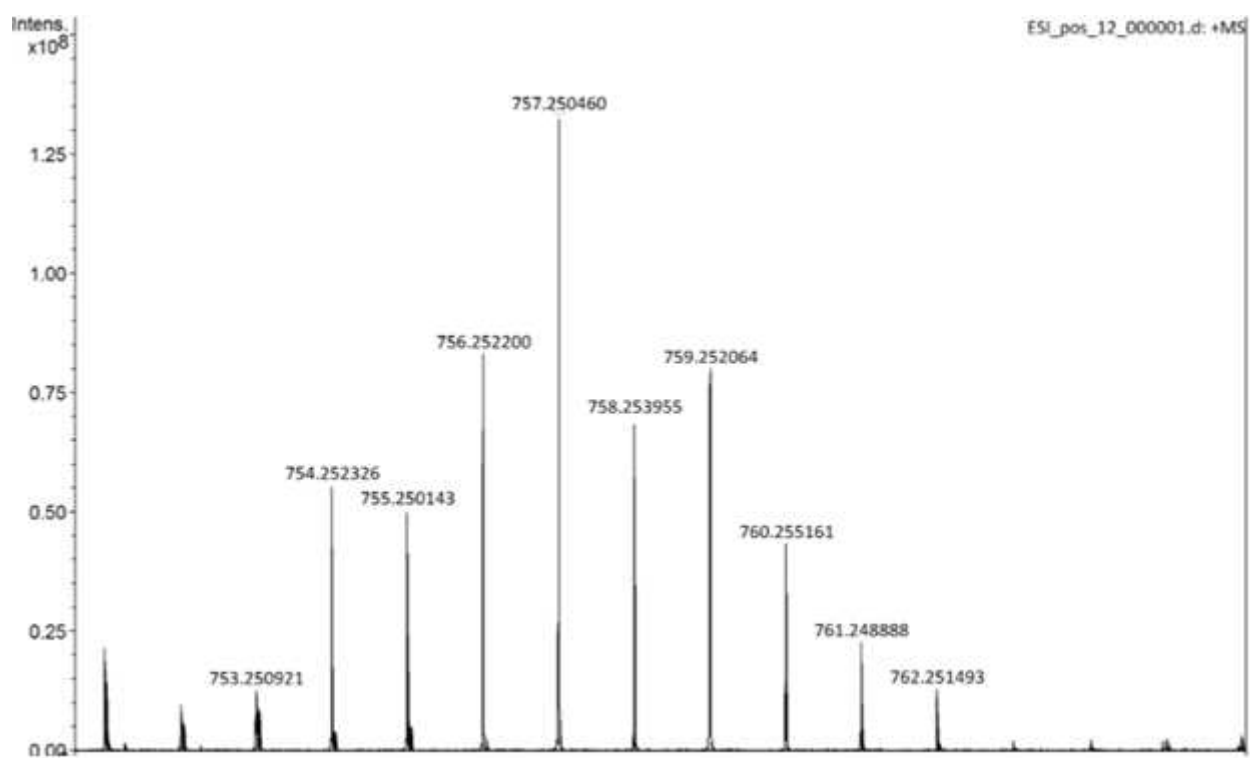
Figure S5.42. ESI-FT-ICR of **39**
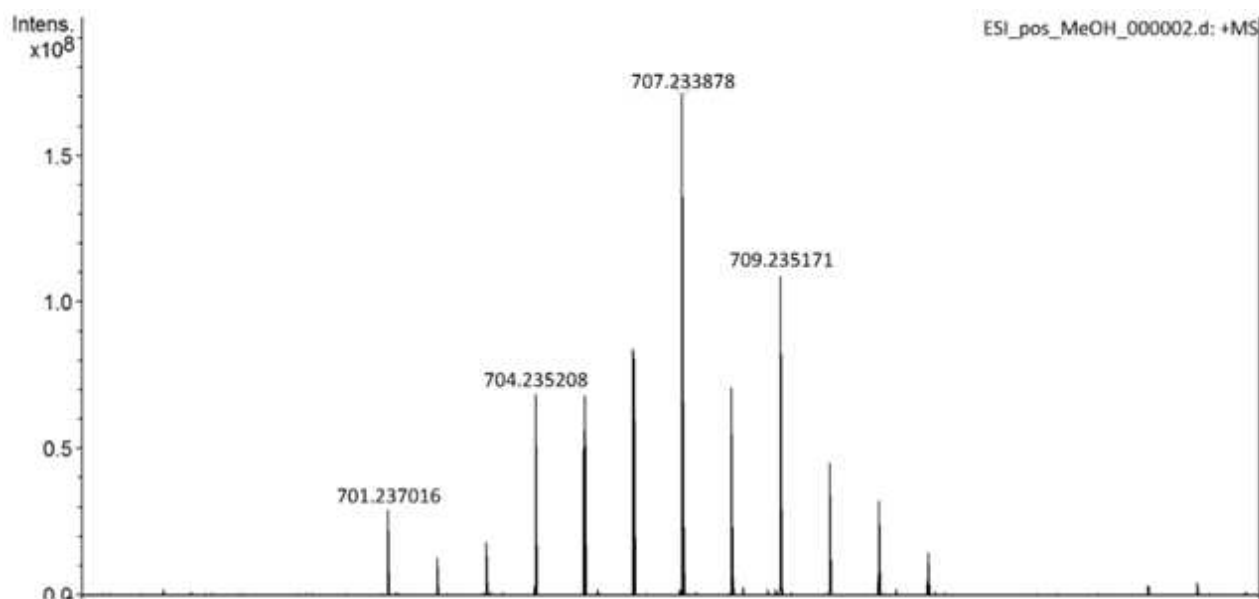
Figure S5.43: ESI-FT-ICR of **40**
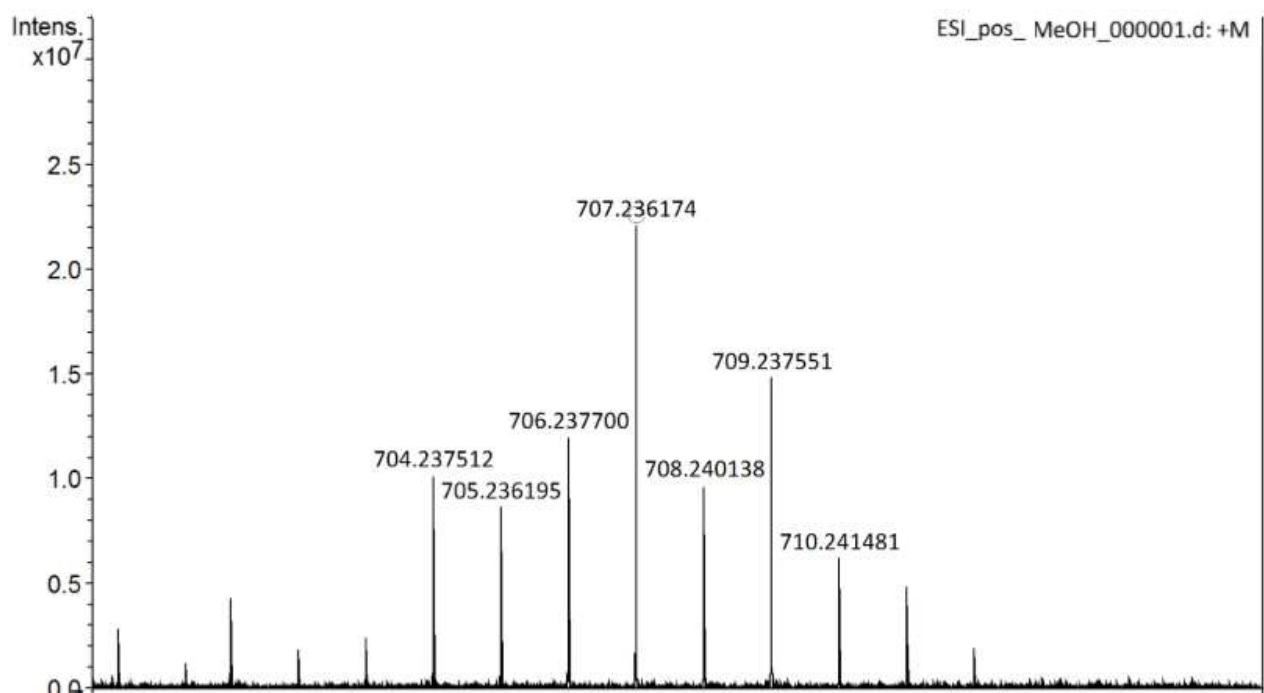
Figure S5.44: ESI-FT-ICR of **41**

5.7.8 X-Ray Diffraction Analysis[112]

The crystal data of compounds **36, 40** and **41** were collected at room temperature using a Nonius Kappa CCD diffractometer with graphite monochromated Mo-Kα radiation. The data sets were integrated with the Denzo-SMN package and corrected for Lorentz, polarization and absorption effects (SORTAV). The structures were solved by direct methods using SIR97 system of programs and refined using full-matrix least-squares with all non-hydrogen atoms anisotropically and hydrogens included on calculated positions, riding on their carrier atoms.

In compound **41** ill-defined regions of residual electron density were found, occupied probably by disordered solvent molecules of benzene and pentane, which cannot be localized. For these reasons the program SQUEEZE was used to cancel out mathematically the effects of the disordered solvent, treated as a diffuse contribution to the overall scattering without specific atom positions. SQUEEZE is part of the PLATON program system.

All calculations were performed using SHELXL-2014/6 and PARST implemented in WINGX system of programs. The crystal data are given in **Table S1**.

A selection of bond distances and angles is given in **Table S2**.

Crystallographic data have been deposited at the Cambridge Crystallographic Data Centre and allocated the deposition numbers CCDC 1533652-1533653-1533654. These data can be obtained free of charge via www.ccdc.cam.ac.uk/conts/retrieving.html or on application to CCDC, Union Road, Cambridge, CB2 1EZ, UK [fax: (+44)1223-336033, e-mail: deposit@ccdc.cam.ac.uk]

---

[112] X-Ray Analysis was performed by Prof. Valerio Bertolasi at University of Ferrara

Table S5.1: Crystallographic data

Compound	36	40	41
Formula	C39H46Cl2N2ORu	C40H46Cl2N2ORu	C40H46Cl2N2ORu
M	730.75	742.76	742.76
Space group	P21/n	C2	C2
Crystal system	Monoclinic	Monoclinic	Monoclinic
a/Å	13.1685(3)	34.4370(11)	22.7452(7)
b/Å	14.2832(4)	8.6779(2)	10.3499(2)
c/Å	19.9018(4)	12.3263(4)	18.4139(5)
β/°	91.668(2)	92.648(1)	91.711(1)
U/Å3	3741.7(2)	3679.7(2)	4332.9(2)
Z	4	4	4
T/K	295	295	295
Dc/g cm-3	1.297	1.341	1.139
F(000)	1520	1544	1544
µ(Mo-Kα)/mm-1	0.593	0.604	0.513
Measured Reflections	35497	18594	16565
Unique Reflections	8158	9518	10684
Rint	0.0602	0.0511	0.0479
Obs. Refl.ns [I≥2σ(I)]	5464	7673	9387
θmin- θmax/°	2.97 – 27.00	2.95 – 30.00	2.81 – 30.00
hkl ranges	-16,16;-17,18;-23,25	-48,48;-9,12; -14,17	-31,31;-12,14; -22,25
R(F2) (Obs.Refl.ns)	0.0419	0.0376	0.0360
wR(F2) (All Refl.ns)	0.1014	0.0892	0.0939
No. Variables/Restraints	413/0	420/1	420/1
Goodness of fit	1.015	1.024	1.067
Δρmax; Δρmin /e Å-3	0.627; -0.654	0.304;-0.526	0.638;-0.538
CCDC Dep. N.	1533652	1533653	1533654

Table S5.2: Selected bond distances and angles (Å and degrees)

Distances	36	40	41
Ru1-Cl1	2.333(1)	2.334(1)	2.330(1)
Ru1-Cl2	2.328(1)	2.339(1)	2.334(1)
Ru1-C1	1.977(3)	1.965(4)	1.974(2)
Ru1-C4	1.825(3)	1.818(5)	1.833(3)
Ru1-O1	2.298(2)	2.283(4)	2.281(2)
C1-N1	1.354(3)	1.351(5)	1.354(4)
C1-N2	1.349(3)	1.360(5)	1.335(3)
Angles			
Cl1-Ru1-Cl2	154.94(3)	155.19(4)	155.49(3)
Cl1-Ru1-C1	95.17(8)	92.41(11)	93.53(8)
Cl1-Ru1-C4	98.88(10)	99.25(13)	99.57(9)
Cl1-Ru1-O1	87.80(6)	87.41(10)	86.88(5)
Cl2-Ru1-C1	88.87(8)	91.20(11)	89.59(8)
Cl2-Ru1-C4	104.38(10)	103.79(13)	103.46(9)
Cl2-Ru1-O1	88.08(6)	88.19(10)	89.47(5)
C1-Ru1-C4	102.47(12)	103.21(16)	102.60(11)
C1-Ru1-O1	176.91(10)	178.14(14)	178.56(9)
C4-Ru1-O1	77.86(10)	78.64(16)	78.68(10)
Ru1-C1-N1	119.8(2)	117.0(3)	118.2(2)
Ru1-C1-N2	132.7(2)	136.7(3)	133.5(2)
N1-C1-N2	107.4(2)	106.3(3)	108.3(2)

5.7.9 Cyclic Voltamograms

$\Delta E_{1/2} = 0.860$ V
$E_a - E_c = 66$ mV

$\Delta E_{1/2} = 0.947$ V
$E_a - E_c = 73$ mV

$\Delta E_{1/2} = 0.960$ V
$E_a - E_c = 102$ mV
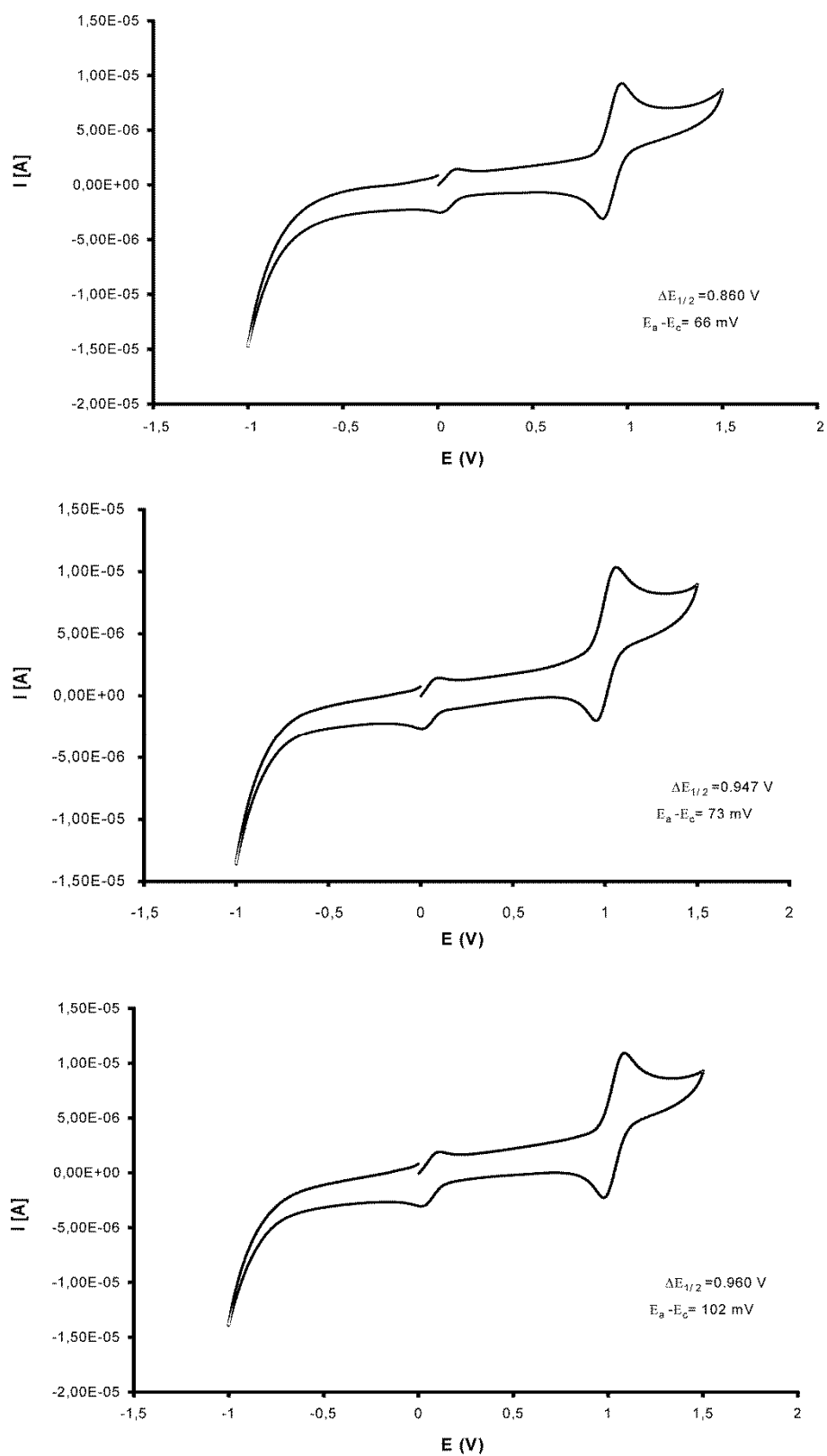
Figure S5.45: Cyclic voltammograms of **HGII,7** and **8**
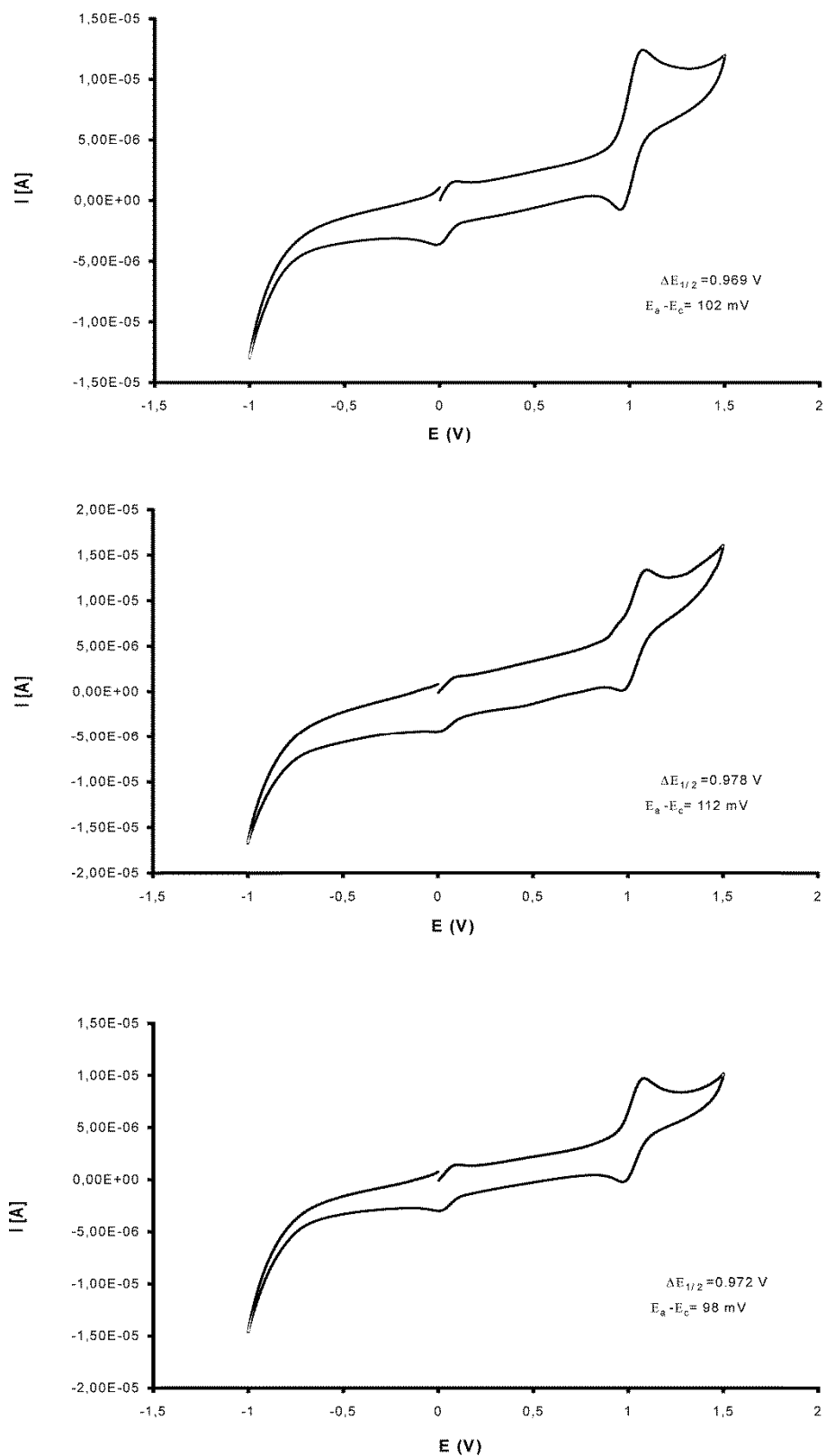
Figure S5.46: Cyclic voltammograms of **36**, **37** and **38**

$\Delta E_{1/2} = 0.976$ V
$E_a - E_c = 112$ mV

$\Delta E_{1/2} = 0.961$ V
$E_a - E_c = 98$ mV

$\Delta E_{1/2} = 0.950$ V
$E_a - E_c = 83$ mV
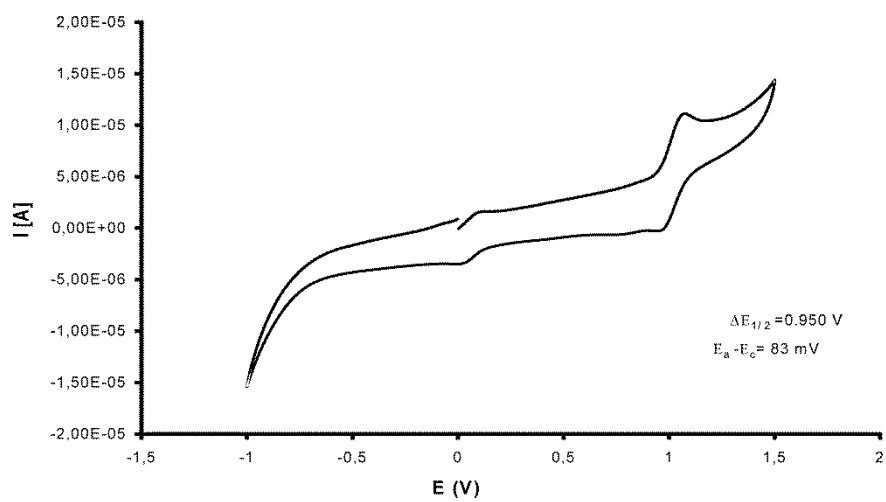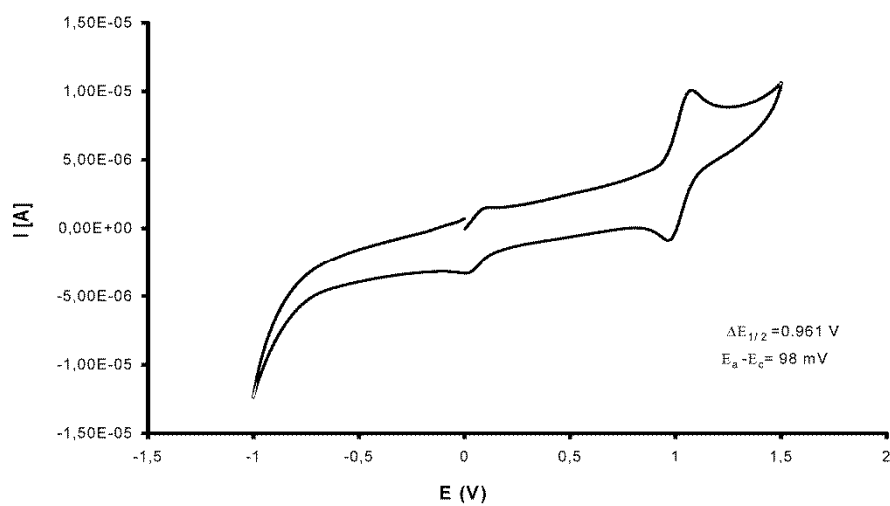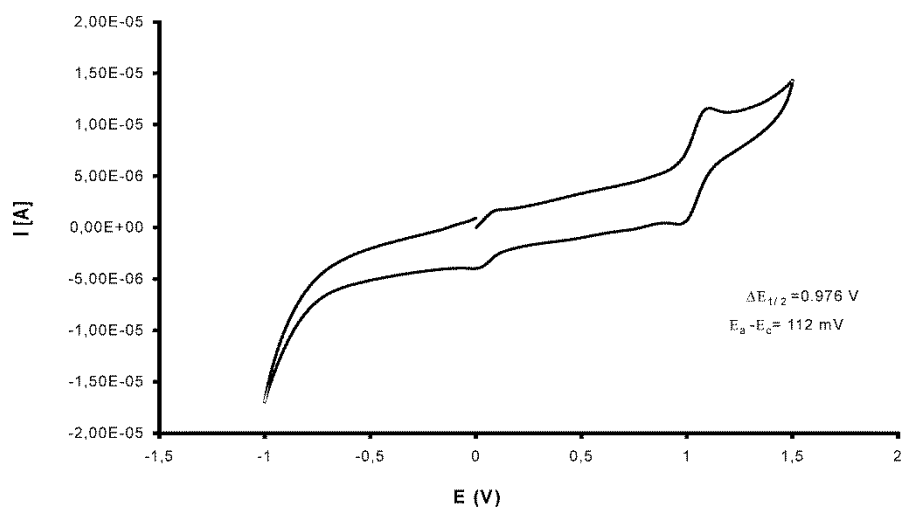
Figure S5.47: Cyclic voltammograms of **39, 40** and **41**

5.7.9 Steric Maps
HII

HII
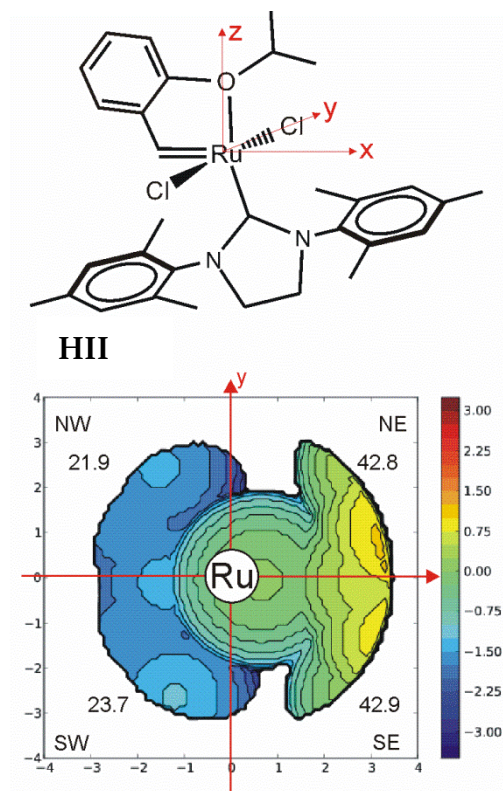
Figure S5.48: Topographic steric map of **HII**

37 and 38 with no π-stacking
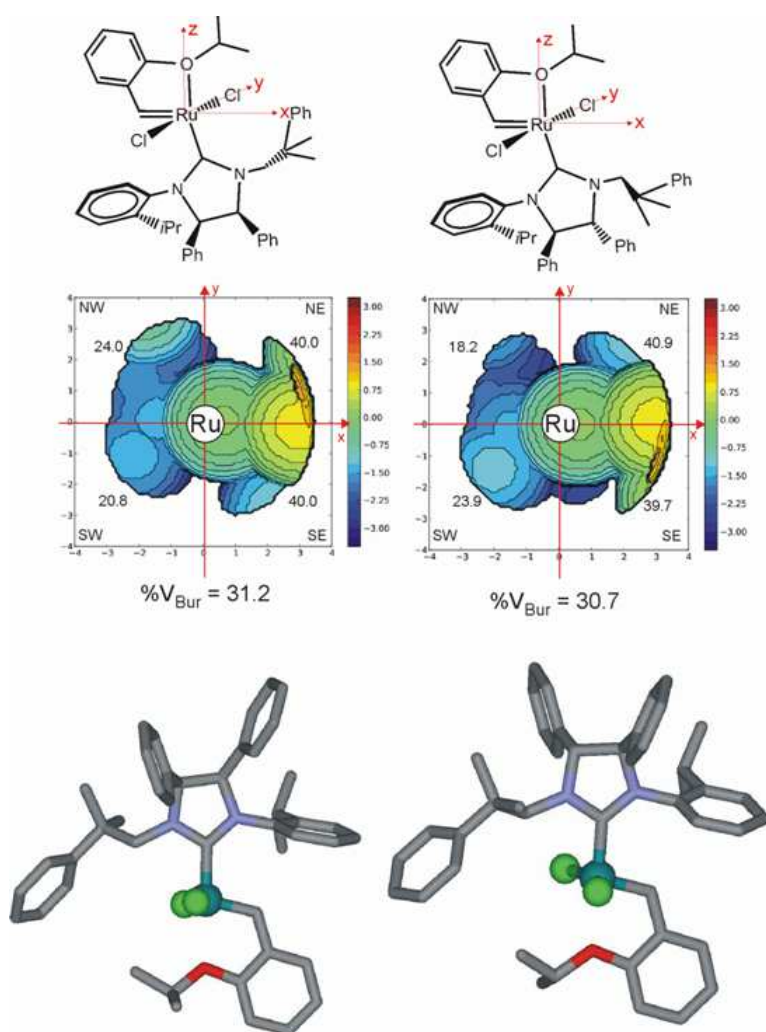
Figure S5.49: Topographic maps, %V_{Bur} and DFT optimized structures of complexes **37** (left) and **38** (right), where neophyl groups do not present any π-stacking with backbone phenyl groups.

5.7.10 Catalysis
Ring Closing Metathesis

General procedure for RCM of malonate and tosyl derivatives have been described in paragraph 3.8.11. Results are summarized in table 5.3, 5.4, 5.5.

Table S5.3: RCM of **23** and **25**

Entry[a]	Substrate	Product	Catalyst (mol%)	Time (min)	Yield[b] (%)
1			**7** (1)	20	>99
2			**8** (1)	4	>99
3	EtOOC COOEt 1%mol [Ru] 0.1M -C_2H_4 **23**	EtOOC COOEt **23a**	**36** (1)	6	99
4			**37** (1)	5	99
5			**38** (1)	8	99
6			**39** (1)	7	99
7			**40** (1)	60	89
8			**41** (1)	37	98
9			**HII** (0.1)	4	>99
10			**7** (1)	60	94
11			**8** (1)	3	>99
12	Tos N 1%mol [Ru] 0.1M -C_2H_4 **24**	Tos N **24a**	**36** (1)	8	99
13			**37** (1)	5	99
14			**38** (1)	13	98
15			**39** (1)	6	99
16			**40** (1)	60	74
17			**41** (1)	60	97
18			**HII** (0.1)	4	>99
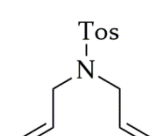
[a] All runs were carried out in C_6D_6 at 60°C. [b] Yields based on NMR analysis.

Table S5.4: RCM of **25** and **26**

Entry[a]	Substrate	Product	Catalyst (mol%)	Time (min)	Yield[b] (%)
1			**7** (1)	60	94
2			**8** (1)	8	>99
3			**36** (1)	30	99
4			**37** (1)	13	99
5			**38** (1)	13	99
6			**39** (1)	10	99
7			**40** (1)	60	60[c]
8			**41** (1)	60	95[c]
9			**HII** (0.1)	7	99
10			**7** (1)	14	99
11			**8** (1)	4	>99
12			**36** (1)	7	99
13			**37** (1)	5	99
14			**38** (1)	12	99
15			**39** (1)	7	>99
16			**40** (1)	60	91[d]
17			**41** (1)	36	99
18			**HII** (0.1)	6	>99

[a] All runs were carried out in C_6D_6 at 60°C. [b]Yields based on NMR analysis. [c]Quantitative yield was observed monitoring reactions after 66 and 17h, respectively. [d]Quantitative yield was observed monitoring reaction after 6h.

Table S5.5: RCM of **27** and **28**

Entry[a]	Substrate	Product	Catalyst (mol%)	Time (min)	Yield[b] (%)
1			**7** (5)	60 [70h]	45 [79]
2			**8** (5)	60	>97
3	EtOOC COOEt 5%mol [Ru]	EtOOC COOEt	**36** (5)	60 [27h]	49 [86]
4	0.1M -C₂H₄		**37** (5)	60 [17h]	88 [>99]
5	27	27a	**38** (5)	60 [72h]	47 [70]
6			**39** (5)	60 [18h]	43 [57]
7			**40** (5)	60 [40h]	- [14]
8			**41** (5)	60 [15h]	- [13]
9			**HII** (5)	60 [8h]	20 [39]
10			**7** (5)	60 [4h]	77 [89]
11			**8** (5)	60	97
12	Tos N 5%mol [Ru]	Tos N	**36** (5)	60 [17h]	86 [>99]
13	0.1M -C₂H₄		**37** (5)	60	97
14	28	28a	**38** (5)	60 [26h]	74 [85]
15			**39** (5)	60 [27h]	75 [88]
16			**40** (5)	60 [21h]	14 [74]
17			**41** (5)	60 [70h]	24 [94]
18			**HII** (5	60 [7h]	72 [93]

[a] All runs were carried out in C_6D_6 at 60°C. [b] Yields based on NMR analysis.

Cross Metathesis

The general procedure for the CM of **30** and **31,** described in paragraph 3.8.11, was followed also for the CM of **55** and **56**.

5.7.11 Ethenolysis

Each component of the ethenolysis reaction mixture was accurately weighted in a vial and these weights were corrected using the component purity percentages (previously determined via GC).

The obtained mixture was injected seven times and, for each peak, an average area was calculated. Then, each average area was divided by the weighted mass and by the average area of **EO** (response factor=1) to obtain the response factor (rf).

Calculated rf are summarised in table S5.6.

Table 5.6: Response factors

Compound	EO	CM1	CM2	SM1	SM2
Response factor	1	0.58	0.74	0.75	0.55

Under a nitrogen atmosphere, in an autoclave, **EO** (5.4 mmol) and dodecane (150 µL) were introduced. At this point, a t = 0 sample was prepared. The autoclave was purged with ethylene three times, and then a toluene solution of the catalyst (20 to 500 ppm) was added. The autoclave was purged with ethylene three times and then charged with a pressure of 150 psi. The reaction mixture was stirred at 50 or 40 °C for 3 or 2 h and then cooled in an ice bath and quenched with ethyl vinyl ether.

After that, GC samples were prepared in hexane. Samples were storedat –20 °C until GC analysis.

Yields, conversions and selectivities were calculated using the following equations:

$$\mathbf{n\ (x)} = \frac{\text{Area (x)}}{\text{rf (x)}} * \frac{1}{\text{MW (x)}} \text{ (for the generic x component)}$$

$$\mathbf{Conversion}\ (\%) = 100 * (1 - \frac{\text{Area (\textbf{EO})sample} * \text{Area (dodecane)t0}}{\text{Area (\textbf{EO})t0} * \text{Area (dodecane)sample}})$$

$$\mathbf{Selectivity}\ (\%) = 100 * (\frac{\text{n}(\textbf{CM1}) + \text{n}(\textbf{CM2})}{\text{n}(\textbf{CM1}) + \text{n}(\textbf{CM2}) + 2(\text{n}(\textbf{SM1}) + \text{n}(\textbf{SM2}))})$$

$$\mathbf{Yield}\ (\%) = \frac{\text{Conversion} * \text{Selectivity}}{100}$$

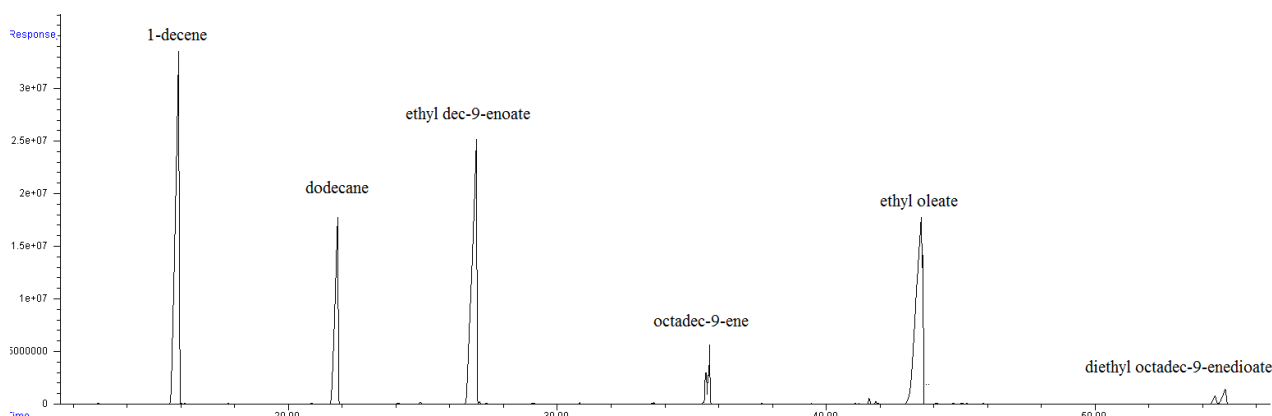$$\mathbf{TON} = \text{Yield}\ (\%) \frac{\text{mol}\ (\textbf{EO})}{\text{mol}\ (\textbf{cat}) * 100}$$

Figure S5.50: Representative chromatogram of ethenolysis reaction mixture. Column: HP 5MS UI 60m*0.25mm. GC method: flow 1mL/min; 60°C for 2 min, then 250°C for 18 min, 5°C/min

Chapter 6

Asymmetric Metathesis Transformations

Chirality of systems is certainly one of the most intriguing features of chemistry. Indeed, the fact that molecules that differ just for the configuration of one stereogenic centre could have a so different chemical response has something fascinating. The accurate evaluation of steric and electronic properties of substituents can, in most of the cases, rationalise or predict molecules' behaviour. However, if one or more stereogenic centres are present, everything should be reconsidered since the disposition of groups in space can turn the tables on.

Synthetic chiral molecules come into everyday life mainly through drugs. The asymmetric nature of biological systems rules the interactions with chiral compounds and determines for them very diverse physiological responses. For this reason pharmaceutical industries, which are always looking for the 'right' enantiomer, are the cornerstone of asymmetric organic chemistry.

As a fundamental reaction for the formation of double carbon-carbon bonds, olefin metathesis has been considered as a crucial step in chiral synthesis and nowadays several asymmetrical metathesis transformations have been developed. One of the strategies to gain enantioselectivity involves the synthesis of novel chiral catalysts (figure 6.1) and considerable advances have been reached in this field.[113]
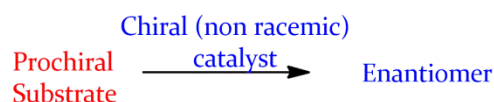
Figure 6.1: Enantioselectivity through the use of a chiral catalyst

In this doctoral work, the role of different backbone configurations of u-NHCs has been studied as an important feature affecting catalytic performances. In this chapter its use as a chiral motif for the synthesis of enantiomerically pure catalysts, as well as complex applications in some model asymmetric metathesis, will be discussed. Seven new chiral ligands have been synthesized: five of them, bearing an anti relative configuration, were obtained through a 'classic' synthesis, which involved the use of a chiral diamine as a starting material; two of them, with a syn backbone configuration, were obtained through chiral resolution, with an approach never used for the synthesis of enantiopure NHC ligands so far.[114]

---

[113] B. Stenne, S. K. Collins, *Enantioselective Olefin Metathesis*, chapter of *Olefin Metathesis: Theory and Practice*, Edited by K. Grela, John Wiley and Sons, Hoboken **2014**

[114] Experimental data reported in this chapter were published in: a) synthesis and asymmetric catalysis with anti catalysts: V. Paradiso, V. Bertolasi, F. Grisi, *Organometallics* **2014**, *33*, 5932; V. Paradiso, V. Bertolasi, C.

6.1 Chiral metathesis catalysts through enantiomerically pure starting materials

The use of a chiral starting material is the easier and most common pathway for the synthesis of new chiral metathesis catalysts.

Starting from (*1R, 2R*)-1,2-diphenylethylendiamine (**13**), through functionalization of nitrogen atoms and subsequent cyclization, five new chiral u-NHC precursors have been obtained (figure 6.2). Their synthesis was described in chapter 3 and chapter 5 and synthetic path for **22** is depicted in scheme 6.1 as a representative example.
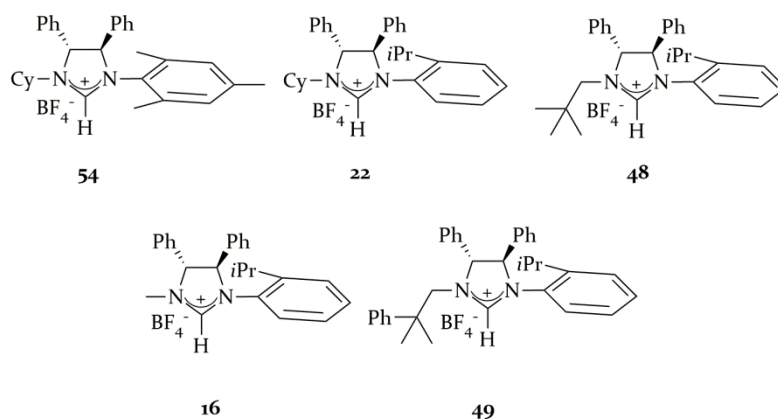
Figure 6.2: Five chiral u-NHC ligands precursors
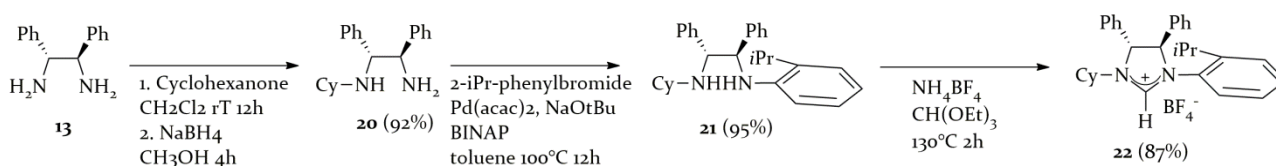
Scheme 6.1: Synthesis of the chiral tetrafluoroborate salt **22**

The reactions used for the construction of the NHC framework **22** did not involve backbone carbons and thus did not alter the configuration. This was also confirmed by X-Ray analysis of the Hoveyda-type and rhodium-COD complexes bearing this ligand (**8** and **35**) in which absolute configuration was unambiguously assigned (see paragraph 3.6).

The successive reaction of **22** and, analogously, of all the other chiral ligand precursors depicted in figure 6.2, led to the synthesis of seven new catalysts bearing enantiomerically pure u-NHCs with an anti backbone relative configuration (figure 6.3).

Unfortunately this facile and efficient approach is limited to anti ligands. In fact (as reported in previous chapters) **9**, the analogue of **13** with syn phenyls on backbone, is a *meso* compound and can just give racemic ligands.

As an example synthesis of **19**, the syn congener of **22**, is depicted in scheme 6.2.

Costabile, F. Grisi, *Dalton Trans.* **2016**, *45*, 561 b) synthesis, resolution and asymmetric catalysis with syn catalysts: V. Paradiso, S. Menta, M. Pierini, G. Della Sala, A. Ciogli, F. Grisi, *Catalysts* **2016**, *6*, 177 .
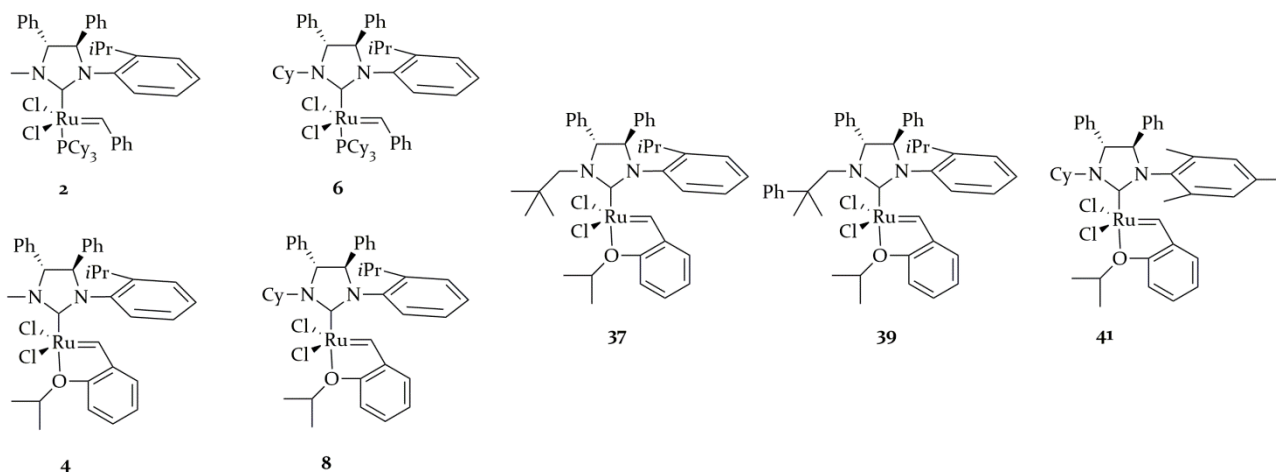
Figure 6.3: Chiral u-NHC ruthenium catalysts with an anti relative configuration of the backbone
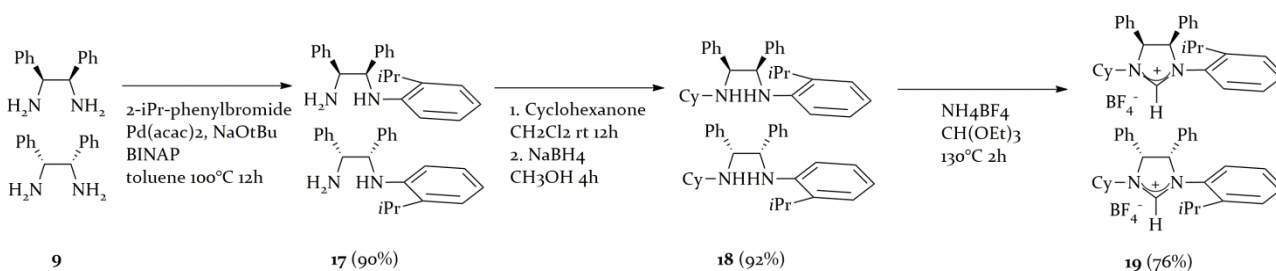
Scheme 6.2: Synthesis of the racemic tetrafluoroborate salt **19** (**9** is a *meso* compound, the two structures reported have to be intended as a visual aid only)

This synthetic approach has made enantiopure catalysts with syn u-NHC backbone configuration inaccessible so far and their potentialities in asymmetric metathesis totally unexplored yet.

6.2 Chiral Metathesis Catalysts *via* resolution of *meso* compounds

The application of enantiopure ruthenium catalysts with syn NHC backbone is an interesting issue, since the presence of backbone groups on the same side of the u-NHC could create a peculiar reactive pocket and could have dramatic effects on enantioselectivity. To explore this side of chiral metathesis transformations it was proposed a completely new approach: derivatisation of the *meso* starting material followed by resolution using high pressure chromatography (HPLC) with a chiral stationary phase (scheme 6.3).

After palladium catalysed Buchwald-Hartwig arylation, the obtained racemic monoarylated diamine underwent separation on chiral HPLC on the polysaccharide-based Chiralpak IA. Chromatograms of the separated enantiomers, obtained in a high level of purity (99.9% *ee* and 98.8% *ee*) are reported in figure 6.4.

The separation step was very efficient however the low solubility of the sample did not allow a complete utilisation of the high loading capacity of the column (the optimised concentration was 50 mg/mL).

Enantiomeric relationship between (+)-**17** and (-)-**17** was confirmed with measurement of the optical rotatory dispersion (ORD) and through Electronic Circular Dichroism (ECD) analysis (figure 6.5).
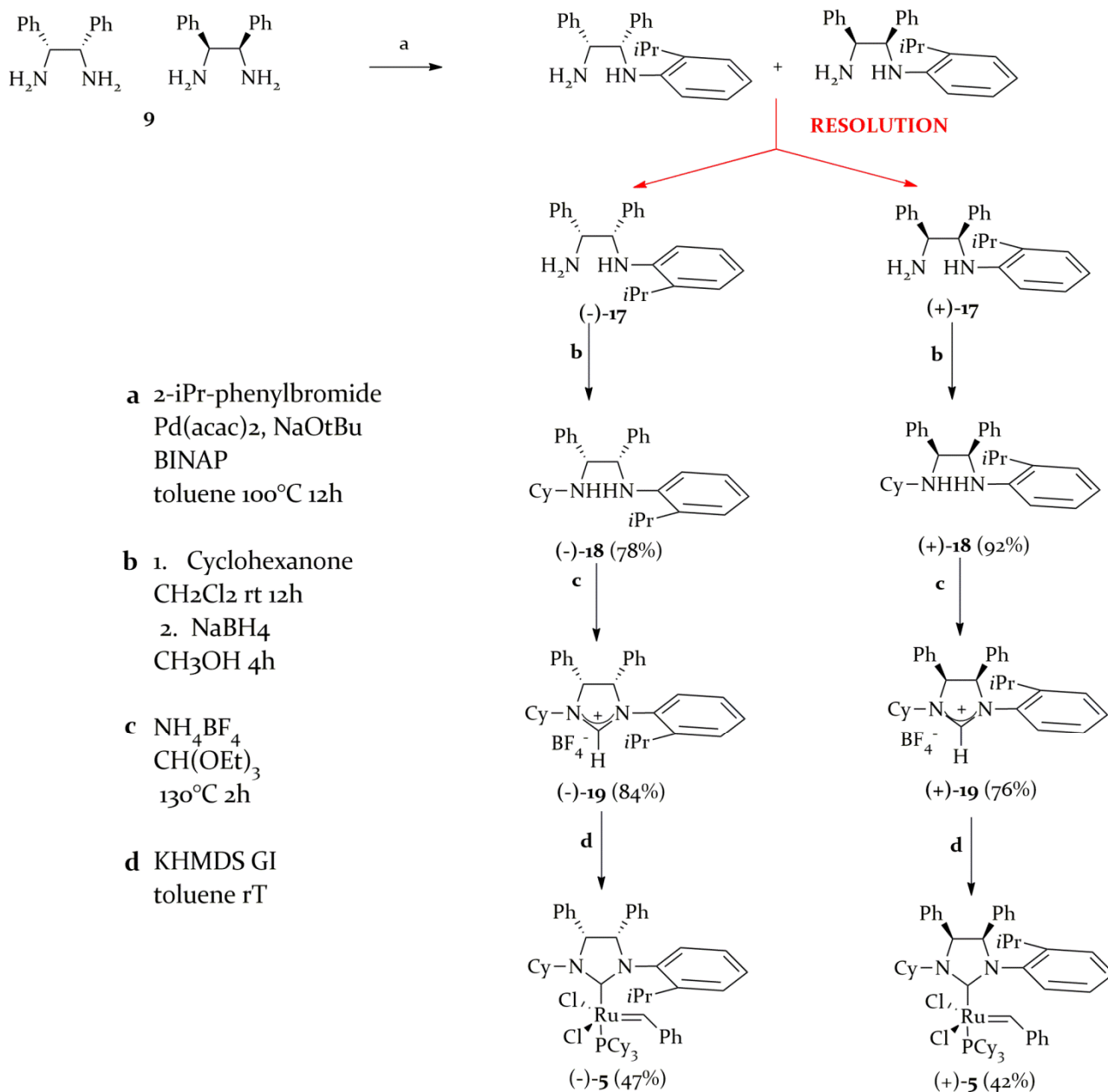
Scheme 6.3: Synthesis of the syn enantiopure catalysts (+)-**5** and (-)-**5** (**9** is a *meso* compound, the two structures reported have to be intended as a visual aid only)
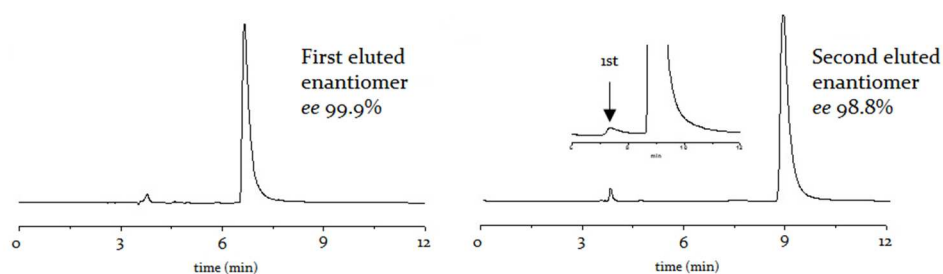
Figure 6.4: Chromatograms of enantiomers (+)-**17** (left) and (-)-**17** (right)

182

ORD was evaluated by measuring the optical rotatory power at different wavelengths. For
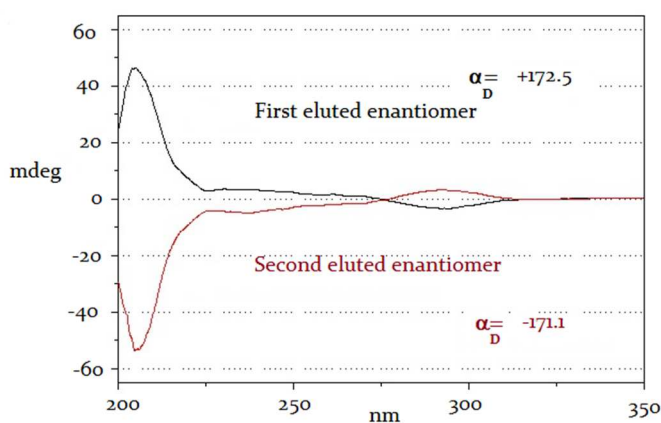
Figure 6.5: ECD and α_D of (+)-**17** and (-)-**17**

(+)-**17** and (-)-**17** the stereoisomeric relation was demonstrated by the very similar absolute values of α (positive for (+)-**17** and negative for (-)-**17**) at wavelengths in the range 405-589 nm.

In order to attribute an absolute configuration to each enantiomer, these measured ORDs were compared with the one of (1R, 2S)-**17**, simulated through DFT calculations.

Experimental and theoretical α_D are summarised in table 6.1. Simulated values of α were positive and increased at lower wavelengths. This trend was perfectly in line with those experimentally observed for (+)-**17**, to which a (1R, 2S) absolute configuration could thus be reasonably assigned.

Table 6.1: ORD of (+)-**17** and (-)-**17** (experimental) and of (1R, 2S)-**17** (simulated)

Wavelength of α_n	α_n of (+)-**17**	α_n of (-)-**17**	α_n of (1R, 2S)-**17**
589	172	-171	186
577	212	-238	-
546	237	-204	-
530	-	-	242
487	-	-	309
443	-	-	473
435	363	-307	-
405	395	-359	-

ECD is the property of a chiral molecule to differently adsorb left-handed and right-handed circularly polarised light. The homonym spectroscopic technique monitors optical activity through the absorption-caused electronic transitions. The analysis of the latter can be used in structural characterisation of molecules.[115]

In the investigation of an enatiomeric relationship, the typical mirror-images profile of the ECD of enantiomers makes this technique very useful and immediate.

ECD spectra of diamines (+)-**17** and (-)-**17** and of catalysts (+)-**5** and (-)-**5** were recorded (figure 6.5 and 6.6, respectively) and enantiomeric relationships were confirmed. For ruthenium compounds, in the spectral investigated window, ECD spectra showed Cotton effects (the change in circular dichroism in the proximity of an absorption band) at 212, 260, 290 and 350 nm: the first two bands presented the same CD sign albeit opposite to the

---

[115]*Circular Dichroism: Principles and Applications, 2nd Edition*, edited by N. Berova, K. Nakanishi, R. W. Woody, Wiley VCH, **2000**

second two (i.e., 212/260 positive and 290/350 nm negative for (+)-**5**) with a single null value (CD sign inversion point) at 280 nm.

To the best of our knowledge, this is the first example of metathesis catalysts characterised through this spectroscopic technique.
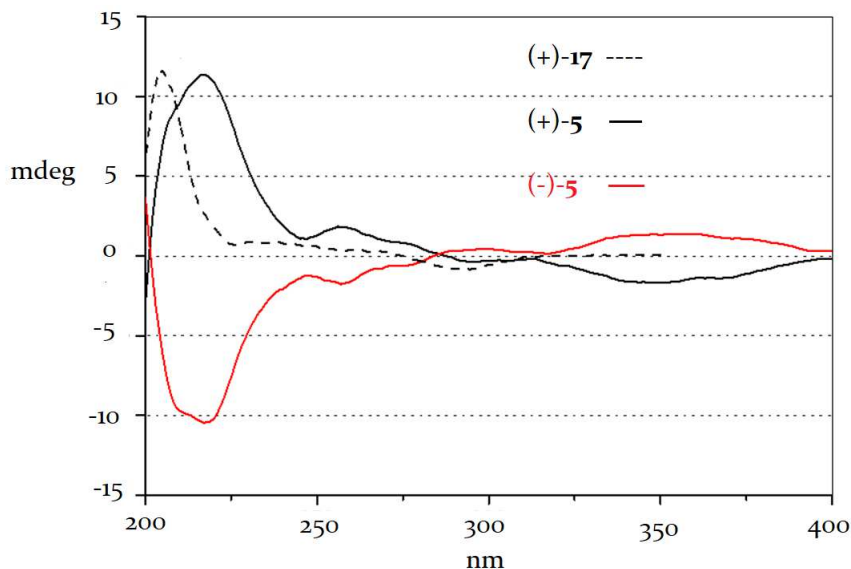
Figure 6.6: ECD spectra of (+)-**5** (black line), (-)-**5** (red line) and (+)-**17** (dashed black line)

6.3 Enantiopure u-NHC catalysts in model asymmetric transformations

Enantiopure catalysts were tested in the ARCM of the model prochiral trienes **58** and **59** (scheme 6.4) and in the AROCM of the *meso*-norbornene derivative **60** with styrene (scheme 6.5).

6.3.1 ARCM of 58 and 59

The results of the ARCM of prochiral trienes catalysed by N-methyl, N'=isopropylphenyl catalysts **2** and **4** and by their N-cyclohexyl congeners **6**, **8** and (-)-**5** are summarised in table 6.2.

Comparing behaviours of phosphine catalyst **2** and **6** with those of their phosphine free analogues **4** and **8** (entries 1-4 and 5-8 for ARCM of **38**, entries 13-16 and 17-20 for ARCM of **39**) it was immediately clear that asymmetric catalytic performances were ruled by the NHC ancillary ligand independentely by the Grubbs-type or Hoveyda-type nature of the catalyst. For this reason, just results of the phosphine catalyst **2** and **6** will be discussed and compared with data obtained with (+)-**5** and with Collins' catalyst (figure 6.7), the most enantioselective backbone substituted unsymmetrical monodentate NHC catalyst to date.
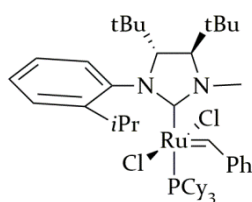
Figure 6.7:
Collins' catalyst

All catalysts were able to very efficiently cyclise **58**. The introduction of the iodide additive, which determined a substitution of the chloride ligands with iodide, affected the conversion only in the case of syn catalyst (+)-**5**. Enantioselectivities were low to moderate (18-53%) and an increase of the enantiomeric excesses was observed if NaI was used. This enhanced enantioselectivity as function of the increased size of the halide ligand is, surprisingly, in contrast with results of Collins' catalyst

having a very similar uNHC ligand and coherent with what observed by Grubbs for symmetrical NHC-based systems.[45]

Scheme 6.4: ARCM of **58** and **59**

Table 6.2: ARCM of **58** and **59** with **2**, **4**, **6**, **8**, (+)-**5** and Collins' catalyst

entry[a]	substrate	catalyst (mol%)	additive	time (h)	yield (%)[b]	ee (%)[c]
1	**58**	**2** (2.5)	None	2	>98	33 (S)
2	**58**	**2** (4.0)	NaI	2	>98	50 (S)
3	**58**	**4** (2.5)	None	2	>98	33 (S)
4	**58**	**4** (4.0)	NaI	2	>98	47 (S)
5	**58**	**6** (2.5)	None	2	>98	18 (S)
6	**58**	**6** (4.0)	NaI	2	>95	53 (S)
7	**58**	**8** (2.5)	None	2	>98	19 (S)
8	**58**	**8** (4.0)	NaI	2	>95	52 (S)
9	**58**	(+)-**5** (2.5)	None	2	>98	37 (S)[d]
10	**58**	(+)-**5** (4.0)	NaI	2	46	44 (S)
11[e]	**58**	**Collins** (2.5)	None	2	>95	82 (S)
12[e]	**58**	**Collins** (4.0)	NaI	3	>95	48 (S)
13	**59**	**2** (2.5)	None	2	>98	25 (R)
14	**59**	**2** (4.0)	NaI	3	-	-
15	**59**	**4** (2.5)	None	2	>98	29 (R)
16	**59**	**4** (4.0)	NaI	3	-	-
17	**59**	**6** (2.5)	None	2	>95	42 (S)
18	**59**	**6** (4.0)	NaI	3	-	-
19	**59**	**8** (2.5)	None	2	>95	42 (S)
20	**59**	**8** (4.0)	NaI	3	-	-
21	**59**	(+)-**5** (2.5)	None	2	>98	14 (R)
22	**59**	(+)-**5** (4.0)	NaI	3	-	-
23[f]	**59**	**Collins** (2.5)	None	3	>95	8 (S)

[a] Runs without additives were carried out at 40°C in dry CD_2Cl_2 while runs with NaI were carried out in dry THF; [b] Yields based on ^1H NMR analysis; [c] Determined with chiral gaschromatography; [d] Values of yields and *ee* with the enantiomer (-)-**5** were coherent, products were obtained with (R) absolute configuration; [e] Taken from reference 56 a; [f] Taken from reference 58.

This demonstrated that enantioselective catalysis with u-NHC occurs with a different mechanism, unfortunately still totally unknown.

Catalyst **2**, differently from the other anti complexes, gave **58a** with an R absolute configuration. This was unexpected and not easy to rationalise. In fact, the low enantioselectivity made risky any computational chemistry hypothesis.

All catalysts were competent in the asymmetric ring closure of **59** but the addition of the iodide addictive harmed complexes' reactivities.

Very interestingly also syn catalyst (+)-**5** was able to reach full conversion: this is not trivial, considering the overall low efficiencies of syn catalysts in the RCM of hindered olefins (see chapters 3 and 5).

Coherently with the ARCM of **58**, enantiomeric excesses were low to moderate (14-42%) but interestingly always higher if compared with those observed in the presence of Collins' catalyst.

At this point, the catalytic behaviour of (+)-**5** (table 6.3) was further investigated under diverse reaction conditions.

Table 6.3: ARCM of **58** with (+)-**5**

entry[a]	loading (mol%)	additive	temperature (°C)	time (h)	yield[b] (%)[b]	*ee* (%)[c]
1	2.5	-	40	2	>98	37 (*S*)
2	2.5	-	22	2	>98	39 (*S*)
3	2.5	-	0	2	>98	39 (*S*)
4	4.0	NaI	40	2	46	44 (*S*)
5	4.0	NaI	40	16	57	44 (*S*)

[a] Runs without additives were carried out at in dry CD_2Cl_2 while runs with NaI were carried out in dry THF, values of yields and *ee* with the enantiomer (-)-**5** were coherent and products were obtained with an (*R*) absolute configuration;; [b] Yields based on ¹H NMR analysis; [c] Determined with chiral gaschromatography;

In the ARCM of **58**, unfortunately, the temperature decrease did not affect enantioselectivity (entries 1-3). In the same reaction, when the halide additive was used, conversion increased with time, however enantiomeric excess remained unchanged (entries 4-5).

Although this particular syn catalyst did not show a pronounced enantioselectivity, the potentialities of the synthetic method developed to its preparation will allow to access to libraries of syn backbone substituted catalysts to test in asymmetric metathesis.

Effects of NHC substitutions on enantioselectivity was further investigated by performing the ARCM of **58** and **59** with the phosphine-free catalysts **37**, **39** and **41** (table 6.4).

Ruthenium compound **37**, bearing an N-neopentyl NHC ligand, showed a comparable behaviour with respect to its N-Cyclohexyl analogue **8**, both in terms of activity and selectivity (entries 7-8 and 19-20 of table 6.2 and entries 1-2 and 10-11 of table 6.4). Behaviour of N-neophyl catalysts **39** was also similar (albeit in this case conversion was affected by the use of the halide additive).

The replacement of isopropylphenyl (**8**) with mesityl (**41**) as the NHC N'-aryl group significantly reduced complex reactivity (entries 7-8 and 19-20 of table 6.2 and entries 6-9 and 14 of table 6.4). In fact, in the ARCM of **58** without addictive, more than 40 hours are

necessary to reach full conversion. Not surprisingly, the use of NaI determined a very poor conversion, even at longer reaction time.

As we expected, **41** was totally inactive in the RCM of **59**.

Table 6.4: ARCM of **58** and **59** with **37**, **39**, and **41**

entry[a]	substrate	catalyst (mol%)	additive	time (h)	yield (%)[b]	ee (%)[c]
1	58	37 (2.5)	None	2	>98	16 (S)
2	58	37 (4.0)	NaI	2	>98	43 (S)
3	58	39 (2.5)	None	2	>98	18 (S)
4	58	39 (4.0)	NaI	2	83	47 (S)
5	58	39 (4.0)	NaI	20	87	43 (S)
6	58	41 (2.5)	None	2	18	7 (R)
7	58	41 (2.5)	None	41	>98	7 (R)
8	58	41 (4.0)	NaI	2	7	24 (S)
9	58	41 (4.0)	NaI	25	7	24 (S)[d]
10	59	37 (2.5)	None	3	>98	41 (R)
11	59	37 (4.0)	NaI	2	-	-
12	59	39 (2.5)	None	3	>95	36 (S)
13	59	39 (4.0)	NaI	2	>98	25 (R)
14	59	41 (2.5)	None	3	-	-

[a] Runs without additives were carried out at 40°C in dry CD_2Cl_2 while runs with NaI were carried out in dry THF; [b] Yields based on ^1H NMR analysis; [c] Determined with chiral gaschromatography.

6.3.2 AROCM of 60 and styrene
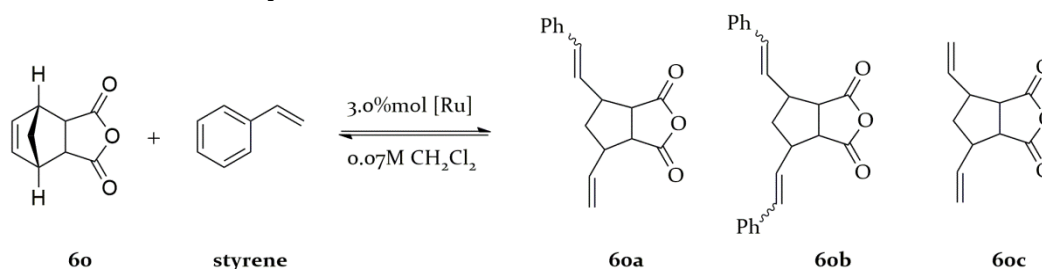
Scheme 6.4: AROCM of **60** and styrene

Hoveyda type catalysts were tested in the AROCM of the norbornene derivative **60** and styrene (table 6.5).

For all catalysts, except to stylbene (the product of the self metathesis of styrene), no other homodimerisation product was detected. Moreover all complexes were selective towards the AROCM desired product **60a**.

The substitution of methyl (**4**) with a more encumbered or ramified alkyl group (**8**, **37** and **39**) slightly increased enantioselectivity. More pronounced was the effect of the N-aryl group. In fact, the introduction of an N'-mesityl aryl group significantly raised the enantiomeric excess up to 43%

Table 6.5: AROCM of **60 and styrene** with **4**, **8**, **37**, **39**, and **41**

entry[a]	catalyst	yield 60a(%)[b]	yield 60b(%)[b]	yield 60c(%)[b]	ee 60a(%)[c]
1	**4**	35	7	24	10 (R, R)
2	**8**	46	15	10	13 (R, R))
3	**37**	57	11	16	19 (R, R))
4	**39**	45	11	16	21 (R, R))
5	**41**	37	16	22	43 (R, R))

[a] Runs were carried out at 40°C in dry CH_2Cl_2; [b] Isolated yields; [c] Determined with chiral HPLC.

6.4 Conclusion

Seven enantiopure backbone substituted u-NHC ligands were synthesized. Above the 'classical' path, which made from chiral starting material just the anti configuration available, a new approach was proposed. This innovative strategy, using chemical derivatisation and chiral resolution, led to achieve complexes with syn backbone relative configuration, whose enantioselectivity was never studied before. Resolution was carried out through chiral HPLC in an easy, non-time consuming step. Enantiomeric relationship between stereoisomers of the monoarylated diamine was proved using optical rotation dispersion (ORD) and electronic circular dichroism (ECD). This latter technique was also involved in the characterisation of the syn metathesis catalysts.

All chiral ruthenium compounds were studied in the ARCM of **58** and **59**. In these reactions, the enantioselectivity were ruled by the NHC ancillary ligand with no influence of the phosphine or phosphine free nature of the catalyst. The use of an halide addictive raised enantiomeric excesses, differently from what observed with the Collins' catalyst.

N-cyclohexyl, N'-isopropylphenyl catalyst **8** showed a very good activity and a poor-moderate enantioselectivity. The substitution of cyclohexyl with neopentyl (**37**) or neophyl (**39**) did not significantly affect catalytic behaviour, while the replacement of isopropylphenyl with mesityl critically reduced both conversion and enantioselectivity.

Syn catalyst (-)-**5** did not show any valuable difference in catalytic performance with respect to the anti analogue.

Hoveyda-type catalysts were tested in the AROCM of **60** with styrene. All ruthenium compounds were selective toward the desired product **60a**. Coherently with ARCM, enantiocontrol was not sensitively affected by the hyndrance and by the ramification of the alkyl group. Differently, the nature of the aryl substituent played a more important role, increasing enantiomeric excesses up to 43%.

6.5 Supporting Information

For all the general information regarding the manipulation of organic and organometallic compounds please see paragraph 3.8.

HPLC gradient grade solvents were obtained from Sigma-Aldrich (St. Louis, MO, USA). Chiral columns were from Chiral Technologies Europe (Illkirch, France). Optical activity for enantiomers of **17** and **18** was determined using a JASCO P2000 polarimeter. Enantiomeric excesses of **58a**, **59a** and **60** were determined by chiral GC (Supelco _DEX 120, 30 m _ 0.25 mm) or by chiral HPLC (JASCO MD-4015 Photo diode array detector, PU4180 RMPLC Pump) and were compared to racemic samples.

6.5.1 NMR characterisation and specific rotations

For compounds **18–19**, (+)-**5** and (-)-**5** , signals of both enantiomers have been found to be coherent with those of the corresponding racemic samples. (+)-**5** and (-)-**5** exist as a mixture of rotational isomers syn: anti ~0.4:1 *(*syn: *N*-alkyl group located on the same side as the benzylidene unit). Representative NMR spectra of (-)-**18**, (−)-**19** and (-)-**5** are reported below. For comparison, NMR analysis of (+)-**5** is also provided.

(–)-**18** (MW= 412.6 g/mol, Yield=78%).
^{1}H NMR (400 MHz, CDCl$_3$): δ 7.25 (br s, 3H); 7.17 (br s, 3H); 7.10 (d, ^3J =7.32 Hz, 1H); 6.98 (br s, 4H); 6.85 (t, ^3J = 7.62 Hz, 1H); 6.61 (t, ^3J = 7.32 Hz, 1H); 6.24 (d, ^3J = 7.93 Hz, 1H); 5.27 (br s, 1H); 4.56 (br s, 1H); 4.30 (d, ^3J =4.27 Hz, 1H); 3.01–2.94 (m, 1H); 2.32 (br t, 1H); 1.90 (br t, 1H); 1.70–1.59 (o m, 3H); 1.57–1.47 (o m, 3H); 1.34 (t, ^3J =6.68 Hz, 3H); 1.28 (t, ^3J =6.68 Hz, 3H); 1.22–0.98 (o m, 3H).
α_D= -13.0 (c = 0.5, CH$_2$Cl$_2$).

(–)-**19** (MW= 511.4 g/mol, Yield=84%).
^{1}H NMR (400 MHz, CDCl$_3$): δ 8.29 (s, 1H); 7.49 (d, ^3J = 8.08 Hz, 1H); 7.30–7.24 (o m, 3H); 7.22–7.15 (o m, 3H); 7.02–6.93 (o m, 5H); 6.86 (d, ^3J = 6.55 Hz, 2H); 6.48 (d, ^3J = 11.81 Hz, 1H); 6.04 (d, ^3J = 11.81 Hz, 1H); 3.46 (m, 1H); 3.19 (m, 1H); 2.26 (br d, 2H); 1.91 (br d, 1H); 1.82–1.69 (o m, 2H); 1.63 (o m, 1H); 1.54 (o m, 1H); 1.34–1.29 (o m, 6H); 1.25–1.13 (o m, 3H).
α_D= -38.8 (c = 0.5, CH$_2$Cl$_2$).

(+)-**5** (MW=965.1 g/mol, Yield=42%)
^{1}H NMR (400 MHz, C$_6$D$_6$): δ 21.06 (minor rotational isomer, d, ^3JHP = 4.0 Hz, 0.4H); 19.75 (major rotational isomer, s, 1H); (only major isomer signals are reported below) 9.02–6.60 (overlapped signals of both isomers); 6.40 (t, ^3J = 7.5 Hz, 1H); 6.15 (br t, 2H); 5.89 (d, 3J = 10.52 Hz, 1H); 5.30 (br t, 1H); 5.16 (d, 3J = 10.52 Hz, 1H); 3.56–3.44 (o m, 2H); 3.23 (br d, 1H); 2.55 (br d, 2H); 2.41–2.38 (o m, 5H); 2.08–0.91 (overlapped signals of both isomers).
^{13}C NMR (C$_6$D$_6$, 100 MHz): δ 299.4 (Ru = CHPh); 221.0 (iNCN, 2JC-P = 79.2 Hz); 152.3; 137.6; 134.4; 134.0; 133.8; 132.2; 130.6; 130.4; 129.8; 129.1; 127.5; 126.3; 125.9; 75.8; 67.5; 61.1; 33.9; 33.7; 33.5; 33.4; 33.0; 30.4; 30.2; 29.9; 29.8; 28.7; 28.6; 27.3; 26.0; 25.9; 25.4; 23.6. 31P NMR (C6D6, 161.97 MHz): δ 24.9; 24.6.

Determination of the specific rotation was not possible due to the rapid decomposition of the complex.

(-)-**5** (MW=965.1 g/mol, Yield=47%)

^{1}H NMR (400 MHz, C$_6$D$_6$) (Figure S4): δ 21.06 (minor rotational isomer, d,3JHP = 4.0 Hz, 0.4H); 19.74 (major rotational isomer, s, 1H); (only major isomer signals are reported below) 9.02–6.57 (overlapped signals of both isomers); 6.41 (t, 3J = 7.5 Hz, 1H); 6.15 (br s, 2H); 5.89 (d, 3J = 10.52 Hz, 1H); 5.29 (br t, 1H); 5.16 (d, 3J =10.52 Hz, 1H); 3.56–3.44 (o m, 2H); 3.25 (br d, 1H); 2.55 (br d, 1H); 2.41–2.38 (o m, 5H); 2.08–0.91 (overlapped signals of both isomers).

^{13}C NMR (C$_6$D$_6$, 100 MHz): δ 299.4 (Ru = CHPh); 221.0 (iNCN, 2JC-P = 79.2 Hz); 152.3; 137.6; 134.4; 134.0; 133.8; 132.2; 130.6; 130.4; 129.8; 129.1; 127.5; 126.3; 125.9; 75.8; 67.5; 61.1; 33.9; 33.7; 33.5; 33.4; 33.0; 30.4; 30.2; 29.9; 29.8; 28.7; 28.6; 27.3; 26.0; 25.9; 25.4; 23.6. 31P NMR (C6D6, 161.97 MHz): δ 24.9; 24.6.

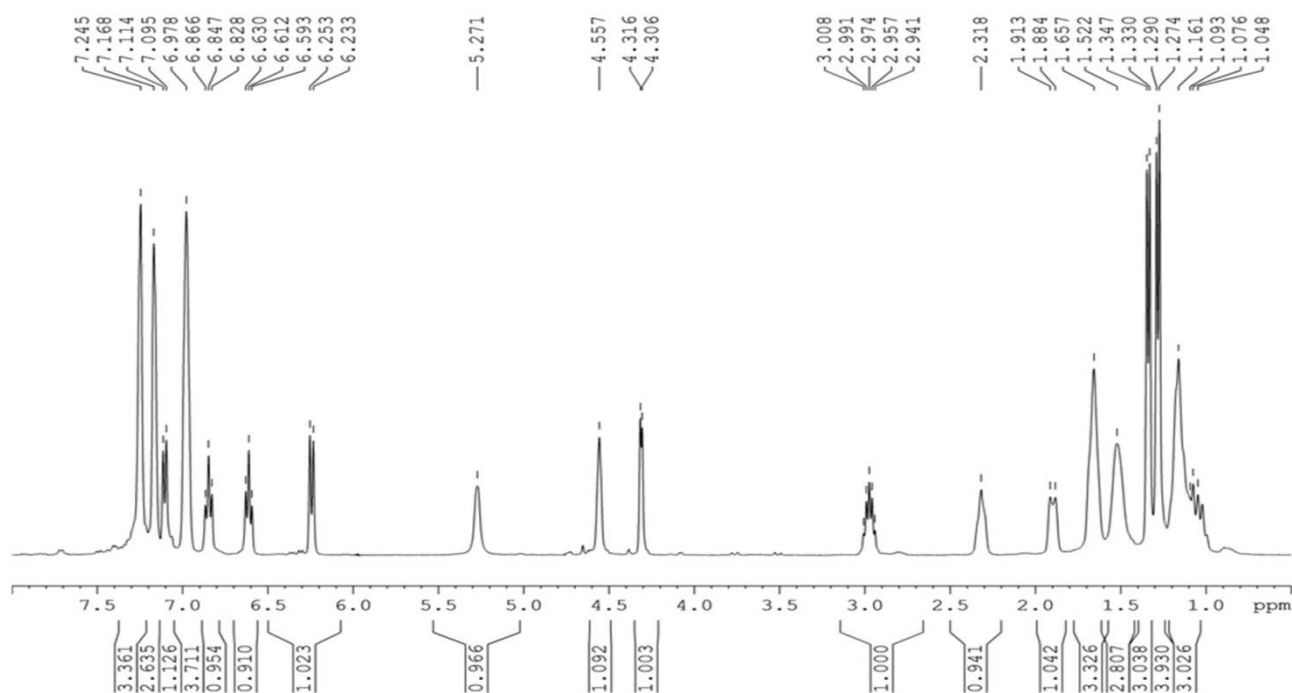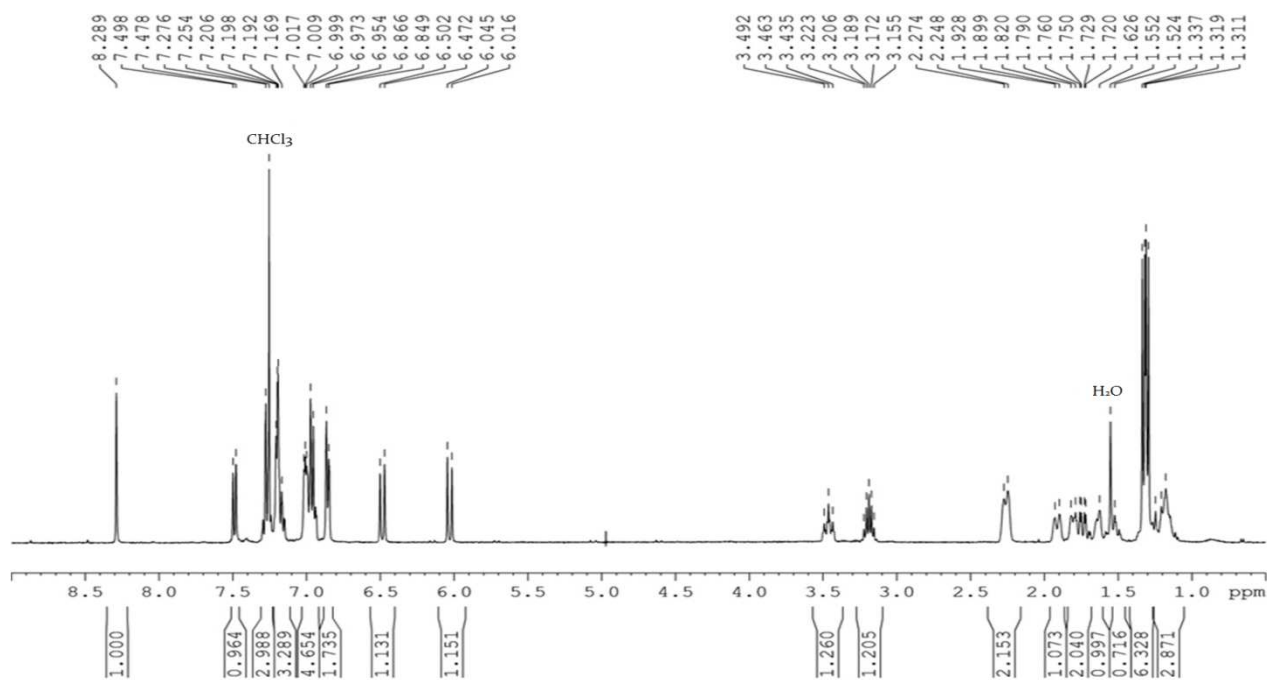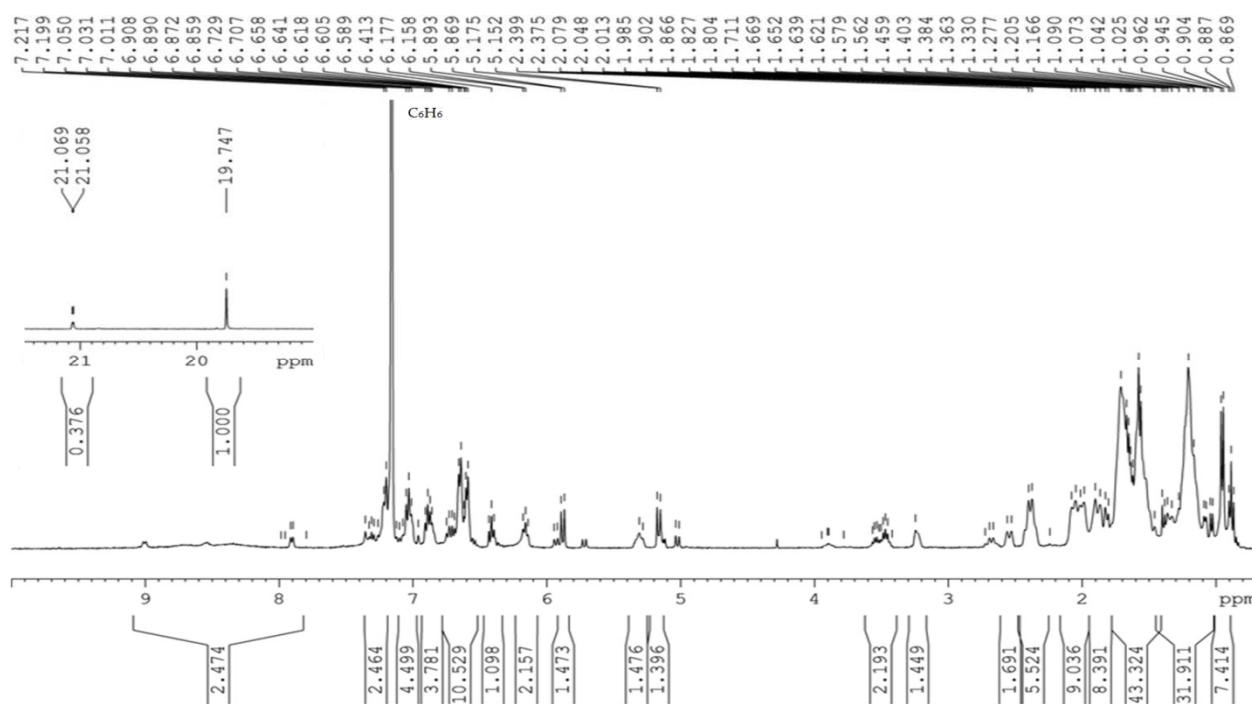Determination of the specific rotation was not possible due to the rapid decomposition of the complex.

Figure S6.1:^{1}H NMR of (–)-**18** (CDCl$_3$, 400 MHz).

Figure S6.2: ¹H NMR of (–)-**19** (CDCl₃, 400 MHz).

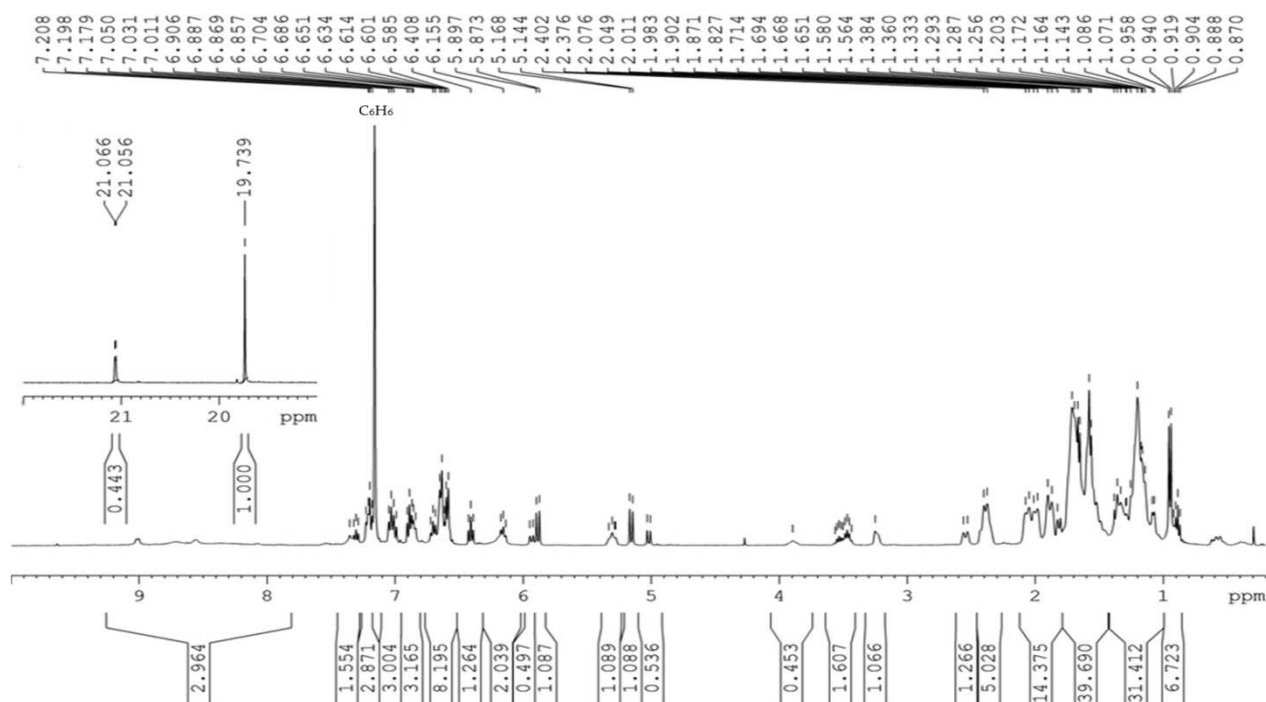**Figure S6.3:** ¹H NMR of (+)-**5** (C₆D₆, 400 MHz).

Figure S6.4: ^{1}H NMR of (-)-**5** (C$_6$D$_6$, 400 MHz).

6.5.2 Enantioselective Chromatography and Chiro-Optical Characterization[116]

Analytical liquid chromatography was performed on a Jasco HPLC system equipped with a PU-980 HPLC pump, a 20 _L loop injector (Rheodyne model 7725i), a 975 series UV detector and a 995-CD series detector. Chromatographic data were collected and processed with Jasco Borwin software (Version 1.50, Jasco Europe, Italy). Semi-preparative liquid chromatography was performed on a Waters chromatograph (Waters, Milford, MA, USA) equipped with a Rheodyne model 7012, 500 _L loop injector and a spectrophotometer UV SpectraMonitor 4100 (Waters, Milford, MA, USA).

The enantiomers of **17** were resolved by using the Chiralpak IA column (250 _ 10 mm ID, 5 _m), n-hexane/isopropanol 90/10 as eluent (flow rate 3.0 mL/min, T: 25 _C and UV detection at 300 nm). The sample was dissolved in hexane/isopropanol/dichloromethane 70/10/20 (c: 50 mg/mL); each injection was of 100 µL (process yield 70%). The enantiomeric excess of each collected enantiomer was determined by analytical HPLC with the Chiralpak IA column (250 _ 4.6 mm ID, 5 _m) under the same elution conditions with a flow rate of 1.0 mL/min and UV/CD detections at 254 and 300 nm respectively.

The off-line ECD spectra of hexane solutions of chromatographically resolved (+)-**17** and (-)-**17** (c = 3 $^*10^{-4}$ M) and the enantiopure catalysts (+)-**5** and (-)-**5** were recorded with a J710 UV-CD Jasco spectrometer. Specific optical rotations of hexane solutions of (+)-**5** and (-)-**5** (c = 0.097% and 0.103%) were measured with a polarimeter P-1020 Jasco (Jasco Europe, Italy) at 25 _C at 589, 577, 546, 435, 405 and 365 nm. HPLC gradient grade solvents were obtained from Sigma-Aldrich (St. Louis, MO).

---

[116] Chiral chromatography, chiro-optical characterization and simulation of the ORD spectrum were performed, respectively, by Dr. Alessia Ciogli, Dr. Sergio Menta and Dr. Marco Pierini at the University of Rome "La Sapienza".

6.5.3 Simulation of the ORD Spectrum of (1R, 2S)-17 [3]

Molecular modeling calculations carried out on the structure of the (1R, 2S)-**17** enantiomer and concerning conformational search and optimization of the so-obtained geometries, were performed by using the computer program SPARTAN 10v1.1.0 (Wavefunction Inc., 18401 Von Karman Avenue,Suite 370, Irvine, CA, USA). The conformational search was performed by molecular mechanic calculations based on the Merck molecular force field (MMFF), according to the systematic algorithm implemented in SPARTAN. All rotatable bonds were varied. Maximum energy gap from the lowest energy geometry for kept conformations was 40 kJ/mol; criterion adopted in the analysis of similarity to define conformers as duplicates was R2 _ 0.9. Such analysis supplied a total of 27 conformations, 22 of which by an energy window of 3 kcal/mol. All the geometries were further optimized at the HF/STO-3G level of theory, which afforded 15 conformations within an energy window of 3 kcal/mol.

Among these latter, the seven more stable conformations from the global minimum (hereafter denoted with the symbol Cn, with n varying between 1 and 7), which covered a range of Boltzmann distribution amounting overall to 79.1%, were, in turn, further optimized by minimizing their energy stability at the level of theory B3LYP/6-31G*. In all such calculations, the effect of the hexane as the solvent, by simulating its presence according to the SM8 model implemented in SPARTAN, was taken into account.

The found relative difference in energy of the conformers C2–7 with respect to C1 were: C2 = 0.11, C3 = 0.41, C4 = 2.04, C5 = 3.39, C6 = 4.66, C7 = 5.03 kcal/mol. The corresponding percentages of Boltzmann distributions were C1 = 42.3, C2 = 35.1, C3 = 21.1, C4 = 1.4, C5 = 0.1, C6 = 0.0 and C7 = 0.0, respectively. Due to the high level of geometric and energetic similarity existing between the two conformers found to be the most stable, C1 and C2 (i.e., the ones differing by only 0.11 kcal/mol), they were clustered in a single global minimum geometry, denoted as C1,2. Thus, among the seven initial conformations optimized by means of the B3LYP method, just the final two geometries C1,2 and C3 were endowed with a significant amount of Boltzmann distribution (65.1% and 32.5%, respectively); they were therefore employed in the next step of the modelling, focused on assessing the relevant optical rotatory dispersion (ORD) spectra of (1R, 2S)-**17**. Conformations C1,2 and C3 were than subjected to assessment of optical rotation values $[\alpha]_n$ at four different wavelengths n, in the range 443–589 nm, which were carried out by using the BLYP method with the TZ2P large core basis set, as implemented in the Amsterdam Density Functional (ADF) package v. 2007.01. The couples of $[\alpha]_n$ values obtained at each wavelength from the geometries of C1,2 and C3 were weighted according to the Boltzmann distributions calculated for the related conformations, and then merged onto each other, thus affording (1R, 2S)-**17** the following final optical rotation values: $[\alpha]_{443}$ = 473 nm; $[\alpha]_{487}$ = 309 nm; $[\alpha]_{530}$ = 242 nm; $[\alpha]_{589}$ = 186 nm.

6.5.4 Catalysis

ARCM of **58** and **59** without additive were carried out by adding the catalyst (0.0028 mmol, 0.025 equiv.) to a 2 mL solution of the prochiral triene (1 equiv., 0.055 M) in dry CD_2Cl_2.

The flask was stirred a 40°C for two hours for **58** and for three hours for **59**. Yields were determined via NMR spectroscopy of the crude product. The reaction mixture was filtered on neutral alumina and injected into the GC system without further purifications.

ARCM of **58** and **59** with additive were implemented by adding NaI (0.055 mmol, 1 equiv.) to a 1 mL THF-d_8 solution of the catalyst (0.0022 mmol, 0.04 equiv.). The reaction mixture was stirred at room temperature for one hour. After that, **58** or **59** (0.055 mmol, 1 equiv.) was added. Then, the flask was stirred a 40 °C for two hours for **58** and three hours for **59**. Yields were determined via NMR spectroscopy of the crude product. The reaction mixture was filtered on neutral alumina and injected into the GC system without further purifications.

AROCM of **60** with styrene was carried out in glove box. **60** (0.43 mol, 1 eq.) and styrene (4.3 mmol, 10 equiv.) were simultaneously added to 7.5 mL of CH_2Cl_2 solution of the catalyst (0.013 mmol, 0.03 equiv.). The flask was stirred at room temperature for three hours. The reaction mixture was then concentrated and purified via column chromatography (petroleum ether : diethyl ether, 1:1) to afford the product as a transparent oil. About 1 mg of the product was dissolved in 1 mL of 2-propanol (HPLC-grade purity), filtered using a syringe filter and then injected into the HPLC system.
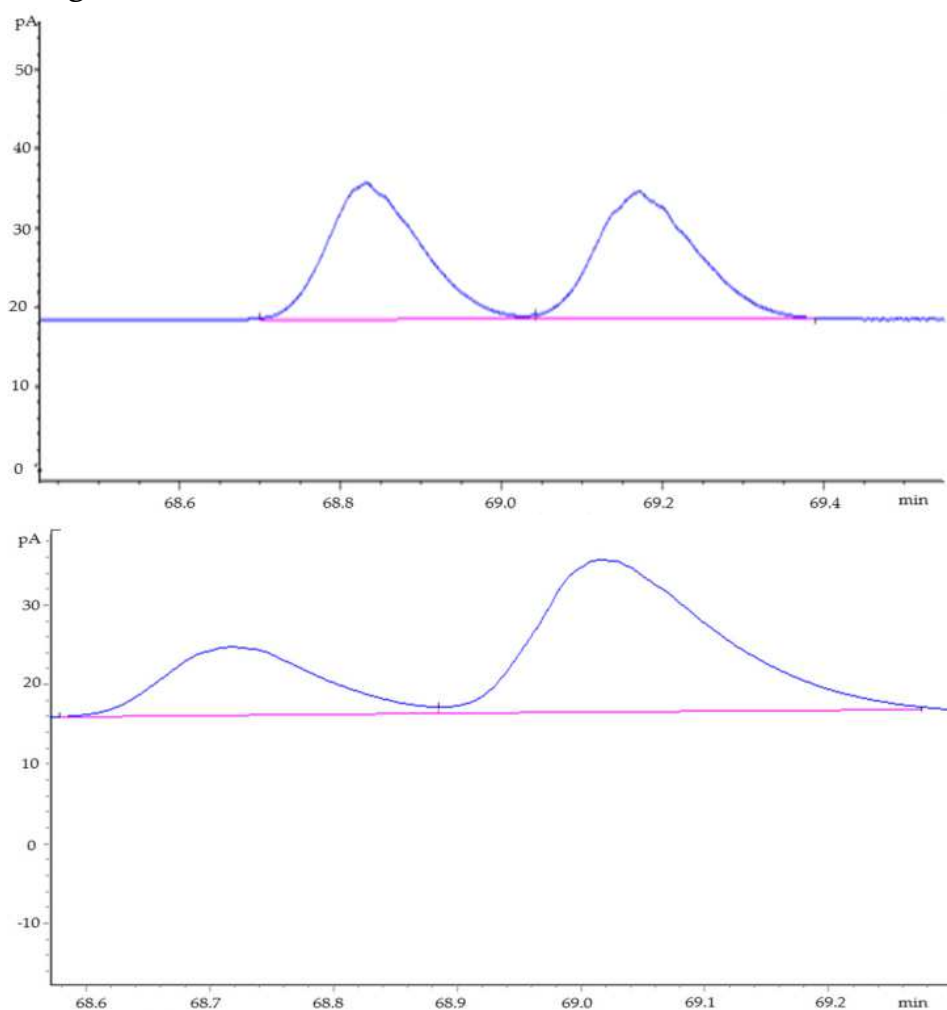
6.5.5 Chromatograms

Figure S6.5: GC analysis of racemic (top) and of enantioenriched **58** (bottom, 43% *ee*).
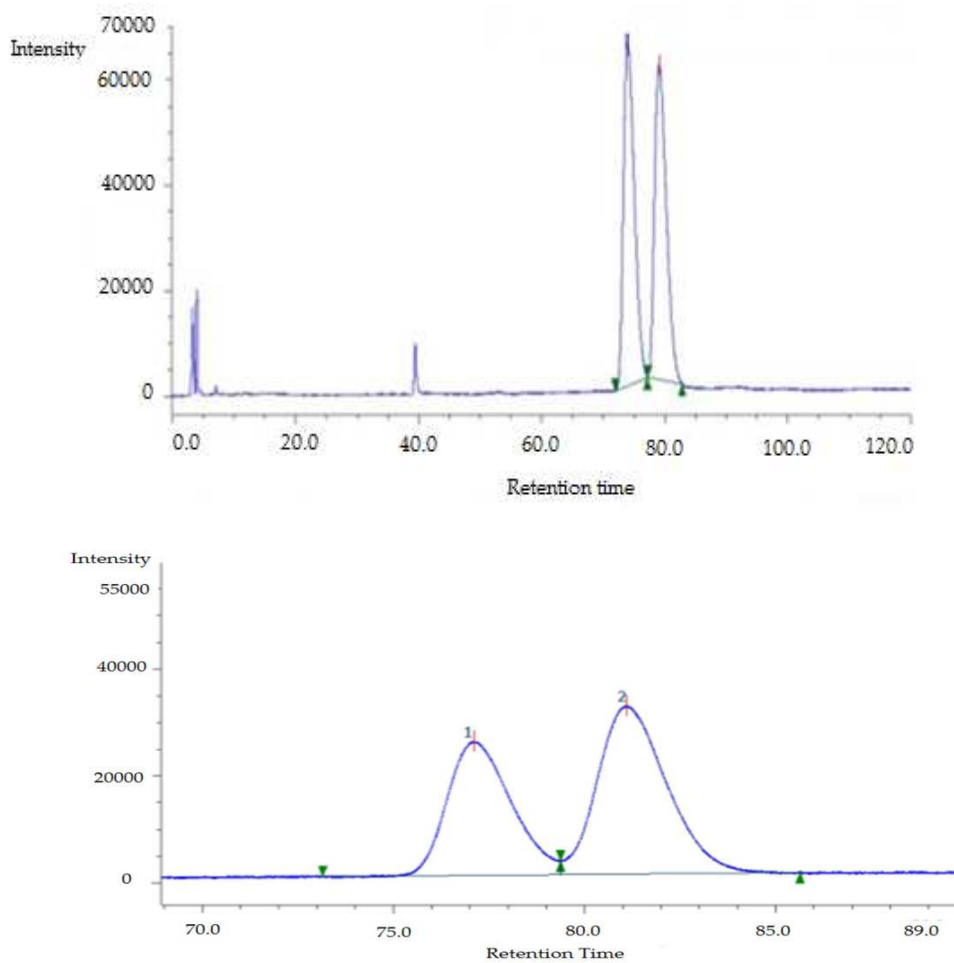
Figure S6.6: HPLC analysis of racemic (top) and of enantioenriched **6oa** (bottom, 15% *ee*).

Conclusion

In this doctoral thesis, novel backbone substituted u-NHC ruthenium complexes were synthesized and characterised.

Evaluation of the catalytic behaviours in standard metathesis reactions showed an interesting backbone configuration effect. In fact, in RCM of model substrates, complexes with an anti backbone relative configuration displayed a higher efficiency with respect to the syn congeners. This was more accentuated in the case of Hoveyda type compound **7** and its anti analogue **8**, bearing an N-cyclohexyl, N'-isopropylphenyl NHC ligand. Moreover, in CM, these two catalysts led to obtain considerably different E/Z ratios, displaying the more consistent backbone induced Z-selectivity observed up to date. The origin of this so peculiar behaviour was studied in depth by investigating the steric and electronic properties of the ligand using DFT calculation and IR spectroscopy

Grubbs type complexes **5** and **6**, bearing the aforementioned N-cyclohexyl, N'-isopropylphenyl NHC ligand, were tested in homo- and copolymerisation. 5, the ruthenium compound with a syn backbone configuration, afforded copolymers with a higher percentage of alternated junctions.

To study the potential effect on catalytic performances of different alkyl (methyl, cyclohexyl, neopentyl, neophyl) or aryl groups (mesityl, isopropylphenyl) on the NHC a new series of u-NHC ruthenium compounds were synthesized. A less prominent backbone effect was observed in standard metatesis reactions promoted by these new catalysts. All the systems developed along with **7-8** were tested in the ethenolysis of ethyl oleate. Very interestingly **41**, the complex bearing an N-cyclohexyl, N'-mesityl ligand, exhibited the highest TON ever observed in the field of metathesis catalysts with N-alkyl, N'-aryl NHC ligands.

Finally, enantiopure catalysts were tested in asymmetric metathesis transformations and led to obtain moderate enantioselectivities. Moreover, a new synthetic strategy for the obtainment of enantiopure catalysts presenting an u-NHC with a syn configuration was proposed.